

Enabling Technologies for Cognitive Optical Networks

Robert Borkowski
Ph.D. Thesis
May 2014

Technical University of Denmark



Enabling Technologies for Cognitive Optical Networks

PhD Thesis

Robert Borkowski

This thesis was supervised by:

Prof. Idelfonso Tafur Monroy Technical University of Denmark

Dr. Darko Zibar Technical University of Denmark

Assessment comitee:

Prof. Leif Katsuo Oxenløwe Technical University of Denmark

Prof. Werner Rosenkranz University of Kiel (Germany)

Prof. Christian G. Schäffer Helmut Schmidt University (Hamburg, Germany)

Thesis delivery date: April 4, 2014.

Thesis defence date: May 20, 2014.

This research was financed in part by the European Union's Seventh Framework Programme for Research (FP7) project CHRON under grant agreement no. 258644.

Parts of this work were carried out in: Huawei Technologies Duesseldorf (Munich, Germany), Centro de Pesquisa e Desenvolvimento em Telecomunicações – CPqD (Campinas, Brazil), and Athens Information Technology – AIT (Greece).

DTU Fotonik

Department of Photonics Engineering

Technical University of Denmark

Ørsted's Plads, Building 343

2800 Kgs. Lyngby

Denmark

DOI:10.11581/DTU:00000007

ISBN: 978-87-93089-28-0

Abstract

Cognition is a new paradigm for optical networking, in which the network has capabilities to observe, plan, decide, and act autonomously in order to optimize the end-to-end performance and minimize the need for human supervision. This PhD thesis expands the state of the art on cognitive optical networks (CONs) and technologies enabling and supporting their implementation. The scientific content presented in this thesis tackles two major research problems. First, formulation of fundamental requirements and objectives of CONs, experimental evaluation of selected aspects of their architecture, and machine learning algorithms that make cognition possible. Secondly, advanced optical performance monitoring (OPM) capabilities performed via digital signal processing (DSP) that provide CONs with necessary feedback information allowing for autonomous network optimization.

The research results presented in this thesis were carried out in the framework of the EU project *Cognitive Heterogeneous Reconfigurable Optical Network (CHRON)*, whose aim was to develop an architecture and implement a testbed of a cognitive network able to self-configure and self-optimize to efficiently use available resources. In order to realize this objective, new CON-supporting functionalities had to be defined, developed, and experimentally verified. This thesis summarizes the main contributions of the author to the project.

Cutting-edge results in experimental evaluation of functionalities of autonomous networks are presented: the first experimental demonstration of the use of case-based reasoning technique in optical communication network for successful quality of transmission estimation in an optical link; cognitively controlled erbium-doped fiber amplifiers to ensure below forward error correction limit performance of all transmitted channels; reconfigurable coherent software-defined receiver supporting various modulation formats and bit rates; experimental evaluation of required optical signal-to-noise ratio for flexible elastic optical networks with mixed modulation formats; evaluation of various

prefilter shapes for high symbol rate software-defined transmitters.

Furthermore, by using the DSP capabilities of a coherent software-defined receiver combined with powerful machine learning methods, optical performance monitoring techniques for next generation networks were conceived, implemented, and tested by numerical simulations and experiments. One of the highlights of this thesis is the first demonstration of a novel modulation format recognition method based on Stokes space parameters, capable of discerning between six different complex modulation formats. Moreover, new chromatic dispersion monitoring metrics were introduced and experimentally tested, while machine learning is shown to tackle constellation distortions due to nonlinearities in long haul fiber-optic links.

In conclusion, the results presented in this thesis lay the groundwork for cognitive optical networks, as well as define and contribute to technologies required for their implementation. Operation of CON-enabling machine learning methods is tested experimentally and DSP-based OPM techniques for software-defined receivers are introduced and verified. The presented set of technologies forms a foundation, upon which next generation fiber-optic data transmission networks will be built.

Resumé

Kognition er et nyt paradigme indenfor optiske netværk, hvor netværket har evne til at observere, planlægge, beslutte og handle selvstændigt for at optimere ende-til-ende ydeevne og minimere behovet for menneskelig overvågning og intervention. Denne ph.d.-afhandling højner stedet indenfor kognitive optiske netværk (cognitive optical network – CON) og tilhørende teknologier, hvilket muliggør og fremmer deres indførelse. Det videnskabelige indhold, som præsenteres i denne afhandling, adresserer to store forskningsmæssige udfordringer. For det første formulering af grundlæggende krav og målsætninger, eksperimentel evaluering af udvalgte aspekter af arkitekturen, og maskinlæringsalgoritmer der muliggør kognition. For det andet avanceret optisk ydeevneovervågning (optical performance monitoring – OPM) af netværket udført vha. digital signalbehandling (digital signal processing – DSP) og tilbagemeldinger, som til sammen giver mulighed for autonom optimering af netværket.

De forskningsresultater, som præsenteres i denne afhandling, blev udført indenfor rammerne af EU-projektet *Cognitive Heterogeneous Reconfigurable Optical Network* (CHRON), hvis formål var at udvikle en arkitektur og etablere en testopstilling af et kognitivt netværk, som er i stand til at konfigurere og optimere sig selv for at opnå effektivt brug af de tilgængelige ressourcer. For at realisere dette mål måtte nye CON-understøttede funktionaliteter defineres, udvikles og eksperimentelt verificeres. Afhandlingen opsummerer de vigtigste bidrag fra forfatteren til nævnte projekt.

Således præsenteres banebrydende resultater vedrørende eksperimentel evaluering af funktionaliteter i autonome netværk: den første eksperimentelle demonstration af anvendelse af case-baseret ræsonnement-teknik til optiske netværk med henblik på en vellykket estimering af transmissionskvaliteten i et optisk link; kognitivt kontrollerede erbium-doteret fiberforstærkere til at sikre grænser for forlæns fejlkorrektion af alle transmitterede kanaler; rekonfigurerbar kohærent softwaredefineret modtager, som understøtter forskellige modulationsformater og bithastigheder; eksperimentel evaluering af krævet optisk

signal støjforhold i fleksible elastiske optiske netværk til blandede modulationsformater; evaluering af forskellige for-filter-former til softwaredefinerede sendere til høj symbolhastighed.

Endvidere, vha. DSP på en kohærent software-defineret modtager i kombination med slagkraftige maskinlæringsmetoder er optiske overvågningsteknikker til næste generation af netværk blevet udtænkt, implementeret og testet i numeriske simuleringer og eksperimenter. Et af højdepunkterne i afhandlingen er den første demonstration af en ny modulationsformat genkendelsesmetode, som er baseret på Stokes rumparametre, og som er i stand til at skelne mellem seks forskellige komplekse modulationsformater. Desuden blev nye kromatisk dispersion overvågningsmetoder introduceret og eksperimentelt afprøvet, mens maskinlæring blev vist at kunne tackle konstellationsforvrængninger som følge af ulineariteter i langdistance fiberoptiske links.

Afslutningsvis konkluderes, at afhandlingens resultater lægger grunden til kognitive optiske netværk, og resultaterne definerer og bidrager til de teknologier, som kræves til implementering af sådanne netværk. Drift af CON-muliggjort maskinlæringsmetoder er blevet testet eksperimentelt, og DSP-baserede OPM-teknikker til softwaredefinerede modtagere er blevet introduceret og verificeret. Det præsenterede sæt af teknologier danner et fundament, hvorpå næste generation af fiberoptiske datatransmissionsnetværk vil blive bygget.

Acknowledgements

I would like to acknowledge my supervisors, Professor Idelfonso Tafur Monroy and Associate Professor Darko Zibar for their guidance and support in my professional development.

Thanks to all my great colleagues. Antonio for his immense help in my personal and scientific development. Miguel for his good spirit in our office. Valeria, Fotini and Bomin without whom long days in the lab wouldn't be the same. Neil for his motivational speeches. Martí, for being a great house mate and a colleague at the same time. Anna, for her care about mother tongue. Silvia for salsa and a rose each year. Xiaodan and Alexander for many interesting discussions at lunch time. Xema for his inspiring ideas. Molly for her American English support hotline. Mario for his readiness to explain physics to an engineer. JJ for his good advice. Jesper for sharing his knowledge of theoretical aspects of our work. Finally, thanks to always helpful Roberto, Thang, Kamau and Maisara. Thanks to Palle for his help with Danish abstract. Thanks to Xu, Jana, Ning and Yi for sharing the office in the past. Thanks to all colleagues from other research groups and the administration of DTU Fotonik.

Thanks to Júlio, Edson, Luis, Eduardo, Juliano, Carol, Ulysses, Marcelo, Victor, Anderson and the rest of the CPqD team. Thanks to all individual CHRON consortium members who made that project so successful. Thanks to all my colleagues at other departments and institutions with whom I had an opportunity to collaborate or discuss my ideas.

Thanks to all friends who supported me throughout this difficult period. Finally, I would like to thank my entire family, in particular my mother, father and aunts Basia and Jagódka, for their great support over the past six years. Thanks to Amaia, for all the good moments and help just before the finish. Thanks to Oxana for her enthusiasm at AMOR.

Finally, thanks to everyone else for whom this page was too short.

Summary of original work

Original publications included in this PhD thesis

- [A] I. Tafur Monroy, D. Zibar, N. Guerrero Gonzalez, and **R. Borkowski**, “Cognitive Heterogeneous Reconfigurable Optical Networks (CHRON): Enabling technologies and techniques,” in *International Conference on Transparent Optical Networks (ICTON)*, vol. 13. Stockholm, Sweden: IEEE, Jun. 2011, paper Th.A1.2.
- [B] I. Tafur Monroy, A. Caballero, S. Saldaña, and **R. Borkowski**, “Cognition-enabling techniques in heterogeneous and flexgrid optical communication networks [Invited],” in *SPIE Photonics West, Optical Metro Networks and Short-Haul Systems V*, W. Weiershausen, B. B. Dingel, A. K. Dutta, and A. K. Srivastava, Eds., vol. 8646. San Francisco, CA, USA: International Society for Optics and Photonics – SPIE, Dec. 2012.
- [C] A. Caballero, **R. Borkowski**, D. Zibar, and I. Tafur Monroy, “Performance monitoring techniques supporting cognitive optical networking,” in *International Conference on Transparent Optical Networks (ICTON)*, vol. 15. Cartagena, Spain: IEEE, Jun. 2013, p. Tu.B1.3.
- [D] A. Caballero, **R. Borkowski**, I. de Miguel, R. J. Durán, J. C. Aguado, N. Fernández, T. Jiménez, I. Rodríguez, D. Sánchez, R. M. Lorenzo, D. Klonidis, E. Palkopoulou, N. P. Diamantopoulos, I. Tomkos, D. Siracusa, A. Francescon, E. Salvadori, Y. Ye, J. L. Vizcaíno, F. Pittalà, A. Tymecki, and I. Tafur Monroy, “Cognitive, heterogeneous and reconfigurable optical networks: the CHRON project,” *Journal of Lightwave Technology*, vol. 32, no. 13, pp. 2308–2323, Jul. 2014.
- [E] **R. Borkowski**, A. Caballero, D. Klonidis, C. Kachris, A. Francescon, I. de Miguel, R. J. Durán, D. Zibar, I. Tomkos, and I. Tafur Monroy,

- “Advanced modulation formats in cognitive optical networks: EU project CHRON demonstration,” in *Optical Fiber Communication Conference (OFC)*. San Francisco, California: Optical Society of America, Mar. 2014, paper W3H.1.
- [F] J. R. Oliveira, A. Caballero, E. Magalhães, U. Moura, **R. Borkowski**, G. Curiel, A. Hirata, L. Carvalho, E. Porto da Silva, D. Zibar, J. Maranhão, I. Tafur Monroy, and J. Oliveira, “Demonstration of EDFA cognitive gain control via GMPLS for mixed modulation formats in heterogeneous optical networks,” in *Optical Fiber Communication Conference (OFC)*. Anaheim, CA, USA: Optical Society of America, Mar. 2013, paper OW1H.2.
- [G] **R. Borkowski**, F. Karinou, M. Angelou, V. Arlunno, D. Zibar, D. Klonidis, N. Guerrero Gonzalez, A. Caballero, I. Tomkos, and I. Tafur Monroy, “Experimental study on OSNR requirements for spectrum-flexible optical networks [Invited],” *Journal of Optical Communications and Networking*, vol. 4, no. 11, pp. B85–B93, Oct. 2012.
- [H] A. Caballero, J. C. Aguado, **R. Borkowski**, S. Saldaña, T. Jiménez, I. de Miguel, V. Arlunno, R. J. Durán, D. Zibar, J. B. Jensen, R. M. Lorenzo, E. J. Abril, and I. Tafur Monroy, “Experimental demonstration of a cognitive quality of transmission estimator for optical communication systems,” *Optics Express*, vol. 20, no. 26, pp. B64–B70, Dec. 2012.
- [I] **R. Borkowski**, L. Carvalho, E. Porto da Silva, J. C. Diniz, D. Zibar, J. Oliveira, and I. Tafur Monroy, “Experimental evaluation of prefiltering for 56 Gbaud DP-QPSK signal transmission in 75 GHz WDM grid,” *Optical Fiber Technology*, vol. 20, no. 1, pp. 39–43, Jan. 2014.
- [J] A. Caballero, N. Guerrero Gonzalez, V. Arlunno, **R. Borkowski**, T. T. Pham, R. Rodes, X. Zhang, M. B. Othman, K. Prince, X. Yu, J. B. Jensen, D. Zibar, and I. Tafur Monroy, “Reconfigurable digital coherent receiver for metro-access networks supporting mixed modulation formats and bit-rates,” *Optical Fiber Technology*, vol. 19, no. 6, pp. 638–642, Dec. 2013.
- [K] **R. Borkowski**, X. Zhang, D. Zibar, R. Younce, and I. Tafur Monroy, “Experimental demonstration of adaptive digital monitoring and compensation of chromatic dispersion for coherent DP-QPSK receiver,” *Optics Express*, vol. 19, no. 26, pp. B728–B735, Dec. 2011.

- [L] **R. Borkowski**, P. Johannisson, H. Wymeersch, V. Arlunno, A. Caballero, D. Zibar, and I. Tafur Monroy, “Experimental demonstration of the maximum likelihood-based chromatic dispersion estimator for coherent receivers,” *Optical Fiber Technology*, vol. 20, no. 2, pp. 158–162, Feb. 2014.
- [M] **R. Borkowski**, D. Zibar, A. Caballero, V. Arlunno, and I. Tafur Monroy, “Stokes space-based optical modulation format recognition for digital coherent receivers,” *IEEE Photonics Technology Letters*, vol. 25, no. 21, pp. 2129–2132, Nov. 2013.
- [N] D. Zibar, O. Winther, N. Franceschi, **R. Borkowski**, A. Caballero, V. Arlunno, M. N. Schmidt, N. Guerrero Gonzalez, B. Mao, Y. Ye, K. J. Larsen, and I. Tafur Monroy, “Nonlinear impairment compensation using expectation maximization for dispersion managed and unmanaged PDM 16-QAM transmission,” *Optics Express*, vol. 20, no. 26, pp. B181–B196, Nov. 2012.

Contributions closely related to this PhD thesis

- [e] C. Kachris, D. Klonidis, A. Francescon, D. Siracusa, E. Salvadori, R. J. Durán Barroso, I. de Miguel, **R. Borkowski**, A. Caballero, I. Tafur Monroy, Y. Ye, A. Tymecki, and I. Tomkos, “Experimental demonstration of a cognitive optical network for reduction of restoration time,” in *Optical Fiber Communication Conference*. San Francisco, California: Optical Society of America, 2014, p. W2A.28.
- [g] **R. Borkowski**, F. Karinou, M. Angelou, V. Arlunno, D. Zibar, D. Klonidis, N. Guerrero Gonzalez, A. Caballero, I. Tomkos, and I. Tafur Monroy, “Experimental demonstration of mixed formats and bit rates signal allocation for spectrum-flexible optical networking,” in *Optical Fiber Communication Conference (OFC)*. Los Angeles, CA, USA: OSA, Mar. 2012, p. OW3A.7.
- [h] A. Caballero, J. C. Aguado, **R. Borkowski**, S. Saldaña, T. Jiménez, I. de Miguel, V. Arlunno, R. J. Durán, D. Zibar, J. B. Jensen, R. M. Lorenzo, E. J. Abril, and I. Tafur Monroy, “Experimental demonstration of a cognitive quality of transmission estimator for optical communication systems,” in *European Conference on Optical Communication (ECOC)*. Los Angeles, CA, USA: OSA, Sep. 2012, p. We.2.D.3.
- [j₁] N. Guerrero Gonzalez, A. Caballero, **R. Borkowski**, V. Arlunno, T. T. Pham, R. Rodes, X. Zhang, M. B. Othman, K. Prince, X. Yu, J. B. Jensen, D. Zibar, and I. Tafur Monroy, “Reconfigurable digital coherent receiver for metro-access networks supporting mixed modulation formats and bit-rates,” in *Optical Fiber Communication Conference (OFC)*. Los Angeles, CA, USA: OSA, Mar. 2011, p. OMW7.
- [j₂] V. Arlunno, N. Guerrero Gonzalez, A. Caballero, **R. Borkowski**, T. T. Pham, R. Rodes, X. Zhang, M. B. Othman, K. Prince, X. Yu, J. B. Jensen, D. Zibar, and I. Tafur Monroy, “Reconfigurable digital coherent receiver for hybrid optical fiber/wireless metro-access networks,” in *Annual Workshop on Photonic Technologies for Access and Biophotonics*, vol. 2, Stanford, CA, USA, 2011.
- [k] **R. Borkowski**, X. Zhang, D. Zibar, R. Younce, and I. Tafur Monroy, “Experimental adaptive digital performance monitoring for optical

DP-QPSK coherent receiver,” in *European Conference on Optical Communication (ECOC)*, vol. 37. Geneva, Switzerland: OSA, Sep. 2011, p. Tu.3.K.5.

- [m] **R. Borkowski**, D. Zibar, A. Caballero, V. Arlunno, and I. Tafur Monroy, “Optical modulation format recognition in Stokes space for digital coherent receivers,” in *Optical Fiber Communication Conference (OFC)*. Anaheim, CA, USA: OSA, Mar. 2013, p. OTh3B.3.
- [n] D. Zibar, O. Winther, N. Franceschi, **R. Borkowski**, A. Caballero, V. Arlunno, M. N. Schmidt, N. Guerrero Gonzalez, B. Mao, K. J. Larsen, and I. Tafur Monroy, “Nonlinear impairment compensation using expectation maximization for PDM 16-QAM systems,” in *European Conference on Optical Communication (ECOC)*. Amsterdam, Netherlands: OSA, Sep. 2012, p. Th.1.D.2.

Remaining scientific contributions published during this PhD

- [1] V. Arlunno, **R. Borkowski**, N. Guerrero Gonzalez, A. Caballero, K. Prince, J. B. Jensen, D. Zibar, K. J. Larsen, and I. Tafur Monroy, “Radio over fiber link with adaptive order n-QAM optical phase modulated OFDM and digital coherent detection,” *Microwave and Optical Technology Letters*, vol. 53, no. 10, pp. 2245–2247, Oct. 2011.
- [2] V. Arlunno, A. Caballero, **R. Borkowski**, D. Zibar, K. J. Larsen, and I. Tafur Monroy, “Counteracting 16-QAM optical fiber transmission impairments with iterative turbo equalization,” *IEEE Photonics Technology Letters*, vol. 25, no. 21, pp. 2097–2100, Nov. 2013.
- [3] V. Arlunno, A. Caballero, **R. Borkowski**, D. Zibar, K. J. Larsen, and I. Tafur Monroy, “Turbo equalization for digital coherent receivers,” *Journal of Lightwave Technology*, vol. 32, no. 2, pp. 275–284, Jan. 2014.
- [4] L. Deng, Y. Zhao, X. Yu, V. Arlunno, **R. Borkowski**, D. Liu, and I. Tafur Monroy, “Experimental demonstration of an improved EPON architecture using OFDMA for bandwidth scalable LAN emulation,” *Optical Fiber Technology*, vol. 17, no. 6, pp. 554–557, Dec. 2011.
- [5] F. Karinou, **R. Borkowski**, D. Zibar, I. Roudas, K. G. Vlachos, and I. Tafur Monroy, “Advanced Modulation Techniques for High-Performance Computing Optical Interconnects,” *IEEE Journal of Selected Topics in Quantum Electronics*, vol. 19, no. 2, p. 3700614, Mar. 2013.
- [6] X. Pang, A. Caballero, A. Dogadaev, V. Arlunno, **R. Borkowski**, J. S. n. Pedersen, L. Deng, F. Karinou, F. Roubeau, D. Zibar, X. Yu, and I. Tafur Monroy, “100 Gbit/s hybrid optical fiber-wireless link in the W-band (75-110 GHz),” *Optics Express*, vol. 19, no. 25, pp. 24 944–24 949, Dec. 2011.
- [7] X. Pang, A. Caballero, A. Dogadaev, V. Arlunno, L. Deng, **R. Borkowski**, J. S. n. Pedersen, D. Zibar, and I. Tafur Monroy, “25 Gbit/s QPSK hybrid fiber-wireless transmission in the W-band (75-110 GHz) with remote antenna unit for in-building wireless networks,” *IEEE Photonics Journal*, vol. 4, no. 3, pp. 691–698, Jun. 2012.

-
- [8] F. Da Ros, **R. Borkowski**, D. Zibar, and C. Peucheret, "Impact of gain saturation on the parametric amplification of 16-QAM signals," in *European Conference on Optical Communication (ECOC)*. Amsterdam, Netherlands: OSA, Sep. 2012, p. We.2.A.3.
- [9] L. Deng, Y. Zhao, X. Yu, V. Arlunno, **R. Borkowski**, D. Liu, and I. Tafur Monroy, "Experimental demonstration of a bandwidth scalable LAN emulation over EPON employing OFDMA," in *Conference on Lasers and Electro-Optics (CLEO)*. Baltimore, MD, USA: OSA, May 2011, p. CThO5.
- [10] F. Karinou, **R. Borkowski**, K. Prince, I. Roudas, I. Tafur Monroy, and K. G. Vlachos, "Performance evaluation of a SOA-based rack-to-rack switch for optical interconnects exploiting NRZ-DPSK," in *European Conference on Optical Communication (ECOC)*. Amsterdam, Netherlands: OSA, Sep. 2012, p. P3.05.
- [11] F. Karinou, **R. Borkowski**, D. Zibar, I. Roudas, and I. Tafur Monroy, "Coherent 40 Gb/s SP-16QAM and 80 Gb/s PDM-16QAM in an optimal supercomputer optical switch fabric," in *Optical Fiber Communication Conference (OFC)*. Anaheim, CA, USA: OSA, Mar. 2013, p. JTh2A.77.
- [12] X. Pang, A. Caballero, L. Deng, X. Yu, **R. Borkowski**, V. Arlunno, A. Dogadaev, D. Zibar, L. F. Suhr, J. J. Vegas Olmos, and I. Tafur Monroy, "100-Gbps hybrid optical fiber-wireless transmission," in *Optoelectronics and Communications Conference (OECC)*, vol. 18, Kyoto, Japan, 2013, pp. ThP3–1.
- [13] D. Zibar, L. Carvalho, J. Estaran, E. Porto da Silva, C. Franciscangelis, V. Ribeiro, **R. Borkowski**, J. Oliveira, and I. Tafur Monroy, "Joint iterative carrier synchronization and signal detection for dual carrier 448 Gb/s PDM 16-QAM," in *European Conference on Optical Communication (ECOC)*, vol. 39. London, United Kingdom: Institution of Engineering and Technology (IET), Jan. 2013, p. P.3.18.

Contents

Abstract	iii
Resumé	v
Acknowledgements	vii
Summary of original work	ix
Original publications	ix
Closely related contributions	xii
Remaining contributions	xiv
1 Introduction	1
1.1 Motivation	1
1.2 Cognitive optical networks	2
1.3 CHRON architecture	4
1.4 Technologies enabling and supporting cognition	6
1.4.1 Flexible and elastic transmission systems	6
1.4.2 Digital and software-defined coherent receivers	8
1.4.3 Optical performance monitoring	10
1.4.4 Machine learning	12
1.5 Outline of the thesis	13
2 State of the art	15
2.1 Cognitive processes	15
2.1.1 Flexible and elastic transmission systems	15
2.1.2 Quality-of-transmission estimation	16
2.2 Software-defined elements	18
2.3 Optical performance monitoring	18
2.3.1 Chromatic dispersion monitoring and compensation	19
2.3.2 Optical modulation format recognition	21

2.3.3	Nonlinearities monitoring and compensation	22
3	Beyond state of the art	23
3.1	Cognitive optical networks and CHRON project	23
3.2	Cognitive processess	25
3.3	Software-adaptable elements	28
3.4	Optical performance monitoring	30
4	Summary	33
4.1	Conclusions	33
4.1.1	Cognitive optical networks	33
4.1.2	Cognitive processes	33
4.1.3	Software-adaptable elements	34
4.1.4	Optical performance monitoring	34
4.2	Future work	35
	Bibliography	37
	List of acronyms	49
	Paper [A]: Cognitive Heterogeneous Reconfigurable Optical Networks (CHRON): Enabling technologies and techniques	53
	Paper [B]: Cognition-enabling techniques in heterogeneous and flexgrid optical communication networks	59
	Paper [C]: Performance monitoring techniques supporting cognitive opti- cal networking	67
	Paper [D]: Cognitive, heterogeneous and reconfigurable optical networks: the CHRON project	73
	Paper [E]: Advanced modulation formats in cognitive optical networks: EU project CHRON demonstration	91
	Paper [F]: Demonstration of EDFA cognitive gain control via GMPLS for mixed modulation formats in heterogeneous optical networks	95
	Paper [G]: Experimental study on OSNR requirements for spectrum- flexible optical networks	99

Paper [H]: Experimental demonstration of a cognitive quality of transmission estimator for optical communication systems	109
Paper [I]: Experimental evaluation of prefiltering for 56 Gbaud DP-QPSK signal transmission in 75 GHz WDM grid	117
Paper [J]: Reconfigurable digital coherent receiver for metro-access networks supporting mixed modulation formats and bit-rates	123
Paper [K]: Experimental demonstration of adaptive digital monitoring and compensation of chromatic dispersion for coherent DP-QPSK receiver	129
Paper [L]: Experimental demonstration of the maximum likelihood-based chromatic dispersion estimator for coherent receivers	139
Paper [M]: Stokes space-based optical modulation format recognition for digital coherent receivers	145
Paper [N]: Nonlinear impairment compensation using expectation maximization for dispersion managed and unmanaged PDM 16-QAM transmission	151

Chapter 1

Introduction

1.1 Motivation

Cisco Visual Networking Index reports that by the end of 2015, annual global IP traffic will exceed one zettabyte (capacity equivalent to one billion modern hard disks 1 TB each) and will reach 1.4 zettabyte per annum by 2017 [1]. This growth is fueled by the explosion of Internet 'anytime, anywhere' over smartphones and tablets, Internet video, cloud services or online gaming. To sustain the need for increasing bandwidth, new transmission technologies are being actively developed [2]. In order to meet this user-driven growth, new network technologies are often deployed alongside old ones, creating very intricate, heterogeneous environments [A, B, C, D]. Moreover, this incremental increase in transmission capacity, where diverse systems share the same fiber, will further impair quality of service (QoS) of existing services and quality of transmission (QoT) of previously deployed technologies. These environments will not only be difficult to manage, but also challenging to optimize with respect to QoS parameters, such as latency, or QoT parameters, e.g. bit error rate (BER) or availability. Another factor contributing to this possible bottleneck is the lack of flexibility in conventional Internet Protocol (IP)/Multi-Protocol Label Switching (MPLS)/Ethernet networks [3]. Considering telecommunications market, operators have to remain competitive and secure their profits by utilizing their infrastructure efficiently. Their operational expenditures (OPEX) has to be minimized while users need to receive the required QoS/QoT. Taking into account the complexity of heterogeneous environments, achieving these goals simultaneously might be very difficult. Firstly, QoS/QoT is typically maintained within the frame of one service/transmission technology only, therefore local optimization may result in suboptimal performance or even unintended

disruption of coexisting services/transmissions. Secondly, the need to control multiple environments simultaneously, typically by human administrators, results in increased OPEX.

Cognitive optical networks (CONs) are trying to address these issues. The main goal behind research in CONs is to improve end-to-end performance (QoS/QoT) through an automatic learning and decision making process implemented at the network level. This will enable self-configuration, self-optimization and autonomous (unmanned) network operation. In order to support these functionalities, many assisting technologies and techniques have to be conceived and designed. This thesis first introduces CONs, which are still a novel paradigm, and subsequently technologies enabling and supporting cognition.

1.2 Cognitive optical networks

It is expected that in future optical networks, a plethora of diverse transmission technologies and services requiring varying QoS/QoT will exist side-by-side. Complexity and challenging management of this type of highly heterogeneous optical network environment [4] is the driving force for new networking paradigms, such as CONs. The foundations of cognition for data networks, have been established within the last decade. Cognitive data and computer networks were first proposed in [5] for military applications by adapting concepts previously known from cognitive radio [6]. These ideas were then crystallized further by Thomas *et al.* [7] and proved to be successful for wireless networks [8, 9].

Definition of a cognitive network, as given in the ground-laying paper [7] reads: “A cognitive network has a cognitive process that can perceive current network conditions, and then plan, decide and act on those conditions. The network can learn from these adaptations and use them to make future decisions, all while taking into account end-to-end goals”. This basic set of actions executed within a cognitive network can be represented graphically as a *cognitive loop*, as shown in Fig. 1.1. The environment, which is the state of the optical network, is observed by network monitors during the *observation* phase. The acquired information is then put into the context and analyzed with previously accumulated knowledge during the *orientation* or *planning* phase. Based on the results of the previous step, a decision is made in the *decision* phase. Both orientation and decision take into account the end-to-end goals of the system. Finally, the decision is executed in the network during the *act* phase. This cycle is continually repeated to handle new events in the environment. A

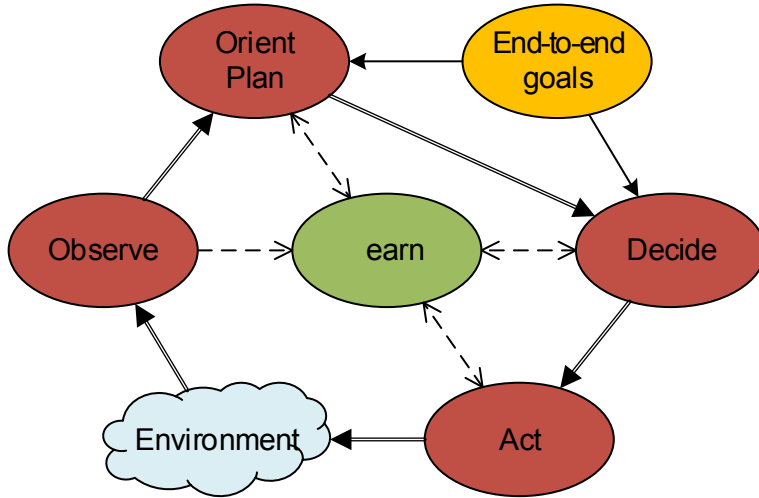


Figure 1.1: Cognitive loop [4].

cognitive network is a type of autonomic network, which is self-optimizing, self-configuring [10] and self-healing [9]. In [4], three main types of building blocks required to create a CON are listed:

- network monitors (NMons), providing the network with information about its current status – *awareness*;
- software adaptable elements (SAEs), providing the network with ability to alter its own state – *adaptivity*;
- cognitive processes, providing the network with ability to learn from the past and reuse the acquired knowledge when taking new decisions – *cognition*.

So far two holistic frameworks for cognitive networks, not targeting any specific physical layer, have been proposed: Thomas *et al.* in [7, 11, 12] and Kliazovich *et al.* [9, section 1.4]. The common denominator of these architectures is that cognitive optimization is to be performed at all network layers: from the physical layer to the application layer. Moreover, traditional network layering model is supported or replaced by a cross-layer cognition enabling full end-to-end optimization.

Centralized and distributed approaches for cognition are considered [4]. In the former case, a single node is responsible for performing the optimizations which are then communicated to other network entities through a control

plane. This approach assumes that the acquired knowledge as well as monitoring information are available in the single node implementing cognition. The latter, distributed cognition approach, delegates the optimization tasks from a central node towards layers of the network, into network nodes or even individual transceivers. This requires implementation of cognitive processes very close to the physical layer of the optical network. The drawback of this approach is the need for exchange of monitoring information across all cognitive elements in the network.

General cognitive network frameworks were later refined and brought into the optical networking domain to become foundations of cognitive optical networks. This led to three proposed architectures. Zervas and Simeonidou devised COGNITION architecture [13], which follows ideas outlined by Thomas *et al.* In this model, cognition is performed per element and per layer and supported by cross-layer optimization. Wei *et al.* in [3] proposes software-defined CON architecture where not only control and management plane but also transport plane is software-defined. Finally, as a result of a European project, Cognitive Heterogeneous Reconfigurable Optical Network (CHRON) architecture has been put forward [14].

1.3 CHRON architecture

In this section we will shortly review the architecture of a particular implementation of a CON, developed within CHRON project. More details can be found in [D, 4, 15, 16, 17]. The project, funded by the European's Seventh Framework Programme lasted from July 2010 until October 2013. The main goal was to develop a CON architecture, which “addresses the challenge of controlling and managing the next generation of heterogeneous optical networks supporting the Future Internet” [14]. The consortium was composed by three partners from academia and four (later three) partners from the industry. It should be noted that the work carried throughout this PhD project was embedded within the framework of this project.

The CHRON architecture is the only one that has been experimentally investigated and whose testbed has been physically created. The project studied both distributed and centralized variant of the architecture, focusing on the latter one for testbed realization. The overview of the CHRON centralized architecture is shown in Fig. 1.2. The core of the architecture is constituted by the cognitive decision system (CDS) which is responsible for managing traffic demands and network events. This element also implements the cognitive behavior, i.e. optimizes network performance by considering its current state

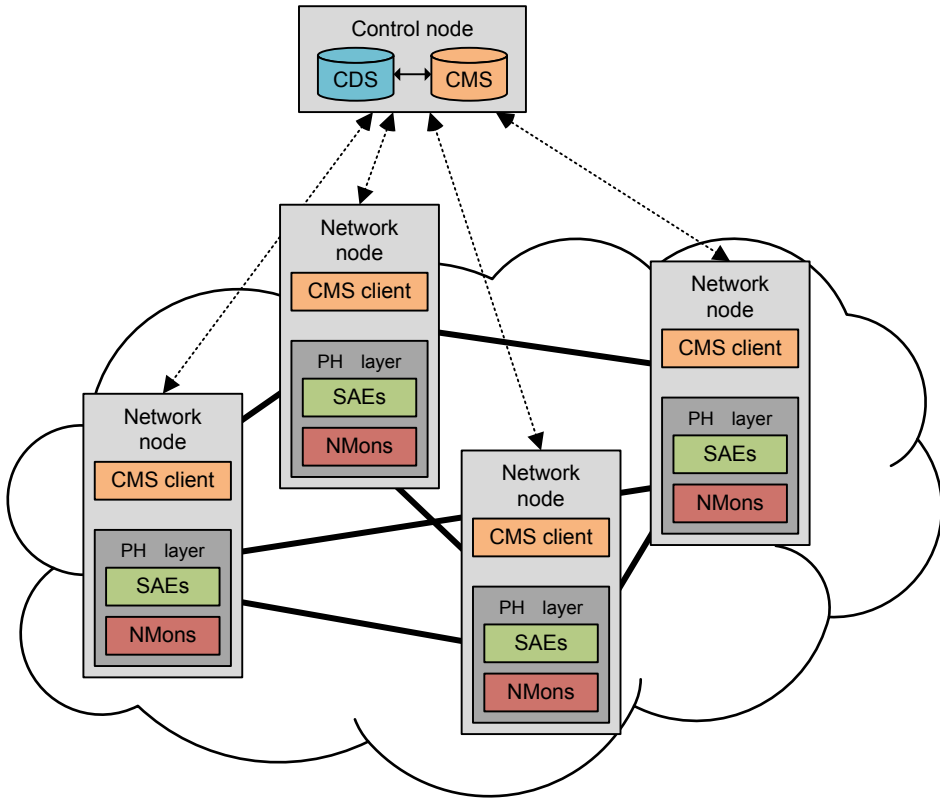


Figure 1.2: Centralized CHRON architecture [D].

and past knowledge. CDS is aided by control and management system (CMS), which is responsible for collecting monitoring information from the network as well as disseminating decisions made by CDS to all nodes. Network monitoring is performed by the network monitoring system (NMS), and specifically by the network monitors (NMons), which provide traffic monitoring information from the network layer as well as optical signal parameters – optical performance monitoring – from the physical layer (cross-layer design). software adaptable elements (SAEs) are controlled via the CDSs in order to reconfigure the network as to e.g. handle traffic requests or optimize operation.

The relation between the recently booming software-defined networking (SDN) and its relation to CONs has to be brought to the attention of the reader. SDN is an emerging concept, in which data and control planes are separated, and moreover, data plane is abstracted and presented to external software controllers. [18]. In other words, the switching fabric can be controlled in a simpli-

fied manner even in multi-vendor hardware environments through standardized software interfaces. The control architecture of SDN allows for centralized network management without having to control all devices individually. On the other hand, the most important ingredient in CON is the cognition itself, and resulting from it end-to-end optimization. CHRON implementation of CON has chosen an architecture based on GMPLS protocol extensions [19]. Cognition is yet another level that builds on top of the standard control architecture, be it Generalized Multi-Protocol Label Switching (GMPLS) (as in CHRON) or SDN. Therefore, it should be viewed as providing unsupervised optimization functionality for, rather than a replacement of, already existing control plane. For that reason, technologies and techniques supporting cognition are equally necessary for CON implementations with any underlying control plane.

1.4 Technologies enabling and supporting cognition

Regardless of CON implementation, three fundamental pillars upon which every CONs is built can be distinguished. Those ingredients are listed in section 1.2 and represented in Fig. 1.3. Subdivision into specific technologies (non-exhaustive) and their mutual relations are also indicated in the figure, along with areas in which this thesis contributes (marked by an asterisk *).

First, software adaptability is achieved by the use of SAEs, such as software-defined receiver (SDR) or software-defined optics. This is further treated in sections 1.4.1 and 1.4.2, respectively.

Secondly, performance monitoring is performed both at the network and physical layer. Network monitoring, including parameters such as latency, traffic load or availability, is not considered in this work. At the physical layer, optical performance monitoring (OPM), described in sections 1.4.3 and 1.4.4 is performed.

Thirdly, cognitive processes are supported by machine learning (ML) algorithms in order to implement intelligence in the network. This is described in section 1.4.4.

1.4.1 Flexible and elastic transmission systems

One of the important technologies allowing the network to perform self-optimization is spectrum flexibility and bandwidth elasticity. Spectrum flexibility tackles the problem of a rigid subdivision of the available transmission window into fixed central frequencies at which channels can be located. Band-

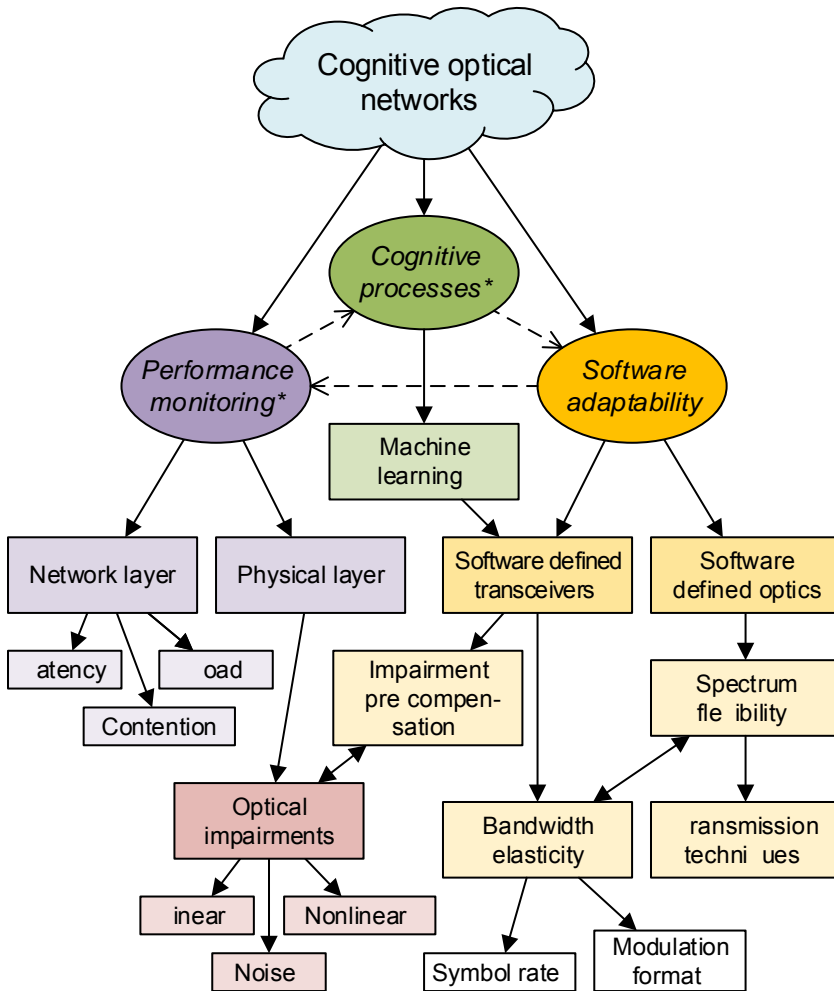


Figure 1.3: Building blocks of a cognitive network and their mutual relations. Asterisk * indicates areas in which this thesis contributes.

width elasticity allows for variable capacity channels, which may increase or decrease their maximum throughput either by changing the symbol rate or modulation (this functionality requires reconfigurable transmitter/receiver pair, described in section 1.4.2). Both concepts are very closely related and allow for fine grained control in the transmission capacity driven by actual user demand. Standard fixed grid scheme [20] may lead to severe underutilization of the available capacity, and as a result, low spectral efficiency (SE). The reason is that the actual spectral occupancy of a channel, required for post-forward error correction (post-FEC) error-free transmission is considerably smaller than the width of the grid slot used (typically 50 GHz for commercial systems). One idea is to abandon fixed grid, as defined by ITU's Telecommunication Standardization Sector (ITU-T) and allow for arbitrary spectral allocation of channels. Although this solution addresses low SE in individual point-to-point links, it may result in new challenges. First, legacy equipment will no longer be compatible with this new model and certain network elements, such as reconfigurable optical add-drop multiplexers (ROADMs), will have to be replaced. Secondly, arbitrary channel assignment with variable bandwidths may severely contribute to increased blocking rate in transparent optical transport networks (OTNs). Therefore the next evolutionary step might be to use narrower grid, such as 25 GHz or use a flexible dense wavelength division multiplexing (DWDM) grid, as specified in [20], where spectrum is allocated in multiples of 12.5 GHz, with central frequencies spaced at 6.25 GHz. Finer control over spectrum allocation and channel bandwidth give CONs additional degree of freedom for optimization. It results not only in increased SE but potentially allows for energy savings by dynamically scaling the network capacity to follow daily traffic patterns. In [G], we perform an experimental assessment of required optical signal-to-noise ratio (ROSNR) required for transmission in symbol-rate spaced grids, where mixed modulation formats, such as quaternary phase shift keying (QPSK) and 16-quadrature amplitude modulation (QAM) are used.

1.4.2 Digital and software-defined coherent receivers

The revival of coherent detection [21] was driven by the increasing need for capacity. Advancements within the field of electronics allowed to realize receivers for coherent detection without phase locked loops (PLLs) [22]. Since the full optical field information (amplitude and phase) is available at the receiver, coherent detection allows for transmission systems with significantly higher SEs. In current digital coherent receivers (DCRs), the signal is first digitized by an analog-to-digital converter (ADC) at or above the Nyquist rate and

the intermediate frequency offset of the free-running local oscillator (LO) is afterwards compensated with a carrier recovery digital signal processing (DSP) algorithm [23, 24], inside a highly parallelized application-specific integrated circuit (ASIC) or field-programmable gate array (FPGA) architecture [25]. Additionally, the presence of a specialized signal processor on the receiver board made possible the implementation of advanced functionalities for OPM and impairment mitigation described in section 1.4.3. The concept of SDR, inherited from the cognitive radio, goes one step further than DCR. The SDR can dynamically reconfigure to receive any modulation format, as the DSP algorithms in the receiver can be modified on demand, e.g. by firmware changes or FPGA reconfiguration. Having both amplitude and phase of the optical field linearly mapped into an electrical domain, SDR can then receive an arbitrary modulation formats. In the ideal case, the only limiting factor for an SDR is the electrical front-end: ADC sampling rate, bandwidth and effective number of bits, transimpedance amplifier (TIA) bandwidth and linearity as well as serial output interface clock speed. Some of the commercially available SDRs implement partial flexibility, where e.g. the modulation can be chosen from a set of two or three alternatives. In paper [J], we experimentally demonstrate an SDR capable of receiving four different modulation formats, and receive four different types of signals after deployed fiber link transmission.

The counterpart of an SDR is a software defined transmitter (SDT). On the transmission side, the processing performed in the digital domain includes digital signal modulation, in place of a dedicated electrical circuit, or digital pulse shaping, replacing conventional fixed analog low pass filter (LPF). The output signal is then synthesized using a digital-to-analog converter (DAC) and fed directly to an optical in-phase/quadrature (I/Q) modulator.

Another important aspect connected with both software-defined paradigm and spectrum flexibility, is programmable optics. Programmable optical elements in the physical layer of the optical network, such as filters or ROADMs enable fine control and management over optical spectrum through a software interface. In paper [I] a programmable optical filter is employed in order to optimize transmission performance of 56 Gbaud polarization division multiplexing (PDM)-QPSK signal.

In short, SDRs offer an important benefit for CONs as they enable both: bandwidth elasticity, either by modulation format or symbol rate adjustment; and ability to implement advanced OPM. By adding programmable optics, full spectrum flexibility can be achieved, which transforms formerly static network into a highly dynamic and reconfigurable environment, autonomously managed by ML-based cognitive control layer.

1.4.3 Optical performance monitoring

Optical performance monitoring (OPM) is a term used to denote a set of techniques used to characterize the quality of optical signals. As the DCRs are now well commercially established, many of the OPM methods are now routinely implemented inside receivers' DSP. Listed are the impairments that are of interest for OPM, categorized according to the place of origin.

- Transmitter:
 - I/Q imbalance,
 - electrical distortions (e.g. saturation, jitter, inter-symbol interference (ISI)),
 - electrical signal-to-noise ratio (SNR),
 - transmitter laser phase noise wavelength drift.
- Optical link:
 - amplified spontaneous emission (ASE) noise,
 - chromatic dispersion (CD),
 - polarization mode dispersion (PMD),
 - polarization dependent loss (PDL),
 - inter-carrier interference (ICI) due to wavelength division multiplexing (WDM) co-propagation,
 - nonlinear noise due to fiber Kerr nonlinearities: four-wave mixing (FWM), self-phase modulation (SPM) or cross phase modulation (XPM) [26].
- Receiver:
 - timing misalignment,
 - local oscillator (LO) phase noise and offset,
 - input state of polarization (SOP).
 - electrical SNR (shot noise)

The ability to monitor the signal is beneficial for optical networks, as it enables the network impairment mitigation, optimization and fault prediction [27]. At the same time, it is required by CONs as it provides feedback regarding signal quality enabling the self-optimization of the network.

Literature distinguishes between data-aided (DA) and blind/non-data-aided (NDA) parameter monitoring [C, 28]. These methods are compared in Table 1.1. The former uses specialized training sequences sent by the transmitter, dedicated optical supervisory channels (OSCs) or frequency pilot tones. In heterogeneous environment, where devices from different vendors coexist, implementation of vendor-specific DA OPM techniques would effectively ban any transmissions between equipment built by different vendors. This problem could be overcome by industrial standardization efforts. Nonetheless, this option is not currently feasible, which necessitates the development of NDA monitoring methods that can perform OPM from the received data.

One of the most crucial NDA compensation algorithms included in most DCRs is CD compensation, which removes the need for link dispersion management. The length of CD impulse response (IR) depends on the fiber length, but already for a transmission over the typical span length (80 km), the time domain equalizer (TDE) adapted by constant modulus algorithm (CMA)/multi-modulus algorithm (MMA) algorithm will not converge unless pre-convergence is applied. Moreover, the number of taps in the TDE required to compensate this amount of CD would exceed 34 per each traversed span at a symbol rate of 28 Gbaud [29]. In order to avoid convergence or overfitting issues, as well as to reduce receiver complexity and power dissipation, the typical number of taps in the TDE does not exceed 21. Bulk of dispersion is compensated in a frequency domain equalizer (FDE), whose complexity scaling is much more favorable than TDE [30].

Even though CD does not significantly fluctuate in time, the ability to rapidly deploy a new link (plug and play), dynamics of network connection, as well as reconfiguration with the purpose of cognitive-driven end-to-end optimization, renders CD monitoring an important feature. CD-induced ISI makes dispersion virtually indistinguishable from noise, unless compensated

	Data-aided	Non data-aided
Pros	<ul style="list-style-type: none"> • High accuracy • Guaranteed convergence • Fast convergence speed 	<ul style="list-style-type: none"> • No bandwidth overhead • Compatible with legacy transmitters • Efficient for short IR
Cons	<ul style="list-style-type: none"> • Bandwidth overhead • No compatibility /standardization 	<ul style="list-style-type: none"> • Inferior accuracy • No convergence for long IR • Slow convergence speed

Table 1.1: Comparison of DA and NDA OPM methods [C].

near perfectly. For that reason, estimation of dispersion cannot be performed using standard optimization algorithms, such as gradient descent. Instead, *sweeping algorithms* are used, where the signal is first compensated and afterwards a metric indicating correct compensation is evaluated. This operation is repeated for every value from the set of possible CD values affecting the signal (spaced by 200-500 ps/nm). After the initial scan is finished, the value of CD indicated by the metric is chosen. Afterwards, the sweep is repeated again, in finer steps (down to 10 ps/nm) around the previously found value, in order to increase estimation accuracy. To take account of residual dispersion, which might be caused by either non-perfect CD estimate given to the FDE or by time-dependent effects, such as CD temperature dependence, the residual dispersion is always cancelled in the subsequent TDE. The quality of the signal after FDE is typically good enough to allow for CMA/MMA operation. Papers [K, L] present CD monitoring algorithms working according to the described principle.

1.4.4 Machine learning

As mentioned earlier, the basic principle of CON is that intelligence, introduced by machine learning (ML) algorithms, is present in the network. These ML algorithms can be implemented at two different levels. First, as techniques enabling the network to learn, orient, decide, and act (c.f. Fig. 1.1). For instance, ML method called case-based reasoning (CBR) is used in [H] to enable the network to use the past experience (in this particular case, a specific configuration of channels and their parameters in an optical link) to subsequently predict the expected QoT of the new connections. By maintaining a knowledge base (KB) containing past network observations, the CDS of a CON can extrapolate from the set of known cases and autonomously derive new empirical rules or exploit data patterns to perform optimization accordingly. This functionality is demonstrated in paper [E], where the QoT (BER) is estimated in intermediate nodes by fitting parameters to a simple model, only knowing BER back-to-back and at the final node. Another use of KB is exploited in paper [F], where gain flatness and noise figures of erbium-doped fiber amplifiers (EDFAs) in a link are autonomously adjusted in order to ensure successful reception of all transmitted channels in a heterogeneous network with different modulation formats and bit rates.

Secondly, ML can be exploited in advanced OPM methods to enable SDRs to perform adaptive adjustment of their algorithms or impairment mitigation schemes. One interesting OPM algorithm exploiting signal statistic through ML is modulation format recognition (MFR). The concept behind MFR is

to automatically discover the modulation format of a received signal without prior knowledge. Once the modulation format is identified, this information is used by the subsequent blocks of the SDR in order to optimize the DSP chain for this particular modulation format. This is especially important for modulation format-opaque (dependent) subsystems, such as digital demodulation, but also for equalizer, which can be switched to decision-directed mode if the received signal constellation is known. In general, instead of using generic, modulation format independent algorithms whose performance might be inferior, their fine-tuned modulation format-specific versions might be used instead to improve receiver performance and thus QoT. Desired qualities of an automatic MFR is insensitivity to impairments and early placement in the DSP chain, to enable modulation format-specific algorithms as early as possible. Another important application of MFR could be in stand-alone MFR monitors, independent of, and cheaper than DCRs. For networks, where the latency of the control plane is significant compared to the data plane (e.g. distributed CONs) or where the control plane overhead is large (e.g. networks where connections are established and torn down at a fast rate), MFR becomes an essential part of a SDR. This functionality may also be seen as a method to enable optical burst switching (OBS) or optical packet switching (OPS) [31], where the per-packet or per-burst modulation format can vary. In [M], a novel MFR algorithm for PDM signals based on Stokes space parameters and variational Bayesian expectation maximization (VBEM) ML method is demonstrated. The underlying principle makes the method insensitive to polarization mixing and carrier frequency offset and can be implemented in any receiver capable of measurement of Stokes parameters. ML can also be used to take advantage of correlations and statistical properties of the signal after passing through the fiber in order to provide accurate estimates/compensation of impairments, such as fiber Kerr nonlinearities or phase noise. In paper [N], influence of those impairments can be monitored and taken account for with the expectation maximization (EM) method (cf. section 3.4, paper [N]).

1.5 Outline of the thesis

This work is divided into three chapters as follows. Chapter 1 provided an introduction to the research carried out throughout this thesis and their context. Section 1.2 gives a brief introduction into the topic of CONs, with particular emphasis on CHRON implementation (section 1.3). Section 1.4 describes the technologies required and supporting cognitive optical networking. Chapter 2 reports on the current state of the art in three key areas supporting CONs:

cognitive network processes in section 2.1, software adaptable elements in section 2.2 and DSP techniques for optical performance monitoring in section 2.3. Chapter 3 describes the novelty behind each of the papers included in this thesis and outlines authors' personal contribution. These research papers, constituting core of this work, are reprinted starting from page 53. The thesis is concluded by chapter 4, which summarizes the main achievements and impact of the presented work in section 4.1. This is followed by an outlook on future prospects of cognitive optical networking in section 4.2.

Chapter 2

State of the art

The topic of cognitive optical networks (CONs) is cross-disciplinary and covers many subareas: from the research on optical networks through machine learning (ML) methods, down to novel receiver concepts and advanced optical performance monitoring (OPM) methods based on digital signal processing (DSP). In this chapter, state of the art analysis of each of the fundamental ingredients necessary for realizing a CON (as listed in section 1.4) is presented. Firstly, in section 2.1 an overview of the current status in implementation of cognitive and autonomous techniques is presented. Secondly, software-defined elements in the network are covered in section 2.2. Finally, in section 2.3, the focus is shifted towards functionalities enabling cognition at the physical layer of the network through DSP-assisted OPM techniques.

2.1 Cognitive processes

A current state in CON architectures was already reviewed in section 1.2. This chapter provides a further overview, with emphasis on demonstrations of autonomous or CON testbeds using policy-based or ML-supported adaptations. The topic of CON is new to optical communication, which is reflected by the sparse literature. For that reason, experiments involving autonomous networks are also included. The main difference between the two is the fact that in the latter, decisions are taken based on policies rather than learning processes [4].

2.1.1 Flexible and elastic transmission systems

The first experimental demonstration of flexible spectrum network with real-time control plane operation was shown by Geisler *et al.* [32]. The goal of

this network testbed was to maintain quality of service (QoS) and high spectral efficiency. A low speed optical supervisory channel (OSC) was used for real-time impairment detection, where the bit error rate (BER) of the OSC was correlated with the expected BER of the transmitted signals. The physical layer supported switching between binary phase shift keying (BPSK), quaternary phase shift keying (QPSK) and 8-phase shift keying (PSK) modulation formats. Next, demonstration by Cugini *et al.* [33] introduced a flexible network architecture based on path computation element (PCE) with Generalized Multi-Protocol Label Switching (GMPLS) control plane. Two scenarios are considered. First, lightpath establishment, where the best possible, in terms of spectral efficiency (SE), modulation format – either 100 Gbit/s polarization division multiplexing (PDM)-16-quadrature amplitude modulation (QAM) or 100 Gbit/s PDM-QPSK – is chosen to establish a new lightpath, given the path optical signal-to-noise ratio (OSNR). Second, restoration, where the working path with 200 Gbit/s PDM-16-QAM has double the capacity of the backup path, routed through a distinct set of nodes. Liu *et al.* [34] also presents an architecture based on PCE, controlled by OpenFlow. Here, the modulation format is switched among BPSK, QPSK, 8-QAM and 16-QAM.

The papers included in this thesis, present following novel work expanding upon this prior art. The CHRON project introduces paper [E] accompanied by [e], originating from the same experiment, presenting for the first time an operational CON testbed with advanced modulation formats, where PDM-16-QAM channel is replaced by two PDM-QPSK channels to maintain capacity and quality of transmission (QoT). Moreover, a demonstration of erbium-doped fiber amplifiers (EDFAs) controlled by a GMPLS control plane in order to enable simultaneous transmission of channels with four different modulation formats is presented in [F].

2.1.2 Quality-of-transmission estimation

Transmission performance predictions in long-haul flexible elastic optical networks are difficult due to the multitude of different effects acting upon signals (cf. section 1.4.3). One way of performance forecasting in this nonlinear transmission regime is by computationally expensive and time consuming simulations. This is not a feasible solution for on-line performance prediction in a CON, where within milliseconds performance estimation of many possible paths has to be considered in order to select the one fulfilling QoT requirement. In order to reduce the complexity, analytical models and approximations for performance prediction, in particular formulas for scaling of nonlinear noise

with channel spacing, symbol rate and transmission distance are an active area of research.

In [35], it is shown that in dispersion uncompensated links, noise inflicted on the constellation due to fiber Kerr nonlinearity has a normal distribution for dense wavelength division multiplexing (DWDM) at symbol rate spacing and PDM-QPSK modulation format. The extended analysis in [36] introduces Gaussian noise (GN) model, described in details in [37], and shows that the nonlinear noise normality holds also for channel spacing exceeding the baud rate. Moreover, required optical signal-to-noise ratio (ROSNR) for transmission using PDM- BPSK, QPSK, 8-, and 16-QAM modulation formats is obtained. Similar conclusion is obtained in [38, 39] for coherent optical (CO)-orthogonal frequency division multiplexing (OFDM) with guard bands using QPSK and 16-QAM PDM transmission. In [40], the normality of nonlinear noise is confirmed. Paper [41], analyzes superchannel transmission with PDM modulation formats: BPSK, QPSK, 8- and 16-QAM and reports on required OSNR limits for superchannel transmission obtained by simulation. The CHRON project consortium created a *QoT Tool* to estimate performance of advanced modulation formats transmitted over uncompensated optical links. The tool, based on the GN model, is validated in [42]. Included in this thesis paper [G], reports on experimental investigation of ROSNR limits for QPSK and 16-QAM superchannels when transmitted in diverse configurations.

Another way of QoT performance estimation is through ML methods. This approach is particularly well suited for CONs for two reasons. First, the analytical approximations are derived for simplified cases, where all transmitted channels (or superchannel subcarriers) have the same parameters: modulation format, symbol rate, channel spacing, etc. This assumption does not hold for heterogeneous networks, where many different technologies and services co-exist and transmit at the same time (such as in [J]). Secondly, analytical estimations do not take into account the performance of actual transmitter-receiver pair, their DSP quality or impairment compensation limits. Therefore different methods have to be considered for those complex scenarios. Knowledge base (KB) of a CON in connection with machine learning methods, in particular case-based reasoning (CBR), can address this challenge by successive on-line learning from a working transmission systems and reuse of past observations [43]. First connection are established blindly. Then, on any subsequent connection attempt, similar connection cases are retrieved from the knowledge base (KB). This information is then reused to estimate the expected performance of new connection. This thesis reports in [H] on the experimental investigation of this method for QoT estimation.

2.2 Software-defined elements

As argued in sections 1.4.1 and 1.4.2, spectrum flexibility and bandwidth elasticity is one of the important concepts supporting CONs. The former was covered in the previous section, along with demonstrations of autonomous networking. Here, a short overview of current research efforts in the latter area is given, including software-defined receivers and transmitters.

The group at Heinrich Hertz Institute (HHI) demonstrated a 32 Gbaud field-programmable gate array (FPGA) transmitter capable of BPSK, QPSK and 16-QAM generation [44]. Researchers from Karlsruhe Institute of Technology, also developed a 28 Gbaud FPGA-based transmitter capable of generating eight different modulation formats at 28 Gbaud: 4- and 6-pulse amplitude modulation (PAM), 2-, 4- and 8-PSK, 16-, 32- and 64-QAM [45]. Later on, the same group presented a real-time OFDM transmitter [46] based on the same software-defined platform. KDDI R&D Laboratories presented their re-configurable transmitter supporting BPSK, QPSK, 8-, and 16-QAM [47]. [48] 2-, 4-, and 8-PSK. Also programmable optics is used to help improve signal quality at the output of high symbol rate systems, where use of software-defined transmitters is not yet feasible due to limitations of digital-to-analog converter (DAC) speeds. In [I] and [49] a programmable optical filter (equalizer) is used at the transmitter to improve BER by pulse shaping in optical domain for, respectively, 56 and 80 Gbaud systems.

Some of these technologies are already available commercially. For instance An optical multi-format transmitter capable of up to 34 Gbaud operation with on-off keying (OOK), QPSK, 8-PSK and 16-QAM modulation formats is available from HHI [50]. Ciena announced availability of coherent transmission chip WaveLogic 3 in 2012 [51, 52], while ClariPhy released LightSpeed-II family of integrated silicon-on-chip circuits in 2014 [53]. Both platforms support PDM formats: BPSK (for submarine applications), QPSK and 16-QAM in order to achieve 400 Gbit/s transport capacity. Finisar's WaveShaper, which is a programmable optical processors, enabling arbitrary spectral shaping has been available already starting from 2010 [54].

Regarding the receiver side, [J] presents a software-defined receiver (SDR) integrating demodulation capabilities for four different modulation formats.

2.3 Optical performance monitoring

Starting from 2004 [21, 22], DSP processing became a default part of a digital coherent receiver (DCR). A multitude of diverse algorithms dealing with all

conventional receiver subsystems were implemented in DSP, including: timing recovery, equalization, polarization demultiplexing and carrier recovery [55]. Many of them were directly adapted from digital wireless or wired data transmission systems, while some, particularly optical impairment monitoring and compensation (optical performance monitoring), were conceived specifically for fiber-optic communication to face the challenges posed by highly dispersive and nonlinear channel. OPM functionalities come almost for free, as DSP is present in the receiver regardless. This chapter presents selected OPM techniques, which were investigated in this thesis.

2.3.1 Chromatic dispersion monitoring and compensation

Many conventional techniques for chromatic dispersion (CD) monitoring have an upper limit on measurable CD value, and thus lost its importance with the introduction of uncompensated links, coherent detection and DSP-enabled receiver [27]. Even advanced direct detection methods, utilizing ML such as eye diagram monitoring using support vector machines [56] or artificial neural networks (ANN) [57], as well as phase portrait monitoring [58, 59] are no longer applicable. The reason is that dispersion maps and accurate dispersion matching prior to the receiver is no longer necessary, whereas already dispersion of a single 80 km standard single-mode fiber (SSMF) span with 17 ps/nm/km at a typical symbol rate of 28 Gbaud closes the eye very efficiently.

Digital chromatic dispersion compensation comes almost at no cost at the DCR and can, in principle, compensate arbitrary amount of CD. For that reason blind monitoring and compensation in receiver's DSP has been investigated thoroughly starting with the work of Savory [29]. The paper presents a method for CD compensation by using a time domain equalizer (TDE) – a finite impulse response (FIR) filter adapted by a constant modulus algorithm (CMA). To guarantee convergence, filter taps were preinitialized in order to speed up CMA convergence. A method for CD monitoring by extracting information from filter taps, which is essentially an inverse operation to taps preinitialization, has been demonstrated in [60]. Since CD transfer function has one degree of freedom proportional to the fiber length, affecting CD values were found by applying a quadratic fit onto the phase of an FIR filter taps. As mentioned in section 1.4.3, due to very long CD impulse response (IR), implementation of such long TDE is infeasible in hardware. To address this issue, a dedicated frequency domain equalizer (FDE) for CD compensation was proposed in [61]. Thanks to the use of fast Fourier transform (FFT), equalization process changes from convolution in time domain (TD) to multiplication in frequency domain (FD), and thus significantly reduces complexity and im-

proves scaling properties [61, 62, 63]. In [30, 62], FDE adapted by sweeping algorithms was used, where the space of possible CD values is explored in steps, and for each a metric value is computed. The metric is used to indicate how accurately dispersion was mitigated and starts to show distinctive feature (minimum) only in the vicinity of value providing correct compensation, when optical eye starts to open. This sweeping algorithm was looking at the TD samples after the FDE equalizer. In this configuration, the TDE is still used following the FDE, however its main function now is to compensate residual CD (originating from imperfect CD compensation in the FDE) and polarization mode dispersion (PMD) as well as polarization demultiplexing. The two stage FDE-TDE equalization (or its variation) is used in virtually all experiments reporting uncompensated link transmission [64], and has been incorporated in commercial line cards for terrestrial and undersea transmission. The FDE is adapted with a sweeping algorithm, while TDE is adapted with a conventional equalization algorithm.

The literature reports on a variety of different sweeping algorithms for dispersion monitoring, working either with TD signal after FDE or FD samples before inverse FFT. The difference between them is in the definition and computation of the metric used to adapt the FDE. A variant of CMA, which penalizes deviation of samples from a constant power is used in [30], and a simplified version of this algorithm is reported [K]. Due to an assumption about constant signal power, those methods are not very general and may not behave well for modulation formats with more than one level of intensity, although operation with 16-QAM is reported in [30]. Moreover, in [K], a novel method based on channel eigenvalue spread is reported and experimentally verified. Measurement of coherent signal at four frequencies, able to estimate up to 3000 ps/nm is reported in [65]. Autocorrelation of signal power waveform from TD signal was used in [66, 67, 68, 69] and the upper estimation limit depends on the signal memory length. Related to it, clock tone search methods, implemented in FD are used in [70, 71, 72]. Delay-tap sampling [58] is used in [73, 74], while Gardner time error detector variance in [75]. A measurement of the width of a notch in a spectrum of the modulus squared of the transmitted signal is used in [76]. Recently, an improvement to sweeping algorithm has been demonstrated, where the sweep and metric calculation is simplified and performed automatically when computing FFT on the autocorrelation of discrete spectrum [77]. Typically, PMD will be a challenge to overcome for many methods. A method based on maximum likelihood estimation (MLE) of CD parameter, insensitive to PMD and modulation format was presented in [78]. Its experimental validation in [L] have shown robustness against PMD and

good estimation accuracy for both QPSK and 16-QAM modulation formats. Finally, simple methods based on peak-to-average power ratio [79] or small signal values [80] which work for channel spacing less than symbol rate have been presented, and an improved version of the latter, insensitive to all-order PMD [81].

2.3.2 Optical modulation format recognition

Techniques for optical modulation format recognition (MFR), also known as modulation format identification (MFI) or modulation format detection (MFD), is under development. In section 1.4.4 motivation for introducing MFR into receivers was given.

First MFR method for fiber-optic transmission was presented in [82] and its applicability for CONs was subsequently argued in [A]. It uses ML technique known as k -means and tests the likelihood of hypothesis that the received constellation diagram contains 4, 8 or 16 clusters and thus represents one of the possible modulation formats: QPSK, 8-PSK, 16-QAM. This method was used for single polarization radio-over-fiber (RoF) system, where the actual signal information is carried in the phase of the transmitted signal, does not undergo severe distortion. In a typical coherent optical transmission system with amplitude and/or phase modulation, this method will not work due to the need for modulation-specific algorithms for impairment equalization, most notably decision-directed equalization. Therefore other methods, such as ANN-based MFR based on direct detection amplitude histograms [83] demonstrated in [84]. A good estimation accuracy, exceeding 99% successful classification attempts was achieved for all modulation formats under consideration: OOK, non-return-to-zero (NRZ) differential BPSK, duobinary, return-to-zero (RZ)-QPSK, PDM-RZ-QPSK and PDM-RZ-16-QAM. Due to the use of ANN a previous neural network training is required to obtain correct classification results. Another method, based on Stokes space parameters and a ML technique known as variational Bayesian expectation maximization (VBEM) was used in [M]. The method relies on the fact that each complex modulation format, when represented in Stokes space, forms a set of points within a lens-like object [85] and their number depends on the modulation format. The Stokes parameters of the received signal are calculated and the number of points forming the Stokes space data is counted with VBEM, which fits 3-dimensional Gaussian mixture model (GMM) into the data and successively reduces the number of mixture components until convergence is achieved. The method is insensitive to polarization multiplexing and carrier frequency due to properties of Stokes transformation. Successful differentiation between various PDM formats is

presented: 2-, 4-, 8-PSK and 8-, 12-, 16-QAM. Another method based on high-order cumulants of the received signal is presented in [86]. By appropriate choice of cumulants and their threshold values, a branching decision tree for MFR was created. Hybrid method based on Stokes space assisted by high-order cumulants was subsequently presented in [87, 88]. Finally, a method based on simple intensity histogram of a signal, requiring polarization demultiplexing and approximate knowledge of OSNR was presented in [89].

2.3.3 Nonlinearities monitoring and compensation

Optical nonlinear compensation methods, such as phase conjugation [90] or new twin waves [34] have been recently presented to mitigate nonlinearities. Nonetheless, the use of DSP-based methods remain active field of research. Techniques based on Volterra kernels [91, 92], channel inversion using digital backpropagation (DBP) [93, 94] and MLE of the transmitted sequence [95, 96, 97]. Even though DBP is considered to be a universal solution for joint mitigation of linear and nonlinear impairments [98], it does not take account of amplified spontaneous emission (ASE) noise, and cannot be used for channel monitoring, as, in order to invert the channel, exact parameters of the fiber are required in advance. On the other hand, MLE was only demonstrated with negligible values of CD, where channel memory and thus inter-symbol interference (ISI) is small. Paper [N] demonstrates a different approach, where the influence of nonlinear impairments, such as self-phase modulation [99] can be monitored from signal statistics using ML technique of expectation maximization (EM). The influence of nonlinear impairments on the BER is then minimized by optimizing decision boundaries of the received constellation.

Chapter 3

Beyond state of the art

The thesis is based on a number of articles already published or submitted for publication in peer-reviewed journals and conference proceedings. This chapter states the main contribution and novelty of each of the included papers as well as defines author's input.

The papers are organized in four following categories, following the division made in the previous chapter as well as the one outlined in Fig. 1.3. Firstly, section 3.1 includes papers [A, B, C, D] which acquaint the reader with the topic of cognitive optical networks (CONs), introduce the framework of the European project CHRON and review enabling technologies. Secondly, section 3.2 presents papers [E, F, G, H] containing results on network demonstrations and transmission experiments involving the use of cognitive techniques. Thirdly, section 3.3 outlines the work in the direction of transmitter and receiver flexibility and software-adaptability [I, J]. Finally, section 3.4 narrows down the focus, and presents novel digital signal processing (DSP) subsystem for digital coherent receivers implementing advanced optical performance monitoring (OPM): chromatic dispersion (CD) monitoring in [K, L], modulation format recognition (MFR) [M], and nonlinear effects monitoring and compensation [N].

3.1 Cognitive optical networks and CHRON project

Paper [A]: Cognitive Heterogeneous Reconfigurable Optical Networks (CHRON): Enabling technologies and techniques

This paper, presented at the *13th International Conference on Transparent Optical Networks (ICTON)* (2011), lays the groundwork for any further paper de-

scribing cognition in the context of Cognitive Heterogeneous Reconfigurable Optical Network (CHRON) project. Motivation for introducing cognition into the current networks is given. The paper explains how cognition can help in optical networks with high degree of heterogeneity with different modulation formats, switching schemes, and quality of transmission (QoT) requirements. It improves upon [13] by presenting advantages stemming from an accurate and detailed digital coherent receiver-based OPM at the transmission level in order to support cognitive decision processes. The paper also emphasized MFR as an important functionality of a cognitive receiver.

The individual author contribution: contributed to the introduction and motivation of the paper; helped in formulating concepts and requirements for cognition in optical networks; reviewed the manuscript.

Paper [B]: Cognition-enabling techniques in heterogeneous and flexgrid optical communication networks

This contribution from the *SPIE Photonics West* (2012) presents novel, at the time of publication, results obtained during first year of the CHRON project. The approach towards OPM in CONs is reviewed and possible use of cognition in order to improve energy efficiency of current networks is described.

The individual author contribution: contributed to the introduction and motivation of the paper; helped in formulating motivation as well as concepts and requirements for cognition in optical networks; authored the section on optical signal monitoring; reviewed the manuscript.

Paper [C]: Performance monitoring techniques supporting cognitive optical networking

This publication presented at the 15th *International Conference on Transparent Optical Networks (ICTON)* (2013) provides an incremental improvement wrt. [B] on the results obtained during the second year of the CHRON project. Following new results are included: OPM method for MFR, machine learning (ML) technique for QoT estimation.

The individual author contribution: authored the section on optical performance monitoring (OPM); acquired data, processed and created Fig. 2 and 3(a,b); prepared and reviewed the manuscript.

Paper [D]: Cognitive, heterogeneous and reconfigurable optical networks: the CHRON project

This article, accepted for *Journal of Lightwave Technology*, is a complete work presenting a survey on various technologies and techniques developed within the CHRON project in order to implement cognition in future CONs. The publication was reviewed after the CHRON project was finalized, thus it provides a comprehensive overview on various aspects of the CHRON architecture developed over the three-year project period. Operation of the cognitive decision system (CDS) as well as its modules such as cognitive algorithms for routing and wavelength assignment (RWA) and routing, modulation format, and spectrum allocation (RMLSA) assignment, virtual topology design, traffic grooming, and QoT estimation have been summarized. Physical layer OPM algorithms have been reviewed.

The individual author contribution: obtained results gathered in Table II; authored section IV on OPM; edited and reviewed the manuscript.

3.2 Cognitive processess

Paper [E]: Advanced modulation formats in cognitive optical networks: EU project CHRON demonstration

This contribution, presented at *Optical Fiber Communication Conference (OFC)* (2014), reports on an experiment in which the control plane of a CHRON-based CON was for the first time combined with a physical testbed. Moreover, advanced modulation formats (QPSK, 16-QAM) were for the first time experimentally transmitted and switched using the CDS of a CON. The modulation format change was triggered by the above-FEC performance of the channel under test. As a result modulation format was downgraded: one 16-quadrature amplitude modulation (QAM) subchannel carrying 192 Gbit/s was, according to the indication of the control plane (CDS), replaced by two quaternary phase shift keying (QPSK) subcarriers, each with 96 Gbit/s, resulting in unchanged total capacity. Due to downgrading modulation format order, bit error rate (BER) has improved considerably and satisfactory QoT (below-FEC BER), could be maintained. This paper is closely related to [e] as both of them originated from the same experimental testbed and show the advantage of CON networks.

The individual author contribution: implemented DSP algorithms for signal

demodulation and code for reporting physical layer OPM data with the control layer; participated in the assembly of the experimental setup and experimental measurements; processed acquired data and analyzed results; prepared, edited, submitted and reviewed the manuscript.

Paper [F]: Demonstration of EDFA cognitive gain control via GMPLS for mixed modulation formats in heterogeneous optical networks

In this paper, a first real-time experimental demonstration on the use of cognition in a Generalized Multi-Protocol Label Switching (GMPLS)-based network in order to optimize erbium-doped fiber amplifiers (EDFAs) gain as to obtain below-FEC performance for all transmitted channels is performed. The testbed used in the experiment is a copy of a part of the Brazilian *GIGA* network between the cities of Campinas and São Paulo. The links are not dispersion compensated. GMPLS is used for control and management of the test network. Four different signals were transported in the testbed: (a) CD-precompensated 10 Gbit/s on-off keying (OOK); (b) 112 Gbit/s polarization division multiplexing (PDM)-QPSK; (c) 224 Gbit/s PDM-16-QAM; and (d) 450 Gbit/s coherent optical (CO)-orthogonal frequency division multiplexing (OFDM) signal. The information about gain flatness (GF) and NF of the EDFAs as a function of both total input and total output power was known and was used to create a metric, where input power is known and output power is adjusted to jointly minimize GF and noise figure (NF). Without cognition, attenuating the signal at the input to the first amplifier in the link by 3 dB resulted in signals (c,d) to have above-FEC threshold performance. With cognition, the EDFAs operational point was automatically adjusted, but reception of signals (b,d) failed due to nonlinear impairments caused by too high launch power. A modified metric, penalizing high total output power, enabled transmission of all signals simultaneously, with below-forward error correction (FEC) limit performance.

The individual author contribution: contributed the expertise on the cognition concepts; assisted in formulating the research aim; reviewed and edited the manuscript.

Paper [G]: Experimental study on OSNR requirements for spectrum-flexible optical networks

Determination of the penalty induced by neighbouring superchannels with different modulation formats is difficult for analytical evaluation and depends on

specific configuration of the superchannel: subcarriers count and their spacing, modulation format, symbol rates, etc. (cf. section 2.1.2). This paper is an invited contribution to *Journal of Optical Communications and Networking*, and along with its short conference version [g], addresses this issue and presents the first experimental investigation of required optical signal-to-noise ratio (ROSNR) values for transmission of superchannels with mixed modulation formats and bit rates. Two 5-subcarrier 14 GHz-spaced, 14 Gbaud, PDM QPSK superchannels separated by a spectral gap, the band of interest (BOI), were transmitted over 252 km long standard single-mode fiber (SSMF) link. The bandwidth of the BOI was varied. The BOI was subsequently filled with another superchannel, constituted by a different number of either 14 Gbaud PDM-QPSK or PDM-16 QAM subcarriers. The optical signal-to-noise ratio (OSNR) required for transmission of the subcarriers inserted into the BOI, depending on: modulation format, number of subcarriers, their spacing and guard band between the neighboring superchannels, was extracted through experimental investigation of different scenarios. The obtained values were interpolated to yield the required OSNR necessary to maintain a 10^{-3} bit error rate of the central BOI subcarrier. The results obtained in this paper are important for CONs as they provide a rule of thumb that can be used to obtain initial estimates on the QoT in case the knowledge base (KB) of the CDS is empty.

The individual author contribution: the original experimental idea of examining OSNR limits for superchannel transmission as important parameter for CON; implemented DSP algorithms for signal demodulation and ROSNR interpolation from experimental data; participated in the assembly of the experimental setup and experimental measurements; processed acquired data and analyzed results; prepared, edited, submitted and reviewed the manuscript.

Paper [H]: Experimental demonstration of a cognitive quality of transmission estimator for optical communication systems

This journal contribution, published in *Optics Express*, extends the work initially reported in [h], in which the first experimental demonstration on the use of case-based reasoning (CBR) machine learning technique in order to assess QoT of the lightpath is performed. First, a set of reference cases is created, where each case corresponds to specific configuration of wavelength division multiplexing (WDM) in the optical link: number of simultaneously active 80 Gbit/s PDM-QPSK channels; launch power per channel; number of 80 km dispersion compensated transmission spans; average loss per span; for

a total number of 153 different sets of the listed parameters. For each case, error vector magnitude (EVM)/OSNR is measured, and this value, along with all WDM parameters, are recorded in the KB. This information is then subsequently used to forecast the QoT of WDM configurations whose parameters were not previously recorded, by predicting if the particular WDM configuration will result in low or high QoT (defined by EVM/OSNR threshold value). Weighted mean-square error of all recorded parameters is used to select the case most similar to the new case and it is assumed that the QoT of the new case will be the same as the QoT of the most similar case. By dividing the KB into training and test subsets, it is shown that even with a KB size of 100 known cases, CBR allows for correct classification of over 80% of new cases when using EVM (low/high threshold of 19.5%) and 98% of new cases, when using OSNR (low/high threshold 26 dB).

The individual author contribution: implemented DSP algorithms for signal demodulation and EVM measurement; participated in the assembly of the experimental setup and experimental measurements; reviewed and edited the manuscript.

3.3 Software-adaptable elements

Paper [I]: Experimental evaluation of prefiltering for 56 Gbaud DP-QPSK signal transmission in 75 GHz WDM grid

Future software defined transmitter (SDT) will have a possibility to modify pulse shaping filters, either electrical DSP-based or those enabled by software-defined optics, as required. This will be performed in order to obtain required BER of the channel under test (CUT) and minimize crosstalk to neighboring channels and thus optimize QoT. This paper, published in *Optical Fiber Technology*, experimentally investigates and compares three different prefilter shapes for 56 Gbaud PDM-QPSK transmission in severe bandwidth limiting conditions. As to the author's knowledge, this paper presents the first investigation of optical pulse shaping performed with a software defined optical filter in a 224 Gbit/s QPSK system. Other demonstrations at high symbol rates, such as [49] typically included a fixed optical equalizer circuit. Transmission using three different optical filter shapes are tested: rectangular, Gaussian and pre-emphasis (M-filter). It was measured that the M-filter with a bandwidth of 75 GHz significantly improved the BER at the receiver compared to other filters and unfiltered case. By using and modifying the filters on de-

mand, software-defined transmitters will be able to support CON optimization by smoothly changing the tradeoff between spectral efficiency and signal quality.

The individual author contribution: the original experimental idea of examining different prefilter shapes in a 56 Gbaud PDM-QPSK transmission system; assembled the experimental setup; acquired experimental measurements; processed experimental data and analyzed results; prepared, edited, submitted and reviewed the manuscript.

Paper [J]: Reconfigurable digital coherent receiver for metro-access networks supporting mixed modulation formats and bit-rates

This journal paper, published in *Optical Fiber Technology* reports on the software-defined receiver (SDR) for heterogeneous metro access network. WDM was used to combine and transmit four different types of signals and a single digital coherent SDR with DSP unifying all the applied modulation formats was used. The signals, transported over a 78 km deployed fiber link, included: 5 Gbit/s OOK; 20 Gbit/s QPSK signal; 2 Gbit/s phase modulated (PM) impulse radio ultra wideband (UWB); and 500 Mbit/s PM coherent OFDM signal at 5 GHz carrier frequency. This scheme demonstrates how powerful SDR technology is, particularly when applied to CONs, with diversified services and transmission technologies. In connection with a SDT it allows for on-the-fly reconfiguration of the modulation format and bit rate in order to optimize the network for capacity, reach, BER, or energy consumption. This innovative work was first presented in [j₁], and received an Honorable Mention (one of 2) in the Corning Outstanding Student Paper Competition at the *Optical Fiber Communication Conference (OFC)* (2011).

The individual author contribution: implemented DSP algorithms for OFDM signal demodulation; assembled the experimental setup for OFDM transmission; acquired experimental measurements with OFDM transmission; processed experimental data and analyzed results for OFDM transmission; reviewed the manuscript.

3.4 Optical performance monitoring

Paper [K]: Experimental demonstration of adaptive digital monitoring and compensation of chromatic dispersion for coherent DP-QPSK receiver

This paper, published in *Optics Express*, is an extended version of contribution [k]. The paper presents experimental evaluation of DSP-based in-service chromatic dispersion metrics for monitoring and subsequent compensation. Two new CD monitoring metrics were introduced and experimentally compared to a reference metric derived from the constant modulus algorithm (CMA) criterion [30] and a method based on frequency spectrum autocorrelation [66]. At the time of publication, the paper was the first to compare different dispersion metrics. The metrics were tested by transmitting a 40 Gbit/s QPSK signal over 80 km of SSMF, which resulted in approximately 1280 ps/nm of chromatic dispersion. This value exceeded the compensation capability of the adaptive time domain equalizer (TDE). Value of the CD was monitored using each of the metrics and the impairment was subsequently compensated according to the value indicated by the metric. By comparing resulting BER, it was found out that all tested metric resulted in virtually the same performance, compared to the reference metric.

The individual author contribution: conceived two new CD dispersion metrics (mean power, eigenvalue spread); implemented DSP algorithms for chromatic dispersion monitoring; acquired experimental measurements; processed experimental data and analyzed results; prepared, edited, submitted and reviewed the manuscript.

Paper [L]: Experimental demonstration of the maximum likelihood-based chromatic dispersion estimator for coherent receivers

This *Optical Fiber Technology* publication, presents an experimental investigation of the maximum likelihood estimation (MLE) CD monitoring metric, and is an experimental counterpart of [78]. A modulation format independent and polarization mode dispersion (PMD) insensitive metric is tested with PDM-QPSK and PDM-16-QAM signals after transmission over 240, 400, 640 and 800 km and compared to the reference method based on constant modulus algorithm (CMA) algorithm [30]. It is found that the MLE method correctly, and more accurately than the reference method, indicates CD value at OSNR below 15 dB and provides precise and repeatable estimates even with signifi-

cant DGD. It is also verified that the MLE estimator can work well with both PDM-QPSK and PDM-16-QAM modulation formats, as in principle it is not modulation format dependent.

The individual author contribution: implemented DSP algorithm for MLE of CD; acquired experimental measurements; processed experimental data and analyzed results; prepared, edited, submitted and reviewed the manuscript.

Paper [M]: Stokes space-based optical modulation format recognition for digital coherent receivers

This paper, published in *IEEE Photonics Technology Letters*, along with its conference version [m], presents a method for modulation format recognition (MFR) for heterogeneous reconfigurable optical networks. As SDT are being used in the network and the reconfiguration of the network is dynamic (cf. section 1.4.4), it is no longer possible to ensure that the receiver will know what modulation format to expect. In order to address this issue, this paper proposes a completely novel method of modulation format detection based on Stokes space signal representation and variational Bayesian expectation maximization (VBEM) ML algorithm. The method is inspired by the observation that different PDM complex modulation formats will result in distinctive signatures, in terms of number of points formed, when transformed to Stokes space and observed in the Poincaré sphere. By using a VBEM ML algorithm, the number of distinctive clusters is counted and the modulation format with the smallest difference between the ideal number of clusters and the counted number of clusters is chosen. Six different PDM modulation formats were considered in numerical simulations: binary phase shift keying (BPSK), QPSK, 8-phase shift keying (PSK), star 8-QAM, 12-QAM, 16-QAM, while QPSK and 16-QAM for experimental evaluation. The modulation format was recognized successfully for all tested cases. This contribution constitutes one of the most important part of this thesis. The idea of Stokes MFR has been taken up by other independent researchers and further developed [87, 88].

The individual author contribution: conceived the original idea of using Stokes space parameters for MFR; implemented DSP algorithms for signal demodulation and Stokes space analysis from experimental data; participated in the assembly of the experimental setup and experimental measurements; processed acquired data and analyzed results; prepared, edited, submitted and reviewed the manuscript.

Paper [N]: Nonlinear impairment compensation using expectation maximization for dispersion managed and unmanaged PDM 16-QAM transmission

The last included paper, published in *Optics Express*, expands upon [n], and presents the use of expectation maximization (EM) machine learning algorithm in order to compensate optical impairments such as fiber Kerr nonlinearities, in-phase/quadrature (I/Q) modulator imperfections and laser phase noise in post-detection. The signal statistics is represented as a superposition of normal distributions – Gaussian mixture model (GMM) – and this model is fit into the received data using EM. Each cluster of the received constellation is modeled with a separate normal distribution. For every cluster forming the GMM, fitted mean will inform about the dislocation of that cluster from ideal position, while non-diagonal covariance matrix will indicate elliptical cluster shape. Both relative cluster dislocations as well as non-circular cluster symmetry are results of either nonlinear effects or laser phase noise. Fitted means and covariance matrices allow for approximation of received signal PDF and are used to find optimal decision boundaries minimizing the BER of the received signal. The influence of nonlinear impairments on the BER is then minimized by optimizing decision boundaries of the received constellation. The method is tested both numerically and experimentally. In experimental investigation, PDM-16-QAM signal is transmitted over 240, 400 and 800 km. An improvement of up to 3 dB in system tolerance in the nonlinear region is measured for 800 km long dispersion compensated transmission. The gain reduces to approximately 0.5 dB for dispersion uncompensated transmission. It is also concluded that EM algorithm may be beneficial for WDM transmission as neighbouring channels will have an imprint on the CUT.

The individual author contribution: helped to develop DSP algorithms for signal demodulation; participated in the assembly of the experimental setup and experimental measurements; reviewed and edited the manuscript.

Chapter 4

Summary

4.1 Conclusions

Optical networks enabling Future Internet will be of highly dynamic and heterogeneous nature and this calls for new paradigm in control and management. Cognitive optical networking is postulated to simplify these tasks by implementing intelligent autonomous behavior of the network. The presence of a decisive “brain” in the network, will require an array of diverse methods, some of which had not existed before. This thesis reports on a pioneering work on technologies and techniques supporting cognitive optical networks operations. The scientific results and achievements presented in this thesis have significantly extended and contributed to state of the art in cognitive optical networks (CONs) and many of the subtopics.

4.1.1 Cognitive optical networks

The basic objectives, requirements and functionalities needed by CONs were outlined in [A, B, C, D]. These includes: cognitive processes, software-adaptable elements, and performance monitoring elements, and the contributions of this thesis cover all three elementary classes. Additionally, [D] provides an overview over the diverse activities of the Cognitive Heterogeneous Reconfigurable Optical Network (CHRON) project within the framework of which this thesis was carried out.

4.1.2 Cognitive processes

Cognitive processes are fundamental for enabling the learning process and utilization of the accumulated knowledge. In [E] a successful experiment com-

binning advanced modulation formats in the physical layer with a cognitive control plane resulted in a first demonstration of modulation format reconfiguration in real-time driven by cognitive algorithms for the purpose of maintaining quality of transmission (QoT). Another demonstration involving real-time optimization of link amplifiers to achieve satisfactory QoT of all transmitted channels in a heterogeneous network was presented in [F]. The demonstration of a machine learning (ML) technique, case-based reasoning (CBR), for QoT estimation was presented in paper [H]. This method enables a CON to use past observations in order to predict expected performance before establishing a connection and therefore decide whether the connection will comply to the required quality of service (QoS) level. Paper [G] reports on experimental evaluation of required optical signal-to-noise ratio (OSNR) for superchannel transmission. The information provided by this experiment can be subsequently used to fill knowledge base (KB) of a cognitive decision system (CDS) and be used in conjunction with techniques, such as CBR.

4.1.3 Software-adaptable elements

Network elements controlled by software allow for optimizations by exploiting spectrum flexibility and bandwidth elasticity, through fine adjustments in the symbol rate, modulation format or signal spectrum shape. The thesis includes two reports related to software adaptability of the network elements. First, in [I] a transmitter with a programmable optical filter is demonstrated. The change of an optical filter shape results in a varied performance of the transmitted channel and can be used for spectral efficiency (SE)-QoT tradeoff decision. A software-defined receiver (SDR) supporting reception of four different modulation formats, simultaneously transmitted over a deployed fiber, has been presented in [J]

4.1.4 Optical performance monitoring

Optical performance monitoring algorithms operate in the physical layer of the network with the aim to monitor signal parameters and its quality. They provide feedback to the cognitive engine allowing the control plane to perform decision based on heuristics rather than blindly and arbitrarily. In paper [K, L], new chromatic dispersion (CD) monitoring algorithms are experimentally evaluated and compared. A novel modulation format recognition (MFR) method insensitive to polarization mixing and carrier offset, with an application for networks with distributed cognition or high-latency control plane, is presented in [M]. Finally, a ML method for improving bit error rate (BER)

of signals affected by nonlinear impairments, such as self-phase modulation (SPM) is presented in [N].

4.2 Future work

This thesis introduces innovative set of tools that focuses on simplified network control and management machinery. Nonetheless many issues still remain to be solved.

One of the most important steps to take in the future, is to design an easy and inexpensive (for operators) upgrade path from current networks towards CONs. As pointed out in [100] Generalized Multi-Protocol Label Switching (GMPLS) fails in many scenarios due to a non-trivial migration scenario, whereas software-defined networking (SDN) offers a smooth transition path. One of the possible points of future work might be to port the concepts of cognition, developed within CHRON project to SDN ground in order encourage operators to adopt cognition in their networks.

Moreover, cognition assumes heavy use of ML techniques. ML-driven functionalities required in the CDS of a CON can be implemented and achieve reasonable runtime scales on a network control node. Nonetheless, implementation of ML techniques in the transceivers is still far from reality. digital signal processing (DSP) algorithms, such as k -means or expectation maximization (EM) are computationally very expensive and are not feasible for hardware implementation at a current stage. Work has to be done in order to reduce complexity of these and similar algorithms without significantly affecting their performance. Taking into account the current trend where the power efficiency pushes the transceivers' DSP clocks towards lower frequencies [25], thereby requiring higher degree of parallelization, new possibilities might be expected to open. For example, Qualcomm has recently unveiled their work on real-time image recognition of objects from moving cars [101]. Such a general-purpose image processors, when combined with relatively slow and parallelized architecture of upcoming transceivers, might finally allow for implementation of advanced optical performance monitoring (OPM) functionalities.

Bibliography

- [1] Cisco, “Cisco Visual Networking Index: Forecast and Methodology, 2012-2017,” Cisco, Tech. Rep., 2013.
- [2] P. J. Winzer, “High-spectral-efficiency optical modulation formats,” *Journal of Lightwave Technology*, vol. 30, no. 24, pp. 3824–3835, 2012.
- [3] W. Wei, C. Wang, and J. Yu, “Cognitive optical networks: key drivers, enabling techniques, and adaptive bandwidth services,” *IEEE Communications Magazine*, vol. 50, no. 1, pp. 106–113, Jan. 2012.
- [4] I. de Miguel, R. J. Durán, T. Jiménez, N. Fernández, J. C. Aguado, R. M. Lorenzo, A. Caballero, I. Tafur Monroy, Y. Ye, A. Tymecki, I. Tomkos, M. Angelou, D. Klonidis, A. Francescon, D. Siracusa, and E. Salvadori, “Cognitive dynamic optical networks [Invited],” *Journal of Optical Communications and Networking*, vol. 5, no. 10, p. A107, Sep. 2013.
- [5] C. Ramming, “Cognitive Networks,” in *DARPA Tech Symposium*, Anaheim, CA, USA, 2004.
- [6] J. III Mitola, “Cognitive radio: an integrated agent architecture for software defined radio [Invited],” PhD dissertation, Royal Institute of Technology (KTH), 2000.
- [7] R. W. Thomas, L. A. DaSilva, and A. B. MacKenzie, “Cognitive networks,” in *IEEE International Symposium on New Frontiers in Dynamic Spectrum Access Networks*, vol. 1. IEEE, 2005, pp. 352–360.
- [8] Q. H. Mahmoud, *Cognitive networks: towards self-aware networks*. Wiley-Interscience, Sep. 2007.
- [9] D. Kliazovich, F. Granelli, and N. L. S. da Fonseca, “Architectures and Cross-Layer Design for Cognitive Networks,” in *Handbook on Sensor*

- Networks*, Y. Xiao, H. Chen, and F. H. Li, Eds. Singapore: World Scientific Publishing, 2010, ch. Chapter 1, pp. 3–24.
- [10] Z. Movahedi, M. Ayari, R. Langar, and G. Pujolle, “A Survey of Autonomic Network Architectures and Evaluation Criteria,” *IEEE Communications Surveys & Tutorials*, vol. 14, no. 2, pp. 464–490, Jan. 2012.
- [11] R. Thomas, D. Friend, L. Dasilva, and A. Mackenzie, “Cognitive networks: adaptation and learning to achieve end-to-end performance objectives,” *IEEE Communications Magazine*, vol. 44, no. 12, pp. 51–57, Dec. 2006.
- [12] R. W. Thomas, “Cognitive networks,” PhD dissertation, Virginia Polytechnic Institute and State University, 2007.
- [13] G. S. Zervas and D. Simeonidou, “Cognitive optical networks: need, requirements and architecture,” in *International Conference on Transparent Optical Networks (ICTON)*, vol. 12. Munich, Germany: IEEE, Jun. 2010.
- [14] CHRON, “The CHRON Project.” [Online]. Available: <http://www.ict-chron.eu/>
- [15] I. Tomkos, M. Angelou, R. J. Durán Barroso, I. de Miguel, R. M. Lorenzo Toledo, D. Siracusa, E. Salvadori, A. Tymecki, Y. Ye, and I. Tafur Monroy, *The Future Internet*, ser. Lecture Notes in Computer Science, F. Álvarez, F. Cleary, P. Daras, J. Domingue, A. Galis, A. Garcia, A. Gavras, S. Karnourkos, S. Krco, M.-S. Li, V. Lotz, H. Müller, E. Salvadori, A.-M. Sassen, H. Schaffers, B. Stiller, G. Tselentis, P. Turkama, and T. Zahariadis, Eds. Berlin, Heidelberg: Springer Berlin Heidelberg, 2012, vol. 7281.
- [16] CHRON, “D3.2 Architecture of the Cognitive Decision System,” The CHRON Project Consortium, Tech. Rep., 2012.
- [17] CHRON, “D3.3 The core of the cognitive system: the cognitive process and the knowledge engineering system,” The CHRON Project Consortium, Tech. Rep., 2012.
- [18] S. Das, “pac.c: A unified control architecture for packet and circuit network convergence,” PhD thesis, Stanford University, 2012.

- [19] D. Siracusa, A. Broglio, A. Francescon, A. Zanardi, and E. Salvadori, "Toward a control and management system enabling cognitive optical networks," in *Proceedings of the 2013 18th European Conference on Network and Optical Communications & 2013 8th Conference on Optical Cabling and Infrastructure (NOC-OC&I)*. IEEE, Jul. 2013, pp. 233–240.
- [20] ITU-T, "Spectral grids for WDM applications: DWDM frequency grid," 2012.
- [21] M. G. Taylor, "Coherent Detection Method Using DSP for Demodulation of Signal and Subsequent Equalization of Propagation Impairments," *IEEE Photonics Technology Letters*, vol. 16, no. 2, pp. 674–676, Feb. 2004.
- [22] R. Noe, "PLL-free synchronous QPSK polarization multiplex/diversity receiver concept with digital I&Q baseband processing," *IEEE Photonics Technology Letters*, vol. 17, no. 4, pp. 887–889, Apr. 2005.
- [23] A. Leven, N. Kaneda, U.-V. Koc, and Y.-K. Chen, "Coherent Receivers for Practical Optical Communication Systems," in *OFC/NFOEC 2007 - 2007 Conference on Optical Fiber Communication and the National Fiber Optic Engineers Conference*. IEEE, Mar. 2007, pp. 1–3.
- [24] E. Ip, A. P. T. Lau, D. J. F. Barros, and J. M. Kahn, "Coherent detection in optical fiber systems," *Optics Express*, vol. 16, no. 2, p. 753, 2008.
- [25] M. Kuschnerov, T. Bex, and P. Kainzmaier, "Energy Efficient Digital Signal Processing," in *Optical Fiber Communication Conference*. San Francisco, California: OSA, 2014, p. Th3E.7.
- [26] R.-J. Essiambre, G. Kramer, P. J. Winzer, G. J. Foschini, and B. Goebel, "Capacity limits of optical fiber networks," *Journal of Lightwave Technology*, vol. 28, no. 4, pp. 662–701, Feb. 2010.
- [27] C. C. K. Chan, Ed., *Optical Performance Monitoring*. Academic Press, 2010.
- [28] M. Kuschnerov, M. Chouayakh, K. Piyawanno, B. Spinnler, E. de Man, P. Kainzmaier, M. S. Alfiad, A. Napoli, and B. Lankl, "Data-Aided Versus Blind Single-Carrier Coherent Receivers," *IEEE Photonics Journal*, vol. 2, no. 3, pp. 387–403, Jun. 2010.
- [29] S. J. Savory, "Digital filters for coherent optical receivers," *Optics Express*, vol. 16, no. 2, pp. 804–817, Jan. 2008.

- [30] M. Kuschnerov, F. N. Hauske, K. Piyawanno, B. Spinnler, A. Napoli, and B. Lankl, "Adaptive Chromatic Dispersion Equalization for Non-Dispersion Managed Coherent Systems," in *Optical Fiber Communication Conference and National Fiber Optic Engineers Conference*. Washington, D.C.: OSA, 2009, p. OMT1.
- [31] S. J. B. Yoo, "Optical Packet and Burst Switching Technologies for the Future Photonic Internet," *Journal of Lightwave Technology*, vol. 24, no. 12, pp. 4468–4492, Dec. 2006.
- [32] D. J. Geisler, R. Proietti, Y. Yin, R. P. Scott, X. Cai, N. K. Fontaine, L. Paraschis, O. Gerstel, and S. J. B. Yoo, "Experimental demonstration of flexible bandwidth networking with real-time impairment awareness," *Optics Express*, vol. 19, no. 26, pp. B736–45, Dec. 2011.
- [33] F. Cugini, G. Meloni, F. Paolucci, N. Sambo, M. Secondini, L. Gerardi, L. Poti, and P. Castoldi, "Demonstration of Flexible Optical Network Based on Path Computation Element," *Journal of Lightwave Technology*, vol. 30, no. 5, pp. 727–733, Mar. 2012.
- [34] L. Liu, H. Y. Choi, R. Casellas, T. Tsuritani, I. Morita, R. Martínez, and R. Muñoz, "Demonstration of a dynamic transparent optical network employing flexible transmitters/receivers controlled by an OpenFlow-stateless PCE integrated control plane [Invited]," *Journal of Optical Communications and Networking*, vol. 5, no. 10, pp. A66–A75, Aug. 2013.
- [35] P. Poggiolini, A. Carena, V. Curri, G. Bosco, and F. Forghieri, "Analytical Modeling of Nonlinear Propagation in Uncompensated Optical Transmission Links," *IEEE Photonics Technology Letters*, vol. 23, no. 11, pp. 742–744, Jun. 2011.
- [36] A. Carena, V. Curri, G. Bosco, P. Poggiolini, and F. Forghieri, "Modeling of the Impact of Nonlinear Propagation Effects in Uncompensated Optical Coherent Transmission Links," *Journal of Lightwave Technology*, vol. 30, no. 10, pp. 1524–1539, May 2012.
- [37] P. Poggiolini, "The GN Model of Non-Linear Propagation in Uncompensated Coherent Optical Systems," *Journal of Lightwave Technology*, vol. 30, no. 24, pp. 3857–3879, Dec. 2012.

- [38] X. Chen and W. Shieh, "Closed-form expressions for nonlinear transmission performance of densely spaced coherent optical OFDM systems." *Optics express*, vol. 18, no. 18, pp. 19 039–54, Aug. 2010.
- [39] G. Gao, X. Chen, and W. Shieh, "Analytical Expressions for Nonlinear Transmission Performance of Coherent Optical OFDM Systems With Frequency Guard Band," *Journal of Lightwave Technology*, vol. 30, no. 15, pp. 2447–2454, Aug. 2012.
- [40] F. Vacondio, O. Rival, C. Simonneau, E. Grellier, A. Bononi, L. Lorcy, J.-C. Antona, and S. Bigo, "On nonlinear distortions of highly dispersive optical coherent systems." *Optics express*, vol. 20, no. 2, pp. 1022–32, Jan. 2012.
- [41] G. Bosco, V. Curri, A. Carena, P. Poggiolini, and F. Forghieri, "On the Performance of Nyquist-WDM Terabit Superchannels Based on PM-BPSK, PM-QPSK, PM-8QAM or PM-16QAM Subcarriers," *Journal of Lightwave Technology*, vol. 29, no. 1, pp. 53–61, Jan. 2011.
- [42] CHRON, "D4.5 Report on a QoT tool for heterogeneous transmission systems," The CHRON Project Consortium, Tech. Rep., 2013.
- [43] T. Jimenez, J. C. Aguado, I. de Miguel, R. J. Duran, M. Angelou, N. Merayo, P. Fernandez, R. M. Lorenzo, I. Tomkos, and E. J. Abril, "A Cognitive Quality of Transmission Estimator for Core Optical Networks," *Journal of Lightwave Technology*, vol. 31, no. 6, pp. 942–951, Mar. 2013.
- [44] J. Hilt, M. Nolle, L. Molle, M. Seimetz, and R. Freund, "32 Gbaud real-time FPGA-based multi-format transmitter for generation of higher-order modulation formats," in *Digest of the 9th International Conference on Optical Internet (COIN 2010)*. IEEE, Jul. 2010, pp. 1–3.
- [45] R. Schmogrow, D. Hillerkuss, M. Dreschmann, M. Huebner, M. Winter, J. Meyer, B. Nebendahl, C. Koos, J. Becker, W. Freude, and J. Leuthold, "Real-Time Software-Defined Multiformat Transmitter Generating 64QAM at 28 GBd," *IEEE Photonics Technology Letters*, vol. 22, no. 21, pp. 1601–1603, Nov. 2010.
- [46] W. Freude, R. Schmogrow, B. Nebendahl, D. Hillerkuss, J. Meyer, M. Dreschmann, M. Huebner, J. Becker, C. Koos, and J. Leuthold, "Software-defined optical transmission," in *2011 13th International Conference on Transparent Optical Networks*. IEEE, Jun. 2011, pp. 1–4.

- [47] H. Y. Choi, T. Tsuritani, and I. Morita, "BER-adaptive flexible-format transmitter for elastic optical networks." *Optics express*, vol. 20, no. 17, pp. 18 652–8, Aug. 2012.
- [48] D. J. Geisler, N. K. Fontaine, R. P. Scott, T. He, L. Paraschis, O. Gerstel, J. P. Heritage, and S. J. B. Yoo, "Bandwidth scalable, coherent transmitter based on the parallel synthesis of multiple spectral slices using optical arbitrary waveform generation." *Optics Express*, vol. 19, no. 9, pp. 8242–53, May 2011.
- [49] G. Raybon, A. L. Adamiecki, S. Randel, C. Schmidt, P. J. Winzer, A. Konczykowska, F. Jorge, J.-Y. Dupuy, L. L. Buhl, S. Chandrasekhar, X. Liu, A. H. Gnauck, C. Scholz, and R. Delbue, "All-ETDM 80-Gbaud (640-Gb/s) PDM 16-QAM Generation and Coherent Detection," *IEEE Photonics Technology Letters*, vol. 24, no. 15, pp. 1328–1330, Aug. 2012.
- [50] "Optical Multi-Format Transmitter." [Online]. Available: <http://www.hhi.fraunhofer.de/fields-of-competence/photonic-networks-and-systems/products-and-services/optical-multi-format-transmitter.html>
- [51] P. Rigby, "Ciena's third generation of WaveLogic processors supports 400G," 2012. [Online]. Available: <http://www.lightwaveonline.com/articles/2012/03/cienas-third-generation-of-wavelogic-processors-supports-400g.html>
- [52] K. Roberts and C. Laperle, "Flexible Transceivers," in *European Conference and Exhibition on Optical Communication*. Washington, D.C.: OSA, 2012, p. We.3.A.3.
- [53] S. Hardy, "ClariPhy unveils 100G Lightspeed-II SoC for coherent CFP transceivers," 2014. [Online]. Available: <http://www.lightwaveonline.com/articles/2014/03/clariphy-unveils-100g-lightspeed-ii-soc-for-coherent-cfp-transceivers.html>
- [54] "Finisar expands WaveShaper programmable optical processors," 2010. [Online]. Available: <http://www.lightwaveonline.com/articles/2010/09/finisar-expands-waveshaper-programmable-optical-processors-103543534.html>
- [55] A. P. T. Lau, Y. Gao, Q. Sui, D. Wang, Q. Zhuge, M. H. Morsy-Osman, M. Chagnon, X. Xu, C. Lu, and D. V. Plant, "Advanced DSP Techniques

- Enabling High Spectral Efficiency and Flexible Transmissions: Toward elastic optical networks,” *IEEE Signal Processing Magazine*, vol. 31, no. 2, pp. 82–92, Mar. 2014.
- [56] R. A. Skoog, T. C. Banwell, J. W. Gannett, S. F. Habiby, M. Pang, M. E. Rauch, and P. Toliver, “Automatic Identification of Impairments Using Support Vector Machine Pattern Classification on Eye Diagrams,” *IEEE Photonics Technology Letters*, vol. 18, no. 22, pp. 2398–2400, Nov. 2006.
- [57] X. Wu, J. Jargon, R. Skoog, L. Paraschis, and A. Willner, “Applications of Artificial Neural Networks in Optical Performance Monitoring,” *Journal of Lightwave Technology*, vol. 27, no. 16, pp. 3580–3589, Aug. 2009.
- [58] T. B. Anderson, S. D. Dods, K. Clarke, J. Bedo, and A. Kowalczyk, “Multi-Impairment Monitoring for Photonic Networks,” pp. 1–4, 2007.
- [59] T. Anderson, A. Kowalczyk, K. Clarke, S. Dods, D. Hewitt, and J. Li, “Multi Impairment Monitoring for Optical Networks,” *Journal of Lightwave Technology*, vol. 27, no. 16, pp. 3729–3736, Aug. 2009.
- [60] F. N. Hauske, J. C. Geyer, M. Kuschnerov, K. Piyawanno, T. Duthel, C. R. Fludger, D. van den Borne, E.-D. Schmidt, B. Spinnler, H. de Waardt, and B. Lankl, “Optical Performance Monitoring from FIR Filter Coefficients in Coherent Receivers,” in *Optical Fiber Communication Conference/National Fiber Optic Engineers Conference*. Optical Society of America, Feb. 2008, p. OThW2.
- [61] B. Spinnler, F. Hauske, and M. Kuschnerov, “Adaptive equalizer complexity in coherent optical receivers,” in *2008 34th European Conference on Optical Communication*. IEEE, 2008, pp. 1–2.
- [62] M. Kuschnerov, F. N. Hauske, K. Piyawanno, B. Spinnler, M. S. Alfiad, A. Napoli, and B. Lankl, “DSP for Coherent Single-Carrier Receivers,” *Journal of Lightwave Technology*, vol. 27, no. 16, pp. 3614–3622, Aug. 2009.
- [63] T. Xu, G. Jacobsen, S. Popov, J. Li, E. Vanin, K. Wang, A. T. Friberg, and Y. Zhang, “Chromatic dispersion compensation in coherent transmission system using digital filters,” *Optics express*, vol. 18, no. 15, pp. 16 243–57, Jul. 2010.

- [64] J.-X. Cai, Y. Cai, C. R. Davidson, D. G. Foursa, A. Lucero, O. Sinkin, W. Patterson, A. Pilipetskii, G. Mohs, and N. S. Bergano, "Transmission of 96Å—100G pre-filtered PDM-RZ-QPSK channels with 300% spectral efficiency over 10,608km and 400% spectral efficiency over 4,368km," pp. 1–3, 2010.
- [65] J. Zweck and C. Menyuk, "A Chromatic Dispersion Estimation Method for Arbitrary Modulation Formats," in *CLEO:2011 - Laser Applications to Photonic Applications*. Washington, D.C.: OSA, 2011, p. CThX4.
- [66] F. Hauske, C. Xie, Z. Zhang, C. Li, L. Li, and Q. Xiong, "Frequency domain chromatic dispersion estimation," pp. 1–3, 2010.
- [67] C. Malouin, P. Thomas, B. Zhang, J. O'Neil, and T. Schmidt, "Natural Expression of the Best-Match Search Godard Clock-Tone Algorithm for Blind Chromatic Dispersion Estimation in Digital Coherent Receivers," in *Proc. SPPCom*. Washington, D.C.: OSA, Jun. 2012, p. SpTh2B.4.
- [68] Q. Sui, A. P. T. Lau, and C. Lu, "Fast and Robust Blind Chromatic Dispersion Estimation Using Auto-Correlation of Signal Power Waveform for Digital Coherent Systems," *Journal of Lightwave Technology*, vol. 31, no. 2, pp. 306–312, Jan. 2013.
- [69] F. C. Pereira, V. N. Rozental, M. Camera, G. Bruno, and D. A. A. Mello, "Experimental Analysis of the Power Auto-Correlation-Based Chromatic Dispersion Estimation Method," *IEEE Photonics Journal*, vol. 5, no. 4, pp. 7901608–7901608, Aug. 2013.
- [70] F. N. Hauske, Z. Zhang, C. Li, C. Xie, and Q. Xiong, "Precise, Robust and Least Complexity CD Estimation," in *Optical Fiber Communication Conference/National Fiber Optic Engineers Conference 2011*. Washington, D.C.: OSA, Mar. 2011, p. JWA032.
- [71] R. A. Soriano, F. N. Hauske, N. Guerrero Gonzalez, Z. Zhang, Y. Ye, and I. Tafur Monroy, "Chromatic Dispersion Estimation in Digital Coherent Receivers," *Journal of Lightwave Technology*, vol. 29, no. 11, pp. 1627–1637, Jun. 2011.
- [72] J. Wang, X. Jiang, X. He, and Z. Pan, "Ultra-wide range in-service chromatic dispersion measurement using coherent detection and digital signal processing," in *SPIE/OSA/IEEE Asia Communications and Photonics*, X. Liu, Ed. International Society for Optics and Photonics, Nov. 2011, p. 83091J.

- [73] D. Wang, C. Lu, A. P. T. Lau, and S. He, "Adaptive Chromatic Dispersion Compensation for Coherent Communication Systems Using Delay-Tap Sampling Technique," *IEEE Photonics Technology Letters*, vol. 23, no. 14, pp. 1016–1018, Jul. 2011.
- [74] V. Ribeiro, S. Ranzini, J. Oliveira, V. Nascimento, E. Magalhães, and E. Rosa, "Accurate Blind Chromatic Dispersion Estimation in Long-haul 112Gbit/s PM-QPSK WDM Coherent Systems," in *Advanced Photonics Congress*. Washington, D.C.: OSA, Jun. 2012, p. SpTh2B.3.
- [75] J. C. Diniz, S. Ranzini, V. Ribeiro, E. Magalhães, E. Rosa, V. Parahyba, L. V. Franz, E. E. Ferreira, and J. Oliveira, "Hardware-Efficient Chromatic Dispersion Estimator based on Parallel Gardner Timing Error Detector," in *Optical Fiber Communication Conference/National Fiber Optic Engineers Conference 2013*. Washington, D.C.: OSA, Mar. 2013, p. OTh3C.6.
- [76] E. Ibragimov, G. Zarris, S. Khatana, and L. Dardis, "Blind Chromatic Dispersion Estimation Using a Spectrum of a Modulus Squared of the Transmitted Signal," in *European Conference and Exhibition on Optical Communication*. Washington, D.C.: OSA, 2012, p. Th.2.A.3.
- [77] C. Malouin, M. Arabaci, P. Thomas, B. Zhang, T. Schmidt, and R. Marcoccia, "Efficient, Non-Data-Aided Chromatic Dispersion Estimation via Generalized, FFT-Based Sweep," in *Optical Fiber Communication Conference/National Fiber Optic Engineers Conference 2013*. Washington, D.C.: OSA, Mar. 2013, p. JW2A.45.
- [78] H. Wymeersch and P. Johannisson, "Maximum-Likelihood-Based Blind Dispersion Estimation for Coherent Optical Communication," *Journal of Lightwave Technology*, vol. 30, no. 18, pp. 2976–2982, Sep. 2012.
- [79] C. Xie, "Chromatic Dispersion Estimation for Single-Carrier Coherent Optical Communications," *IEEE Photonics Technology Letters*, vol. 25, no. 10, pp. 992–995, May 2013.
- [80] N. Stojanovic, B. Mao, and F. Karinou, "Efficient and low-complexity chromatic dispersion estimation in coherent optical systems," in *2013 21st Telecommunications Forum Telfor (TELFOR)*. IEEE, Nov. 2013, pp. 153–156.
- [81] N. Stojanovic, F. Karinou, and B. Mao, "Chromatic Dispersion Estimation Method for Nyquist and Faster Than Nyquist Coherent

- Optical Systems - OSA Technical Digest (online),” in *Optical Fiber Communication Conference*. San Francisco, California: Optical Society of America, 2014, p. Th2A.19.
- [82] N. Guerrero Gonzalez, D. Zibar, and I. Tafur Monroy, “Cognitive digital receiver for burst mode phase modulated radio over fiber links,” in *European Conference and Exhibition on Optical Communication*, vol. 36. IEEE, Sep. 2010, pp. 1–3.
- [83] N. Hanik, A. Gladisch, C. Caspar, and B. Strebel, “Application of amplitude histograms to monitor performance of optical channels,” *Electronics Letters*, vol. 35, no. 5, p. 403, 1999.
- [84] F. N. Khan, Y. Zhou, A. P. T. Lau, and C. Lu, “Modulation format identification in heterogeneous fiber-optic networks using artificial neural networks,” *Optics Express*, vol. 20, no. 11, pp. 12 422–31, May 2012.
- [85] B. Szafraniec, T. S. Marshall, and B. Nebendahl, “Performance Monitoring and Measurement Techniques for Coherent Optical Systems,” *Journal of Lightwave Technology*, vol. 31, no. 4, pp. 648–663, Feb. 2013.
- [86] P. Isautier, A. Stark, K. Mehta, R. de Salvo, and S. Ralph, “Autonomous software-defined coherent optical receivers,” in *Optical Fiber Communication Conference*, 2013.
- [87] P. Isautier, A. Stark, K. Mehta, and S. E. Ralph, “Autonomous Software-Defined Coherent Optical Receivers Performing Modulation Format Recognition in Stokes-Space,” in *European Conference and Exhibition on Optical Communication*, vol. 39. Institution of Engineering and Technology, 2013, pp. 1035–1037.
- [88] P. Isautier, J. Pan, and S. Ralph, “Robust Autonomous Software-Defined Coherent Optical Receiver,” in *Optical Fiber Communication Conference*. Washington, D.C.: OSA, 2014, p. W1G.7.
- [89] J. Liu, Z. Dong, K. P. Zhong, A. P. T. Lau, C. Lu, and Y. Lu, “Modulation Format Identification Based on Received Signal Power Distributions for Digital Coherent Receivers - OSA Technical Digest (online),” in *Optical Fiber Communication Conference*. San Francisco, California: Optical Society of America, 2014, p. Th4D.3.
- [90] R. A. Fisher, B. R. Suydam, and D. Yevick, “Optical phase conjugation for time-domain undoing of dispersive self-phase-modulation effects,” *Optics Letters*, vol. 8, no. 12, p. 611, Dec. 1983.

- [91] K. V. Peddanarappagari and M. Brandt-Pearce, "Volterra series transfer function of single-mode fibers," *Journal of Lightwave Technology*, vol. 15, no. 12, pp. 2232–2241, 1997.
- [92] H. Song and M. Brandt-Pearce, "A 2-D Discrete-Time Model of Physical Impairments in Wavelength-Division Multiplexing Systems," *Journal of Lightwave Technology*, vol. 30, no. 5, pp. 713–726, Mar. 2012.
- [93] X. Li, X. Chen, G. Goldfarb, E. Mateo, I. Kim, F. Yaman, and G. Li, "Electronic post-compensation of WDM transmission impairments using coherent detection and digital signal processing," *Optics Express*, vol. 16, no. 2, p. 880, 2008.
- [94] E. Ip and J. Kahn, "Fiber Impairment Compensation Using Coherent Detection and Digital Signal Processing," *Journal of Lightwave Technology*, vol. 28, no. 4, pp. 502–519, Feb. 2010.
- [95] Y. Cai, D. G. Foursa, C. R. Davidson, J.-X. Cai, O. Sinkin, M. Nissov, and A. Pilipetskii, "Experimental Demonstration of Coherent MAP Detection for Nonlinearity Mitigation in Long-Haul Transmissions," in *Optical Fiber Communication Conference*. Washington, D.C.: OSA, 2010, p. OTuE1.
- [96] D. Marsella, M. Secondini, E. Forestieri, and R. Magri, "Detection Strategies in the Presence of Fiber Nonlinear Effects," in *European Conference and Exhibition on Optical Communication*. Washington, D.C.: OSA, 2012, p. P4.06.
- [97] T. Koike-Akino, C. Duan, K. Parsons, K. Kojima, T. Yoshida, T. Sugihara, and T. Mizuochi, "High-order statistical equalizer for nonlinearity compensation in dispersion-managed coherent optical communications," *Optics express*, vol. 20, no. 14, pp. 15 769–80, Jul. 2012.
- [98] E. Ip, "Nonlinear compensation using backpropagation for polarization-multiplexed transmission," *Journal of Lightwave Technology*, vol. 28, no. 6, pp. 939–951, Mar. 2010.
- [99] A. P. T. Lau and J. M. Kahn, "Signal Design and Detection in Presence of Nonlinear Phase Noise," *Journal of Lightwave Technology*, vol. 25, no. 10, pp. 3008–3016, Oct. 2007.

- [100] S. Das, G. Parulkar, and N. McKeown, "Why OpenFlow/SDN Can Succeed Where GMPLS Failed," in *European Conference and Exhibition on Optical Communication*. Amsterdam, Netherlands: OSA, 2012, p. Tu.1.D.1.
- [101] R. C. Johnson, "Qualcomm reveals neural network progress," 2013. [Online]. Available: http://www.eetimes.com/document.asp?doc_id=1319767

List of acronyms

ADC	analog-to-digital converter	DCR	digital coherent receiver
ANN	artificial neural networks	DSP	digital signal processing
ASE	amplified spontaneous emission	DWDM	dense wavelength division multiplexing
ASIC	application-specific integrated circuit	EDFA	erbium-doped fiber amplifier
BER	bit error rate	EM	expectation maximization
BOI	band of interest	EVM	error vector magnitude
BPSK	binary phase shift keying	FD	frequency domain
CBR	case-based reasoning	FDE	frequency domain equalizer
CD	chromatic dispersion	FEC	forward error correction
CDS	cognitive decision system	FFT	fast Fourier transform
CHRON	Cognitive Heterogeneous Reconfigurable Optical Network	FIR	finite impulse response
CMA	constant modulus algorithm	FPGA	field-programmable gate array
CMS	control and management system	FWM	four-wave mixing
CO	coherent optical	GF	gain flatness
CON	cognitive optical network	GMM	Gaussian mixture model
CUT	channel under test	GMPLS	Generalized Multi-Protocol Label Switching
DA	data-aided	GN	Gaussian noise
DAC	digital-to-analog converter	ICI	inter-carrier interference
DBP	digital backpropagation	IP	Internet Protocol
		I/Q	in-phase/quadrature
		IR	impulse response
		ISI	inter-symbol interference

ITU	International Telecommunication Union	PDF	probability density function
ITU-T	ITU's Telecommunication Standardization Sector	PDL	polarization dependent loss
KB	knowledge base	PDM	polarization division multiplexing
LO	local oscillator	PLL	phase locked loop
LPF	low pass filter	PM	phase modulated
MFR	modulation format recognition	PMD	polarization mode dispersion
ML	machine learning	PSK	phase shift keying
MLE	maximum likelihood estimation	QAM	quadrature amplitude modulation
MMA	multi-modulus algorithm	QoS	quality of service
MPLS	Multi-Protocol Label Switching	QoT	quality of transmission
NDA	non-data-aided	QPSK	quaternary phase shift keying
NF	noise figure	RMLSA	routing, modulation format, and spectrum allocation
NMon	network monitor	ROADM	reconfigurable optical add-drop multiplexer
NMS	network monitoring system	RoF	radio-over-fiber
NRZ	non-return-to-zero	ROSNR	required optical signal-to-noise ratio
OBS	optical burst switching	RWA	routing and wavelength assignment
OFDM	orthogonal frequency division multiplexing	RZ	return-to-zero
OOK	on-off keying	SAE	software adaptable element
OPEX	operational expenditures	SDN	software-defined networking
OPM	optical performance monitoring	SDR	software-defined receiver
OPS	optical packet switching	SDT	software defined transmitter
OSC	optical supervisory channel	SE	spectral efficiency
OSNR	optical signal-to-noise ratio	SNR	signal-to-noise ratio
OTN	optical transport network	SOP	state of polarization
PAM	pulse amplitude modulation	SPM	self-phase modulation
PCE	path computation element	SSMF	standard single-mode fiber

TD	time domain	VBEM	variational Bayesian expectation maximization
TDE	time domain equalizer	WDM	wavelength division multiplexing
TIA	transimpedance amplifier	XPM	cross phase modulation
UWB	ultra wideband		

Paper [A]: Cognitive Heterogeneous Reconfigurable Optical Networks (CHRON): Enabling technologies and techniques

Idelfonso Tafur Monroy, Darko Zibar, Neil Guerrero Gonzalez, and **Robert Borkowski**. Cognitive Heterogeneous Reconfigurable Optical Networks (CHRON): Enabling technologies and techniques. In *13th International Conference on Transparent Optical Networks (ICTON)*, paper Th.A1.2, Stockholm, Sweden, June 2011. IEEE.

Cognitive Heterogeneous Reconfigurable Optical Networks (CHRON): Enabling Technologies and Techniques

Idelfonso Tafur Monroy, Darko Zibar, Neil Guerrero Gonzalez, Robert Borkowski

*DTU Fotonik, Department of Photonics Engineering, Technical University of Denmark,
DK-2800 Kgs. Lyngby, Denmark*

idtm@fotonik.dtu.dk

ABSTRACT

We present the approach of cognition applied to heterogeneous optical networks developed in the framework of the EU project CHRON: Cognitive Heterogeneous Reconfigurable Optical Network. We introduce and discuss in particular the technologies and techniques that will enable a cognitive optical network to observe, act, learn and optimizes its performance, taking into account its high degree of heterogeneity with respect to quality of service, transmission and switching techniques.

Keywords: all-optical networks, coherent communication.

1. INTRODUCTION

It is noteworthy that services such as telephony, TV broadcast, signalling, SMS, MMS, e-health (EHR), e-commerce, bank transfers and video on demand among others are expected to change their share in global market traffic in different pace during following years. The biggest increase of global internet traffic will come from advanced video services, in majority working on basis of hyper-connectivity. On the other hand it is anticipated that service providers will continue offering some of today's services and differentiate their quality according to services agreements with end users. Therefore, network operators are facing the challenge of supporting such a plethora of services with different requirements in terms of Quality of Service (QoS) as well as their optical transport networks composed of different transmission technologies in aspects such as coding and modulation formats, or data rates.

To support the heterogeneity of the service provision and the resulting traffic, it is important to utilize mixed line transmission technologies that enable the efficient migration to higher capacity systems. Moreover, in the short and medium term, single optical network architecture may simultaneously support different switching paradigms such as semi-static and dynamic circuit switching. As a consequence it is of primary importance to provide mixed transmission techniques associated with intelligent network management to be able to run new generation services on legacy networks.

Since cognitive networks typically perform cross-layer design and multi-objective optimization in order to support trade-offs between multiple goals, they also become a promising option to optimize the performance of optical networks in a cost efficient way. In addition, the use of cognitive techniques in optical networks can offer much more flexibility to telecom operators by tuning various physical layer components characteristics (modulation format, forward error correction, wavelength capacity, etc) and networking layer parameters (bandwidth, number of simultaneous lightpaths, QoS, etc) depending on application or service requirements. Thus, the CHRON architecture proposes an integrated platform to tackle the challenges stemming from the management of the future high-capacity core network [1].

2. COGNITIVE RECONFIGURABLE OPTICAL NETWORKS (CHRON)

The aim of CHRON is to develop and showcase network architecture and a control plane which efficiently use resources in a heterogeneous scenario while fulfilling QoS requirements of each type of services and applications supported by the network. For that aim, CHRON relies on cognition, so that control decisions must be made with an appropriate knowledge of current status, and supported by a learning process to improve performance with acquired experience. The physical layer of such a network reflects the current and upcoming situation faced by network operators, with high level of heterogeneity of physical interfaces and transmission systems such as modulation formats, wavelength capacity or coherent and non-coherent techniques.

Therefore, the basic conceptual network architecture of CHRON consists of the building blocks shown in Fig. 1. Basically a cognitive decision system is fed by the service and traffic demands, takes into account the current network status from a network monitoring system and learns from previous actions to output a decision to the control and management system, which forwards the commands from the cognitive system as well as offers communications between the different elements of the architecture. The knowledge base stores previous scenarios, the decisions taken and the results of those decisions. Thus, the knowledge base makes it possible to learn from past decisions taken in similar scenarios and use that learning capability to influence future behavior.

A brief summary of functions to be developed and integrated for designing future optical networks is presented below.

- Optical performance monitoring (OPM).

- Path diagnosis and quality of transmission (QoT): to identify or predict possible sources of possible anomaly observed in link characteristics by comparing it with the link design.
- Path-specific supervision and path performance optimization by jointly tuning the parameters between the transceivers.
- Energy saving.

Monitoring the physical properties of the optical signal is a key building block that provides the needed information to the network management entity. Therefore optical performance monitoring (OPM) is the required tool to face up the network challenges and comply with quality of service (QoS) requirements that fulfil user demands. Digital coherent receivers in combination with analog-to-digital converter (ADC) give a complete representation of the optical field into the electrical domain providing amplitude, phase, and polarization information from the incoming optical signal. Using that digitized signal, linear channel distortions can be fully compensated by digital signal processing (DSP) algorithms [2].

Those algorithms, after convergence sequence have reached steady state, approximate the inverse transfer function of the corresponding impairments on digital filters realization. As result, signal statistics and channel impairment properties can be extracted from mentioned adaptive process. Accordingly, OPM techniques can be successfully applied for impairment estimation taking advantage of such signal processing [3, 4], opening the door for estimation of all deterministic linear optical channel parameters like chromatic dispersion (CD), polarization mode dispersion (PMD) and polarization-dependent loss (PDL). At the same time other transmission parameters, such as amplified spontaneous emission (ASE) noise, or polarization rotation can be monitored, as long as are equalized by the converged filtering process.

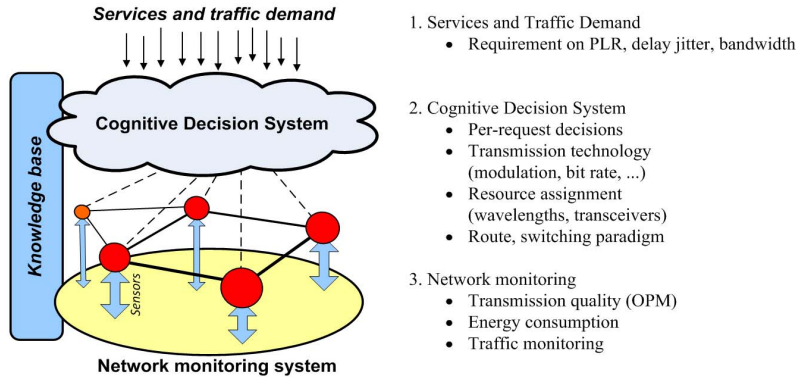


Figure 1. Main subsystems to OODA (Observe-Orient-Decide-Act) tasks.

3. COHERENT DETECTION AND DIGITAL SIGNAL PROCESSING (DSP)

Optical performance monitoring exploits the fact of having the estimated inverse optical channel response related to the filter impulse response implemented in the digital coherent receiver given an optimum adaptation process for the FIR equalizer. Furthermore, digital signal processing (DSP)-based OPM does not require any additional optical hardware and can be seamlessly combined with digital data coming from the coherent receiver. Most convenient location for an electronic CD monitoring module is alongside digital coherent receiver circuitry, in an ASIC directly located on a printed circuit board (PCB) of the device (see Fig. 2). It is also possible to build a standalone CD monitor and compensation device, a bulk compensator that would equalize CD from an electrical signal provided by the coherent receiver not equipped in on-board DSP processing unit. So far, only computer simulations of blind CD equalization realized in monitoring module preceding timing recovery stage were reported in literature [2, 4]

Depending on the nature of OPM methods, they can be divided onto two different categories, distinguishing between blind parameter estimation algorithms commonly designed as non data-aided (NDA) methods, and data-aided (DA) techniques. DA techniques have been proved to provide good performance [5] and even increased accuracy, with the drawbacks of transmission bandwidth wasted for training sequences overhead, and the severe requirements for synchronization. On the other hand, algorithms based on NDA provide a simple approach for optical parameter estimation. Also relaxed requirements for the estimations are needed, trusting typically in converged equalizer filter parameters or scanning methods.

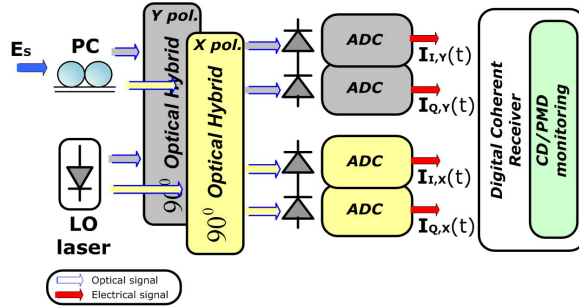


Figure 2. System model of PDM-DQPSK optical transmission with coherent detection.

4. RECONFIGURABLE DIGITAL COHERENT RECEIVERS

In addition to DSP-based OPM, algorithms for automatic signal parameters detection are required to maximize the use of channel capacity in highly heterogeneous environments [6]. Indeed, digital photonic receivers for the next generation cognitive heterogeneous reconfigurable optical networks supporting different modulation formats and bit rates must be capable of autonomous transmission-settings recognition without any prior information. The most relevant autonomous transmission-setting recognition is perhaps automatic modulation format detection (AMFD) in the current context of highly heterogeneous environments [6]. AMFD can be described as statistical process in estimating the modulation scheme of an unknown signal based on multiple hypotheses with a high probability of success in a short observation time.

Figure 3 shows a parallel between a schematic diagram of a generic cognitive process model and the corresponding automatic modulation format detection (AMFD) function integrated to the digital coherent receiver [7].

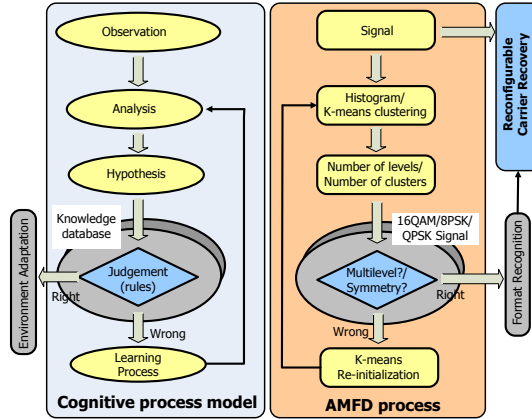


Figure 3. Schematic diagrams of cognitive process model and the automatic modulation format detection module.

AMFD is based on the statistical analysis of the signal and will provide the updating information to the carrier recovery module for subsequent demodulation. A first step is the estimation of the number of clusters (or expected m-PSK/QAM complex symbols) on the two-dimensional (2D) I&Q constellation diagram and the number of levels on the histogram (hypothesis stage). The operation of finding the number of clusters is achieved by the *k*-means clustering algorithm on the constellation diagram. According to the generic cognitive process depicted in Fig. 2 (left) a testing stage based on rules follows.

Rules for AMFD are derived according to modulation type characteristics and stored on a knowledge database. The two criteria to be judge for AMFD are the number of levels on the magnitude histogram of vectors formed by the complex data symbols, and the number of clusters on the constellation diagram.

In the case of classification between QAM and PSK signals, AMFD is based on the number of levels detected on the histogram (first rule). For AMFD among *m*-PSK modulation formats, a condition of symmetry

must be satisfied after clustering operation on the constellation diagram. If the condition is not satisfied, the initial state of the k -means algorithm (the number of expected clusters to be found) is varied. Successful automatic modulation format detection is achieved when the symmetry condition is satisfied for the number of clusters found on the constellation.

4. CONCLUSION AND FUTURE WORK

Cognitive heterogeneous reconfigurable optical networks are expected as a breakthrough technology to implement future optical communication networks in highly heterogeneous environment. Indeed, the integration of cognitive processes into the network will allow perceiving optical network conditions for optimum data-signal routing as well as efficient network management in order to optimize network resources utilization and reduce system power consumption. Most relevant research challenges to exploit the full potential of cognitive optical networks are how to implant cognitive entities (devices) into the existing optical network architecture and map intelligence into such devices. DSP-based coherent detection is a promising technology to integrate cognitive activities such as recognition, decision making, monitoring and prediction to the physical layer of the future heterogeneous optical networks.

A natural evolution for DSP may be the integration of transmitter and receiver functions over a single platform (software-define transceivers). However, at least two challenges to implement software-define transceivers can be envisaged at date: 1) Digital integration of optical-electrical components including data converters and field programmable gate arrays (FPGAs) allowing the size, cost and power consumption to be reduced and 2) algorithm design to facilitate the detection of burst of data overcoming nonlinear channel effects and the presence of non-Gaussian noise.

ACKNOWLEDGEMENTS

The research leading to these results is partially supported by the CHRON project (Cognitive Heterogeneous Reconfigurable Optical Network) with funding from the European Community's Seventh Framework Programme [FP7/2007-2013] under grant agreement n° 258644.

REFERENCES

- [1] Deliverable D2.1, Specification of the network scenario and service requirements, The European FP7 CHRON Project: Cognitive Heterogeneous Reconfigurable Optical Networks, www.ict-chron.eu.
- [2] M. Kushnerov, F. N. Hauske, K. Piyawanno, B. Spinnler, M. S. Alfiad, A. Napoli, and B. Lankl: DSP for coherent single-carrier receivers, *Journal of Lightwave Technology*, vol. 27, no. 16, pp. 3614-3622, Aug. 2009.
- [3] C. C. K. Chan: *Optical Performance Monitoring*, Elsevier, Academic Press, 2010, chapter 1, 10.
- [4] F. N. Hauske, M. Kushnerov, B. Spinnler, and B. Lankl: optical performance monitoring in digital coherent receivers, *Journal of Lightwave Technology*, vol. 27, no. 16, pp. 3623-3630, Aug. 2009.
- [5] M. Kushnerov, M. Chouayakh, K. Piyawanno, B. Spinnler, E. de Man, P. Kainzmaier, M. S. Alfiad, A. Napoli, and B. Lankl: Data-aided versus blind single-carrier coherent receivers, *IEEE Photonics Journal*, vol. 2, no. 3, pp. 387-403, Jun. 2010.
- [6] W. Su, J.L. Xu, and M. Zhou: Real-time modulation classification based on maximum likelihood, *IEEE Communications Letters*, vol. 12, no. 11, pp. 801-803, 2008.
- [7] N.G. Gonzalez, D. Zibar, I. Tafur Monroy: Cognitive digital receiver for burst mode phase modulated radio over fiber links", in *Proc. 36th European Conference on Optical Communication, ECOC'2010*, Torino, Italy, Paper P6.11, Sept. 2010.

Paper [B]: Cognition-enabling techniques in heterogeneous and flexgrid optical communication networks

Idelfonso Tafur Monroy, Antonio Caballero, Silvia Saldaña, and **Robert Borkowski**. Cognition-enabling techniques in heterogeneous and flexgrid optical communication networks. In Werner Weiershausen, Benjamin B. Dingel, Achyut K. Dutta, and Atul K. Srivastava, editors, *Optical Metro Networks and Short-Haul Systems V*, vol. 8646, San Francisco, CA, USA, December 2012. International Society for Optics and Photonics – SPIE.

Cognition-Enabling Techniques in Heterogeneous and Flexgrid Optical Communication Networks

Idelfonso Tafur Monroy, Antonio Caballero, Silvia Saldaña Cercós and Robert Borkowski
DTU Fotonik – Department of Photonics Engineering, Technical University of Denmark,
Oersteds Plads 343, 2800 Lyngby, Denmark

ABSTRACT

High degree of heterogeneity of future optical networks, such as services with different quality-of-transmission requirements, modulation formats and switching techniques, will pose a challenge for the control and optimization of different parameters. Incorporation of cognitive techniques can help to solve this issue by realizing a network that can observe, act, learn and optimize its performance, taking into account end-to-end goals. In this letter we present the approach of cognition applied to heterogeneous optical networks developed in the framework of the EU project CHRON: Cognitive Heterogeneous Reconfigurable Optical Network. We focus on the approaches developed in the project for optical performance monitoring and power consumption models to implement an energy efficient network.

Keywords: optical networks, cognition, energy consumption, optical performance monitoring

INTRODUCTION

Optical networks are nowadays becoming more heterogeneous, ranging from different types of services, switching paradigms to physical interfaces. Therefore, network operators are facing the challenge of supporting a plethora of services, each with individual requirements on quality of service (QoS) while their optical transport networks utilize different transmission technologies, such as coding, modulation formats or data rates. Moreover, in the short and medium term, a single optical network architecture may simultaneously support different switching paradigms such as semi-static and dynamic circuit switching. Hence, a key issue of highly heterogeneous networks is how to efficiently control and manage network resources while fulfilling user demands and complying with QoS requirements.

A solution for such a scenario may come from cognitive networks. A cognitive network is defined as "a network with a process that can perceive current network conditions, and then plan, decide and act on those conditions. The network can learn from these adaptations and use them to make future decisions, all while taking into account end-to-end goals"¹. Hence, a cognitive network should provide better end-to-end performance than a non-cognitive network. Cognitive networks have already shown to be a promising solution for wireless networks^{2,3}. Cognition is also applicable to optical communication architectures^{4,7} since it can offer flexibility to telecom operators by optimizing simultaneously physical layer components characteristics (modulation format, forward error correction (FEC), wavelength capacity, etc.) and network layer parameters (bandwidth, number of simultaneous lightpaths, QoS, etc.) depending on application or service requirements. Another advantage comes from a potential decrease in energy consumption by deciding how to handle new traffic demands according to the current network status provided by the monitoring system and to set devices to low power consumption mode when appropriate.

The aim of CHRON is to develop a showcase network architecture and a control plane that efficiently uses resources in a heterogeneous scenario while fulfilling QoS requirements of each type of services and applications. For that aim, CHRON relies on cognition, so that control decisions must be made with an appropriate knowledge of current status, and supported by a learning process to improve the performance with the acquired experience.

In this paper we first present the CHRON architecture and its implementation of optical performance monitoring (OPM). In section 3 we cover energy efficiency in elastic networks defining a multi-objective genetic algorithm and network modeling. We finish with conclusions and future work in section 4.

COGNITIVE HETEROGENEOUS RECONFIGURABLE OPTICAL NETWORK (CHRON)

The central element of our proposed CHRON architecture is a cognitive decision system (CDS), which contains a cognitive decision process in charge of taking decisions based on the appropriate response according to the observed network behavior. Figure 1 presents the building blocks of a module of the CDS, as well as their relationship to the network monitoring system and the control and management system. This architecture shows how the CDS implements the cognitive loop². The network monitoring system gathers the network status to a generic knowledge base. Separately, there are specific knowledge bases containing all the information associated with each of the cognitive processes. Therefore, there are as many specific knowledge bases as cognitive processes in the CDS. These data bases are updated through a specific learning module which is associated to a single cognitive process. Consequently, the cognitive process module can access these two data bases to retrieve and update them. Finally, the specific cognitive process provides the decision and action information to the control plane when request arrives. Based on this architecture, a robust optical signal monitoring needs to be developed in order to feed the CDS and implement this intelligence into the network.

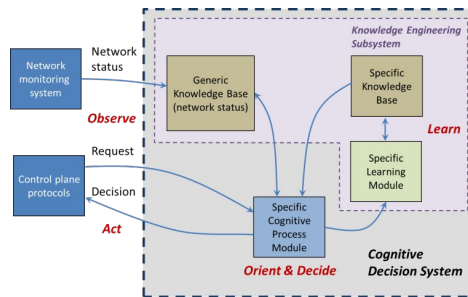


Figure 1. Building blocks of the cognitive decision system as defined in the CHRON project

Optical signal monitoring

OPM is a basic mechanism providing inputs to the cognitive processes. In traditional scenarios, OPM is performed by monitoring the signal tapped before the receiver with devices such as an oscilloscope or an optical spectrum analyzer⁸. Combining the advantage of coherent detection, where both amplitude and phase are recovered with digital sampling and signal processing, forms an inexpensive and robust alternative to traditional OPM methods. Figure 2 a) shows placement of an OPM subsystem in the digital signal processing (DSP) module of a coherent receiver. The received optical field is transferred into electrical domain for further treatment with DSP algorithms. In the sense used here, monitoring can be understood twofold: 1) as the observation of the received signal performance parameters that indicate the detrimental effects of the signal generation, fiber-optic transmission and reception (OPM); and 2) as the analysis of the received signal to enable advanced functionalities of the receiver such as reconfiguration of the software-defined digital coherent receiver.

Typical performance indicators used in the digital communication systems include quality factor Q^2 , error vector magnitude (EVM), modulation error ratio (MER), or pre- and ultimately post- FEC bit error rate (BER). Those are, however, synthetic indicators where information about the contribution of each specific impairment affecting the signal is lost. Since in a digital coherent receiver it is possible to compensate deterministic linear impairments, it is highly desirable to separate the influence of all impairments acting upon the signal in order to efficiently mitigate them in DSP.

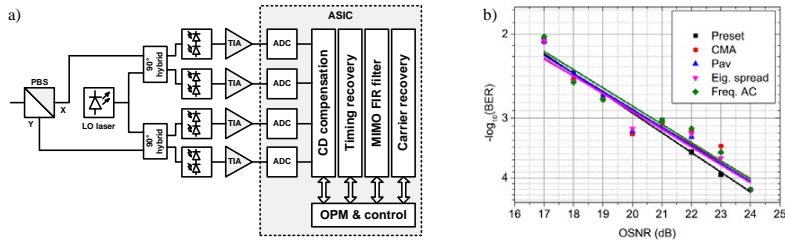


Figure 2. a) Typical structure of a digital coherent receiver with CD monitoring and equalization block. b) BER curves as a function of OSNR showing performance of different CD compensation methods¹⁰. Methods: Preset – reference; CMA – constant modulus algorithm; Pav – mean signal power; Eig. spread – eigenvalue spread; Freq. AC – frequency spectrum autocorrelation.

Most of impairments that affect the signal performance in the coherent fiber-optic transmission system are listed in Table 1, which includes effects originating in the transmitter, fiber-optic link and the receiver⁹. OPM techniques can be divided into data-aided (DA) and non-data-aided (NDA). Comparison between both approaches is shown in Table 2.

Table 1. Important impairments in a fiber-optic coherent transmission system

Transmitter	Link
In-phase/quadrature (I/Q) imbalance	Amplifier spontaneous emission (ASE)
Electrical saturation/clipping in the generation stage	Chromatic dispersion (CD)
	Differential group delay (DGD)
	Polarization mode dispersion (PMD)
Receiver	Polarization dependent loss (PDL)
Timing misalignment	Nonlinear effects due to high input power
Local oscillator offset	Linear and nonlinear effects due to copropagation
Polarization mixing angle	

Table 2. Summary of advantages and disadvantages of NDA and DA techniques for digital OPM⁹.

	Data-aided	Non-data-aided
Pros	High accuracy Guaranteed convergence Short convergence length	No training overhead Compatible with legacy nodes Efficient for short memory channels
Cons	Training overhead Incompatible with legacy nodes	Long convergence time Inferior accuracy

In DA approach, a training sequence (TS) is transmitted along the message. Based on the received TS and knowing the ideal transmitted TS, the receiver can estimate the transfer function of the system (zero-forcing solution). This allows for accurate channel monitoring. The NDA approach on the other hand does not use any predefined sequences and relies on

statistics of random transmitted data. An example of blind estimation performance is shown in Figure 2.b) for CD estimation of PDM-QPSK system after 80 km of fiber transmission using four different estimation methods¹⁰.

Another important contribution in the monitoring subsystem is the modulation format recognition (MFR) which enables software-defined algorithms of the receiver. Since for every modulation format the algorithms that shall be applied for optimal signal demodulation differ slightly, the MFR block shall continually observe the signal to determine the modulation format used and load the appropriate software. At the same time it allows for a fallback solution if the monitored impairments exceed marginal values and cannot be compensated.

At the same time MFR allows for operation of dynamically switched networks in which the arriving signal may be of unknown nature and the receiver has to determine the way to demodulate it.

COGNITION TO DESIGN ENERGETICALLY EFFICIENT OPTICAL NETWORKS

The upcoming focus of research on increasing the network capacity, leads to an increase in power consumption as well. However, there is a gap between the pace of reduction of the total energy needed to transmit end-to-end a single bit of information and the network traffic growth. Therefore, despite current researches achieve an annual decrease of 10% in the total energy per bit¹¹, it is estimated 34% annual growth in the traffic demand, consequently, the overall energy consumed per user has grown. Thus, energy efficiency has become a major concern among optical network research community to meet the current traffic demands. There are two complementary research lines to cope with the arising energy efficiency challenges: Firstly, devising a model to estimate the overall power consumption and secondly, designing and implementing algorithms aiming at minimizing the overall network power consumption. Both lines have to take into consideration that energy consumption has an impact on backbone telecommunication networks in a multilayer manner¹². Thus, while modeling and discourse upon power consumption it is important to define the most power-hungry elements and contributors within cross-layers approaches.

The proposed CHRON architecture provides enhanced benefits compared to traditional optical networks, due to the fact that relies on cognition to manage and handle energy efficiency from a network design and operation perspectives. This is achieved by a rearrangeable architecture which accommodates mixed transmission techniques, where different bit rates and advanced modulation formats are employed, such as 10 Gbps non return to zero-on off keying (NRZ-OOK), 40 Gbps return to zero-differential phase shift keying (RZ-DPSK) and 100 Gbps polarization division multiplexed-QPSK (PDM-QPSK). Based on a self-learning process, physical interfaces and transmission systems are adjusted dynamically to improve performance in terms of energy efficiency while ensure QoS and quality-of-transmission (QoT).

Within CHRON scenario, different work has been carried out. In the first stage, power consumption network modeling has been assessed, offering a comparison between flex-grid OFDM and fixed grid WDM to offer bandwidth elasticity^{13,14}. The second line investigated within this project focuses on wavelength-routed optical networks (WRONs), where genetic algorithms are used to reduce power consumption⁴.

Bandwidth elasticity

There are several tradeoffs concerning power consumption in the network design environment. Among them, there is the compromise between spectral efficiency and energy efficiency. Investigations on energy efficiency network upgrade problem are assessed. It has been presented a multi-line rate (MLR) scheme with 10, 40 and 100 Gbps demonstrating its cost-effective and energy-efficient approach compared to single line rate (SLR) scheme¹⁵. Using MLR optical network as a scenario, it is demonstrated that between disruptive and non-disruptive upgrades, non-disruptive approach for network upgrade presents lower cost but higher energy consumption than the disruptive case.

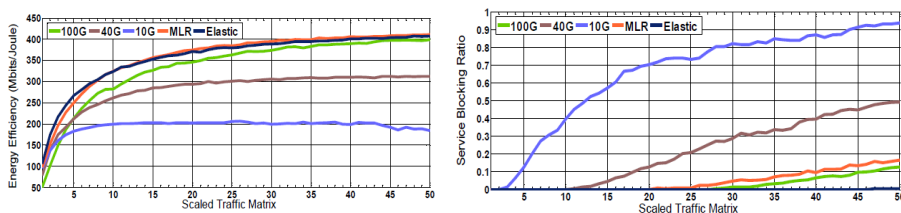


Figure 3. a) DT Network: Energy efficiency b) DT Network: Service blocking ratio

Within CHRON framework, an energy consumption simulation for flex-grid OFDM and fixed-grid WDM (for both SLR and MLR) has been presented^{12, 13}. This work shows that OFDM is more energy-efficient in a traffic demand time-varying scenario. Validation is done in two different network topologies with different geographical spans: 1) a Deutsche Telekom network (Germany), and 2) GEANT-2 network (Europe). As shown in Figure 3, better results for OFDM are obtained compared to fixed WDM. Besides reducing the blocking ratio while having high volume of traffic, its fine granularity and use of different modulation formats allows a decreased number of really energy-hungry transmission regenerators. Dynamic-routing heuristic algorithms have also been implemented and carried out to check performance in terms of energy efficiency.

Multi-objective genetic algorithm on network layer

Reduction of energy consumption is usually accompanied by an increase of network congestion, higher blocking ratio or a decrease of spectral efficiency. These trades off have raised the need for implementing multi-objective algorithms. Within the cognitive reconfigurable environment, genetic algorithms have been analyzed and validated by simulation tools in order to minimize the energy consumption while complying with other network requirements such as capacity demands, delay or QoT⁴. The novel genetic algorithm developed within CHRON project⁴ conceives a design of the logical topology without considering the impact of physical parameters such as modulation format. The two-layered architecture presented in this paper is meant to develop a method to reduce the energy consumption¹⁸.

Power consumption modeling

As it is presented above, for both elastic networks or for implementing multi-objective optimization tools, it is necessary to devise an end-to-end energy consumption model for heterogeneous transmission links with mixed modulation formats and bit rates. This model is under development within CHRON to be included as a building block of a self-learning cognitive network as a network optimization tool.

CONCLUSION AND FUTURE WORK

Cognitive heterogeneous reconfigurable optical networks are expected as a breakthrough technology to implement future optical communication networks in highly heterogeneous environment. In this paper we have described the approach followed in the CHRON project to include cognitive techniques in order to efficiently control and manage the network to optimize network resources utilization and reduce system energy consumption. In this context, there are several research lines that CHRON is working with. In optical performance monitoring, the development of robust algorithms for signal monitoring is being investigated to provide accurate and fast information to the cognitive decision system on the status of the physical layer. The optimization of the network with respect to energy consumption is also being investigated in CHRON, to provide an accurate end-to-end model of the energy consumption to the network and, together with the development of algorithms, to include the energy consumption in the multi-objective optimization.

ACKNOWLEDGEMENT

The research leading to these results was partly supported by the CHRON project (Cognitive Heterogeneous Reconfigurable Optical Network) with funding from the European Community's Seventh Framework Program [FP7/2007-2013] under grant agreement n° 258644.

REFERENCES

- [1] Thomas, R. W., Friend, D. H., Dasilva, L. A. & Mackenzie, A. B., "Cognitive networks: adaptation and learning to achieve end-to-end performance objectives," *IEEE Commun. Mag.*, 44(12), 51-57, (2006).
- [2] MacKenzie, A., Reed, J., Athanas, P., Bostian, C., Buehrer, R., DaSilva, L., Ellingson, S., Hou, Y., Hsiao, M., Park, J.-M., Patterson, C., Raman, S. & da Silva, C. "Cognitive Radio and Networking Research at Virginia Tech," *Proc. IEEE*, 97, 660-688 (2009).
- [3] Devroye N., Vu M., and Tarokh V., "Cognitive radio networks," *IEEE Signal Process. Mag.*, 25(6), 12-23 (2008).
- [4] Durán, R.J., de Miguel, I., Merayo, N., Sánchez, D., Angelou, M., Aguado, J.C., Fernández, P., Jiménez, T., Lorenzo, R.M., Tomkos, I., Abril E.J. and Fernández, N., "Cognition to Design Energetically Efficient and Impairment Aware Virtual Topologies for Optical Networks," in *Proc. ONDM*, 1-6. (2012)
- [5] Zervas G. S. and Simeonidou, D., "Cognitive optical networks: Need, requirements and architecture," in *Proc. ICTON We.C1.3* (2010).
- [6] Zervas, G., Baniyas, K., Rofoee, B. R., Amaya, N. and Simeonidou, D., "Multi-core, multi-band and multi-dimensional cognitive optical networks: An architecture on demand approach," in *Proc. ICTON* (2012).
- [7] Wei, W., Wang, C. and Yu, J., "Cognitive optical networks: key drivers, enabling techniques, and adaptive bandwidth services," *IEEE Comm. Mag.*, 50(1), 106-113 (2012).
- [8] Chan, C. K., Optical performance monitoring: advanced techniques for next-generation photonic networks, Elsevier (2010).
- [9] Kuschnerov, M., Hauske, F., Piyawanno, K., Spinnler, B., Alfiad, M., Napoli, A. and Lankl, B., "DSP for Coherent Single-Carrier Receivers," *IEEE/OSA J. Lightw. Technol.*, 27(16) 3614-3622 (2009).
- [10] Borkowski, R., Zhang, X., Zibar, D., Younce, R. and I. Tafur Monroy, "Experimental demonstration of adaptive digital monitoring and compensation of chromatic dispersion for coherent DP-QPSK receiver," *Opt. Express* 19, B728-B735 (2011).
- [11] Tucker, R. S., Parthiban, R., Baliga, J., W. A. Ayre R. and Sorin, W. V. "Evolution of WDM Optical IP Networks: A Cost and Energy Perspective," *IEEE/OSA J. Lightw. Technol.*, 27(3), 243-252, (2009).
- [12] Van Heddeghem, W., Idzikowski, F., Vereecken, W., Colle, D., Pickavet, M. and Demeester, P. "Power consumption modeling in optical multilayer networks," *Photonic Network Communications*, 23(1), 1-15, (2012).
- [13] Ye Y., Tafur Monroy, I and López Vizcaíno, J., "Energy efficiency in elastic-bandwidth optical networks," in *Proc. NOF 7a.02* (2011).
- [14] Ye Y., Monroy, I. T. and López Vizcaíno, J., "Energy efficiency analysis for dynamic routing in optical transport networks," in *Proc. ICC ONS01.04* (2012).
- [15] Nag, A., Tornatore, M., Wang, T. and Mukherjee, B., "Energy-efficient capacity upgrade in optical networks with mixed line rates," in *Proc. OFC OM2G.2* (2012).
- [16] Borkowski, R., Karinou, F., Angelou, M., Arlunno, V., Zibar, D., Klonidis, D., Gonzalez, N. G., Caballero, A., Tomkos, I. and Monroy, I. T., "Experimental Demonstration of Mixed Formats and Bit Rates Signal Allocation for Spectrum-flexible Optical Networking," in *Proc. OFC OW3A.7* (2012).
- [17] Shen, G. and Tucker, R., "Energy-minimized design for IP over WDM networks," *IEEE/OSA J. Optical Comm. and Network.*, 1(1) 176-186 (2009).

Paper [C]: Performance monitoring techniques supporting cognitive optical networking

Antonio Caballero, **Robert Borkowski**, Darko Zibar, and Idelfonso Tafur Monroy. Performance monitoring techniques supporting cognitive optical networking. In *15th International Conference on Transparent Optical Networks (ICTON)*, paper Tu.B1.3, Cartagena, Spain, June 2013. IEEE.

Performance Monitoring Techniques Supporting Cognitive Optical Networking

Antonio Caballero, Robert Borkowski, Darko Zibar and Idelfonso Tafur Monroy

DTU Fotonik – Department of Photonics Engineering, Technical University of Denmark,
Oersteds Plads 343, 2800 Lyngby, Denmark

Tel: (+45) 4525 5173, Fax (+45) 4593 6581, e-mail: acaj@fotonik.dtu.dk

ABSTRACT

High degree of heterogeneity of future optical networks, such as services with different quality-of-transmission requirements, modulation formats and switching techniques, will pose a challenge for the control and optimization of different parameters. Incorporation of cognitive techniques can help to solve this issue by realizing a network that can observe, act, learn and optimize its performance, taking into account end-to-end goals.

In this letter we present the approach of cognition applied to heterogeneous optical networks developed in the framework of the EU project CHRON: Cognitive Heterogeneous Reconfigurable Optical Network. We focus on the approaches developed in the project for optical performance monitoring, which enable the feedback from the physical layer to the cognitive decision system by providing accurate description of the performance of the established lightpaths.

Keywords: optical networks, cognition, dynamic optical networks, optical performance monitoring.

1. INTRODUCTION

Optical networks are nowadays becoming more heterogeneous, ranging from different types of services, switching paradigms to physical interfaces. Therefore, network operators are facing the challenge of supporting a plethora of services, each with individual requirements on quality of service (QoS). Operators have also available different transmission technologies for their optical transport networks, such as coding, modulation formats or data rates. Moreover, in the short and medium term, optical networks may simultaneously support different switching paradigms such as semi-static and dynamic circuit switching. Hence, a key issue of highly heterogeneous networks is how to efficiently control and manage network resources while fulfilling user demands and complying with QoS requirements.

A solution for such a scenario may come from cognitive networks. A cognitive network is defined as “a network with a process that can perceive current network conditions, and then plan, decide and act on those conditions. The network can learn from these adaptations and use them to make future decisions, all while taking into account end-to-end goals” [1]. Hence, a cognitive network should provide better end-to-end performance than a non-cognitive network. Cognitive paradigm have already shown to be a promising solution for wireless networks [1,2]. Cognition is also applicable to optical communication architectures [3-5], since it can offer flexibility to telecom operators by optimizing simultaneously physical layer components’ characteristics (modulation format, forward error correction – FEC, wavelength capacity, *etc.*) and network layer parameters (bandwidth, number of simultaneous lightpaths, QoS, *etc.*) depending on application or service requirements.

The aim of CHRON is to develop a showcase network architecture and a control plane that efficiently uses resources in a heterogeneous scenario, while fulfilling the QoS requirements of each type of services. To achieve this goal, CHRON relies on cognition, so that control decisions must be made with an appropriate knowledge of current status, and supported by a learning process to improve the performance with the acquired past knowledge. In this paper, we present in Section 1.1 the global CHRON architecture. In Section 2 we describe the approaches followed in CHRON for optical performance monitoring (OPM). In Section 3 we describe a Quality-of-Transmission (QoT) estimator that combines OPM with cognition. We finish with conclusions and future work in Section 4.

1.1 CHRON Architecture

The central element of our proposed CHRON architecture is a cognitive decision system (CDS). CDS runs a generic cognitive decision process which is in charge of taking decisions, which are in turn based on the observed network behavior. Figure 1 presents the building blocks of the CDS module, as well as their relationship to the network monitoring system and the control and management system. This architecture shows how the CDS implements the cognitive loop [1]. The network monitoring system gathers the network status and store it into a generic knowledge database. Separately, there are several specific knowledge databases, containing all the information associated with each of the cognitive processes. Therefore, there are as many specific knowledge databases as cognitive processes in the CDS. These databases are updated through a specific learning module, which is associated to a single cognitive process per database. Consequently, the cognitive process module can access the general and specific databases to retrieve and update them. Finally, the specific cognitive

process provides the decision and action information to the control plane when request arrives. Based on this architecture, a robust optical signal monitoring needs to be developed in order to feed the CDS with information and implement intelligence into the network.

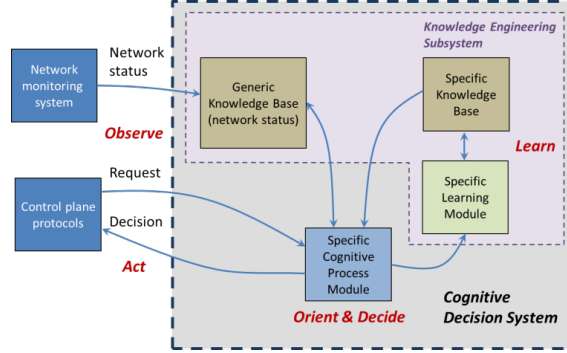


Figure 1. Building blocks of the cognitive decision system as defined in the CHRON project.

2. OPTICAL PERFORMANCE MONITORING

OPM is a basic mechanism providing inputs to the cognitive processes. In traditional scenarios, OPM is performed by monitoring the signal tapped before the receiver with devices such as an oscilloscope or an optical spectrum analyzer [6]. Combining the advantage of coherent detection, where both amplitude and phase are recovered with digital sampling and signal processing, forms an inexpensive and robust alternative to traditional OPM methods. Figure 2a) shows location of an OPM subsystem in the digital signal processing (DSP) module of a coherent receiver. The received optical field is transferred into electrical domain for further treatment with DSP algorithms. In the sense used here, monitoring can be understood twofold: 1) observation of the received signal performance parameters that indicate detrimental effects of signal generation, fiber-optic transmission and reception (OPM); and 2) observation of the received signal to enable advanced receiver functionalities, such as reconfiguration of the software-defined digital coherent receiver.

Typical performance indicators used in the digital communication systems include quality factor Q^2 , error vector magnitude (EVM), modulation error ratio (MER), or pre- and ultimately post-FEC bit error rate (BER). Those are, however, synthetic indicators where information about the contribution of each specific impairment affecting the signal is lost. Since in a digital coherent receiver it is possible to compensate deterministic linear impairments, it is highly desirable to separate the influence of all impairments acting upon the signal in order to efficiently mitigate them in DSP. Most of impairments that affect the signal performance in the coherent fiber-optic transmission system are listed in Table 1, which includes effects originating in the transmitter, fiber-optic link and the receiver [7]. OPM techniques can be divided into data-aided (DA) and non-data-aided (NDA). Comparison between both approaches is shown in Table 2.

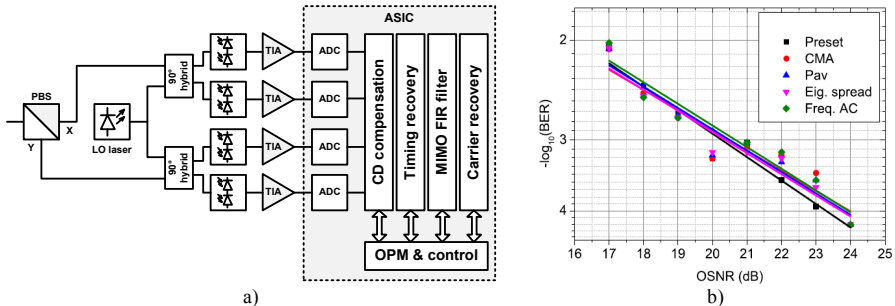


Figure 2: a) Typical structure of a digital coherent receiver with CD monitoring and equalization block; b) Performance of different CD compensation methods [8]. Methods: Preset – reference; CMA – constant modulus algorithm; Pav – mean signal power; Eig. spread – eigenvalue spread; Freq. AC – frequency spectrum autocorrelation.

Table 1. Important impairments in a fiber-optic coherent transmission system

Transmitter	Link
In-phase/quadrature (I/Q) imbalance Electrical distortion in the generation stage	Amplifier spontaneous emission (ASE) Chromatic dispersion (CD) Differential group delay (DGD) Polarization mode dispersion (PMD) Polarization dependent loss (PDL) Nonlinear effects due to high input power Linear and nonlinear effects due to co-propagation
Receiver	
Timing misalignment Local oscillator offset Polarization mixing angle	

Table 2. Summary of advantages and disadvantages of NDA and DA techniques for digital OPM [7].

	Data-aided	Non-data-aided
Pros	High accuracy Guaranteed convergence Short convergence length	No training overhead Compatible with legacy nodes Efficient for short memory channels
Cons	Training overhead Incompatible with legacy nodes	Long convergence time Inferior accuracy

In DA approach, a training sequence (TS) is transmitted along the message. Based on the received TS and knowing the ideal transmitted TS, the receiver can estimate the transfer function of the system (zero-forcing solution). This allows for accurate channel monitoring [9,10]. The NDA approach on the other hand does not use any predefined sequences and relies on statistics of random transmitted data. An example of blind estimation performance is shown in Fig. 2b) for CD estimation of polarization division multiplexed (PDM) quadrature phase shift keying (QPSK) system after 80 km of fiber transmission using four different estimation methods [8].

Another important contribution in the monitoring subsystem is the modulation format recognition (MFR) which enables software-defined algorithms of the receiver. Since for every modulation format the algorithms that shall be applied for optimal signal demodulation differ slightly, the MFR block shall continually observe the signal to determine the modulation format used, and use the most optimal DSP algorithms. At the same time MFR allows for operation of dynamically switched networks in which the arriving signal may be of unknown nature and the receiver has to determine the way to demodulate it. We have developed a technique for modulation format recognition that is insensitive to frequency offset and polarization mixing based on Stokes space receiver and Bayesian expectation maximization and Gaussian mixture models [11]. Figure 3 shows the experimental results for PDM-QPSK and PDM-16-quadrature and amplitude modulation (PDM-16QAM) demodulated and the corresponding clustering identification using the Stokes space MFR.

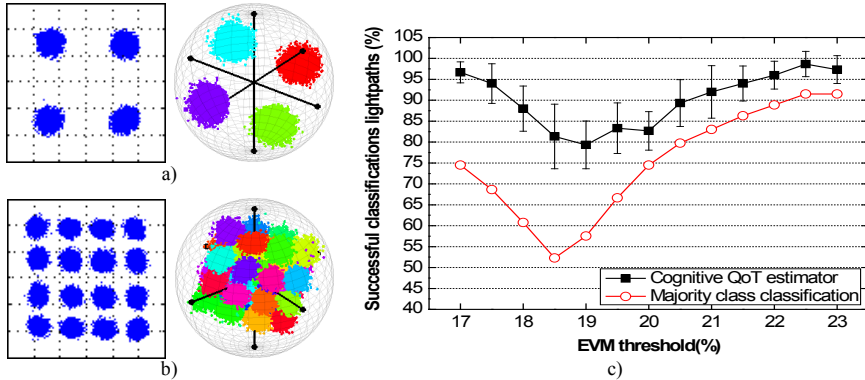


Figure 3. Modulation format recognition in Stokes space, experimental results for: a) DP-QPSK b) DP-16QAM; c) Experimental demonstration of QoT based on CBR for PD-QPSK WDM networks with high successful ratio for small KB [13].

3. QUALITY-OF-TRANSMISSION ESTIMATOR

The aim of the QoT estimator is to make a prediction of signal quality of the new lightpaths to be established in the network and to address its impact on existing connections. The approach of CHRON combines the

information of past history and the feedback from the network monitoring system. This information may be used to update its knowledge base and thus adapt to changing conditions, like component ageing or substitution.

The cognitive operation of this module relies on the utilization of a data mining technique called case-based reasoning (CBR). The CBR approach achieves more than 99% successful classifications of optical connections, and is much faster for on-line operation than an existing non-cognitive approach, thus demonstrating the advantages of cognition. In [12] the basic cognitive QoT estimator was enhanced by including learning and forgetting capabilities. These capabilities are used to optimize the set of experiences stored in the knowledge base, and thus to improve performance accelerating the classification procedure by an order of magnitude. The CBR QoT estimator was experimentally validated in [13]. We implemented a wavelength division multiplexed, homogeneous point-to-point optical transmission system consisting of 5 channels carrying 80 Gb/s PDM-QPSK, with a number of adjustable parameters such as: optical launch power, fiber link length, and number of co-propagating channels, in order to support different lightpath and system configurations. The estimator performance is shown in Fig. 3c), where a total of 150 different link configurations were measured and channel error-vector magnitude (EVM) calculated. The estimator was able to show high successful classification ratio, over 75% even for small KB of only 150 cases.

4. CONCLUSION AND FUTURE WORK

Cognitive heterogeneous reconfigurable optical networks are expected as a breakthrough technology to implement future optical communication networks in highly heterogeneous environment. In this paper we have described the approach followed in the CHRON project to include cognitive techniques in order to efficiently control and manage an optical network. In this context, there are several research lines that CHRON is working on. In optical performance monitoring, the development of robust algorithms for signal monitoring is being investigated to provide accurate and fast information to the cognitive decision system on the status of the physical layer.

ACKNOWLEDGMENT

The research leading to these results was partly supported by the CHRON project (Cognitive Heterogeneous Reconfigurable Optical Network) with funding from the European Community's Seventh Framework Program [FP7/2007-2013] under grant agreement n° 258644.

REFERENCES

- [1] R. W. Thomas *et al.*: Cognitive networks: adaptation and learning to achieve end-to-end performance objectives, *IEEE Commun. Mag.*, vol. 44 no. 12, pp. 51-57, 2006.
- [2] N. Devroye *et al.*: Cognitive radio networks, *IEEE Signal Process. Mag.*, vol. 25 no. 6, pp. 12-23 (2008).
- [3] R. J. Durán *et al.*: Cognition to Design Energetically Efficient and Impairment Aware Virtual Topologies for Optical Networks, in *Proc. ONDM*, 1-6, 2012.
- [4] G. S. Zervas and D. Simeonidou: Cognitive optical networks: Need, requirements and architecture, in *Proc. ICTON 2010*, paper We.C1.3.
- [5] W. Wei *et al.*: Cognitive optical networks: key drivers, enabling techniques, and adaptive bandwidth services, *IEEE Comm. Mag.*, vol. 50, pp. 106-113, 2012.
- [6] C. K. Chan: Optical performance monitoring: Advanced techniques for next-generation photonic networks, ed. Elsevier, 2010.
- [7] M. Kushnerov *et al.*: DSP for Coherent Single-Carrier Receivers, *IEEE/OSA J. Lightw. Technol.*, vol. 27, pp. 3614-3622, 2009.
- [8] R. Borkowski *et al.*: Experimental demonstration of adaptive digital monitoring and compensation of chromatic dispersion for coherent DP-QPSK receiver, *Opt. Express* vol. 19, pp. B728-B735, 2011.
- [9] F. Pittala *et al.*: Data-aided frequency-domain channel estimation for CD and DGD monitoring in coherent transmission systems, in *Proc. Photonics Conference (PHO) 2011*, pp. 897-898, Oct. 2011.
- [10] F. Pittala *et al.*: Joint PDL and in-band OSNR monitoring supported by data-aided channel estimation, in *Proc. OFC/NFOEC 2012*, Mar. 2012, paper OW4G.2.
- [11] R. Borkowski *et al.*: Optical modulation format recognition in Stokes space for digital coherent receivers, in *Proc. OFC/NFOEC 2013*, Mar. 2013, paper OTh3B.3.
- [12] T. Jiménez *et al.*: A cognitive quality of transmission estimator for core optical networks, *IEEE/OSA J. Lightw. Technol.*, vol. 31, pp. 942-951, 2013.
- [13] A. Caballero *et al.*: Experimental demonstration of a cognitive quality of transmission estimator for optical communication systems, *Opt. Express*, vol. 20, pp. B64-B70, 2012.

Paper [D]: Cognitive, heterogeneous and reconfigurable optical networks: the CHRON project

Antonio Caballero, **Robert Borkowski**, Ignacio de Miguel, Ramón J. Durán, Juan Carlos Aguado, Natalia Fernández, Tamara Jiménez, Ignacio Rodríguez, David Sánchez, Rubén M. Lorenzo, Dimitrios Klonidis, Eleni Palkopoulou, Nikolaos P. Diamantopoulos, Ioannis Tomkos, Domenico Siracusa, Antonio Francescon, Elio Salvadori, Yabin Ye, Jorge López Vizcaíno, Fabio Pittalà, Andrzej Tymecki, and Idelfonso Tafur Monroy. Cognitive, heterogeneous and reconfigurable optical networks: the CHRON project. *IEEE/OSA Journal of Lightwave Technology*, vol. 32, no. 13, pp. 2308–2323, July 2014. IEEE.

Cognitive, Heterogeneous and Reconfigurable Optical Networks: The CHRON Project

Antonio Caballero, Robert Borkowski, Ignacio de Miguel, Ramón J. Durán, Juan Carlos Aguado, Natalia Fernández, Tamara Jiménez, Ignacio Rodríguez, David Sánchez, Rubén M. Lorenzo, Dimitrios Klonidis, Eleni Palkopoulou, Nikolaos P. Diamantopoulos, Ioannis Tomkos, Domenico Siracusa, Antonio Francescon, Elio Salvadori, Yabin Ye, Jorge López Vizcaíno, Fabio Pittalà, Andrzej Tymecki, and Idelfonso Tafur Monroy

Abstract—High degree of heterogeneity of future optical networks, stemming from provisioning of services with different quality-of-transmission requirements, and transmission links employing mixed modulation formats or switching techniques, will pose a challenge for the control and management of the network. The incorporation of cognitive techniques can help to optimize a network by employing mechanisms that can observe, act, learn and improve network performance, taking into account end-to-end goals. The EU project CHRON: Cognitive Heterogeneous Reconfigurable Optical Network proposes a strategy to efficiently control the network by implementing cognition. In this paper we present a survey of different techniques developed throughout the course of the project to apply cognition in future optical networks.

Index Terms—Cognition, cognitive networks, energy consumption, heterogeneous optical networks, optical performance monitoring (OPM).

I. INTRODUCTION

NETWORK operators are facing the challenge of supporting a plethora of services, each with individual requirements on quality of service (QoS). At the same time, their

optical transport networks utilize many diverse transmission technologies concurrently: different modulation formats, data rates, transmission grids or coding schemes [1]–[3]. Thus, optical networks are nowadays becoming more heterogeneous, both in terms of supported services and physical interfaces. Moreover, in the short and medium term, a single optical network architecture will need to simultaneously support different switching paradigms such as semi-static and dynamic circuit switching.

A solution for the control of those heterogeneous networks comes from the use of cognitive networks [4]–[6]. A cognitive network is defined as “a network with a process that can perceive current network conditions, and then plan, decide, and act on those conditions. The network can learn from these adaptations and use them to make future decisions, all while taking into account end-to-end goals” [4]. Hence, a cognitive network should provide better end-to-end performance than a non-cognitive network. In fact, cognitive networks have already shown to be a promising solution for wireless networks [5]–[7]. Nonetheless, this paradigm is also applicable to optical communication architectures [1]–[3], [8] and offers flexibility to telecom operators by jointly optimizing aspects of the underlying physical layer (modulation format, forward error correction, wavelength, etc.) and network layer parameters (bandwidth, number of simultaneous lightpaths, latency, etc.) depending on application or service requirements to support determined objective (e.g. maintain QoS level). Furthermore, the energy consumption of the network can be decreased by deciding how to handle new traffic demands according to the current network status provided by the monitoring system and to set devices to low power consumption mode when appropriate.

Cognitive networks involve the utilization of three different types of elements [8]: monitoring elements, enabling the network to be aware of current conditions; software adaptable elements, enabling the network to adapt to changing conditions; and cognitive processes, which learn or make use of past history to improve performance. Cognitive processes are typically based on machine learning techniques [9], consisting of a number of mechanisms such as neural networks, genetic algorithms, ant colony optimization and learning automata, to name just a few.

Most of the work on cognitive networks has been done in the context of radio communications [5]–[7], to obtain seamless adaptation of radio link parameters: improved utilization of the wireless spectrum, modulation and waveform

Manuscript received September 20, 2013; revised December 17, 2013 and March 18, 2014; accepted April 2, 2014. Date of publication April 20, 2014; date of current version June 20, 2014. This work was supported in part by the European Community's FP7/2007–2013 Programme, CHRON Project, under Grant 258644 and the Spanish Ministry of Science and Innovation (TEC2010–21178-C02-02).

A. Caballero, R. Borkowski, and I. T. Monroy are with the DTU Fotonik, Technical University of Denmark, 2800 Kongens Lyngby, Denmark (e-mail: antonio.caballero@accacia-inc.com; rbor@fotonik.dtu.dk; idtm@fotonik.dtu.dk).

I. de Miguel, R. J. Durán, J. C. Aguado, N. Fernández, T. Jiménez, I. Rodríguez, D. Sánchez, and R. M. Lorenzo are with the Universidad de Valladolid, 47002 Valladolid, Spain (e-mail: ignacio.miguel@tel.uva.es; rduran@tel.uva.es; jaguado@tel.uva.es; nfersor@delibes.tel.uva.es; tamara.jimenez@tel.uva.es; irodper@ribera.tel.uva.es; dscarabias@gmail.com; rublor@tel.uva.es).

D. Klonidis, E. Palkopoulou, N. P. Diamantopoulos, and I. Tomkos are with the Athens Information Technology, GR-19002 Peania, Greece (e-mail: dkl@ait.gr; elenip@ait.gr; nidi@ait.gr; itom@ait.edu.gr).

D. Siracusa, A. Francescon, and E. Salvadori are with CREATE-NET, 38123 Trento, Italy (e-mail: domenico.siracusa@create-net.org; antonio.francescon@create-net.org; elio.salvadori@create-net.org).

Y. Ye, J. L. Vizcaíno, and F. Pittalà are with the European Research Center, Huawei Technologies, 80992 Munich, Germany (e-mail: yeyabin@huawei.com; Jorge.vizcaino@huawei.com; Fabio.Pittalà@huawei.com).

A. Tymecki is with Orange Labs, 02-691 Warsaw, Poland (e-mail: Andrzej.Tymecki@orange.com).

Color versions of one or more of the figures in this paper are available online at <http://ieeexplore.ieee.org>.

Digital Object Identifier 10.1109/JLT.2014.2318994

selection to adapt to the current wireless environment, and their integration into the network that intelligently takes end-to-end goals into account. However, several cognitive architectures have been also proposed that are applicable to wired networks [4], [10]. In the particular case of optical communications, various proposals are targeting cognitive dynamic optical networks, such as Zervas and Simeonidou [3], Wei *et al.* [2], and the CHRON project [1], [8], [11]; these architectures show that cognition can be implemented in different dimensions, in terms of devices and protocol layers [8].

The aim of CHRON [11] is to develop and showcase a network architecture and a control plane that efficiently uses resources in a heterogeneous scenario while fulfilling the QoS requirements of each type of service and application. To achieve that goal, CHRON relies on cognition, so that control decisions must be made with appropriate knowledge of current status, supported by a learning process to improve the performance with the acquired experience.

In this paper, we present a survey of the CHRON approach for cognitive optical networks. First of all, we define the concept of cognition applied to optical networks. Then, in Section II, we describe the CHRON architecture, including an explanation of different modules of its core element, the cognitive decision system (CDS). In Section III, we describe operation techniques developed in the project. Section IV is focused on novel optical performance monitoring (OPM) techniques for heterogeneous networks developed in CHRON. We conclude with Section V: a future outlook for cognitive optical networks.

II. CHRON ARCHITECTURE

The CHRON project proposes a strategy to efficiently control the network by cognitively taking decisions on the most efficient use of its resources to match the best transmission and switching technology to satisfy the end-to-end service requirements. The focus of the CHRON project is on a reconfigurable transport optical network, where a reconfigurable virtual topology by means of optical connections (lightpaths) is established, which can accommodate new traffic demands by routing them through existing lightpaths, establishing new lightpaths or reconfiguring the virtual topology to better adapt to current network conditions. Moreover, additional lightpaths can be added/removed on user demand, for instance to provide private circuit services. The physical layer of such a network reflects the current and upcoming situation faced by network operators, with high level of heterogeneity of physical interfaces and transmission systems in terms such as modulation formats, wavelength capacity or coherent and non-coherent transmission.

A. General Architecture

The central element of the proposed CHRON architecture is a CDS [12], which determines how to handle traffic demands or network events, and optimizes network usage and performance by taking into account both the current status of the network and past history. The CDS also instructs the control plane to configure network elements accordingly. Cognition can be implemented in either centralized or distributed manner, depending on

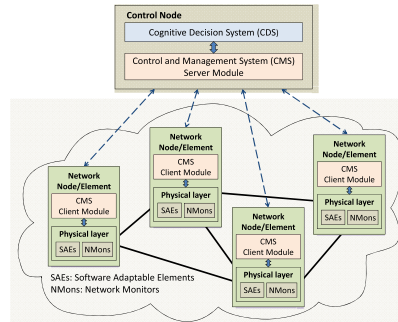


Fig. 1. The CHRON architecture for a network with centralized cognition.

whether the CDS is a single instance running on a single control node in the entire network or it is implemented across different network nodes. In the CHRON project we have focused on the centralized architecture [13], shown in Fig. 1.

The CDS is assisted by a control and management system (CMS) [13], which feeds the CDS with updates regarding network status and resource availability, grants the delivery of the decisions made by the CDS to all the interested nodes, and watches over the device configuration process, notifying any malfunctioning or anomaly.

The architecture also includes software-adaptable elements and network monitors. *The software-adaptable elements are configured according to the decisions made by the CDS and thus enable adaptation of the network to current conditions. On the other hand, the network monitors (as part of the Network Monitoring System) provide traffic status and optical performance measurements to the CDS. The functionalities of adaptability and monitoring are handled in each network element through a physical layer manager, which works as a common interface towards the CMS.*

B. Cognitive Decision System in CHRON

The CDS is involved in various tasks related to network control and optimization. Thus, rather than implementing the whole CDS as a monolithic module, it is divided into different modules, each offering a functionality (or a set of related functionalities), and all of them exploiting cognition.

Thus, each module implements a feedback loop where interactions with the environment guide current and future interactions. Moreover, the feedback loop not only observes and provides decisions, but a learning module is also implemented in order to prevent mistakes from previous interactions being made on future interactions. Therefore, each module implements the so-called cognitive loop [4], as shown in Fig. 2. The CDS modules consist of two main parts

- 1) *The Cognitive Process*, which implements the algorithms to make decisions and takes into account the current network status and previous history.

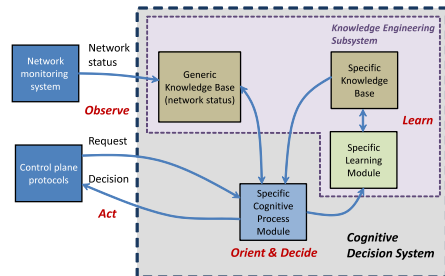


Fig. 2. Cognitive loop in the CHRON cognitive decision system: relationship between a cognitive process and its associated knowledge base [12].

- 2) *The Knowledge Engineering Subsystem*, which handles the information used by the cognitive process. This element consists of a knowledge base (KB) and a learning module, which links the cognitive process with its associated KB and executes methods to update the KB with acquired experience.

Fig. 2 presents the building elements of a module of the CDS, as well as their relationship to the network monitoring system and the CMS. The network monitoring system gathers the network status to a generic (KB). Separately, there is a specific KB containing all the information associated with that cognitive process, which is updated by a specific learning module. A cognitive process can access these two KBs (generic and specific) to retrieve information and to update them. Finally, when a decision is made to handle a request or network event, the decision is communicated to the CMS for its execution.

Nevertheless, it is important to note that the cognitive process and the knowledge engineering subsystem (in particular the learning modules) may be strongly or loosely coupled, depending on the cognitive technique employed. On the other hand, the structure and size of the KB is also dependent on the technique employed.

Before going ahead, we will provide a couple of examples showing how the different elements in Fig. 2 work together.

As we will later see in more detail, when a request coming from the control plane demands the establishment of a lightpath, the cognitive process assesses the quality of transmission (QoT) of a potential solution to establish that optical connection (i.e., a combination of a route and the required network resources), taking into account the current status of the network (in particular, the set of lightpaths already established). To achieve that, it searches for similar scenarios stored in a specific KB. If, based on that information, the cognitive process determines that the potential solution complies with QoT requirements, it will *decide* to use it: the control plane protocols will *act* and establish that connection. Once the connection is established, its real QoT performance will be *observed* by means of network monitors. If the QoT does not really comply with requirements, the connection will be released and the cognitive process will *learn* by updating the KB with this new information in order to avoid repeating this mistake in future.

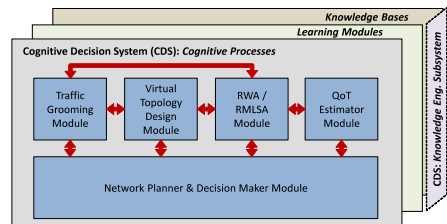


Fig. 3. CHRON Cognitive Decision System in a centralized architecture [12].

Another example is proactive restoration. While some network failures are abrupt and unpredictable, other failures (like bit error rate—BER—degradation) may have a relatively slow transient, and thus proactive recovery mechanisms can be executed. For that reason, each time a request for lightpath establishment is received, a route for path restoration is also pre-computed. Then, cognition is used in two different ways. First, the time that would be required for restoring the connection is dynamically estimated by taking into account the time required to setup paths of similar lengths to that of the calculated restoration path (which is *observed* from the network). Second, the evolution of BER is forecasted from past *observations* to predict when it will reach the critical value in terms of QoT requirements. By combining these two estimates: how long it would take the restoration and how much time is left before failure occurs, the cognitive process *decides* when to trigger a proactive restoration procedure (i.e., an *action*). This ensures that a backup lightpath is available before actual failure occurs, simultaneously minimizing establishment of backup lightpaths that are not really required. In this case, the cognitive process and the knowledge engineering subsystem are strongly coupled, and a formal KB, with e.g. a set of past experiences, is replaced by a set of parameters which are dynamically adjusted as a function of past history, and thus incorporate *learning*.

C. Processes and Knowledge Bases in the CHRON CDS

The CDS in the CHRON centralized architecture consists of five cognitive modules running in parallel, as shown in Fig. 3. A description of the functionalities of each module follows.

- 1) *Traffic Grooming (TG) module*, which is in charge of routing non-optical traffic demands, for example time division multiplexed (TDM) label-switched paths (LSPs) through existing lightpaths composing the current virtual topology.
- 2) *Virtual Topology Design (VTD) module*, which is responsible for (re)designing the virtual topology and thus the set of lightpaths to be established in the network. This module is used for optimizing network performance by rearranging existing connections.
- 3) *RWA/RMLSA module*, which in networks following the ITU-T grid solves the routing and wavelength assignment (RWA) problem in the physical network, as well as determines the modulation format. In elastic networks, it solves

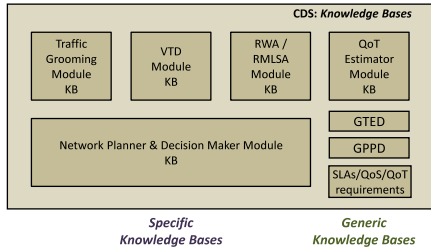


Fig. 4. Knowledge bases included in the CHRON Cognitive Decision System.

the routing, modulation format and spectrum allocation (RMLSA) problem.

- 4) *QoT estimator module*, which predicts QoT of new lightpaths to be established in the network as well as the impact on existing connections when setting up a new one. Thus, the establishment of impairment-aware optical connections relies on this module. It provides an estimation of the QoT and once a new lightpath is established, verifies the real QoT (which is provided by network monitors) and uses this information to improve the performance of the module for future estimations.
- 5) *Network Planner & Decision Maker (NPDM) module*, which receives user requests and determines how to serve them by using the functionalities offered by the other modules. It also performs forecasting functionalities to trigger proactive decisions for network optimization like virtual topology reconfiguration or proactive restoration (as previously described). Thus, the NPDM coordinates the operation of the different modules of the CDS, communicates the actions to be performed to the network nodes through control plane protocols, and handles the information received from the network monitoring system.

As previously discussed, each module in the CDS has an associated KB in the knowledge engineering subsystem, which is linked to the cognitive process by means of a learning module. Therefore, there are as many specific knowledge bases as cognitive processes in the CDS (see Fig. 4).

The CDS also includes generic databases that can be read by all modules, since they contain service requirements as well as current network status. These generic databases, also shown in Fig. 4, are

- 1) *Global Traffic Engineering Database (GTED)* contains information about traffic status and resource availability in the network.
- 2) *Global Physical Parameters Database (GPPD)* contains information about the physical topology of the network, and physical monitoring data.
- 3) *SLAs/QoS/QoT requirements* contains the service level agreements (SLAs) QoS and QoT parameters associated with different services. Hence, when the cognitive system receives a request associated with a class of service, it can

obtain the values of QoT that should be guaranteed when handling that request.

III. NETWORK OPERATION TECHNIQUES DEVELOPED IN CHRON AND PERFORMANCE EVALUATION

Within the project, we have developed different network operation techniques. In this section, we present an overview of some of the methods developed for QoT assessment, path computation, virtual topology design and reconfiguration, as well as strategies for energy efficiency improvement and a few comments on the joint operation of the system.

A. QoT Evaluation Techniques

The aim of the QoT estimator module of the CDS is to make a prediction of the signal quality of new lightpaths to be established in the network, as well as to address its impact on the performance of existing connections. Therefore, this module works in cooperation with other modules of the CDS architecture, and in particular with the RWA/RMLSA module, in order to minimize blocking probability and spectrum fragmentation (in case of elastic networks), while maintaining the required maximum BER.

The QoT assessment mechanisms should have information about a number of parameters, including: the network topology, spectral windows, link characteristics, signal types (baud rate and modulation format), and lightpaths currently established in the network (so as to consider the impact of co-propagating channels) in order to provide an accurate estimation. By taking into account all the aforementioned characteristics, the QoT estimator should provide a relatively accurate estimate of the QoT of the lightpaths. However, a practical version of a QoT estimator should require relatively short execution times to provide those estimates, so that these results are available to the other modules of the CDS within adequate time. This means that part of the aforementioned characteristics may need to be simplified, or even neglected if the complexity of calculation (execution time) is too high.

We have approached two different types of scenarios: traditional fixed-grid dispersion compensated networks, and emerging flex-grid uncompensated networks, and have proposed QoT assessment mechanisms for each of those scenarios.

1) *QoT Assessment in Fixed-Grid Dispersion Compensated Networks*: For fixed-grid dispersion-compensated network, and in particular for 10 Gb/s systems, significant work has been done. In particular, Azodolmolky *et al.* [14], [15], have proposed a QoT estimation tool (the Q-Tool), which combines in a single framework a number of well investigated and verified analytical models, together with a numerical split-step Fourier method. However, the tool is only valid for 10 Gb/s on-off keying (OOK) networks, and due to the complex calculations required, the computation time is very long, ranging from 1 to 1000 s, depending of the scenario [16]. We have proposed an alternative approach for predicting the QoT of lightpaths in an optical network (i.e. before being established), which relies on cognition. By exploiting previous realizations, which are stored in a KB, fast and correct decisions on whether a lightpath fulfills

QoT requirements or not, can be made without having to resort to complex methods.

The cognitive operation of this module relies on the use of a KB, where the features of lightpaths previously established in the network (including parameters like their route, wavelength or the number of co-propagating channels) and their QoT values (like BER, error vector magnitude—EVM—or Q-factor obtained from the monitoring system) are stored. Then, by using data mining techniques [17]—such as naïve Bayes estimator, decision trees or a case-based reasoning (CBR) technique [18]—operating on that KB, the QoT of new lightpaths can be estimated. With the first set of techniques, a model is built *a priori* by using the information stored in the KB which is then used in real time to determine whether a lightpath complies with QoT requirements or not. The CBR technique does not build any model *a priori*, but conducts searches in real time on the KB when assessing the QoT of lightpaths. It compares the features of the lightpath whose QoT is to be assessed with those stored in the KB and assumes that the QoT is that of the most similar lightpath stored in the KB. Moreover, the measurements obtained from the network monitoring system (BER, EVM or Q-factor), and, in particular, the feedback obtained when establishing new lightpaths helps improving the contents of the KB. A complete description of the CBR technique is provided in [19], where pragmatic procedures for building the initial KB are discussed, and where we also proposed a mechanism to enhance the cognitive QoT estimator with the execution of periodic maintenance stages where the KB is updated and optimized by learning new cases, but also by forgetting uninteresting ones. Such an optimized KB slightly improves the percentage of successful classifications, but also accelerates the classification procedure by one order of magnitude due to the lower size of the KB.

Fig. 5 shows the percentage of successful classifications of lightpaths into high or low QoT categories when using different types of data mining techniques including a naïve Bayes classifier, several types of decision trees (decision tree, random forest, J4.8 tree), and the CBR approach previously described, for the 34-node GÉANT2 dispersion-compensated network with 64 wavelengths assuming 10 Gb/s OOK transmission [8]. As shown in Fig. 5, and as demonstrated in [19], the CBR approach achieves more than 99% successful classifications of optical connections. Moreover, the use of the CBR system is much faster for on-line operation than the Q-Tool, thus demonstrating the advantages of cognition. For instance, in the 14-node Deutsche Telekom (DT) network, with an optimized KB consisting of less than 1000 cases (lightpaths stored), the computation time to assess QoT of a lightpath is below 0.06 ms while the Q-Tool requires ~770 ms. Larger networks require bigger KBs, which in turn increases the computation time. For instance, for the 34-node GÉANT2, with an optimized KB of less than 15000 cases, the time increases to ~35 ms, but it is still faster than the Q-Tool, which takes ~3.6 s.

The joint operation of the QoT estimator together with the RWA module was studied in [8] from a techno-economic perspective, in order to assess the impact of erroneous classifications of the cognitive QoT estimator. Those erroneous

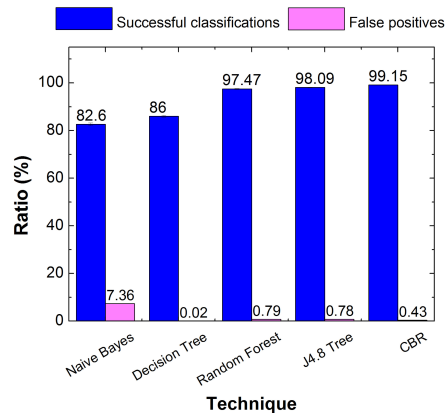


Fig. 5. Success ratio of different QoT estimators, showing the high value obtained by the case-based reasoning technique [8].

classifications are divided into false negatives (i.e., estimating erroneously that a lightpath does not comply with QoT requirements) and false positives (i.e., estimating erroneously that a lightpath complies with QoT requirements). False negatives lead to a potential loss of revenues for the operator, as connections that could be established are not. The impact of false positives (which are also represented in Fig. 5) requires an additional consideration. When a new lightpath is going to be established, not only its QoT has to be assessed, but also that of co-propagating lightpaths which are currently established in the network (in order to ensure that they are not disrupted by the new connection). The false positive error has much more impact if committed when assessing any of those copropagating lightpaths, as it implies a disruption event. However, we have found that those events are virtually inexistent (i.e., basically all false positives are committed when assessing the QoT of the new lightpath). In fact, the results of the techno-economic analysis (which considers the impact of those errors) show that the revenues that a network operator can obtain by relying on the CBR technique are very close to those obtained if an ideal QoT estimator would be available (i.e. if no classification errors were made).

Finally, while the analysis in [19] focused on 10 Gb/s and relied on simulation studies, the CBR QoT estimator was experimentally validated in [20], where we also demonstrated its applicability to other modulation formats. We implemented a wavelength division multiplexed (WDM), dispersion compensated, point-to-point optical transmission system, with 5 channels carrying 80 Gb/s polarization division multiplexed (PDM) quaternary phase-shift keying (QPSK), with a number of adjustable parameters such as optical launch power, fiber link length and number of co-propagating channels, in order to support different lightpath and system configurations. The cognitive

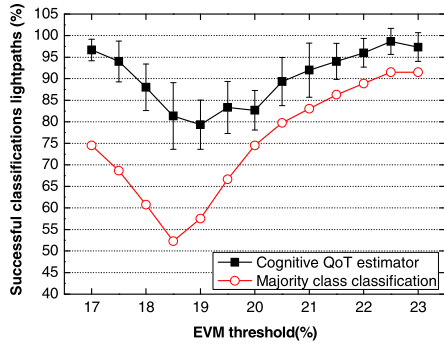


Fig. 6. Experimental demonstration of QoT based on CBR for PDM-QPSK WDM networks with high successful ratio for small KB [20]. Percentage of successful classifications of lightpaths into high/low QoT categories according to an EVM threshold, for the cognitive QoT estimator (based on CBR) and a majority class classificatory.

QoT estimator was used to classify lightpaths into high and low QoT category, using different thresholds on the EVM or OSNR, respectively. Even with a small and not optimized KB of only 153 cases, it achieved between 79% and 98.7% successful classifications of lightpaths into high or low QoT classes when the classification was done according to predicted EVM (see Fig. 6), and nearly 100% when the OSNR was used instead.

2) *QoT Estimation in Flexible Uncompensated Networks:* Second, we have focused on flex grid uncompensated networks [21]–[23]. In contrast to fixed-grid dispersion compensated scenarios, relatively accurate and fast methods for QoT estimation based on analytical expressions have been proposed [24]–[28] and evaluated in [29]. However, these methods have been developed for the performance evaluation of multi-channel NWDM, quasi-NWDM and dense WDM ([24], [25] and [28]), as well as OFDM ([26], [27]) signal transmission over point-to-point links, composed by a cascade of uncompensated amplified spans with fixed lengths. As such the aforementioned work does not consider the transmission effects over different network optical paths composed by multi-span optical links with different span lengths and a variable number of either NWDM- or OFDM-based multiplexed channels per link.

The work performed within CHRON adopts a performance estimation tool for dynamic end-to-end super-channel connections, taking into consideration the induced transmission impairments per optical link (i.e. node-to-node) and therefore providing optimized allocation of the network resources when combined with the CDS. The model, adopts the latest (to the best of our knowledge) analytical models for the calculation of the non-linear induced penalty of NWDM [28] and OFDM [27] schemes, in a new flexible transmission performance estimation tool (*flexible TPE-Tool*) that is applicable in multi-path and multi-node optical meshed networks. For the proper use of the flexible TPE-Tool in the evaluation of various optical net-

working scenarios with flexible spectrum allocation for each connection, one must consider that multiple lightpaths may co-exist, sharing common optical links. In practice, there are multiple lightpaths that are established, resulting in optical links accommodating a varying number of channels from different end-to-end connections. Therefore, for a given lightpath the signal related characteristics are not the same for each link and depend on the existing preestablished connections. As a result the TPE-Tool needs to be designed in such a way that it provides an estimate separately for each optical link in-between nodes. Then, the overall performance estimation of the lightpath should be estimated by concatenating the degradation effects from each link in the OSNR value according to

$$\frac{1}{\text{OSNR}_T} = \frac{1}{\text{OSNR}_{B2B}} + \sum_{i=1}^N \frac{1}{\text{OSNR}_i} \quad (1)$$

where OSNR_i is the OSNR value of the i th optical link that is attributed only to the P_{ASE} and P_{NLI} noise terms over the link. The back-to-back OSNR performance, OSNR_{B2B} , is added to the total OSNR value. It is important to note that the assumption regarding the summation of the OSNR values for the individual optical links across the lightpath is valid for the case of the ASE noise term that has purely Gaussian characteristics, but in general invalid for the case of nonlinear impairments (NLI). In order to remain valid also in the latter case, the analytical formulas derived in [27] and [28] need to be corrected by adding a correction factor ε to take into consideration the accumulation of NLI over links with different span lengths. However, comparisons between the TPE-Tool and the original analytical formulas in [27] and [28] for the same transmission distances and number of spans have shown that the accuracy error becomes negligible (i.e. less than 0.2 dB in terms of Q factor) when the performance is evaluated at the optimum launch power, where the NLI induced noise is minimum. This indicates that TPE-Tool approach is valid for realistic networking applications.

It is noted that recently a similar model has been developed and applied for the dynamic routing and spectrum assignment of OFDM channels in multi-node elastic optical networks by the authors in [30]. This model uses a closed-form expression to estimate the OSNR that is derived by the power spectral density of fiber nonlinearity noises. However, it is based on the formulas reported in [26] and [27] and therefore it is applicable for the cases of densely spaced coherent OFDM signals.

The applicability of the TPE-tool in an optical network scenario is explained through the illustrative network topology example shown in Fig. 7. Flexible multi-carrier super-channels are assumed for each lightpath with different number of channels per super-channel as it is shown in the inset table on the right of the figure. The allocation of the different super-channels in spectrum is also presented. Various link-distances are assumed with a larger number of spans and used later for the evaluation of the methodology presented here.

In Fig. 7, let us assume that super-channel Sch1 is to be established between nodes A and D over the links AC and CD while all the rest of the super-channels are already established. In order to examine the performance of Sch1, the total number of

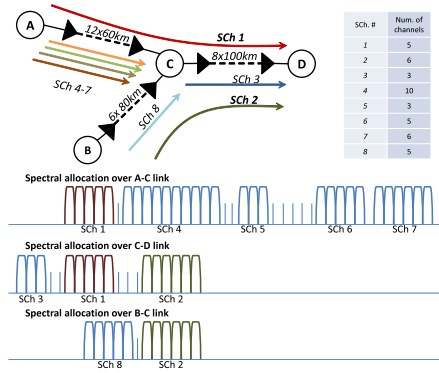


Fig. 7. Example on the use of TPE-Tool in a multi-path network environment. All super-channels are PM-QPSK at 28 Gbaud, with 30 GHz subchannel separation. EDFA's NF is 5 dB.

co-propagating channels over the links AC and CD is required. The total number of channels to be considered is the Sch1 channels plus the channels that affect the Sch1 performance. In this example, it is shown that for link AC, Sch4 is one spectral slot away from Sch1 and that Sch5 is 2 slots away from Sch4. Also Sch6 is 5 slots away from Sch5. If the super-channels consist of NWDW subchannels, then the slot-width is determined by the symbol rate of the individual channels. Assuming that the NWDW subchannels are transmitted at 28 Gbaud and are placed close to the Nyquist limit, at 30 GHz, then a two-slot spectral gap is equal to 60 GHz. In this case Sch5 and of course Sch6 and Sch7 can be neglected from the calculation of the transmission performance of Sch1. However Sch4 that is only one-slot away (and thus affecting the performance) will be considered. Therefore, the TPE-Tool will be called with the parameter "number of channel" being equal to 15 (5 from Sch1 and 10 from Sch4) for the link AC. Similar for link CD, both Sch3 and Sch2 can be neglected since they are allocated two or more slots away from Sch1.

According to the network schematic shown in Fig. 7, link AC is composed of 12 spans of 60 km, link CD by 8 spans of 100 km and link BC by 6 spans of 80 km. Using the TPE-Tool the performance evaluation of the channels within Sch1 will be estimated by considering 15 and 5 co-propagating channels over links AC and CD respectively. For the evaluation of the Sch2 channels the total number of considered channels will be 11 for link BC and 6 for link CD. However, for comparison reasons, two additional cases are considered which set the decision rule to include the neighboring channels at 2 slots and even 3 slots away resulting in an increased number of channels per link. The results of this study for the various cases are summarized in Table I. The effect of the decision rule on the estimated performance values is relatively small, since the deviation in terms of Q factor value between a 1-slot and a 3-slot decision

TABLE I
QOT ESTIMATED FROM THE TPE-TOOL FOR THE SCENARIOS PRESENTED IN FIG. 7

Mon. SChs	Decision rule	ch. 1 st link	ch. 2 nd link	TPE-Tool	
				Q (dB)	BER
Sch1	50GHz → 1slot	15	5	12.69	8.2e-6
	75GHz → 2slots	18	8	12.54	1.1e-5
	100GHz → 3slots	18	14	12.43	1.4e-5
Sch2	50GHz → 1slot	11	6	12.91	4.9e-6
	100GHz → 3slots	11	14	12.73	7.4e-6

rule is less than 0.3 dB, which correspond to almost a factor of 2 in terms of BER for the specific example.

Following this brief discussion about motivation and capabilities of TPE-Tool and the example of its application to a realistic scenario, we can conclude that it provides a fast and relatively accurate estimation of signal transmission quality over multi-path networks with different signal and physical layer characteristics and can calculate an end-to-end performance of optical paths composed of several optical links carrying a different number of co-propagated optical channels.

For quasi-Nyquist WDM systems, the penalty induced by the modulation format of neighboring carriers and their proximity is, in general, difficult to evaluate analytically as it depends on the actual implementation of the transceivers and DSP algorithm. In [32], we performed an experimental study on required OSNR (ROSNR) levels for maintaining a 10^{-3} BER for numerous scenarios. Traffic demands requiring different bit rates were served with 14 Gbaud PDM-16-quadrature-amplitude modulation (16-QAM) and PDM-QPSK formats, within the unused spectral gap (band-of-interest—BOI) within a heterogeneous optical super-channel. The measured performance for these scenarios provides an input that allows one to create an empirical model of a super-channel transmission. We implemented a number of transmission scenarios for different BOI bandwidths and wavelength allocation schemes, as well as for different modulation formats. Evaluated scenarios are illustrated in the second column of Table II. In all cases, the optical spectrum consists of three bands. Two outer interfering PDM-QPSK bands, each comprising four subcarriers (see red dashed arrows in Table II), surrounding the central band, i.e. the BOI (shaded area). In scenarios A, B, C, and D, two DP-16-QAM subcarriers with a variable spacing occupy the BOI. In scenarios G, H, F, and E a variable number of PDM-QPSK subcarriers occupy the BOI, as shown in Table II. We investigated BOIs with bandwidths of 98 GHz (scenarios A, B, G, H), 70 GHz (C, F), and 42 GHz (D, E). Those numbers follow from the fact that only BOIs with bandwidths equal to an integer multiple of the spacing of interfering subcarriers (14 GHz) could have been generated.

B. Path Computation Mechanisms

The QoT estimator module that we have just reviewed, works in close cooperation with the RWA/RMLSA module of the CDS. The RWA/RMLSA module offers the functionality of

TABLE II
INVESTIGATED SCENARIOS AND OBTAINED ROSNR LEVELS [32]

Scenario	Spectrum allocation (14 GHz grid)			BOI (GHz)	BOI capacity (GHz)	Total capacity (Gbs)	Spectral efficiency (b/s/Hz)	ROSNR for BER 1×10^{-3} (dB)
	16-QAM in BOI	QPSK in BOI	Outer QPSK					
A	↑↑↑↑↑	↑↑↑↑↑	↑↑↑↑↑	98	224	672	2.29	27.3
B	↑↑↑↑↑	↑↑↑↑↑	↑↑↑↑↑	98	224	672	2.29	30.9
G	↑↑↑↑↑	↑↑↑↑↑	↑↑↑↑↑	98	168	616	1.71	19.6
H	↑↑↑↑↑	↑↑↑↑↑	↑↑↑↑↑	98	280	728	2.86	20.1
C	↑↑↑↑↑	↑↑↑↑↑	↑↑↑↑↑	70	224	672	3.20	32.7
F	↑↑↑↑↑	↑↑↑↑↑	↑↑↑↑↑	70	168	616	2.40	21.0
D	↑↑↑↑↑	↑↑↑↑↑	↑↑↑↑↑	42	224	672	5.33	—
E	↑↑↑↑↑	↑↑↑↑↑	↑↑↑↑↑	42	168	616	4.00	22.0

determining the routes and wavelengths (or spectrum) for the connections to be established in the network. Regarding this issue, a similar role (although with less capabilities) is performed by the Path Computation Element (PCE) [33], defined by IETF, and which has lately received increasing attention in optical networks. Assuming a fixed-grid network, the CDS receives requests for lightpath establishment, and then computes a route and a wavelength for that connection according to the current network state, which is stored in the Generic Traffic Engineering Database (GTED). The result of such computation (once validated by the QoT estimator module) is used to establish the connection by means of the Resource-Reservation Protocol- Traffic Engineering (RSVP-TE) protocol [34]. Then, the CDS can either take care itself of performing the updates to the GTED, or rely on the use of the Open Shortest Path First-TE (OSPF-TE) protocol, which implies that the GTED will be updated after some time. Therefore, in the latter case, the CDS may decide to assign to an incoming request a resource that has already been assigned to another lightpath, but for which the confirmation from OSPF-TE has not yet reached the central GTED (so, according to the GTED, those resources are available, but they have already been taken, and thus this connection will be blocked at some point by the RSVP-TE protocol). Hence, relying on OSPF-TE to update the GTED leads to increasing the blocking probability when compared to a scenario where the GTED is directly updated by the CDS.

Cognition offers a solution to improve performance and, moreover, that solution can also be easily applied in stateless PCE-based networks. For those environments where the GTED (or simply TED in PCE parlance) is updated by OSPF-TE, we have proposed the elapsed times matrix (ETM) heuristic [35], which aims at avoiding the selection of resources which have been recently assigned by the CDS (or by a PCE) to another

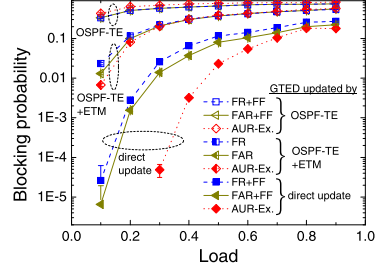


Fig. 8. Dynamic lightpath establishment: Blocking probability versus load (when the duration of a lightpath is ~ 40 times the OSPF-TE update time) [35].

request. This is because those recently assigned resources will be very probably unavailable: the GTED has not been updated yet, but the RSVP-TE mechanism has already reserved those resources. For that reason, every time that a request arrives at the CDS/PCE, a matrix of elapsed times is built. That table stores the time elapsed since the CDS/PCE assigned a certain wavelength channel in a fiber to any lightpath request for the last time. Based on that information, together with that stored in the GTED, a combination of route and wavelength for that lightpath request is selected (see [35] for details). Thus, by exploiting recent past history, the method avoids selecting resources which have been recently assigned to other requests. In contrast with other proposals, this technique can be easily introduced in stateless PCEs without the need for protocol extensions, as it only implies the modification of an underlying PCE algorithm.

Fig. 8 shows the blocking probability versus the network load when using Fixed Routing (FR) [36], Fixed Alternate Routing (FAR) [36] –considering three alternative routes–, and AUR-Exhaustive mechanisms (AUR-Ex) [37] in the 14-node DTnetwork. For each method, three scenarios have been considered: one assuming that the CDS directly updates the GTED, another assuming that OSPF-TE is used to update the GTED, and another assuming that OSPF-TE is used to update the GTED, but the RWA module of the CDS also employs the ETM mechanism. In the first two scenarios, the First Fit (FF) technique for wavelength assignment [36] has been used with FR and FAR. In the third scenario, as described in [35], the use of the ETM method leads to the joint selection of route and wavelength even when FR and FAR are used. As shown in Fig. 8, the ETM method, when combined with FR, FAR or AUR-Ex heuristics significantly reduces the blocking probability (although, obviously, optimal results are only obtained if the GTED is directly updated by the CDS). Moreover this method can also be extended to flexible grid optical networks.

C. Virtual Topology Design and Reconfiguration

Besides supporting dynamic lightpath establishment on user demand, a reconfigurable virtual topology to transport IP traffic is also set up in CHRON by the network operator. The virtual topology thus refers to a specific set of lightpaths that are

established in the network by the operator itself, rather than by network clients, in order to transport the IP traffic demand faced by the operator. Hence, we do not refer here to the concept of virtual optical networks [38], where different slices of the network are hired to different clients or devoted to different tasks, but to the classical definition of virtual topologies as given in [39], [40].

In order to reduce the total cost of ownership, the design of an optimized virtual topology (including an efficient selection of transceivers, routes and wavelengths for its connections), and the determination of its associated traffic grooming is essential. Thus, the adequate joint design of virtual topology, routing and wavelength assignment, and traffic grooming, can further optimize the costs as opposed to splitting the design problem into separate subproblems. That task is mainly performed by VTD module of the CDS, but in collaboration with other modules both internal and external to the CDS. For instance, such a design can also take advantage of the traffic forecasting capabilities provided by the NPDM module, and of the traffic monitoring capabilities provided by the network monitoring system, in order to determine when and how to reconfigure the virtual topology with the aim of improving performance.

We have proposed a number of algorithms for VTD [41]–[43], including CONGA-VTD (Cost Optimization Genetic Algorithm for the Virtual Topology Design) [43]. CONGA-VTD is a multiobjective genetic algorithm for virtual topology design in reconfigurable environments, which aims at minimizing network congestion, reducing the reconfiguration disruption, and minimizing the operational costs (OPEX), which are calculated according to the model in [44]. Two cognitive techniques have been included in the reconfiguration process to enhance the performance of the whole mechanism. First of all, by forecasting future traffic demands (for which the AutoRegressive Integrated Moving Averages—technique is used) which are then used to feed the VTD algorithm, and second, by complementing the virtual topology design algorithm with a KB where solutions successfully used in the past are stored for potential reuse in the future. That is, when a virtual topology proposed by CONGA-VTD is established (i.e., the network is reconfigured with that solution), it is stored in the KB. Then, when the method is launched again to find new virtual topologies for a future time slot, it uses those solutions from the KB that better fit to the current traffic and network state, as starting points of the genetic algorithm (together with a set of randomly generated virtual topologies and other special ones, calculated ad-hoc, as described in [45]). Thanks to the use of the KB, CONGA-VTD finds better solutions in less time.

The performance of the virtual topology design and reconfiguration process has been analyzed by simulation, assuming the 14-node DT network and a traffic-varying scenario, where the virtual topology is reconfigured every hour as required. The computing time of VTD process can be adjusted by changing the parameters of the evolutionary procedure of the genetic algorithm, but with ~ 20 s very good solutions are obtained. Fig. 9 shows the OPEX over a period of 8 days when using a reconfigurable virtual topology and two static virtual topologies (SVT). As shown there, OPEX is not constant during the simulation,

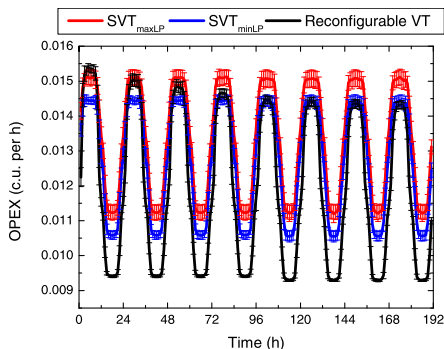


Fig. 9. OPEX per hour along 8 simulated days when cognitive virtual topology design and reconfiguration is compared with two static virtual topology approaches [43].

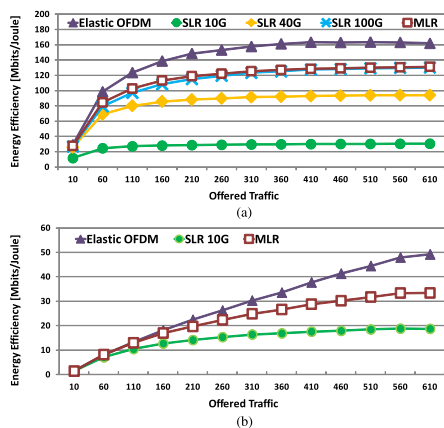


Fig. 10. Energy efficiency for different line rate cards in a dynamic scenario for diverse traffic demands for two reference networks: (a) Telefónica's Spanish network, (b) GÉANT2 network [48].

but follow the traffic variations due to power consumption of the IP layer. By exploiting the reconfiguration advantages, OPEX is reduced when compared to a static solution, mainly in the out-of-peak traffic periods. Moreover, the impact of the learning process is also shown in the figure, as the results improve with time, i.e. lower cost values are obtained as the CDS learns from past experiences.

D. Energy Efficiency Improvements

Every year, energy required to transmit end-to-end one bit of information decreases by 10% [44], [46], while the traffic

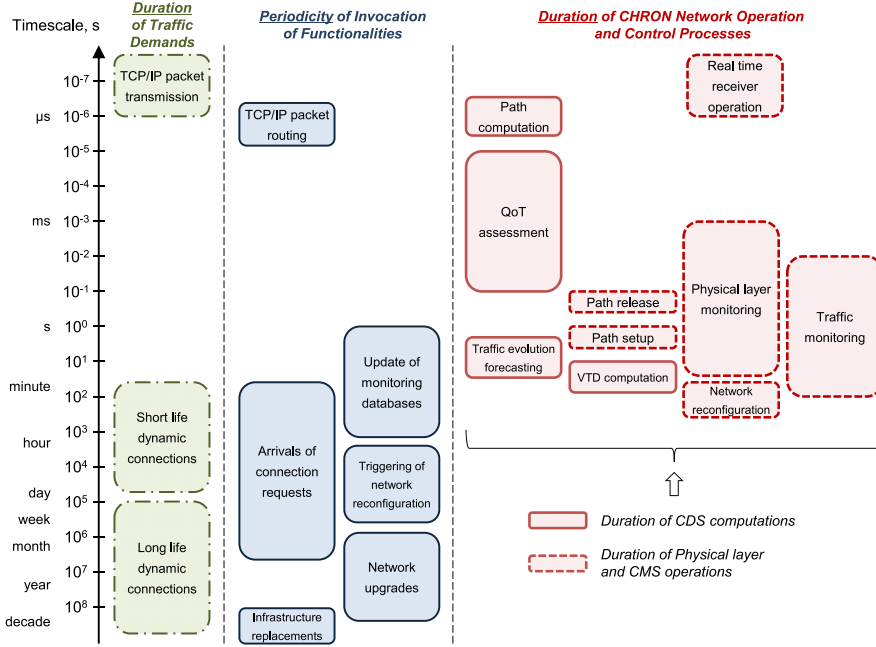


Fig. 11. A time-base view of the network functions analyzed in this paper.

demands grow by 34%. Hence, the total power consumption of networks is increasing and so is the concern of the operators about energy efficiency in their networks. Models to estimate power consumption as well as algorithms aimed at minimization of power waste are being implemented. In CHRON, an energy efficiency evaluation has been carried out for flex-grid OFDM and fixed-grid WDM with single line rate (SLR) and mixed line rate (MLR) [47], [48]. Thus, power consumption models for both flex-grid and fixed-grid WDM have been proposed and used in a set of energy-aware dynamic-routing heuristic algorithms (included in the RWA/RMLSA module) to evaluate their energy efficiency. As shown in Fig. 10, a flex-grid elastic OFDM-based network is more energy-efficient than fixed-grid approaches in a dynamic scenario with time-varying traffic demands. Besides improving the overall energy efficiency of the network, the elastic OFDM approach also reduces network blocking and decreases number of required transmission regenerators due to used distance-adaptive modulation.

Reduction in energy consumption is usually accompanied by an increased probability of network congestion, higher blocking ratio or a decrease in spectral efficiency. These trade-offs necessitate the need for implementing multi-objective algorithms. Therefore, the power consumption models have also been

included in the family of genetic algorithms for VTD previously mentioned. In this way, they also minimize energy consumption within the cognitive reconfigurable environment, while complying to network requirements such as capacity demands or QoT [45].

E. Joint Operation of CDS Modules

In the operation of an optical network different time scales are involved [49]. A time-based view of the network functions analyzed in this paper is shown in Fig. 11. Periodically, every few months or years, investments for network upgrades are required. However, as shown in techno-economic studies [50], [51], the use of cognitive techniques leads to a more efficient use of resources and thus enables postponing upgrades in time. Moreover, the knowledge acquired (e.g., by evolutionary learning through VTD) can help further decrease the upgrade costs. In the meantime, control mechanisms have to deal with different processes like the establishment of dynamic connections (which can range from short connections of a few minutes to connections spanning months or years), and dynamically varying IP traffic, showing peaks and valleys along the day. The different modules of the CDS are able to deal with those different requirements. On the one hand, requests for lightpath establishment are

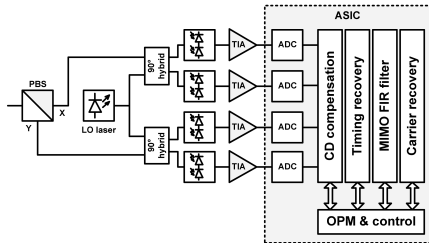


Fig. 12. Typical structure of a digital coherent receiver with CD monitoring and an equalization block [55], [60].

forwarded by the NPDM module to the RWA/RMLSA module, which quickly computes a potential route and set of resources (e.g., by using the method shown in Section III-B), and assesses its QoT (and that it does not disrupt existing connections) by relying on the cognitive QoT estimator (see Section III-A). If low QoT is estimated, the RWA/RMLSA module can iteratively test other solutions. On the other hand, the use of a reconfigurable virtual topology (as described in Section III-C) addresses the variations of IP traffic by adapting the set of lightpaths devoted to IP transport to those changes.

Moreover, the use of a centralized control scheme facilitates the joint operation of the reconfigurable virtual topology and dynamic lightpath establishment. The CDS handles the different procedures in an orchestrated way, and takes care of the different computing requirements of the different procedures. For instance, requests for dynamic lightpath establishment are queued in the CDS if a virtual topology design calculation is in progress, in order to avoid allocating resources to that request being considered by the VTD process in its evolutionary computation. Nevertheless, since the VTD calculation process takes around 20 s and is executed e.g. every hour, such a delay is not significant in pragmatic environments. Additionally, the joint operation, leads to improved resource sharing (by using suitable policies), and enables that those resources not in use for the virtual topology in a certain period of time become available for dynamic lightpath establishment, thus leading to a decrease on blocking probability.

IV. OPTICAL PERFORMANCE MONITORING

CHRON networks with reconfigurable optical components, various modulation formats, flexible switching and wavelength routing require sophisticated OPM due to the increased probability of different system failures. Thus, accurate and fast parameter monitoring techniques are required to provide an overview of a current network status to the CDS, so that it can make more effective and informed decisions on how to handle traffic requests and network events. In addition, it enables advanced functionalities such as software-defined reconfiguration of digital transceivers.

Within CHRON project, various techniques for OPM have been developed and used. Since the receivers are equipped with

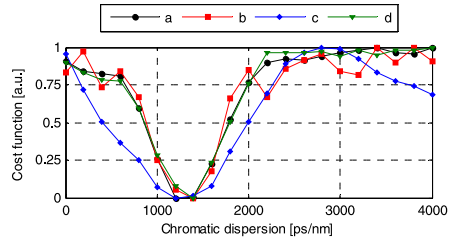


Fig. 13. CD estimation using NDA scanning techniques showing results of four different methods from [59]: (a) CMA, (b) average power, (c) eigenvalue spread, (d) frequency autocorrelation. Minimum of the cost functions indicates correct value for compensation (1280 ps/nm) [59].

digital signal processing capabilities, the entire OPM can be performed in electronic domain [52], [53], without the need for, usually expensive, external devices [54]. This approach greatly enhances the system's functionality and flexibility, which is particularly important in CHRON. Fig. 12 shows the placement of an OPM subsystem in the DSP module of a coherent receiver. It adopts a dual stage equalization approach [47], where the first static equalization stage compensates for the bulk of chromatic dispersion (CD) and a second adaptive finite impulse response (FIR) 2×2 multiple-input multiple-output (MIMO) equalizer compensates for residual CD, polarization mode dispersion (PMD) and performs tracking of other time-varying effects. Coefficients of the equalizer may be adapted by blind techniques, also called non-training-aided (NTA). Alternatively, training-aided (TA) estimation [56] based on the use of training sequences (TS) can be employed. Static effects with long channel impulse response, in particular CD, are typically compensated using NTA scanning algorithms [57]–[59]. A digital CD compensator gradually scans the space of possible CD values in coarse steps. At every step, a cost function is evaluated on the signal at the output of the compensator. The cost function indicates if the dispersion was successfully mitigated. Typically the cost function is flat except for the vicinity of correct CD value (cf., Fig. 13), which makes gradual adaptation of this filter infeasible. Although the coefficients of the 2×2 MIMO equalizer are widely adapted by NTA algorithms (typically in time domain) like constant-modulus algorithm (CMA) or decision-directed (DD) least mean square (LMS) which converge to the minimum-mean square-error (MMSE) solution, TA channel estimation (CE) and equalization (usually in frequency domain) can also provide the zero-forcing (ZF) solution required for precise and accurate OPM [60]. Additionally, TA-CE with equalization in frequency domain requires low-complexity implementation, exhibits high performance stability and transparency with respect to the modulation-format of the user data [56], [61]–[63].

Optimum TS for 2×2 MIMO CE and synchronization are based on perfect-square minimum-phase (PS-MP) constant amplitude zero-autocorrelation (CAZAC) sequence [64] of length N symbols by using the single-block (SB) and double-block (DB) schemes described in [65]. Each TS block is surrounded

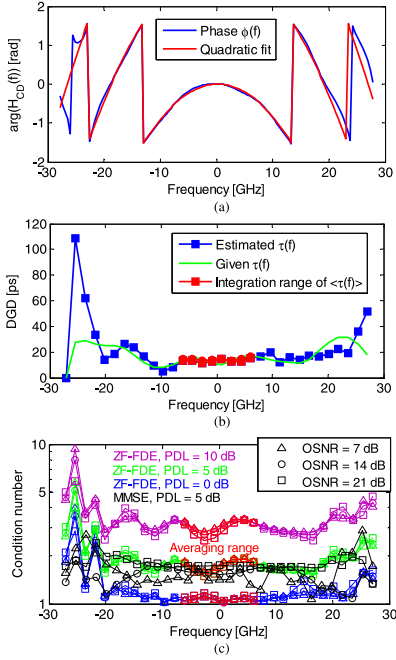


Fig. 14. CD estimation using the quadratic fit method [62], $\arg(H_{CD})$ the phase variation in frequency for the estimated induced dispersion and its quadratic fit. (left), DGD estimation averaging the DGD spectrum over a limited range of integration [66], [67] (center), condition number of each filter tap for different values of PDL and OSNR (right) [66], [67].

by a couple of guard intervals of length $N/4$ symbols. The constellation plot of a PS-MP CAZAC sequence is a $\log_2(N)$ -phase-shift keying (PSK) modulated signal. The receiver calculates the ZF CE for SB-TS [63] for DB-TS [66]. The residual CD is estimated from the quadratic fit of the resulting parabolic phase function (see Fig. 14, left) [66]. The DGD estimation is achieved by averaging over the central taps of the DGD spectrum (see Fig. 14, center) [66]. The PDL is estimated by averaging over the central taps of the ZF filter matrix (see Fig. 14, right) [64]. The ZF filter only compensates for inter-symbol interference (ISI), whereas the MMSE filter jointly optimizes the mitigation of ISI and noise attenuating the eigenvalue spread of the filter taps. Therefore, accurate estimation of PDL could not be possible from an MMSE filter. The TA-OSNR monitoring requires systems calibration as described in [67].

DSP-based OPM is demonstrated based on a simulated 28 Gbaud PDM-QPSK system. Table III provides a summary of the evaluation of the OPM based on DB-TS and SB-TS. Fast, accurate and precise CD estimation can be obtained with estima-

TABLE III
OPM CHANNEL ESTIMATION BASED ON 2×2 MIMO TRAINING SEQUENCES;
 w : WORST CASE, σ : STANDARD DEVIATION, m : MEAN VALUE OF THE
ESTIMATION ERROR; W & W/O AVERAGE: WITH OR WITHOUT CHANNEL
ESTIMATES AVERAGING (10 ESTIMATES) [66], [67]

	TS length	CD (ps/nm)					
		w/o average			w/ average		
		w	σ	m	w	σ	m
DB-TS	16	± 460	42.4	0	± 140	12.8	0
	64	± 60	14.3	0	± 30	6.9	0
SB-TS	16	± 510	43.1	0	± 160	20.1	0
	64	± 50	12.6	0	± 40	8.4	0

	TS length	DGD (ps)					
		w/o average			w/ average		
		w	σ	m	w	σ	m
DB-TS	16	-42,+34	9.8	0	-4,+44	7.1	12
	64	-60,+30	11.3	-6	-10,+42	8.6	10
SB-TS	16	-68,+22	9.4	-6	-20,+38	6.6	0
	64	-24,+28	7.2	-2	-20,+38	7.0	2

tion error as low as ± 30 ps/nm. From the DGD estimation results obtained, it would be desirable to further reduce the estimation error. However, it should be considered that a typical deviation of around 7 ps corresponds to 20% of the symbol duration of a 28 Gbaud system. Judging on the requirement for sufficient equalizer memory, this would not make a significant difference with a deviation relating to less than 1 tap (18 ps) for DSP with 2 samples/symbol. Finally, the PDL and OSNR estimation prove accuracy within ± 0.6 dB and ± 1 dB, respectively [68].

V. CONCLUSION AND FUTURE WORK

Cognitive heterogeneous reconfigurable optical networks are expected to become a breakthrough technology to implement future optical communication networks, especially in highly heterogeneous environment. In this paper we have described the approach developed within the CHRON project to include cognitive techniques in order to efficiently control and manage the network: to optimize network resources utilization and reduce system energy consumption. In this context, there are several research lines that CHRON is working on: cognitive algorithms for RWA and RMLSA assignment, virtual topology design, traffic grooming, and QoT estimation. In OPM, the development of robust algorithms for signal monitoring is being investigated to provide accurate and fast information to the CDS on the status of the physical layer. The optimization of the network with respect to energy consumption is also being investigated in CHRON, to provide an accurate end-to-end model of the energy consumption to the network, and to include the energy consumption in the multiobjective optimization.

REFERENCES

- [1] I. Tomkos *et al.*, "Next generation flexible and cognitive heterogeneous optical networks," in *the Future Internet—Future Internet Assembly 2012: From Promises to Reality*. New York, NY, USA: Springer, 2012, pp. 225–236.
- [2] W. Wei, C. Wang, and J. Yu, "Cognitive optical networks: Key drivers, enabling techniques, and adaptive bandwidth services," *IEEE Commun. Mag.*, vol. 50, no. 1, pp. 106–113, Jan. 2012.

- [3] G. S. Zervas and D. Simeonidou, "Cognitive optical networks: Need, requirements and architecture," presented at the Int. Conf. Transparent Opt. Netw., Munich, Germany, 2010, Paper We.C1.3.
- [4] R. W. Thomas, D. H. Friend, L. A. DaSilva, and A. B. MacKenzie, "Cognitive networks: Adaptation and learning to achieve end-to-end performance objectives," *IEEE Commun. Mag.*, vol. 44, no. 12, pp. 51–57, Dec. 2006.
- [5] J. Mitola III, *Cognitive Radio Architecture: The Engineering Foundations of Radio XML*. New York, NY, USA: Wiley, 2006.
- [6] Q. H. Mahmoud, *Cognitive Networks: Towards Self-Aware Networks*. New York, NY, USA: Wiley, 2007.
- [7] A. B. MacKenzie et al., "Cognitive radio and networking research at Virginia tech" *Proc. IEEE*, vol. 97, no. 4, pp. 660–688, Apr. 2009.
- [8] I. de Miguel et al., "Cognitive dynamic optical networks [Invited]" *IEEE/OSA J. Opt. Commun. Netw.*, vol. 5, no. 10, pp. A107–A118, Oct. 2013.
- [9] M. A. L. Thathachar and P. S. Sastry, *Networks of Learning Automata*. New York, NY, USA: Springer, 2004.
- [10] D. Klazovich, F. Granelli, and N. L. S. Da Fonseca, "Architectures and cross-layer design for cognitive networks," in *Handbook of Sensor Networks*. Singapore: World Scientific, 2010.
- [11] EU FP7 CHRON Project <http://www.ict-chron.eu>
- [12] R. J. Durán et al., "A cognitive decision system for heterogeneous reconfigurable optical networks" in *Proc. Future Netw. Mobile Summit*, 2012, pp. 1–9.
- [13] D. Siracusa et al., "A control plane framework for future cognitive heterogeneous optical networks" in *Proc. Int. Conf. Transparent Opt. Netw.*, 2012, pp. 1–4.
- [14] S. Azodolmoky et al., "Experimental demonstration of an impairment aware network planning an operation tool for transparent/translucent optical networks" *J. Lightw. Technol.*, vol. 29, no. 4, pp. 439–448, Feb. 2011.
- [15] S. Azodolmoky, P. Kokkinos, M. Angelou, E. Varvarigos, and I. Tomkos, "DICONET NPOT: An impairments aware tool for planning and managing dynamic optical networks," *J. Netw. Syst. Manage.*, vol. 20, no. 1, pp. 116–133, Mar. 2012.
- [16] Y. Qin et al., "Demonstration of C/S based hardware accelerated QoT estimation tool in dynamic impairment-aware optical network," presented at the Eur. Conf. Exhib. Opt. Commun., Torino, Italy, 2010, Paper P5.17.
- [17] I. H. Witten, E. Frank, and M. A. Hall, *Data Mining: Practical Machine Learning Tools and Techniques*, 3rd ed. San Mateo, CA: Morgan Kaufmann, 2011.
- [18] A. Aamodt and E. Plaza, "Case-based reasoning: Foundational issues, methodological variations, and system approaches," *Artif. Intell. Commun.*, vol. 7, no. 1, pp. 39–59, 1994.
- [19] T. Jiménez et al., "A cognitive quality of transmission estimator for core optical networks" *J. Lightw. Technol.*, vol. 31, no. 6, pp. 942–951, Mar. 2013.
- [20] A. Caballero et al., "Experimental demonstration of a cognitive Quality of Transmission estimator for optical communication systems" *Opt. Exp.*, vol. 20, no. 26, pp. B64–B70, Dec. 2012.
- [21] O. Gerstel et al., "Elastic optical networking: A new dawn for the optical layer" *IEEE Commun. Mag.*, vol. 50, no. 2, pp. S12–S20, Feb. 2012.
- [22] X. Liu et al., "448-Gb/s reduced-guard-interval CO-OFDM transmission over 2000 km of ultra-large-area fiber and five 80-GHz-grid ROADMs" *J. Lightw. Technol.*, vol. 29, no. 4, pp. 483–490, Feb. 2011.
- [23] S. Chandrasekhar, X. Liu, B. Zhu, and D. W. Peckham, "Transmission of a 1.2-Tb/s 24-carrier no-guard-interval coherent OFDM superchannel over 7200-km of ultra-large-area fiber," presented at the Eur. Conf. Opt. Commun., Vienna, Austria, Paper PD2.6.
- [24] P. Poggiolini et al., "Analytical modeling of nonlinear propagation in uncompensated optical transmission links" *IEEE Photon. Technol. Lett.*, vol. 23, no. 11, pp. 742–744, Jun. 2011.
- [25] A. Carena, V. Curri, G. Bosco, P. Poggiolini, and F. Forghieri, "Modeling of the impact of non-linear propagation effects in uncompensated optical coherent transmission links," *J. Lightw. Technol.*, vol. 30, no. 10, pp. 1524–1539, May 2012.
- [26] X. Chen and W. Shieh, "Closed-form expressions for nonlinear transmission performance of densely spaced coherent optical OFDM systems," *Opt. Exp.*, vol. 18, no. 18, pp. 19039–19054, Aug. 2010.
- [27] G. Gao, X. Chen, and W. Shieh, "Analytical expressions for nonlinear transmission performance of coherent optical OFDM systems with frequency guard band," *J. Lightw. Technol.*, vol. 30, no. 15, pp. 2447–2454, Aug. 2012.
- [28] P. Poggiolini, "The GN model of non-linear propagation in uncompensated coherent optical systems," *J. Lightw. Technol.*, vol. 30, no. 24, pp. 3857–3879, Dec. 15, 2012.
- [29] S. Kilmurray, T. Fehenberger, P. Bayvel, and R. I. Killey, "Comparison of the nonlinear transmission performance of quasi-Nyquist WDM and reduced guard interval OFDM," *Opt. Exp.*, vol. 20, no. 4, pp. 4198–4205, Feb. 2012.
- [30] H. Beyranvand and J. A. Salehi, "A quality-of-transmission aware dynamic routing and spectrum assignment scheme for future elastic optical networks," *J. Lightw. Technol.*, vol. 31, no. 18, pp. 3043–3054, Sep. 2013.
- [31] M. Jinno et al., "Distance-adaptive spectrum resource allocation in spectrum-sliced elastic optical path" *IEEE Commun. Mag.*, vol. 48, no. 8, pp. 138–145, Aug. 2012.
- [32] R. Borkowski, F. Karinou et al., "Experimental study on OSNR requirements for spectrum-flexible optical networks [Invited]" *IEEE/OSA J. Opt. Commun. Netw.*, vol. 4, no. 11, pp. B85–B93, Oct. 22, 2012.
- [33] A. Farrel, J.-P. Vasseur, and J. Ash, "A path computation element (PCE)-based architecture," presented at the IETF RFC, 2006, Paper 4655.
- [34] L. Berger, "Generalized multi-protocol label switching (GMPLS) signaling resource reservation protocol-traffic engineering (RSVP-TE) extensions," in *Proc. IETF RFC*, 2003, Paper 3473.
- [35] I. Rodríguez et al., "Minimization of the impact of the TED inaccuracy problem in PCE-based networks by means of cognition," presented at the Eur. Conf. Exhib. Opt. Commun., London, U.K., 2013, Paper We.4.E.2.
- [36] H. Zang, J. Jue, and B. Mukherjee, "A review of routing and wavelength assignment approaches for wavelength-routed optical WDM networks," *Opt. Netw. Mag.*, vol. 1, no. 1, pp. 47–60, Jan. 2000.
- [37] A. Mokhtar and M. Azizoglu, "Adaptive wavelength routing in all-optical networks," *IEEE/ACM Trans. Netw.*, vol. 6, no. 2, pp. 197–206, Apr. 1998.
- [38] R. Nejibati, E. Escalona, S. Peng, and D. Simeonidou, "Optical network virtualization," in *Proc. Int. Conf. Opt. Netw. Design Modeling*, 2011, pp. 1–5.
- [39] B. Mukherjee, *Optical Communication Networks*. New York, NY, USA: McGraw-Hill, 1997.
- [40] R. Ramaswami, K. N. Sivarajan, and G. Sasaki, *Optical Networks: A Practical Perspective*, 3rd ed. San Mateo, CA, USA: Morgan Kaufmann, 2009.
- [41] N. Fernández et al., "Cognitive algorithm to solve the impairment-aware virtual topology design problem in reconfigurable optical networks" in *Proc. IEEE Int. Conf. Cognitive Methods Situation Awareness Decision Support*, 2012, pp. 170–173.
- [42] N. Fernández et al., "Cognitive genetic algorithms to design impairment-aware virtual topologies in optical networks" in *Proc. Opt. Fiber Commun. Conf. Expo./Nat. Fiber Opt. Eng.*, Mar. 4–8, 2012, pp. 1–3.
- [43] N. Fernández et al., "Virtual topology design and reconfiguration using cognition: Performance evaluation in case of failure" in *Proc. RNDM*, 2012, pp. 132–139.
- [44] R. Tucker, "Green optical communications - part I: Energy limitations in transport," *IEEE J. Sel. Topics Quantum Electron.*, vol. 17, no. 2, pp. 245–260, Mar. 2011.
- [45] N. Fernández et al., "Cognition to design energetically efficient and impairment aware virtual topologies for optical networks" in *Proc. Int. Conf. Opt. Netw. Design Modeling*, Apr. 17–20, 2012, pp. 1–6.
- [46] W. Van Heddeghem et al., "Power consumption modeling in optical multilayer networks" *Photon. Netw. Commun.*, vol. 23, no. 1, pp. 1–15, Feb. 2012.
- [47] J. López Vizcaíno et al., "Energy Efficiency Improvement with the Innovative Flexible-grid Optical Transport Network," *Green Networking and Communications Green Networking and Communications*. Auerbach Publications, CRC Press, Taylor & Francis Group, USA, to be published in 2013.
- [48] J. Lopez Vizcaíno, Y. Ye, and I. Tafur Monroy, "Energy efficiency in elastic-bandwidth optical networks," in *Proc. Int. Conf. Netw. Future*, 2011, pp. 1–3.
- [49] M. Pióro and D. Medhi, *Routing, Flow, and Capacity Design in Communication and Computer Networks*. San Mateo, CA, USA: Morgan Kaufmann, 2004.
- [50] N. Fernández, R. J. Durán, E. Palkopoulou, I. de Miguel, I. Stiakogiannakis, N. Merayo, I. Tomkos, and R. M. Lorenzo, "Techno-economic advantages of cognitive virtual topology design," in *Proc. Eur. Conf. Exhib. Opt. Commun.*, 2013, pp. 1–3.

- [51] E. Palkopolou, I. Stiakogiannakis, D. Klonidis, T. Jiménez, N. Fernández, J. C. Aguado, J. López, Y. Ye, and I. Tomkos, "Cognitive heterogeneous reconfigurable optical network: A techno-economic evaluation," in *Proc. Future Netw. Mobile Summit*, 2013, pp. 1–10.
- [52] C. K. Chan, *Optical Performance Monitoring—Advanced Techniques for Next-Generation Photonic Networks*. Amsterdam, The Netherlands: Elsevier, 2010.
- [53] D. Kilper *et al.*, "Optical performance monitoring" *J. Lightw. Technol.*, vol. 22, no. 1, pp. 294–304, Jan. 2004.
- [54] F. Buchali, "Electronic dispersion compensation for enhanced optical transmission," presented at the Opt. Fiber Commun. Conf., Anaheim, CA, USA, Mar. 2006.
- [55] F. Pittalà *et al.*, "Data-aided frequency-domain 2×2 MIMO equalizer for 112 Gbit/s PDM-QPSK coherent transmission systems," presented at the Opt. Fiber Commun. Conf. Expo./Nat. Fiber Opt. Eng., Los Angeles, CA, USA, 2012 Paper OM2H.4.
- [56] M. Kuschnerov *et al.*, "Data-aided versus blind single-carrier coherent receivers" *IEEE Photon. J.*, vol. 2, no. 3, pp. 387–403, Jun. 2010.
- [57] R. A. Soriano *et al.*, "Chromatic dispersion estimation in digital coherent receivers" *J. Lightw. Technol.*, vol. 29, no. 11, pp. 1627–1637, Jun. 2011.
- [58] S. Qi, A. P. T. Lau, and L. Chao, "Fast and robust blind chromatic dispersion estimation using auto-correlation of signal power waveform for digital coherent systems," *J. Lightw. Technol.*, vol. 31, no. 2, pp. 306–312, Jan. 2013.
- [59] R. Borkowski *et al.*, "Experimental demonstration of adaptive digital monitoring and compensation of chromatic dispersion for coherent DP-QPSK receiver" *Opt. Exp.*, vol. 19, no. 26, pp. B728–B735, Dec. 6, 2011.
- [60] F. Hauske, M. Kuschnerov, B. Spinnler, and B. Lankl, "Optical performance monitoring in digital coherent receivers," *J. Lightw. Technol.*, vol. 27, no. 16, pp. 3623–3631, Aug. 2009.
- [61] B. Spinnler, "Equalizer design and complexity for digital coherent receivers," *IEEE J. Sel. Topics Quantum Electron.*, vol. 16, no. 5, pp. 1180–1192, Sep/Oct. 2010.
- [62] F. Pittalà, F. N. Hauske, Y. Ye, N. G. Gonzalez, and I. Tafur Monroy, "Data-aided frequency-domain channel estimation for CD and DGD monitoring in coherent transmission systems," in *Proc. IEEE Photon. Conf.*, Oct. 9–13, 2011, pp. 897–898.
- [63] F. Pittalà *et al.*, "Efficient training-based channel estimation for coherent optical communication systems," presented at the Signal Process. Photon. Commun. Conf., Colorado Springs, CO, USA, 2012 Paper SpTu3A.4.
- [64] U. H. Rohrs and L. P. Linde, "Some unique properties and applications of perfect squares minimum phase CAZAC sequences," in *Proc. South African Symp. Commun. Signal Process.*, Sep. 1992, pp. 155–160.
- [65] http://www.ict-chron.eu/Content/Deliverables_details_4_2.aspx
- [66] F. Pittalà *et al.*, "Fast and robust CD and DGD estimation based on data-aided channel estimation," presented at the Int. Conf. Transparent Opt. Netw., Stockholm, Sweden, 2011 Paper We.D1.5.
- [67] F. Pittalà, F. N. Hauske, Y. Ye, N. G. Gonzalez, and I. Tafur Monroy, "Joint PDL and in-band OSNR monitoring supported by data-aided channel estimation," in *Proc. Opt. Fiber Commun. Conf. Expo. Nat. Fiber Opt. Eng.*, Mar. 4–8, 2012, pp. 1–3.
- [68] F. Pittalà, F. N. Hauske, Y. Ye, N. G. Gonzalez, I. T. Monroy, and J. A. Nossek, "PDL monitoring based on the eigenvalues spread of a data-aided zero-forcing frequency domain equalizer," presented at the Signal Process. Photon. Commun. Top. Meeting, Colorado Springs, CO, USA, 2012, Paper SpTh2B.5.

Antonio Caballero received the Ph.D. degree on high speed radio-over-fiber links, focusing on the photonic detection using digital coherent receivers in 2011.

He is currently a Postdoctoral Researcher in metro-access and short-range systems at DTU Fotonik, Kongens Lyngby, Denmark, working in the European Research Project CHRON on cognitive optical networking. He was a Visiting Researcher at the Photonic and Networks Research Lab at Stanford University, Stanford, CA, USA, in 2010.

Robert Borkowski received the M.Sc.Eng. and Ph.D. degrees from the Technical University of Denmark in 2011 and 2014, respectively. He is currently a postdoctoral researcher at the Department of Photonics Engineering, Technical University of Denmark. He has been actively involved in the European FP7 project CHRON (Cognitive Heterogeneous Reconfigurable Optical Network).

Dr. Borkowski had been a visiting researcher at Centro de Pesquisa e Desenvolvimento em Telecomunicações (CPQD) in Campinas, Brazil in 2012. His research interests are in the area of digital signal processing and machine learning for optical communications.

Ignacio de Miguel received the Telecommunication Engineer and the Ph.D. degrees from the Universidad de Valladolid (UVA), Valladolid, Spain, in 1997 and 2002, respectively.

Since 1997, he has been a Lecturer at UVA. He has also been a Visiting Research Fellow at the University College London, working in the Optical Networks Group. His research interests include the design and performance evaluation of optical networks, especially hybrid optical networks, cognitive optical networks, as well as IP over WDM.

Dr. de Miguel received the 1997 Innovation and Development Regional Prize for his Graduation Project, and the Nortel Networks Prize for the best Ph.D. thesis on optical internet in 2002, awarded by the Spanish Institute and Association of Telecommunication Engineers.

Ramón J. Durán was born in Cáceres, Spain, in 1978. He received the Telecommunication Engineer and the Ph.D. degrees from the University of Valladolid, Valladolid, Spain, in 2002 and 2008, respectively.

Since 2002, he has been a Junior Lecturer at the University of Valladolid and is currently the Deputy Director of the Faculty of Telecommunication Engineering. His current research interests include the design and performance evaluation of cognitive heterogeneous optical networks. He is the author of more than 60 papers in international journals and conferences.

Juan Carlos Aguado received the Telecommunication Engineer and Ph.D. degrees from the University of Valladolid, Valladolid, Spain, in 1997 and 2005, respectively.

He has been a Junior Lecturer at the University of Valladolid since 1998. His current research interests include the design and evaluation of cognitive methods applied to physical-layer modeling and traffic routing in heterogeneous optical networks.

Natalia Fernández received the Telecommunication Engineer degree from the University of Valladolid, Valladolid, Spain, in 2008, where she is currently working toward the Ph.D. degree in the Optical Communications Group.

Her current research interests include the design and performance evaluation of cognitive optical networks (especially virtual topology design and reconfiguration).

Tamara Jiménez received the Telecommunication Engineer degree from the University of Valladolid, Valladolid, Spain, in 2008, where she is currently working toward the Ph.D. degree in the Optical Communications Group.

Her current research interests include the design and performance evaluation of optical networks (especially long reach passive optical networks, and cognitive optical networks).

Ignacio Rodríguez received the Telecommunication Engineer degree from the University of Valladolid, Valladolid, Spain, in 2010.

He was a Risk Analyst for Deloitte S.L. in revenue assurance projects and auditing tasks for one year. He is currently with the Optical Communications Group, University of Valladolid working on the design and performance evaluation of optical networks. In particular, he has been engaged in research on path computation mechanisms, and dynamic routing and spectrum assignment algorithms in elastic optical networks.

David Sánchez received the Telecommunication Engineer degree and the M.Res. degree in information and communication technologies, both from the University of Valladolid, Valladolid, Spain, in 2009 and 2012, respectively.

From 2008 to 2012, he was a Project Engineer in the Centre for the Development of Telecommunications, Castilla y León, Spain, and he participated in different European research projects both in the e-learning and telematics fields. Then, he moved to the Optical Communications Group, University of Valladolid. Since 2010, he has been involved in the Cognitive Heterogeneous Reconfigurable Optical Network European project (FP7/2007–2013) within the optical communications field. His current research interests includedemonstrating, both in simulation and emulation scenarios, how cognition can be exploited to provide effective decisions on the operation of a heterogeneous reconfigurable optical network.

Rubén M. Lorenzo received the Telecommunication Engineer and Ph.D. degrees from the University of Valladolid, Valladolid, Spain, in 1996 and 1999, respectively.

From 1996 to 2000, he was a Junior Lecturer at the University of Valladolid, and joined the Optical Communications Group, where since 2000, he has been a Lecturer. He is also the Head of the Faculty of Telecommunication Engineering, University of Valladolid. His research interests include integrated optics, optical communication systems and optical networks.

Dimitrios Klonidis received the degree in electrical and computer engineering from the Aristotle University of Thessaloniki, Thessaloniki, Greece, in 1998, the M.Sc. degree in telecommunication and information systems, and the Ph.D. degree in optical communications and networking, both from the University of Essex, Essex, U.K., in 2001 and 2006, respectively.

In September 2005, he joined the high-speed Networks and Optical Communications Group, Athens Information Technology, Peania, Greece, as a Faculty Member and Senior Researcher. He has been actively involved in several European funded research projects and gained technical expertise in various research and development areas, including optical network architecture design and optimization for access, metro and core networks, optical transmission and switching technology development and performance evaluation, and network planning control and management. His research activities have resulted in more than 100 publications in international journals and conferences.

Eleni Palkopoulou received her Diploma degree in Electrical and Computer Engineering from the National Technical University of Athens (NTUA), Greece in 2005, her M.Sc. in Communications Engineering from the Munich University of Technology (TUM), Germany in 2007, and her Ph.D. degree her Ph.D. from the Chemnitz University of Technology in 2012. In September 2011 she joined the High Speed Networks and Optical Communications Research Group of Athens Information Technology (AIT). Prior to AIT she was with the Multi-Layer Networks and Resilience Group of Nokia Siemens Networks (NSN) Research in Munich and with Siemens, Corporate Technology in Munich. Her research interests include network architectures and multi-layer optimization, techno-economic studies, heterogeneous optical networks, resilience mechanisms, grooming, and routing. She is the co-recipient of the Best Paper Award of the 7th International Workshop on the Design of Reliable Communication Networks (DRCN) 2009.

Nikolaos P. Diamantopoulos, biography not available at the time of publication.

Ioannis Tomkos has been with Athens Information Technology (AIT), Peania, Greece, since September 2002 (serving as the Professor, Research Group Head, and Associate Dean). In the past, he was a Senior Scientist at Corning Inc., Corning, NY, USA (1999–2002) and a Research Fellow at the University of Athens, Athens, Greece (1995–1999). He has represented AIT as the Principal Investigator in about 20 European Union and industry funded research projects (including nine currently active projects) and has a consortium-wide initiator/leader role. His fields of expertise are telecommunication systems, networks and photonics, as well as technoeconomic analysis and business planning of ICTs. Together with his colleagues and students, he has authored more than 450 peer-reviewed archival scientific articles, including more than 120 journal/magazine/book publications and 330 conference/workshop proceedings papers.

Dr. Tomkos was elected in 2007 as the Distinguished Lecturer of the IEEE Communications Society for the topic of optical networking. He has served as the Chair of the International Optical Networking Technical Committee of the IEEE Communications Society (2007–2008) and the Chairman of the IFIP Working Group on Photonic Networking (2008–2009). He is currently the Chairman of the OSA Technical Group on Optical Communications (2009–2012) and the IEEE Photonics Society Greek Chapter (2010–2012). He is also the Chairman of the Working Group “Next Generation Networks” of the Digital Greece 2020 Forum. He has also been General Chair, Technical Program Chair, Subcommittee Chair, Symposium Chair, or/and Member of the steering/organizing committees for the major conferences/workshops. In addition, he is/was a Member of the Editorial Boards of the IEEE/OSA JOURNAL OF LIGHTWAVE TECHNOLOGY, the IEEE/OSA JOURNAL OF OPTICAL COMMUNICATIONS AND NETWORKING, the IET Journal On Optoelectronics, and the International Journal on Telecommunications Management.

Domenico Siracusa received the M.Sc. degree in telecommunications engineering from Politecnico di Milano, Milan, Italy, in December 2008, with a thesis on carrier Ethernet technologies. He received the Ph.D. in information technology from Politecnico di Milano, Milan, in March 2012.

He is currently a Researcher of the Future Networks area at CREATE-NET, Trento, Italy. In his Ph.D. thesis, he has investigated the architectures, the methods, and the algorithms to control switching in optical networks. He is (and has been) involved in European and industrial projects on optical switching technologies and on control and management solutions. He has authored a number of publications for international conferences on optical and transport networking technologies.

Antonio Francescon received the degree in computer engineering in 2005 from the University of Padua, Padua, Italy.

Since June 2005, he has been working in CREATE-NET, Trento, Italy, as a Research Engineer, first designing and developing software for energy saving wireless sensor networks, then moving into optical networks and working on the design and implementation of GMPLS control planes for resource optimization. He is currently involved in EC-funded research projects on optical technologies.

Elio Salvadori received the degree in telecommunications engineering from Politecnico di Milano, Milan, Italy, in 1997. He received the Ph.D. degree in computer science from the University of Trento, Trento, Italy, in 2005.

He was a Systems Engineer in Nokia Networks and then Lucent Technologies until November 2001. He had been acting as Area Head of the Engineering & Fast Prototyping group until July 2012, while he is currently the CEO of Trentino NGN Srl, while keeping a position as Senior Advisor in CREATE-NET, Trento, Italy. His team is (and has been) involved in several European and industrial projects on SDN and optical technologies, as well as on future Internet experimental facilities. He has authored a number of publications in the area of optical networks and software-defined networking.

Yabin Ye received the B.E. and Ph.D. degrees in electronic engineering from Tsinghua University, Beijing, China, in 1997 and 2002, respectively.

From September 2002 to July 2004, he was a Research Scientist with the Institute for Infocomm Research, Singapore. From August 2004 to October 2008, he was a Senior Researcher with Create-Net, Italy. He is currently a Senior Researcher at the European Research Center, Huawei Technologies, Munich, Germany. His research interests include optical networking, transmission technologies as well as hybrid optical/wireless access technologies. He has authored more than 100 papers in international journals and conferences.

Jorge López Vizcaíno received the M.Sc. degree in telecommunications engineering from the Technical University of Denmark, Kongens Lyngby, Denmark. In 2011, he carried out research at the European Research Center of Huawei Technologies, Munich, Germany, within the scope of the M.Sc. thesis at DTU Fotonik. He is currently working toward the Ph.D. degree at Huawei Technologies, Munich, Germany.

His research interests include network planning, network protocols, and optical networks.

Fabio Pittalà received the M.Sc. degree in telecommunication engineering from the Technical University of Denmark, Kongens Lyngby, Denmark, in 2011. He is currently working toward the Ph.D. degree at the Technical University of Munich, Munich, Germany.

He is also a Researcher at the Huawei European Research Center, Munich. He was a Visiting Student at the Universidad Autónoma de Madrid, Madrid, Spain, in 2007, and a Research Assistant at the National Technical University of Athens, Athens, Greece, in 2008. His research interests include the field of high-speed digital signal processing for optical transmission systems with emphasis in synchronization, channel estimation, equalization, and optical performance monitoring.

Andrzej Tymecki received the Master's degree from the Technical University of Lublin, Lublin, Poland, in 1996.

He is currently with Orange Labs, Warsaw, Poland, keeping the position of an R&D Expert responsible for new telecommunications technologies. He specializes in fibre optic tests and measurements, impairments compensation/mitigations techniques, and fibre optic passive components. He is the author of numerous national and international publications in the area of fibre optic technologies.

Mr. Tymecki is a Member of CENELEC CLC/TC 86BXA and IEC SC86A, SC86B and SC86C Standardization Committees and numerous project teams in international and corporate projects. He is the Chairman of KT282 Fibre Optic Committee in Polish Committee for Standardization. He is the Project Manager of FP7 ALPHA, CHRON, FBOS projects in Orange Labs.

Idelfonso Tafur Monroy is currently a Professor at the Technical University of Denmark, Kongens Lyngby, Denmark, and the Head of the Metro-access and Short-range Communications Group, of the Department of Photonics Engineering, DTU Fotonik, Kongens Lyngby. He has more than 15 years of experience in participation in European research projects (e.g., APEX, STOLAS, LASAGNE, MUFINS, ALPHA, BONE, EURO-FOS, and GigaWaM). He is also the Technical Coordinator of European Project CHRON. He also leads projects granted by the Danish Research Council and within the Marie Curie IIF Schemes (WoPROF, WisCON).

Paper [E]: Advanced modulation formats in cognitive optical networks: EU project CHRON demonstration

Robert Borkowski, Antonio Caballero, Dimitrios Klonidis, Christoforos Kachris, Antonio Francescon, Ignacio de Miguel, Ramón J. Durán, Darko Zibar, Ioannis Tomkos, and Idelfonso Tafur Monroy. Advanced modulation formats in cognitive optical networks: EU project CHRON demonstration. In *Optical Fiber Communication Conference (OFC)*, paper W3H.1, San Francisco, CA, USA, March 2014. OSA.

Advanced Modulation Formats in Cognitive Optical Networks: EU project CHRON Demonstration

Robert Borkowski¹, Antonio Caballero¹, Dimitrios Klonidis², Christoforos Kachris², Antonio Francescon³, Ignacio de Miguel⁴, Ramón J. Durán⁴, Darko Zibar¹, Ioannis Tomkos² and Idelfonso Tafur Monroy¹

¹ DTU Fotonik – Department of Photonics Engineering, Technical University of Denmark

² Athens Information Technology, Greece

³ CREATE-NET, Italy

⁴ Universidad de Valladolid, Spain

¹ rbor@fotonik.dtu.dk, ² itom@ait.gr, ³ antonio.francescon@create-net.org

Abstract: We demonstrate real-time path establishment and switching of coherent modulation formats (QPSK, 16QAM) within an optical network driven by cognitive algorithms. Cognition aims at autonomous configuration optimization to satisfy quality of transmission requirements.

OCIS codes: (060.4250) Networks; (060.4510) Optical communications; (060.1660) Coherent communications

1. Introduction

In modern optical fiber communication networks there exists a vast spectrum of available technologies and services and their number as well as their diversity will continue to grow with time. In order to support dynamically reconfigurable heterogeneous scenarios, and taking into account that service provisioning decisions have to be made as rapidly as possible, it is of vital importance to introduce automatic or semi-automatic decision making process at the network management and control level. Cognitive optical networking, in particular the architecture proposed by the EU project CHRON (Cognitive Heterogeneous Reconfigurable Optical Network) [1] (cf. Fig. 1(a)), is a suitable candidate to introduce this functionality. CHRON implements “a network with a process that can perceive current network conditions, and then plan, decide, and act on those conditions. The network can learn from these adaptations and use them to make future decisions, all while taking into account end-to-end goals” [2].

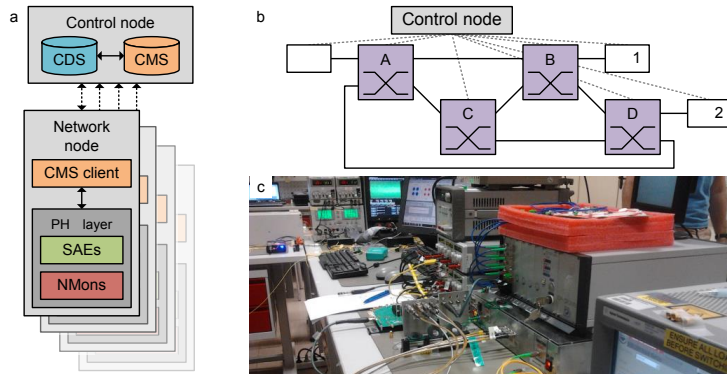


Fig. 1. (a) Outline of the centralized CHRON architecture; CDS: cognitive decision system, CMS: control and management system, PHY: physical, SAEs: software-adaptable elements, NMons: network monitors. (b) Configuration of the experimental network testbed; A-D: network nodes, Tx: transmitter, Rx1/2: receivers. (c) A photograph showing the experimental setup for CHRON network testbed with coherent modulation formats.

In this paper, we report on an experimental demonstration of transmission of advanced modulation formats (quaternary phase-shift keying: QPSK and 16-ary quadrature amplitude modulation: 16QAM) in the CHRON project testbed. By using a Cognitive Decision System (CDS) [3], various advanced networking scenarios are realized. In particular, we experimentally investigate modulation format change scenario, where the modulation format used for transmission is dynamically adjusted to maintain required quality of transmission (QoT) level.

2. Testbed

2.1 Network setup

The network configuration of the CHRON testbed is presented in Fig. 1(b). The testbed is a partly connected mesh network with four nodes and a central control node that implements network cognition. Coherent transmitter is connected at Node A, while receivers are located at nodes C and D. All experimental transmissions originate from node A and are being sent to the destination over a selected route. Each node is equipped with a strictly non-blocking 8×8 optical cross-connect (OXC). Outputs of two WDM demultiplexers (DMUX), each supporting four wavelengths (ITU-T DWDM G.694.1 channels C28-C31) by directing each channel to a dedicated output fiber, are connected to OXC inputs. All eight OXC outputs are grouped into two bundles of four fibers. Fibers in each bundle are coupled together. In this way we obtain a 2×2 strictly non-blocking switch supporting 4λ channels on each input. Moreover, nodes are equipped with power monitors, observing for potential signal failures.

In the transmitter (Tx in Fig. 1(b)), four decorrelated copies of pseudorandom binary sequence of length $2^{15}-1$ (PRBS-15) at 24 Gbit/s are generated with a bit pattern generator (BPG). The electrical signals are used to drive a commercial 100G dual polarization (DP) QPSK lithium-niobate optical modulator. The modulator is supplied by an optical signal originating from four 100 kHz-linewidth lasers at 100 GHz spacing (C28-C31: 1554.94 nm, 1554.13 nm, 1553.33 nm, 1552.52 nm). The output of the modulator is then split in a 3 dB coupler. One of its copies is then used as-is, to provide DP-QPSK signal at a line rate of 96 Gbit/s. The other output of the splitter is passed through a carefully aligned polarization controller and a polarization beam splitter in order to generate 16QAM signal via angular superposition of polarizations [5]. This results in a single polarization (SP) 16QAM signal which is later polarization-multiplexed by combining it with its delayed copy in the orthogonal polarization. As a result, four DP-16QAM channels, each carrying 192 Gbit/s become available. As both QPSK and 16QAM at the same wavelengths are simultaneously generated, we can easily switch between those modulation formats, emulating an actual reconfigurable transmitter.

Signal reception (Rx1/2 in Fig. 1(b)) is performed with a standard preamplified coherent detection receiver. The received signal is mixed in a 90° optical hybrid with a local oscillator signal from another 100 kHz-linewidth laser source whose frequency is separated by a couple of hundreds of MHz from the measured signal. Next, the signal is photodetected, sampled with a real-time sampling oscilloscope and demodulated with algorithms operating in near-real time (NRT), which provide up to one measurement approximately every five seconds. The bit error rate (BER) is estimated from error vector magnitude (EVM) of the received constellation diagram.

3. Experimental scenarios

In order to show advantages obtained by using cognition in the network, a range of different scenarios were designed and implemented in the testbed [6].

3.1 New lightpath establishment by cognition

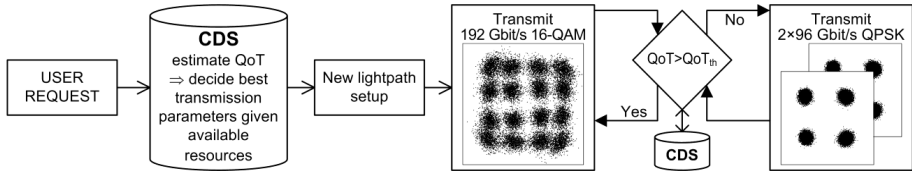


Fig. 2. A simplified concept of the lightpath establishment and subsequent modulation format change.

The concept of this and subsequent scenario is outlined in Fig. 2. First, the CDS receives user request regarding required capacity between two nodes. Next, CDS determines the route as well as the transmission parameters (bandwidth, modulation format) given available resources while ensuring that QoT is maintained. In our case, QoT is only constituted by the BER, and thus QoT threshold (QoT_{th}) is determined by a FEC limit. Nonetheless, more advanced scenarios may use a composite QoT figure which would be a combination of multiple signal quality parameters. As a next step, CDS requests the source node to configure the route via the control plane. Once finished, destination node notifies CDS about successful path establishment and data is being sent with transmission parameters configured by the CDS. Finally, the monitoring plane continually updates CDS with the performance data regarding the QoT of the established connection.

3.2 Modulation format change (QoT degradation without rerouting)

The CDS may decide to autonomously change connection parameters in an answer to external or unexpected factors affecting QoT. In modulation format change scenario, the modulation format is downgraded from high order QAM

to a simpler and more robust, phase-shift keyed signal. The CDS obtains monitoring data from power monitors and optical signal-to-noise ratio monitors along the path, as well as BER from end nodes. Based on this information, CDS computes QoT figure. If measured QoT is below QoT_{th} and CDS expects that the QoT will be restored due to modulation format change, this change is implemented in the network. This concept is outlined in the flow diagram in Fig. 2. Additionally, CDS contains a knowledge base (KB) which store past network behavior, such as previously observed QoT of each lightpath to improve upon current decisions.

Experimental investigation of real-time path establishment and modulation format change was performed in the testbed. We investigate establishment of one-channel lightpath ACBDAB with 192 Gbit/s DP-16QAM modulation format assuming KB of the CDS is empty. The performance of 16QAM transmission in the testbed is presented in Fig. 3 (filled markers). We see that BER for this particular lightpath is below the assumed 7% forward error correction (FEC) limit of 3.8×10^{-3} . However, the CDS does not have any prior performance data on this or similar lightpath (is empty) and initiates transmission using 16QAM. As a result, QoT is unsatisfactory (i.e., $QoT < QoT_{th}$) and the cognitive process inside CDS takes a decision to downgrade the modulation format to DP-QPSK carrying 96 Gbit/s (c.f. Fig. 2). To maintain the same capacity, another channel with the same bit rate is added to the lightpath. The modulation format change process is autonomous and transparent to the user, who does not need to specify any parameters of the optical transmission.

The information about 16QAM failure when transmitted over the investigated lightpath is then stored in the KB to make sure that subsequent requests to establish this or similar lightpath will not result in attempts to use 16QAM. Moreover the simple fact of measuring 16QAM performance over ACBDAB lightpath in the first connection attempt can be used by the CDS to predict performance of 16QAM at other nodes (cf. Fig. 3). Methods, such as in [3], are also involved to estimate the performance. If QoT_{th} is to decrease in future (e.g. by introducing a stronger FEC variant), the modulation format may be autonomously upgraded to 16QAM by the cognitive process.

3.3 Other scenarios supported by cognition

The link failure scenario occurs when one of the links fails. The aim is to demonstrate that CDS learns patterns of failure and can provide superior path rerouting time to a non-cognitive network. Another scenario is OSNR degradation (QoT degradation with rerouting), where links are OSNR limited. Only a certain number of channels can be established before QoT will fall below QoT_{th} . In order to avoid decrease of QoT of already established channels, new channels are set up using a different route. For both of those scenarios, a similar process is followed: 1) monitoring plane notifies CDS of a failure/decreasing performance; 2) CDS decides that the specific lightpath has to be rerouted as to avoid broken fiber/OSNR limited link; 3) CDS tears down previous path and establishes a new one with sufficient QoT; 4) each node is reconfigured accordingly and CDS is notified; 5) the new lightpath is monitored.

4. Conclusions

We experimentally demonstrated chosen scenarios and capabilities of a cognitive networking testbed developed within the EU project CHRON. For example we show that the cognitive decision system developed within the project is successful in autonomous establishment of a lightpath carrying 192 Gbit/s 16QAM. Due to insufficient quality of transmission (QoT), the modulation format over the established lightpath is downgraded to two 96 Gbit/s QPSK channels, providing the same total line rate.

5. Acknowledgements

The research leading to these results was partly supported by the CHRON (Cognitive Heterogeneous Reconfigurable Optical Network) project with funding from the EU FP7 Programme (FP7/2007-2013) under grant agreement no. 258644. We acknowledge u² Photonics AG for the provided equipment.

6. References

- [1] CHRON (Cognitive Heterogeneous Reconfigurable Optical Network) project, <http://www.ict-chron.eu/>
- [2] R.W. Thomas et al., "Cognitive networks: adaptation and learning to achieve end-to-end performance objectives," *IEEE Commun. Mag.* 44, 51-57 (2006).
- [3] T. Jiménez et al., "A cognitive quality of transmission estimator for core optical networks," *J. Lightw. Technol.* 31, 942-951 (2013).
- [4] I. de Miguel et al., "Cognitive dynamic optical networks [Invited]," *IEEE J. Opt. Commun. Netw.* 5, A107-A118 (2013).
- [5] I. Morohashi et al., "16 QAM synthesis by angular superposition of polarization using dual-polarization QPSK modulator," in *Proc. ECOC*, P3.14 (2010).
- [6] CHRON Consortium, "D6.1 Specification of the CHRON testbed," (2012).

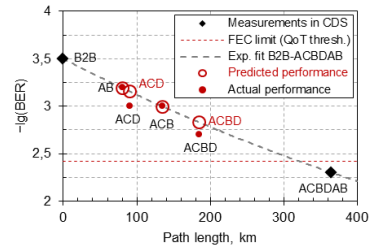


Fig. 3. Performance of 16QAM in the testbed (filled markers). By simple engineering rules, performance at other nodes can be easily inter- or extrapolated (open markers) and used for future decisions by the CDS.

Paper [F]: Demonstration of EDFA cognitive gain control via GMPLS for mixed modulation formats in heterogeneous optical networks

Juliano R. Oliveira, Antonio Caballero, Eduardo Magalhães, Uiara Moura, **Robert Borkowski**, Giovanni Curiel, Alberto Hirata, Luis Carvalho, Edson Porto da Silva, Darko Zibar, José Maranhão, Idelfonso Tafur Monroy, and Júlio Oliveira. Demonstration of EDFA cognitive gain control via GMPLS for mixed modulation formats in heterogeneous optical networks. In *Optical Fiber Communication Conference (OFC)*, paper OW1H.2, Anaheim, CA, USA, March 2013. OSA.

Demonstration of EDFA Cognitive Gain Control via GMPLS for Mixed Modulation Formats in Heterogeneous Optical Networks

Juliano Oliveira⁽¹⁾, Antonio Caballero⁽²⁾, Eduardo Magalhães⁽¹⁾, Uíara Moura⁽¹⁾, Robert Borkowski⁽²⁾, Giovanni Curiel⁽¹⁾, Alberto Hirata⁽¹⁾, Luis Hecker⁽¹⁾, Edson Porto⁽¹⁾, Darko Zibar⁽²⁾, José Maranhão⁽³⁾, Idelfonso Tafur Monroy⁽²⁾, Julio Oliveira⁽¹⁾

⁽¹⁾ CPqD Foundation, Rod. Campinas/Mogi Mirim, km 118.5, Campinas, SP, Brazil, jrfo@cpqd.com.br

⁽²⁾ DTU Fotonik, Tech. Univ. of Denmark, DK-2800 Kgs. Lyngby, Denmark, acaj@fotonik.dtu.dk

⁽³⁾ PADTEC, Rod. Campinas/Mogi Mirim, km 118.5, Campinas, SP, Brazil, jmaranhao@padtec.com.br

Abstract: We demonstrate cognitive gain control for EDFA operation in real-time GMPLS controlled heterogeneous optical testbed with 10G/100G/200G/400G lightpaths. Cognitive control maintains the network BER below FEC-limit for up to 6 dB of induced attenuation penalty.

OCIS codes: (060.4250) Networks; (060.4510) Optical communications.

1. Introduction

Next generation optical networks will be of a highly heterogeneous nature, ranging from elastic bandwidth, mixed modulation formats and flexible grid for spectrum allocation [1–5]. One implication of this new paradigm is that optical elements, like the omnipresent erbium-doped fiber amplifiers (EDFAs), need to dynamically support lightpaths with different characteristics. Control algorithms to stabilize EDFAs channel power control in networks with ROADMs have been reported [6]. Solely, it does not provide dynamic control of gain flatness (GF) and noise figure (NF), relevant for links supporting advanced modulation formats, such as dual-polarization (DP) quadrature phase-shift keying (QPSK) or 16-ary quadrature amplitude modulation (16-QAM) in dense wavelength division multiplexed (DWDM) networks.

We propose the use of a novel cognitive approach, in particular the capability of learning from previous knowledge [4, 5], for EDFA gain control to ensure stable quality of transmission (QoT) for heterogeneous optical lightpaths. In this paper, we present the first experimental demonstration of real-time cognitive EDFA gain control in a GMPLS controlled autonomous testbed. The testbed is based on a replication of Brazilian GIGA network branch, with 10/100/200/400G lightpaths including mixed-modulation formats: DP-QPSK, 16-QAM and coherent optical (CO) orthogonal frequency division multiplexing (OFDM) DP-QPSK superchannel. The cognitive control includes the EDFAs fitness power mask used in the testbed to ensure bit error rate (BER) below 7% of forward error correction (FEC) threshold for all network lightpaths under attenuation penalty of up to 6 dB.

2. Cognitive EDFA control concept

The use of cognition for optimizing EDFAs operation point is based on the knowledge of a fitness power mask for each EDFA in the network. In our reported experiment, all EDFAs were characterized with respect to GF and NF. We considered 40 non-modulated WDM channels in a 100 GHz grid (entire C-band) as the input signal to each EDFA. The characterization procedure consisted of measuring the GF and NF values for each combination of gain and total input power, see Fig. 1. For the purpose of illustration, Fig 1(a) and (b) shows an example of such characterization. For each total input power and gain value combination, a plot of $NF \times GF$ was built for each EDFA, as exemplified in Fig. 1(c) for the case of input power of -15 dBm. A target vector optimization method [7] was implemented to simultaneously optimize NF and GF, acting on the objective space as illustrated in Fig. 1(c).

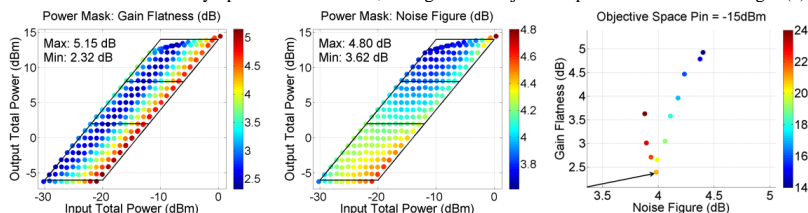


Fig. 1: Optical amplifier operational point adjustment: (a) Gain flatness, (b) Noise figure, (c) Example of objective space optimization for input power of -15 dBm.

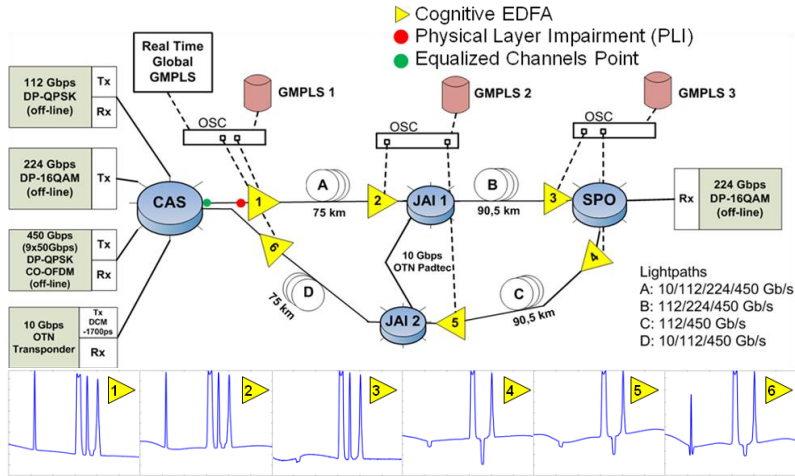


Fig. 2: Experimental setup of the implemented heterogeneous optical network. OSC: Optical supervisory channel.

A setpoint gain value is associated with each point in the objective space for the measured input power. The lowest Euclidian distance from the point to origin denotes the gain setpoint that gives better fitness result (lowest GF and NF). An example in Fig. 1(c) shows that the optimized setpoint gain is 21 dB for -15 dBm input power. In our testbed, the GMPLS control plane was adapted for EDFAs monitoring and configuration, implementing the corresponding collection, and communication via control channels. In this way, we were able to run live the above cognitive EDFA control algorithm, performing real time setpoint gain adjust in less than 1 second for all EDFAs in the testbed. As high values of optical power may induce undesirable non-linear fiber transmission impairments, two regimes are considered. LP1 regime makes strict restriction on allowed maximum launch power (LP) to minimize potential non-linear effects, but does not highly optimizes GF and NF. LP2 makes the trade-off between the minimization of NF and GF values for tolerance to non-linear effects. The allowed LP for LP1 is -2 dBm and for LP2 is 2 dBm. These values are accounted in the optimization algorithm restricting the adjusted gains to limit output powers below LP1 and LP2 levels.

3. Experimental implementation

Fig. 2 shows the experimental testbed, based on a replication of Brazilian GIGA experimental network branch Campinas (CAS), Jundiaí (JAI), São Paulo (SPO), with implemented GMPLS real time control. Four different wavelengths were used, carrying different modulation formats: 10 Gb/s on-off keying (OOK) with chromatic dispersion (CD) pre-compensation (1535.82 nm), 112 Gb/s NRZ-DP-QPSK with offline coherent detection (1550.12 nm), 224 Gb/s pre-filtered 33% RZ-DP-16QAM with offline coherent detection (1547.72 nm), 450 Gb/s NRZ-CO-OFDM, (9x12.5 Gbaud DP-QPSK) with offline coherent detection (1545.32 nm). In Fig. 2 insets are shown each amplifier output power spectrum for the transmitted channels.

The testbed was composed of 3 nodes and 4 fiber spans, see Fig. 2. The first node (CAS) acted as a transmitter (Tx) for all 4 channels and receiver (Rx) for the 10 Gb/s, 112 Gb/s and 450 Gb/s. The 4 channels were transported to JAI1, where the 10 Gb/s channel was dropped. At SPO the 224 Gb/s 16-QAM channel was detected, whereas the 112 Gb/s QPSK and 450 Gb/s CO-OFDM were routed back to JAI2 where they were combined with the 10 Gb/s from JAI1 and transported all together to CAS. Induction of physical layer impairments (PLI) were generated by adding 3 or 6 dB attenuation at the input of the amplifier 1, the same point where channels were equalized, see Fig. 2.

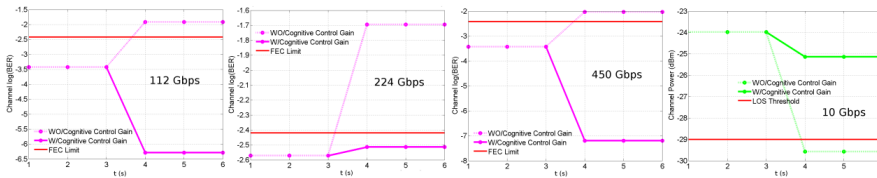
A distributed GMPLS control plane, comprising a standard GMPLS protocols stack with adaptations for DWDM layer is implemented. EDFAs were configured through the optical link management protocol (OLMP) using a centralized monitor. This monitor reads both EDFA dynamic (input power, output power and current calculated optical gain) and static parameters (device model) for all amplifiers along the GMPLS nodes, executes the cognitive EDFA control algorithm and configures all amplifiers in real time operation.

Tab. 1: Results of the cognitive EDFA with respect to launch power restriction method. OK/Fail =below/above FEC threshold.

PLI Att. (dB)	Channel Bit rate (Gb/s)	EDFA w/o cognition BER	Cognitive EDFA					
			No LP restriction		LP1 regime		LP2 regime	
			G1-G6 After (dB)	BER	G1-G6 After (dB)	BER	G1-G6 After (dB)	BER
3	10	OK		OK		OK		OK
	112	OK	21/23/24/ 21/23/21	Fail	14/22/22/ 14/23/23	OK	16/23/20/ 14/23/21	OK
	224	Fail		OK		OK		OK
	450	Fail		Fail		OK		OK
6	10	Fail		OK		OK		OK
	112	Fail	20/23/20/ 23/23/21	OK	15/23/20/ 15/23/23	OK	18/23/21/ 14/23/21	OK
	224	Fail		OK		Fail		OK
	450	Fail		OK		OK		OK

4. Experimental results

Tab. 1 gathers the results for different attenuation PLI levels (3 and 6 dB) and launch power restriction methods performed in the testbed. OK/Fail indicates BER below/above the FEC threshold. Initially, considering the system without PLI, the gain of all the EDFAs were set to 17 dB, as it was enough to overcome all span losses with all channels operating below FEC limit. When a 3 dB PLI is induced in a system without EDFA cognition, only 10 Gb/s and 112 Gb/s channels are properly received. For 6 dB PLI, none of the channels are below the FEC threshold. When cognitive EDFA control is applied, without LP control, the performance is improved and only the 112 Gb/s and 450 Gb/s channels fail for 3 dB PLI due to nonlinearities caused by the high amplifier launch power levels. Next, when cognitive EDFA control with LP1 launch power constrain is implemented, the performance is improved even further and just the 224 Gb/s channel fails for 6 dB PLI due the low OSNR value. Finally, when cognitive EDFA LP2 control is employed, all channels are successfully detected for both 3 or 6 dB PLI. Fig. 3 shows an example of live time control of EDFAs with LP2 cognitive control, for the case of 6 dB induced PLI. We can clearly observe how at time 3s (Fig. 3) cognitive EDFA LP2 adjust the gain, to achieve BER performance below FEC-limit for 112/224/450 Gb/s channels, and beyond loss of signal (LOS) threshold for the 10 Gb/s channel.

**Fig. 3:** BER measurements (purple) for 112/224/450 Gb/s channels and power (green) for 10 Gb/s channel after a 6dB attenuation event.

5. Conclusions

We experimentally demonstrated the benefits of cognitive EDFA gain control through a real-time GMPLS control plane for heterogeneous optical networks. The reported testbed includes 10/100/200/400G lightpaths with mix-modulation formats. Our result shows that under dynamic operation and induced attenuation events of up to 6 dB, the BER of lightpaths were maintained below 7% FEC threshold. The results show clearly the prospect of cognition to achieve self-perception and self-adaption to the current physical layer conditions which is of relevance in flexible and heterogeneous optical networks.

6. References

- [1] S. Azodolmolky et al., "Experimental demonstration of an impairment aware network planning and operation tool for transparent/translucent optical networks" J. of Lightwave Technol. **29**, 4, 439–448 (2011).
- [2] N. Amaya et al., "Gridless optical networking field trial: flexible spectrum switching, defragmentation and transport of 10G/40G/100G/555G over 620-km field fiber", Optics Express **19**, 26, B277–B282, (2011).
- [3] D. J. Geisler et al., "The First Testbed Demonstration of a Flexible Bandwidth Network with a Real-Time Adaptive Control Plane," ECOC'11, Th.13.K.2 (2011).
- [4] I. T. Monroy et al., "Cognitive Heterogeneous Reconfigurable Optical Networks (CHRON): Enabling technologies and techniques," ICTON, 2011, Th.A1.2 (2011).
- [5] E. C. Magalhães et al., "Multi-Rate (10/112G) GMPLS based Autonomous Optical Testbed considering Physical IA Constraints," Photonics in Switching (PS), Fr-S38-O18 (2012).
- [6] Frank Smyth et al., "Applied Constant Gain Amplification in Circulating Loop Experiments," J. Lightwave Technol. **27**, 4686–4696 (2009).
- [7] Chien-Ho Ko and Shu-Fan Wang, "Precast production scheduling using multi-objective genetic algorithms," Expert Systems With Applications **38**, 7, 8293–8302, (2011).

Paper [G]: Experimental study on OSNR requirements for spectrum-flexible optical networks

Robert Borkowski, Fotini Karinou, Marianna Angelou, Valeria Arlunno, Darko Zibar, Dimitrios Klonidis, Neil Guerrero Gonzalez, Antonio Caballero, Ioannis Tomkos, and Idelfonso Tafur Monroy. Experimental study on OSNR requirements for spectrum-flexible optical networks. *Journal of Optical Communications and Networking*, vol. 4, no. 11, pp. B85–B93, October 2012.

Experimental Study on OSNR Requirements for Spectrum-Flexible Optical Networks [Invited]

Robert Borkowski, Fotini Karinou, Marianna Angelou, Valeria Arlunno, Darko Zibar, Dimitrios Klonidis, Neil Guerrero Gonzalez, Antonio Caballero, Ioannis Tomkos, and Idelfonso Tafur Monroy

Abstract—The flexibility and elasticity of the spectrum is an important topic today. As the capacity of deployed fiber-optic systems is becoming scarce, it is vital to shift towards solutions ensuring higher spectral efficiency. Working in this direction, we report an extensive experimental study on adaptive allocation of superchannels in spectrum-flexible heterogeneous optical network. In total, three superchannels were transmitted. Two 5-subcarrier 14-GHz-spaced, 14 Gbaud, polarization-division-multiplexed (PDM) quadrature-phase-shift-keyed (QPSK) superchannels were separated by a spectral gap, the band of interest (BOI). The bandwidth of the BOI was varied. The BOI was subsequently filled with another superchannel, constituted by a different number of either 14 Gbaud PDM-QPSK or PDM-16-ary quadrature amplitude modulation (16-QAM) subcarriers. The optical signal-to-noise ratio (OSNR) for transmission of the subcarriers inserted into the BOI, depending on the modulation format, subcarrier count and spacing to the neighboring superchannels, was extracted through experimental implementation of different scenarios. The obtained values were interpolated to yield the required OSNR necessary to maintain a 1×10^{-3} bit error rate of the central BOI subcarrier. The results provide a rule of thumb that can be exploited in resource allocation mechanisms of future spectrum-flexible optical networks.

Index Terms—Coherent detection; Elastic optical networking; Flexible optical networking; Optical networking; Optical transmission.

I. INTRODUCTION

Because of ever-increasing traffic demands, the limited resources of currently deployed fiber-optic systems are approaching their capacity [1]. Among many factors, limited amplifier bandwidth and modulation schemes with low spectral efficiency are contributing to this exhaustion. The reintroduction of coherent detection [2] allowed for advanced

optical phase and amplitude modulation schemes such as quadrature phase-shift keying (QPSK), and more notably for 16-ary quadrature amplitude modulation (16-QAM), with high spectral efficiency. To further improve available resource utilization, the concept of elasticity and flexible spectrum allocation was put forward [3,4]. Spectrum flexibility is implemented via adaptation of wavelength, symbol rate, or modulation format and is enabled by coherent detection [5,6]. Bandwidth-variable transponders and optical cross-connects (OXC) have been introduced to allow for an efficient utilization of spectrum by allocating only the required resources [7]. Flexibility, however, comes at the expense of complex routing and traffic allocation algorithms that have to fulfill strict requirements in the operational phase of the network when the route, wavelength, modulation format, or symbol rate has to be decided and allocated in real time. Owing to the nature of the network traffic, the capacity is allocated and released in a dynamic manner, which may result in a heavily fragmented optical spectrum where unused gaps are scattered throughout the entire operating window used by a transmission system [8]. The task of the routing and traffic allocation algorithms in spectrum-flexible networks is to minimize blocking probability and spectrum fragmentation while maintaining the required bit error rate (BER). It is of crucial importance for the underlying algorithms to have full information about many parameters, including i) network topology, ii) route-dependent impairments such as optical signal-to-noise ratio (OSNR) degradation, iii) available spectral windows, iv) their neighboring (interfering) channels (subcarriers), and v) penalties due to intercarrier interference (ICI) between subcarriers already present and those to be established. This requires determination of relations such as dependency of modulation format and spectral window—referred to as band of interest (BOI)—bandwidth on the BER.

In this paper we expand on the experiment reported in [9], in which an experimental study on required OSNR (ROSNR) levels for maintaining a 1×10^{-3} BER was concluded. To determine the ROSNR for numerous scenarios, an extensive experimental configuration has been set up. Traffic demands requiring different bit rates were served with 14 Gbaud polarization-division-multiplexed- (PDM-) 16-QAM and PDM-QPSK formats within the unused spectral gap (BOI) of a heterogeneous optical superchannel. The measured performance for these scenarios constitutes the required input

Manuscript received June 4, 2012; revised September 1, 2012; accepted September 3, 2012; published October 22, 2012 (Doc. ID 169826).

Robert Borkowski (e-mail: rbor@fotonik.dtu.dk), Valeria Arlunno, Darko Zibar, Neil Guerrero Gonzalez, Antonio Caballero, and Idelfonso Tafur Monroy are with DTU Fotonik, Department of Photonics Engineering, Technical University of Denmark, Ørstedsgade 343, 2800 Kgs. Lyngby, Denmark.

Fotini Karinou is with the University of Patras, Patras, Greece.

Marianna Angelou, Dimitrios Klonidis, and Ioannis Tomkos are with the Athens Information Technology Center, Peania, Greece.

Digital Object Identifier 10.1364/JOCN.4.000B85

TABLE I
INVESTIGATED SCENARIOS AND OBTAINED ROSNR LEVELS

Scenario	Spectrum allocation (14 GHz grid)	BOI (GHz)	BOI capacity (GHz)	Total capacity (Gb/s)	Spectral efficiency (b/s/Hz)	ROSNR for BER 1×10^{-3} (dB)
A		98	224	672	2.29	28.0
B		98	224	672	2.29	30.7
G		98	168	616	1.71	19.6
G2		98	168	616	1.71	18.6
H		98	280	728	2.86	20.1
C		70	224	672	3.20	32.8
F		70	168	616	2.40	23.9
D		42	224	672	5.33	—
E		98	392	616	4.00	24.9
		70	280			
		42	168			

that allows the network to adjust with respect to capacity, spectral efficiency, or reach in order to achieve the required characteristics.

II. IMPLEMENTED CONCEPT

In the flexible network, every connection between a pair of nodes consists of bands of spectrum with variable width (depending on the number of subcarriers and the requested traffic demand). During network operation the spectral occupancy changes dynamically with time, leaving unused spectral windows available for future demands [10]. When allocating traffic, the source node can use an entire available spectral window, a part of it, or combine several disjoint windows to fulfill a particular traffic demand. The part of the spectrum that is being allocated for a given demand is referred to as a BOI. The BOI is subsequently populated with adequate subcarriers that differ in wavelength, modulation format, or bit rate. This assignment should be determined based on system performance knowledge acquired from past events and/or extrapolated from already known physical layer performance parameters [11].

To represent such events, we implemented a number of transmission scenarios for different BOI bandwidths and wavelength allocation schemes, as well as for different modulation formats. Evaluated scenarios are illustrated in the second column of Table I. In all our cases, the optical spectrum consists of three bands. Two outer interfering PDM-QPSK

bands, each constituted by four subcarriers (red dashed arrows in Table I), surround the central band, i.e., the BOI (shaded area). In scenarios A, B, C, and D two DP-16-QAM subcarriers with a variable spacing occupy the BOI. In scenarios G, G2, H, F, and E a variable number of PDM-QPSK subcarriers occupy the BOI, as shown in Table I. We investigated BOIs having bandwidths of 98 (scenarios A, B, G, G2, H), 70 (C, F), and 42 GHz (D, E). Those numbers follow from the fact that only BOIs with bandwidths equal to an integer multiple of the spacing of interfering subcarriers (14 GHz) could have been generated.

III. EXPERIMENTAL SETUP

The experimental setup is shown in Fig. 1(a). Two independent transmitters, one generating an optical 16-QAM signal and the other one for QPSK, both at 14 Gbaud, were employed.

A. Transmitters

1) *16-QAM*: The 16-QAM transmitter was equipped with two independent external cavity lasers (ECLs) whose wavelength separation can be varied. Outputs of both lasers were combined, polarization-aligned, and fed to a double-nested Mach-Zehnder modulator (I/Q modulator). The I/Q modulator was driven by two independent four-level electrical signals at 14 Gbaud which resulted in a 56 Gbit/s data signal. The detailed description of the generation technique that was used can be found in [12], while the outline of its electrical part is shown in Fig. 1(b).

2) *QPSK Transmitter*: The QPSK transmitter generates frequency-locked subcarriers with a spacing of 14 GHz from a 100-kHz-linewidth ECL seed laser, using a recirculating frequency shifter (RFS) based on frequency conversion in a single sideband modulator [5]. The schematic of the RFS (comb generator) is shown in Fig. 1(c). Sixteen of the generated subcarriers (comb lines) had peak powers equalized within an accuracy of 1 dB. The generated comb was then passed through a programmable optical filter (POF), which was used to reject undesired (unequalized) lines. The POF had a frequency setting resolution of ± 1 GHz with an accuracy of ± 2.5 GHz, and bandwidth setting resolution of ± 1 GHz with an accuracy of ± 5 GHz. The insertion loss of the POF was around 4.5 dB. The function of the transmitter was twofold. First, it was used to output two groups of CW lines—one group at wavelengths lower than the wavelength used by the 16-QAM transmitter, the other one at wavelengths higher, referred to as lying in the “outer QPSK” band. Second, for some networking scenarios, QPSK subcarriers were used inside the BOIs replacing the 16-QAM subcarriers, so the POF was configured to allow those subcarriers to pass through. Effectively, the POF was acting as a replacement for three separate tunable optical bandpass filters (OBPFs) and an attenuator. Selected CW subcarriers were applied to the I/Q modulator, which in this transmitter was driven by two binary outputs of a pulse pattern generator (PPG) independent of the one used in the 16-QAM transmitter. Since both the RFS and the PPG had to be driven by two

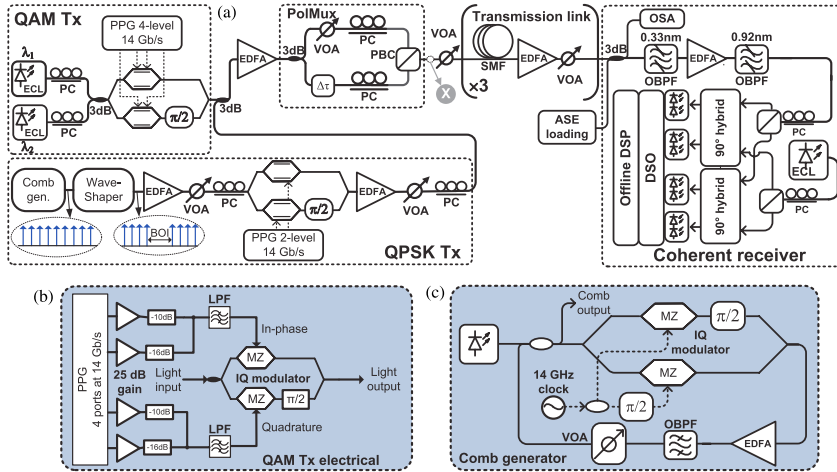


Fig. 1. (Color online) (a) General overview of the experimental setup. QAM Tx: 16-QAM transmitter; QPSK Tx: QPSK transmitter; ECL: external cavity laser; PC: polarization controller; PPG: pulse pattern generator; Comb gen.: 14 GHz comb generator; EDFA: erbium-doped fiber amplifier; VOA: variable optical attenuator; PolMux: polarization multiplexing stage; SMF: single-mode fiber; ASE loading: amplified spontaneous emission loading stage; OSA: optical spectrum analyzer; OBPF: optical bandpass filter; DSO: digital sampling oscilloscope; offline DSP: offline digital signal processing stage. X is a monitoring point at which the spectra in Fig. 4 were taken. (b) Electrical part of the 16-QAM transmitter. LPF: low-pass filter; MZ: Mach-Zehnder modulator. (c) Details of the comb generator.

complementary outputs of the same clock, the symbol rate of the generated QPSK signal was effectively locked to the subcarrier spacing.

B. Heterogeneous Superchannel

Signals coming from both transmitters were then combined in an optical coupler and amplified. A PDM emulator was then used to create a dual polarization signal by combining the single polarization signal with its delayed copy in the orthogonal polarization.

Due to a nonstandard baud rate subcarrier spacing (14 GHz) and lack of appropriate demultiplexer and multiplexer, generated subcarriers could not be split into odd and even and decorrelated. For that reason all QPSK subcarriers were transmitted while being correlated, and the same applies to 16-QAM subcarriers. In [13] it is shown that the OSNR is decreasing as the data correlation coefficient is increasing. Therefore the lowest OSNR is achieved for full data correlation, which was the case in our experimental testbed. The obtained results are influenced by a heavy WDM crosstalk from adjacent subchannels that deteriorate the subchannel under measurement. Therefore the measured penalties may be thought of as being the worst case, or upper bound on the OSNR, for given conditions.

Next, the signal was sent through a fiber link consisting of three concatenated standard single-mode fiber (SMF)

spans. The launch power into each span of the 252-km-long transmission link was set at -2 dBm/channel.

C. Receiver

A preamplified receiver, outlined in Fig. 1(a) (Coherent receiver) was used at the receiving end. First, the heterogeneous superchannel was passed through an OBPF with a bandwidth of 0.33 nm for two reasons: i) to select the desired subcarrier that was targeted, and ii) to ensure that the gain experienced in the follow-up erbium-doped fiber amplifier (EDFA) by the subcarrier under measurement was not varying too much when the number of subcarriers in the superchannel was altered and at the same time avoid the problem of receiver photodiode saturation. The signal was then filtered with another OBPF having a bandwidth of 0.92 nm in order to suppress out-of-band amplified spontaneous emission (ASE) noise from the EDFA. Next, the signal was received with an integrated phase- and polarization-diverse coherent optical receiver. An intradyne reception, where the local oscillator (LO) was set in the range of up to ± 300 MHz, was used. The detailed procedure of demultiplexing the measured signal can be found in [5]. For scenarios E, F, G, and H the central subcarrier of the BOI was measured, while for scenarios A, B, C, and D the subcarrier at the lower wavelength inside the BOI was measured. In scenario G2, the subcarrier at a lower wavelength neighboring the central BOI subcarrier was measured. The electrical outputs of the coherent receiver

were digitized at 40 GS/s using a real-time digital sampling oscilloscope (DSO) and processed offline using digital signal processing (DSP) algorithms presented in the next section.

D. Digital Signal Processing

An outline of the DSP chain is presented in Fig. 2. The sampled signal was first passed through a 4th-order Butterworth filter with a 10.5 GHz cutoff frequency (75% of the symbol rate) as a filter for noise and ICI. The filter type and parameters were found experimentally to provide the best possible BER. Especially the ICI is important for a system with baud-rate-spaced carriers like the one used. The Gram–Schmidt orthogonalization technique was then used for quadrature imbalance compensation [14]. The output of this digital filter was then resampled from 40 GS/s to 28 GS/s in order to obtain a signal with 2 samples/symbol for further processing. An equalizer driven by the constant modulus algorithm (CMA) was used for polarization demultiplexing [15] followed by a decision-directed phase locked loop for frequency and phase offset estimation [16].

IV. RESULTS AND DISCUSSION

A. Single Carrier

First, single-carrier back-to-back trials were performed as a benchmark for the experimental testbed. The obtained results are shown in Fig. 3. The performance was measured for a single, 14 Gbaud modulated carrier for both PDM-QPSK and PDM-16-QAM modulations, centered at 1551.505 nm, which was the middle of the BOI for all investigated scenarios. The obtained BER curves as a function of OSNR measured in a 0.1 nm bandwidth show that the ROSNR for obtaining a 1×10^{-3} BER is 14 dB and 24 dB for PDM-QPSK and PDM-16-QAM, respectively. This shows a penalty of the implemented experimental testbed and demodulator to the theoretical limits [17] of approximately 4 dB for QPSK and 7 dB for 16-QAM. The excess penalty of 3 dB between 16-QAM and QPSK modulation formats may stem from i) use of two different transmitters (especially PPG), each resulting in a different hardware penalty, or ii) unoptimized algorithms implemented for 16-QAM (in particular, a simple CMA equalizer not designed for multilevel signals was used). The insets in Fig. 3 show directly detected optical eye diagrams captured in monitoring point X (see Fig. 1(a)). The quality of the eye diagrams is good, and different amplitude levels are well separated, indicating that a major part of the hardware penalty may originate from the receiver.

B. Scenarios

The conceptual outlines presented in Table 1 were then executed in the experimental setup. Figure 4 shows the actual spectra captured at monitoring point X, i.e., before the fiber transmission. The spectra before applying modulation to QPSK subchannels are denoted by the letter of the respective scenario

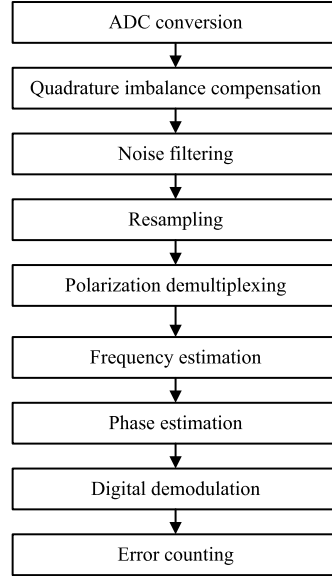


Fig. 2. Outline of the offline digital signal processing algorithm chain.

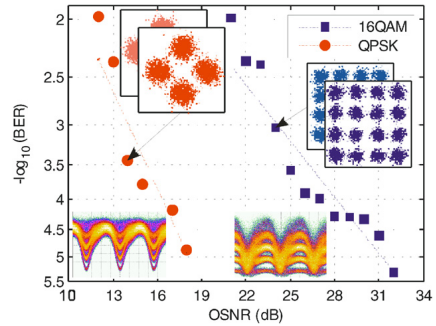


Fig. 3. (Color online) Back-to-back performance of single-carrier 14 Gbaud PDM-16-QAM (squares) and PDM-QPSK (circles) in the experimental setup. Upper insets show both received constellations at a BER of approximately 1×10^{-3} , while lower insets depict optical intensity eye diagrams captured at monitoring point X (see Fig. 1) for respective modulation formats.

and superscript 0 and are shown to clearly emphasize the spectral composition of the BOI (marked by a gray background) and interfering bands; A^0 and C^0 are not available. The spectra after turning on the QPSK modulation are denoted

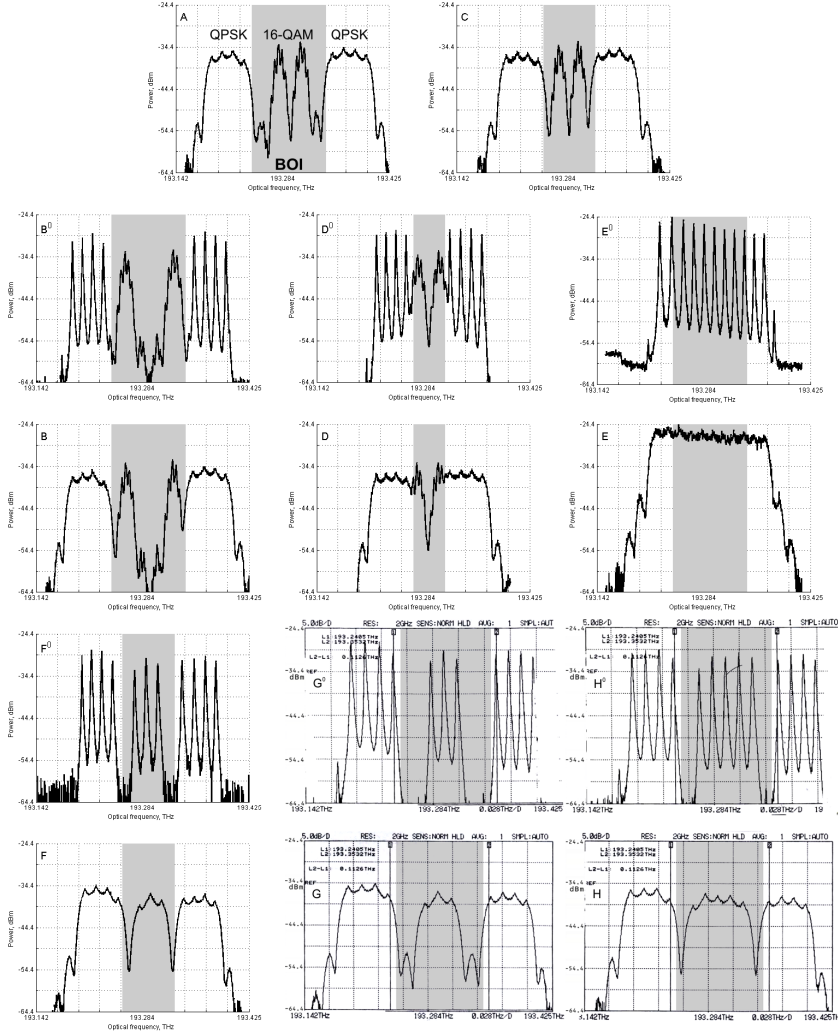


Fig. 4. Modulated and unmodulated (denoted by superscript 0) spectra for all scenarios A–H. The BOI is marked by a gray background.

by the respective letter without the superscript. Scenario G2 is represented by exactly the same spectrum as G, since the only difference between those two scenarios was the subcarrier under test. In each case, the BOI subcarriers, as well as interfering bands surrounding the BOI, can be easily identified from the spectrum.

In order to evaluate the performance of the heterogeneous superchannel, BER measurements were performed as a function of OSNR (0.1 nm) for each of the flexible traffic allocation scenarios considered here. The obtained results are presented in Fig. 5. The parameters A and B of the exponential fit $-\log(\text{BER}) = A \cdot 10^{B \cdot \text{OSNR}}$ were found and used for analytical

determination of the ROSNR by using $\text{ROSNR} = 1/B \cdot \log(3/A)$, i.e., the crossing of the fitted curve with a 1×10^{-3} BER level.

ROSNR levels were determined by finding a curve fitting the measured BER performance for each scenario followed by analytical calculation of the expected BER at the OSNR of 1×10^{-3} . This is depicted in Fig. 5, where the solid curves were obtained by fitting; the dashed horizontal line denotes the 1×10^{-3} BER level, and vertical dashed rays are the projection onto the OSNR axis of the crossing between both, directly showing the ROSNR level.

In addition, Table I shows a) the spectral width of the BOI; b) the BOI capacity; c) the total capacity of the superchannel; d) the achievable BOI spectral efficiency, defined as the ratio of the aggregated traffic within a BOI over the total spectral width of the available BOI; and d) the OSNR (ROSNR) required in order to achieve a BER of 1×10^{-3} for the targeted channel in the BOI.

1) 98 GHz BOI Bandwidth: The conducted study reveals that a 98 GHz (7 subcarriers of 14 GHz) BOI can be filled with up to 7 subcarriers with the PDM-QPSK format (scenario E) if the ROSNR is above 24.9 dB. When the number of allocated PDM-QPSK subcarriers within the BOI is reduced to 5 (scenario H), the ROSNR drops to 20.1 dB. A further decrease in the bandwidth demand is shown in scenario G, where the ROSNR for 3 subcarriers is 19.6 dB when measuring the central BOI subcarrier or 18.6 dB for the subcarrier at a lower wavelength. This difference is due to the fact that the central subcarrier has neighboring subcarriers spaced at 14 GHz from both sides, while the one at lower wavelength has one of its neighbors located 42 GHz away. Reduction in the number of subcarriers across scenarios E, H, and G/G2 results in a decreasing OSNR; this, however, comes at the expense of reduced BOI spectral efficiency. It is important to notice that the performance of scenario E is significantly degraded, as compared with scenario H, because of the entire comb's being correlated. In an actual flexible network implementation it would be important to consider the interplay between the traffic demand, BOI bandwidth, and available OSNR margin

and to balance those parameters accordingly. It is conceivable that ROSNR levels can be interpolated for the cases of 6, 4, and 2 PDM-QPSK subcarriers, since these are expected to lie between the ROSNR levels of the cases with 7, 5, and 3 subcarriers.

Alternatively, the 98 GHz BOI can be filled with two PDM-16-QAM subcarriers (scenario A) at a ROSNR level of at least 28 dB. In this case, the PDM-16-QAM subcarriers have been located 28 GHz apart, symmetrically within the BOI with the interfering QPSK channels being spaced 42 GHz. Additional studies (scenario B) show that, if the two PDM-16-QAM subcarriers are located further apart from each other (56 GHz spacing), but closer to the interfering channels (28 GHz separation), then the ROSNR increases to 30.7 dB. The increase is due to the fact that the correlated QPSK subcarriers in the interfering band are degrading the 16-QAM performance. This result indicates that a traffic allocation mechanism should also take into consideration the spectral position of the channels within the BOI.

2) 70 GHz BOI Bandwidth: Considering a narrow BOI of 70 GHz (5 subcarriers of 14 GHz) being initially filled with 3 PDM-QPSK subcarriers (scenario F), a ROSNR level of 23.9 dB is observed. This ROSNR level is larger than that of scenario G, indicating that the performance is affected mainly by the spectral distance of the allocated subcarriers from the interfering channels. The performance of the full PDM-QPSK subcarrier allocation within the 70 GHz BOI is defined again by scenario E (24.9 dB ROSNR).

The same BOI of 70 GHz can also be filled with 2 PDM-16-QAM subcarriers (scenario C), resulting in an increased ROSNR level of 32.8 dB because of the close spectral proximity between the central BOI subcarrier and interfering channels.

3) 42 GHz BOI Bandwidth: Finally, it was observed that a narrow BOI of 42 GHz could not accommodate two PDM-16-QAM channels (scenario D), since the narrow spectral

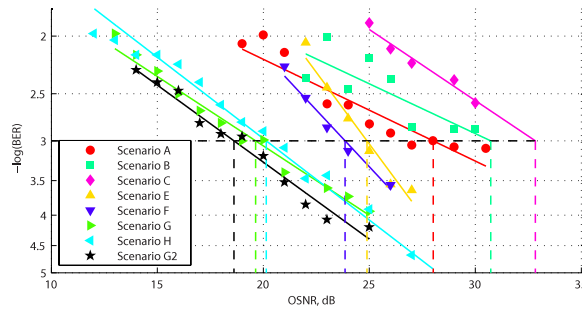


Fig. 5. (Color online) BER performance of all scenarios, except for D. Solid curves were fitted to the measured data points. Thick horizontal dashed line denotes the BER threshold set at 1×10^{-3} . Thick vertical lines in respective colors show the OSNR corresponding to a crossing between fitted curves and the BER threshold, indicating the ROSNR level for each scenario.

spacing (14 GHz) of the nonorthogonal channels leads to high ICI and severely impairs the signal. On the other hand, the allocation of three PDM-QPSK orthogonal channels is acceptable and refers to scenario E, resulting in a ROSNR of 24.9 dB.

V. CONCLUSION

We have experimentally investigated the OSNR requirements for a spectrum-flexible heterogeneous optical superchannel. We have determined ROSNR levels for a BER of 1×10^{-3} for a number of scenarios with variable BOI bandwidths being dynamically filled with PDM-QPSK and PDM-16-QAM with different bit rates. The obtained results are important, as they form a basis for traffic allocation mechanisms in flexible optical networks. Empirically determined values of the ROSNR provided here may be used as an upper bound on the OSNR necessary to transmit given a particular BOI, traffic demand, and superchannel that may be inserted into the BOI to serve this demand.

ACKNOWLEDGMENTS

We thank LeCroy for providing WaveMaster DSOs, Finisar for the WaveShaper and ID Photonics for CoBrite DX1 lasers. We also thank Jesper B. Jensen for help in setting up the comb generator, Anton Dogadaev and Xiaodan Pang for operating the WaveShaper, and Teit Poulsen from Altuo ApS for renting us equipment.

REFERENCES

- [1] M. Jinno, T. Ohara, Y. Sone, A. Hirano, O. Ishida, and M. Tomizawa, "Elastic and adaptive optical networks: possible adoption scenarios and future standardization aspects," *IEEE Commun. Mag.*, vol. 49, no. 10, pp. 164–172, Oct. 2011.
- [2] D. van den Borne, "Robust optical transmission systems: modulation and equalization," Ph.D. dissertation, Technische Universiteit Eindhoven, 2008 [Online]. Available: <http://repository.tue.nl/633535>.
- [3] L. Velasco, M. Klinkowski, M. Ruiz, V. López, and G. Junyent, "Elastic spectrum allocation for variable traffic in flexible-grid optical networks," in *Nat. Fiber Optic Engineers Conf.*, 2012, JTh2A.39.
- [4] Y.-K. Huang, E. Ip, P. N. Ji, Y. Shao, T. Wang, Y. Aono, Y. Yano, and T. Tajima, "Terabit/s optical superchannel with flexible modulation format for dynamic distance/route transmission," in *Optical Fiber Communication Conf.*, 2012, OM3H.4.
- [5] S. Chandrasekhar, X. Liu, B. Zhu, and D. W. Peckham, "Transmission of a 1.2-Tb/s 24-carrier no-guard-interval coherent OFDM superchannel over 7200-km of ultra-large-area fiber," in *35th European Conf. on Optical Communication (ECOC)*, Sept. 2009, vol. 2009-Supplement, pp. 1–2.
- [6] T. Xia, G. Wellbrock, Y.-K. Huang, E. Ip, M.-F. Huang, Y. Shao, T. Wang, Y. Aono, T. Tajima, S. Murakami, and M. Cvijetic, "Field experiment with mixed line-rate transmission (112-Gb/s, 450-Gb/s, and 1.15-Tb/s) over 3560 km of installed fiber using filterless coherent receiver and EDFAs only," in *Optical Fiber Communication Conf.*, 2011, PDPA3.
- [7] M. Jinno, H. Takara, B. Kozicki, Y. Tsukishima, Y. Sone, and S. Matsuoka, "Spectrum-efficient and scalable elastic optical path network: architecture, benefits, and enabling technologies," *IEEE Commun. Mag.*, vol. 47, no. 11, pp. 66–73, Nov. 2009.
- [8] K. Christodouloupoulos, I. Tomkos, and E. Varvarigos, "Elastic bandwidth allocation in flexible OFDM-based optical networks," *J. Lightwave Technol.*, vol. 29, no. 9, pp. 1354–1366, May 2011.
- [9] R. Borkowski, F. Karinou, M. Angelou, V. Arlunno, D. Zibar, D. Klonidis, N. G. Gonzalez, A. Caballero, I. Tomkos, and I. T. Monroy, "Experimental demonstration of mixed formats and bit rates signal allocation for spectrum-flexible optical networking," in *Optical Fiber Communication Conf.*, 2012, OW3A.7.
- [10] K. Christodouloupoulos, I. Tomkos, and E. Varvarigos, "Dynamic bandwidth allocation in flexible OFDM-based networks," in *Optical Fiber Communication Conf.*, 2011, OTu15.
- [11] I. Tafur Monroy, D. Zibar, N. Guerrero Gonzalez, and R. Borkowski, "Cognitive Heterogeneous Reconfigurable Optical Networks (CHRON): enabling technologies and techniques," in *13th Int. Conf. on Transparent Optical Networks (ICTON)*, June 2011.
- [12] P. J. Winzer, A. Gnauck, C. Doerr, M. Magarini, and L. Buhl, "Spectrally efficient long-haul optical networking using 112-Gb/s polarization-multiplexed 16-QAM," *J. Lightwave Technol.*, vol. 28, no. 4, pp. 547–556, Feb. 2010.
- [13] W. Qiu, S. Yu, J. Zhang, J. Shen, W. Li, H. Guo, and W. Gu, "The nonlinear impairments due to the data correlation among sub-carriers in coherent optical OFDM systems," *J. Lightwave Technol.*, vol. 27, no. 23, pp. 5321–5326, Dec. 2009.
- [14] S. J. Savory, "Digital coherent optical receivers: algorithms and subsystems," *IEEE J. Sel. Top. Quantum Electron.*, vol. 16, no. 5, pp. 1164–1179, Sept.–Oct. 2010.
- [15] K. Kikuchi, "Polarization-demultiplexing algorithm in the digital coherent receiver," in *2008 Digest of the IEEE/LEOS Summer Topical Meetings*, July 2008, pp. 101–102.
- [16] D. Zibar, R. Sambaraju, A. Caballero, J. Herrera, U. Westergren, A. Walber, J. Jensen, J. Marti, and I. Monroy, "High-capacity wireless signal generation and demodulation in 75- to 110-GHz band employing all-optical OFDM," *IEEE Photon. Technol. Lett.*, vol. 23, no. 12, pp. 810–812, June 2011.
- [17] R.-J. Essiambre, G. Kramer, P. Winzer, G. Foschini, and B. Goebel, "Capacity limits of optical fiber networks," *J. Lightwave Technol.*, vol. 28, no. 4, pp. 662–701, Feb. 2010.



Robert Borkowski was born in Lodz, Poland, in 1987. He received the M.Sc. degree in telecommunications from the Technical University of Denmark in 2011 and the M.Sc. degree in electronics and telecommunications from the Technical University of Lodz in 2012. He is now working towards his Ph.D. degree in the field of optical communications in the Metro-Access and Short Range Systems group at DTU Fotonik, Department of Photonics Engineering, Technical University of Denmark. He is involved in the EU FP7 project CHRON (Cognitive Heterogeneous Reconfigurable Optical Networks). His research interests are in the areas of optical performance monitoring, coherent transmission systems and digital signal processing for fiber-optic communications.



Fotini Karinou was born in Arta, Greece, in 1983. She received the Diploma in Electrical and Computer Engineering, with specialization in Telecommunications and Information Theory, from the University of Patras, Rio, Greece, in 2007, where she is currently working towards the Ph.D. degree. From October 2006 to May 2007, she was an exchange student at the Institute for Quantum Optics and Quantum Information (IQOQI), at Vienna University of Technology, participating in the initial attempts for the realization of a commercial prototype of a quantum key distribution (QKD) system based on polarization entanglement. From June 2011 to December 2012 she was an exchange researcher at the Denmark Technical University, in the Department DTU Fotonik, where she worked towards her Ph.D. and towards cognitive optical networks. She has been involved in the EU FP6 SECOQC, EU FP7 ICT-BONE, and EU FP7 CHRON projects. Her research interests lie in the fields of optical interconnects and advanced modulation formats. Ms. Karinou has been a member of the Technical Chamber of Greece and an OSA student member since 2009.



Marianna Angelou (S'09) received a degree in Computer Science from the Aristotle University of Thessaloniki, Greece, in 2005. She received the M.Sc. in Information and Telecommunication Technologies from Athens Information Technology in 2008 and the Ph.D. degree from Universitat Politècnica de Catalunya, Barcelona, in April 2012. In January 2008 she joined the High-speed Networks and Optical Communications Group of Athens Information Technology, as a Research Scientist, working within the framework of EC-funded research projects. Her research activities focus on cross-layer optimization techniques for optical networks and cover a broad range of topics in that area including physical layer modeling, energy-efficiency, and networking with flexible/adaptive transmission characteristics.



Valeria Arlunno received the M.Sc. degree in telecommunication engineering from the Politecnico di Torino, Torino, Italy, in 2009. She is currently pursuing a Ph.D. in optical communications engineering at DTU Fotonik, Technical University of Denmark, with the Metro-Access and Short Range Systems research group of the department of Photonics Engineering. Her research interests are in the areas of coherent optical communications and digital signal processing.



Darko Zibar was born in Belgrade, in the former Yugoslavia, on September 9, 1978. He received the M.Sc. degree in telecommunication and Ph.D. degree in optical communications from the Technical University of Denmark, Lyngby, Denmark, in 2004 and 2007, respectively. He was a Visiting Researcher with the Optoelectronic Research Group, University of California, Santa Barbara, during January–August 2006 and in January 2008 where he was involved in coherent receivers for phase-modulated analog optical links. From February to July 2009, he was a Visiting Researcher with Nokia-Siemens Networks where he worked on 112 Gbit/s polarization multiplexed systems. He is currently an Associate Professor at DTU Fotonik, Technical University of Denmark. His research interests include coherent optical communication, with the emphasis on digital demodulation and compensation techniques. Dr. Zibar is the recipient of the Best Student Paper Award at the IEEE Microwave Photonics Conference 2006, the Villum Kann Rasmussen Postdoctoral Research Grant in 2007, and the Villum Foundation Young Investigator Program in 2011.



Dimitrios Klonidis is an Assistant Professor at the Athens Information Technology Center, Greece. He was awarded his Ph.D. degree in the field of optical communications and networking from the University of Essex, UK, in 2006. He has several years of research and development experience, working on a large number of national and European projects in the field of optical switching, networking and transmission. He has more than 90 publications in international journals and refereed major conferences. His main research interests are in the area of optical communication networks, including optical transmission and modulation, signal processing and equalization, fast switching and node control.



Neil Guerrero Gonzalez was born on July 19, 1982, in Cucuta, Colombia. He received the B.Sc. degree in Electronic Engineering in 2005 and the M.Sc. degree in 2007 from the National University of Colombia. During his Ph.D. studies in Photonics at the Technical University of Denmark (2008–2011), he developed a novel approach to implement joint phase, frequency and signal modulation format estimation for signal detection and demodulation in phase-modulated radio-over-fiber systems. In 2010, he was working on optical performance monitoring within the framework of the EU FP7 project “BONE” at Huawei Technologies in Munich. He is a recipient of an honorable mention in the 2011 Corning Outstanding Student Paper Competition, OFC 2011, for his work on a novel reconfigurable digital coherent receiver for metro-access networks supporting mixed modulation formats and bit rates. Since January 2012 Dr. Guerrero Gonzalez has worked as an Optical Researcher in the European Research Center, Huawei Technologies Duesseldorf GmbH, in Munich. His research interests are in hybrid optical–wireless communication systems, coherent detection technologies and digital photonic receivers for wireless and wireline optical fiber transmission links. Currently he is engaged in the design and implementation of high-capacity optical communication systems.



Antonio Caballero was born in 1985 in Zaragoza, Spain. He received the B.Sc. and M.Sc. degrees in Telecommunications Engineering from Centro Politécnico Superior, Zaragoza, Spain, in 2008. He received his Ph.D. in Optical Communications Engineering at DTU Fotonik, Technical University of Denmark, in September 2011, with a thesis on high-capacity radio-over-fiber links. He was a Visiting Researcher at The Photonics and Networking Research Laboratory at Stanford University from February to June 2010, under supervision of Prof. Leonid G. Kazovsky. He is currently a postdoctoral researcher at DTU Fotonik. His research interests are in the area of coherent optical communications as well as radio-over-fiber links.



Ioannis Tomkos has been with AIT since September 2002 (serving as Professor, Research Group Head and Associate Dean). In the past he was a Senior Scientist at Corning Inc., USA (1999–2002) and a Research Fellow at the University of Athens, Athens, Greece (1995–1999). Dr. Tomkos has represented AIT as Principal Investigator in about 20 European Union and industry funded research projects (including 8 currently active projects) and has a consortium-wide initiator/leader role. Through his activities he has managed to attract over 6,000,000 Euros in funding for AIT. His fields of expertise are telecommunication systems and networks, as well as techno-economic analysis and business planning

of ICTs. Together with his colleagues and students he has authored about 450 peer-reviewed archival scientific articles, including over 120 journal/magazine/book publications and 330 conference/workshop proceedings papers. His published articles have received in excess of 2200 citations (increasing at a rate of 500 annually). Dr. Tomkos was elected in 2007 as a Distinguished Lecturer of the IEEE Communications Society for the topic of optical networking. He has served as the Chair of the International Optical Networking Technical Committee of the IEEE Communications Society (2007–2008) and the Chairman of the IFIP working group on Photonic Networking (2008–2009). He is currently the Chairman of the OSA Technical Group on Optical Communications (2009–2012) and the Chairman of the IEEE Photonics Society Greek Chapter (2010–2012). He is also Chairman of the working group “Next Generation Networks” of the Digital Greece 2020 Forum. He has been General Chair, Technical Program Chair, Subcommittee Chair, Symposium Chair, or/and member of the steering/organizing committees for the major conferences in the area of telecommunications/networking (more than 100 conferences/workshops). In addition, he is a member of the Editorial Boards of the *IEEE/OSA Journal of Lightwave Technology*, the *IEEE/OSA Journal of Optical Communications and Networking*, *IET Optoelectronics*, and the *International Journal on Telecommunications Management*. He is a Fellow of the Institute of Engineering and Technology (IET).



Idelfonso Tafur Monroy is currently a Professor and the Head of the Metro-Access and Short Range Systems group of the Department of Photonics Engineering at the Technical University of Denmark. He graduated from the Bonch-Bruевич Institute of Communications, St. Petersburg, Russia, in 1992, where he received a M.Sc. degree in multichannel telecommunications. In 1996 he received a Technology Licentiate degree in telecommunications

theory from the Royal Institute of Technology, Stockholm, Sweden. In the same year he joined the Electrical Engineering Department of the Eindhoven University of Technology, The Netherlands, where he earned a Ph.D. degree in 1999 and worked as an Assistant Professor until 2006. He has participated in several European research framework projects in photonic technologies and their applications to communication systems and networks. At the moment he is involved in the ICT European projects GigaWaM and EURO-FOS and is the technical coordinator of the CHRON project. His research interests are in hybrid optical–wireless communication systems, high-capacity optical fiber communications, digital signal processing for optical transceivers for baseband and radio-over-fiber links, application of nanophotonic technologies in the metropolitan and access segments of optical networks as well as in short range optical–wireless communication links.

Paper [H]: Experimental demonstration of a cognitive quality of transmission estimator for optical communication systems

Antonio Caballero, Juan Carlos Aguado, **Robert Borkowski**, Silvia Saldaña, Tamara Jiménez, Ignacio de Miguel, Valeria Arlunno, Ramón J. Durán, Darko Zibar, Jesper Bevensee Jensen, Rubén M. Lorenzo, Evaristo J. Abril, and Idelfonso Tafur Monroy. Experimental demonstration of a cognitive quality of transmission estimator for optical communication systems. *Optics Express*, vol. 20, no. 26, pp. B64–B70, December 2012.

Experimental demonstration of a cognitive quality of transmission estimator for optical communication systems

Antonio Caballero,^{1,*} Juan Carlos Aguado,² Robert Borkowski,¹ Silvia Saldaña,¹ Tamara Jiménez,² Ignacio de Miguel,² Valeria Arlunno,¹ Ramón J. Durán,² Darko Zibar,¹ Jesper B. Jensen,¹ Rubén M. Lorenzo,² Evaristo J. Abril,² and Idelfonso Tafur Monroy¹

¹DTU Fotonik, Tech. Univ. of Denmark, DK-2800 Kgs. Lyngby, Denmark

²University of Valladolid, Paseo de Belén 15, 47011, Valladolid, Spain

*acaj@fotonik.dtu.dk

Abstract: The impact of physical layer impairments in optical network design and operation has received significant attention in the last years, thereby requiring estimation techniques to predict the quality of transmission (QoT) of optical connections before being established. In this paper, we report on the experimental demonstration of a case-based reasoning (CBR) technique to predict whether optical channels fulfill QoT requirements, thus supporting impairment-aware networking. The validation of the cognitive QoT estimator is performed in a WDM 80 Gb/s PDM-QPSK testbed, and we demonstrate that even with a very small and not optimized underlying knowledge base, it achieves between 79% and 98.7% successful classifications based on the error vector magnitude (EVM) parameter, and approximately 100% when the classification is based on the optical signal to noise ratio (OSNR).

©2012 Optical Society of America

OCIS codes: (060.4250) Networks; (060.4510) Optical communications.

References and links

1. S. Azodolmolky, M. Klinkowski, E. Marin, D. Careglio, J. Solé Pareta, and I. Tomkos, "A survey on physical layer impairments aware routing and wavelength assignment algorithms in optical networks," *Comput. Netw.* **53**(7), 926–944 (2009).
2. S. Azodolmolky, J. Perelló, M. Angelou, F. Agraz, L. Velasco, S. Spadaro, Y. Pointurier, A. Francescon, C. V. Saradhi, P. Kokkinos, E. Varvarigos, S. Al Zahr, M. Gagnaire, M. Gunkel, D. Klonidis, and I. Tomkos, "Experimental demonstration of an impairment aware network planning and operation tool for transparent/translucent optical networks," *J. Lightwave Technol.* **29**(4), 439–448 (2011).
3. Y. Qin, K. Cheng, J. Triay, E. Escalona, G. S. Zervas, G. Zarris, N. Amaya-Gonzalez, C. Cervoello-Pastor, R. Nejabati, and D. Simeonidou, "Demonstration of C/S based Hardware Accelerated QoT Estimation Tool in Dynamic Impairment-Aware Optical Network," in *European Conference in Optical Communications (ECOC 2010)*, Torino, IT, paper P5.17 (2010).
4. P. Poggiolini, "The GN model of non-linear propagation in uncompensated coherent optical systems," *J. Lightwave Technol.* (to be published).
5. T. Jiménez, J. C. Aguado, I. de Miguel, R. J. Durán, N. Fernandez, M. Angelou, D. Sánchez, N. Merayo, P. Fernández, N. Atallah, R. M. Lorenzo, I. Tomkos, and E. J. Abril, "A cognitive system for fast quality of transmission estimation in core optical networks," in *Optical Fiber Communication Conference (OFC 2012)*, Los Angeles, CA, USA, paper OW3A.5 (2012).
6. A. Aamodt and E. Plaza, "Case-based reasoning: Foundational issues, methodological variations, and system approaches," *Artificial Intelligence Communications* **7**(1), 39–59 (1994).
7. T. Jiménez, J. C. Aguado, I. de Miguel, R. J. Durán, D. Sánchez, M. Angelou, N. Merayo, P. Fernández, N. Fernández, R. M. Lorenzo, I. Tomkos, and E. J. Abril, "Optimization of the knowledge base of a cognitive quality of transmission estimator for core optical networks," *16th Optical Network Design and Modeling Conference (ONDM 2012)*, Colchester, UK, (2012).
8. D. W. Aha, "Tolerating noisy, irrelevant and novel attributes in instance-based learning algorithms," *Int. J. Man-Machine Studies* **36**(2), 267–287 (1992).

1. Introduction

Next generation optical networks will be of a highly heterogeneous nature, as they will support mixed bit-rates, mixed modulation formats and even a flexible grid for spectrum allocation. That arising scenario brings new challenges in terms of transmission robustness, optical monitoring and mechanisms for control and management. One of those challenges is the need for new estimation techniques to predict the quality of transmission (QoT) of optical connections before being established in the network, thus supporting impairment-aware networking [1].

A number of solutions have been proposed to assess the QoT of optical connections. In [2], a real-time QoT estimator, the Q-Tool, has been presented. The tool receives a network topology and a set of lightpaths based on 10 Gb/s on-off keying (OOK), and then computes their associated Q-factors, which are indicators of the QoT, as they are directly related to the bit error rate (BER). Although the tool is extremely useful to check *a priori* whether the computed lightpaths will comply with QoT requirements when they are established on the network, its high computing time (from 1 to 1000 seconds, depending on the scenario) is a significant issue [3]. In [4], a Gaussian noise (GN) model which is able to estimate accurately the optical signal to noise ratio (OSNR) of the optical channels in uncompensated coherent transmission systems has been proposed. However, it does not yet address network scenarios (where channels coming from different locations are multiplexed in an optical fiber at optical cross-connects), and it is not valid for dispersion-compensated systems.

On the other hand, we have recently proposed a different approach for assessing the QoT. It consists in taking advantage of previous experiences which are stored on a knowledge base, i.e., it relies on cognition. Thus, in [5] we proposed a novel cognitive QoT estimator which is able to predict whether a new lightpath to be established in an optical network will comply with QoT requirements (and if it will not have a significant impact on the currently established ones). This estimator employs case-based reasoning (CBR) techniques [6]. CBR is an artificial intelligence mechanism which solves a new problem by looking for the most similar problems (or cases) faced in the past, and by reusing that knowledge, either directly or after some adaptation, to provide a solution. In this way, by exploiting previous experiences, which are stored on a knowledge base (KB), the QoT estimator is able to provide fast and correct decisions on whether a lightpath fulfills QoT requirements or not, before being established, without having to rely on complex methods. Using the proposed estimator, we have demonstrated, by means of simulation, that lightpaths in a 10 Gb/s OOK 14-node wavelength-routed optical network (the Deutsche Telekom network) are correctly classified into high or low QoT categories in more than 99% of cases, with a very low computing time: three orders of magnitude lower than that required by the Q-Tool in that scenario [5]. These results were extended and improved by incorporating learning and forgetting capabilities to optimize the underlying KB on which the cognitive estimator relies [7]. As demonstrated there, the use of those techniques slightly increases the rate of successful classifications and, more importantly, it significantly reduces the size of the KB, which in turn leads to additional computing time reductions. Thus, when operating with the optimized KB, the computing time is around four orders of magnitude faster when compared with a non-cognitive approach, the Q-Tool.

In this paper, we push forward our previous work by experimentally demonstrating that cognition can be successfully employed to predict the QoT of optical channels, and also by showing that it can be employed for other modulation formats than OOK. At this stage, rather than implementing a whole network, a wavelength division multiplexed (WDM), homogeneous point-to-point optical transmission system has been built, consisting of 5 80 Gb/s polarization division multiplexed (PDM) quadrature phase-shift keying (QPSK), with a

number of adjustable parameters such as the optical launch power, the fiber link length and the number of co-propagating channels, in order to support different lightpath and system configurations.

2. Experimental testbed

Figure 1 shows the WDM experimental setup for the quality of transmission experiment of PDM-QPSK at 80 Gbit/s through 480 km of a dispersion-compensated fiber link. At the transmitter side, 5 laser sources spaced 50 GHz apart are combined using a 50 GHz arrayed waveguide grating (AWG), 4 of them distributed feedback lasers (3 MHz linewidth) and an external cavity laser (ECL) with 100 kHz linewidth placed in the central channel. 20 Gbit/s electrical signals are generated using a 5 Gbit/s pulse pattern generator (PPG) with PRBS $2^{15}-1$ and a 4:1 electrical interleaver (IL). The electrical signals are used to drive a double-nested Mach-Zehnder modulator fed by the 5 optical sources. Polarization division multiplexing (Polmux) is emulated by multiplexing the signal with its delayed copy in the orthogonal polarization. Afterwards the odd and even channels are decorrelated using a 50 GHz optical interleaver and a 3 dB optical coupler, by introducing an optical delay of 23 ps between odd and even channels. After that, an erbium-doped fiber amplifier (EDFA) is used to amplify the signal to the desired launch power.

Fiber transmission is realized over a maximum of 6 fiber spans of 80 km standard single mode fiber (SSMF) and matched dispersion compensating fiber (DCF), for a total maximum distance of 480 km. After each fiber span, the optical signal is amplified in a double-stage EDFA with the DCF placed between the two stages. The gain of the amplification stage is adjusted to compensate for each span and DCF losses. In some scenarios 4 dB extra span losses are added at the end of each fiber span to achieve 22 dB of losses per span, thus emulating changes on the link losses due to fiber aging, new splices, etc. At the receiver side, a preamplified coherent detection scheme is used. It consists of a 0.3 nm optical filter for channel selection, a pre-amp EDFA, a 2 nm optical filter to remove amplified spontaneous emission excess noise and a polarization-diversity coherent receiver with integrated balanced photodiodes. An ECL with 100 kHz linewidth is employed as local oscillator (LO). A digital sampling oscilloscope (DSO) with 40 GS/s of sampling rate and 13 GHz bandwidth is used to digitize the photodiodes outputs. The acquired data is processed offline with a digital signal processing-based (DSP-based) receiver that includes a digital filter, constant modulus algorithm (CMA), carrier phase recovery and root mean squared (RMS) error vector magnitude (EVM) calculation.

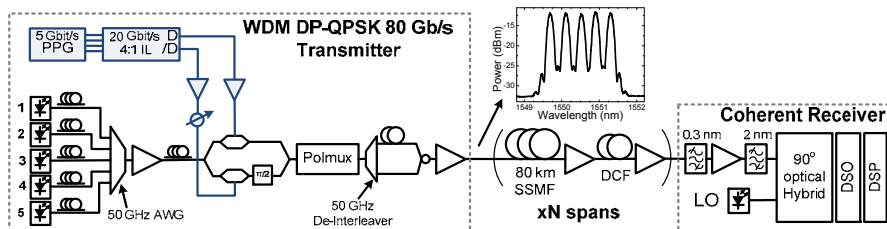


Fig. 1. Experimental testbed.

In order to emulate different lightpaths and system configurations in an optical network, the experimental setup allows for the modification of some parameters:

- number of simultaneously active channels in the link (from 2 to 5),
- launch power per channel (from -4 to 4 dBm in steps of 2 dB),
- number of spans (3 or 6, thus testing lightpath lengths of 240 and 480 km),

- average losses per span (18 or 22 dB).

Different scenarios have been configured, and the EVM of each of the active channels in each configuration has been experimentally measured, which is an indicator of the QoT of each channel. Apart from the EVM, the OSNR has also been measured. An example of the type of experimental measurements which were used to populate the KB of the cognitive QoT estimator (as it will be later described) is shown in Table 1. The set corresponds to the variation of the launch power per channel when the 5 channels are propagating through 6 fiber spans. The measured channel is the third one, placed in the middle. It can be observed that, in this example experiment, whereas the OSNR increases with the launch power, the EVM follows a different trend, and there is an optimal launch power, 0 dBm, where the EVM reaches a minimum. Therefore, the classification of a lightpath into one or another QoT category depends on the parameter used to make the decision.

Table 1. Example of experimental measurements used to populate the KB. Only one of the QoT parameters (OSNR or EVM) is included in the KB.

Channel measured	Channels (on = 1)					P_{in}/ch (dBm)	# of spans	Span loss (dB)	OSNR dB/0.1 nm	EVM (%)
	1	2	3	4	5					
3	1	1	1	1	1	-4	6	18	23.5	21.4
3	1	1	1	1	1	-2	6	18	25.4	19.6
3	1	1	1	1	1	0	6	18	27.3	19.2
3	1	1	1	1	1	2	6	18	29.1	21.1
3	1	1	1	1	1	4	6	18	30.8	24.9

3. A cognitive QoT estimator based on CBR

We have developed a cognitive QoT estimator, based on CBR, for the testbed described above. The estimator is able to classify a lightpath into a high or low QoT category, depending on the predicted value of its quality of transmission parameter, which can be either the EVM or the OSNR. The KB of the cognitive estimator is composed by a number of cases, each consisting of a description of the lightpath and its associated experimentally measured QoT value (EVM or OSNR). The description of the lightpath contains the channel wavelength, the value of launch power, the losses per span and the number of spans (i.e., the lightpath length), the set of active wavelength channels (i.e., the active lightpaths) in the link, the total input power to the link, and the total power carried by the adjacent channels of the lightpath considered, as well as that carried by those located 2, 3 and 4 channel slots apart from it. The measured QoT value in the experimental testbed for each lightpath and each configuration is also stored in the KB. It is important to remark that only one QoT parameter (EVM or OSNR) is used by the cognitive system and thus included in the KB, whereas the other is not considered at all.

Let us assume that the QoT of a new lightpath must be assessed. The cognitive QoT estimator works as follows. First of all, it retrieves the most similar lightpath from the KB to the one to be analyzed. In order to assess the similarity when comparing the new lightpath with those contained in the KB, the weighted Euclidean distance is calculated [8] according to Eq. (1),

$$Similarity(x, y) = -\sqrt{\sum_{a=1}^n W_a^2 \cdot (x_a - y_a)^2} \quad (1)$$

where a represents each attribute of the lightpaths x and y , W_a is the weight associated to that attribute, and n is the set of attributes. Thus, higher values (i.e., closer to zero values) of Eq. (1) mean higher similarity of the cases. The set of weights used is previously determined by means of a linear regression calculated on the KB.

The QoT parameter of the new lightpath is assumed to be the same one than that of the retrieved case, and that value is used to decide whether the lightpath fulfills the QoT

requirements or not. For that purpose, the QoT parameter is compared with a threshold. If the QoT parameter is the EVM, and the value obtained is lower than the threshold, the lightpath is classified into the high QoT category; otherwise it is classified into the low QoT category. If the QoT parameter is the OSNR, the classification is done the other way round. If the OSNR is higher than the threshold, the lightpath is classified into the high QoT category, and otherwise into the low QoT class.

4. Performance results of the cognitive QoT estimator

In order to evaluate the performance of the cognitive QoT estimator, we have set the testbed with different configurations and measured the EVM and the OSNR of the different channels. In that way, a total of 153 cases have been experimentally compiled, with EVM values ranging from 14.4% to 24.9%, and OSNR values from 20.5 to 33.4 dB. Then, we have used the 10-fold cross validation technique, a standard technique to analyze the success rate of machine learning algorithms [9]. The available data (the set of 153 cases) is randomly permuted and then divided into 10 parts. 9 parts are used to compose the KB (and then the weights, W_a , to be used in the similarity computation are calculated by means of a linear regression), and the remaining part is used to test the cognitive estimator (i.e., the cases of that part are classified by the estimator and the ratio of successful classifications is calculated). The procedure is repeated 10 times (each time using a different portion for the test set, and the remaining parts to build the KB), and the results are averaged.

First, we have focused on classifying the lightpaths according to the EVM value. As previously mentioned, the OSNR values are not considered and hence not included in the KBs. Figure 2(a) represents the percentage of successful classifications provided by the cognitive QoT estimator when setting different values of the EVM as the threshold to differentiate between high and low QoT categories. The results are compared with a majority class classification. Let S_h be the success ratio obtained if all the lightpaths are classified into the high QoT class, and S_l be the success ratio obtained if all the lightpaths are classified into the low QoT category. Then, the majority class classification provides $\max(S_h, S_l)$. In other words, the results are compared with the percentage of cases belonging to the most likely class. The cognitive QoT estimator improves the ratio of successful classifications between 5.8 (for an EVM threshold of 23%) and 29.0 (for an EVM threshold of 18.5%) percentage points when compared with the majority class classification. Moreover, the successful classifications are higher than 79% in all cases, and even higher than 90% except when the EVM threshold is set between 18 and 20.5%. The success ratio is lower than that obtained previously [5,7], but it should be noted that the scenario is different and, more importantly, that in this case the size of the KB is very small (nine-tenths of 153, i.e., 135 cases) and has not been optimized.

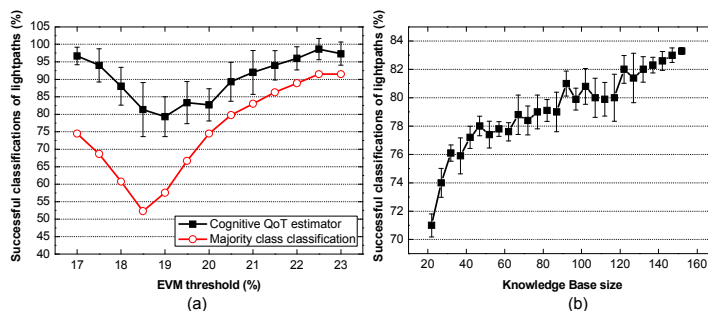


Fig. 2. (a) Percentage of successful classifications of lightpaths into high/low QoT categories according to an EVM threshold. (b) Impact of the size of the knowledge base on the percentage of successful classifications for the case of 19.5% EVM threshold.

Secondly, to further analyze the impact of the size of the KB, we have studied the performance of the cognitive QoT estimator for different KB sizes, from 22 to 152 cases, when considering an EVM threshold of 19.5%. In this occasion, a leave- n -out cross validation technique has been used, setting n to different values in order to get the desired size of the KB. As shown in Fig. 2(b), the success ratio of the classifications increases with the KB size.

Finally, we have repeated the former analysis using the OSNR as the QoT parameter that determines the category of a lightpath, proving that the cognitive QoT estimation technique is generic enough to be used with other performance parameters. The EVM values have not been considered, and thus have not been included in the KBs. Figure 3(a) represents the percentage of successful classifications provided by the cognitive QoT estimator when setting different values of the OSNR as the threshold to differentiate between high and low QoT categories. The results are again compared with a majority class classification. The cognitive estimator performs a nearly perfect classification ($\sim 100\%$ success ratio) independently of the OSNR threshold. Figure 3(b) shows the performance of the cognitive QoT estimator as a function of the size of the KB (for an OSNR threshold of 26 dB), which improves more steadily than when the EVM is used as QoT parameter.

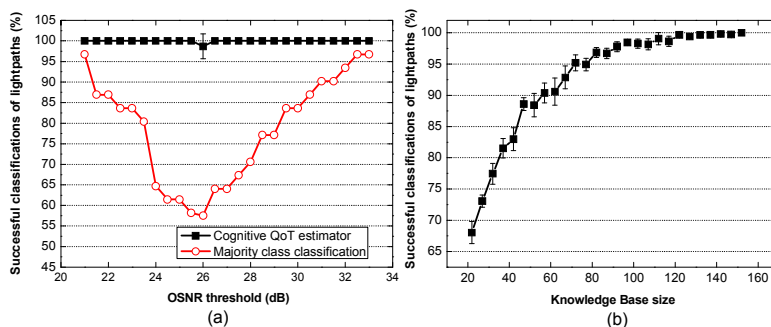


Fig. 3. (a). Percentage of successful classifications of lightpaths into high/low QoT categories according to an OSNR threshold. (b). Impact of the size of the knowledge base on the percentage of successful classifications for the case of 26 dB OSNR threshold.

5. Conclusions

We have experimentally demonstrated the use of a case-based reasoning technique to assess whether lightpaths comply with QoT requirements or not in a WDM 80 Gb/s PDM-QPSK dispersion-compensated testbed. Even with a small and not optimized KB of only 153 cases, it achieves between 79% and 98.7% successful classifications of lightpaths into high or low QoT classes according to predicted EVM values, and approximately 100% when the OSNR is used instead. These results complement previous work where we show, by means of simulation studies, the excellent performance of the cognitive QoT estimator in a 10 Gb/s OOK dispersion-compensated wavelength-routed optical network, not only in terms of successful classifications (based on the Q-factor), but also in terms of computing time, as it is around four orders of magnitude than an existing non-cognitive approach. Therefore, this shows that the case-based reasoning technique is generic enough for being used for QoT assessment in diverse networking scenarios, with different modulation formats and/or QoT parameters, hence showing its potential for application in cognitive optical networking.

Acknowledgments

This work has been partly supported by the CHRON (Cognitive Heterogeneous Reconfigurable Optical Network) project, with funding from the European Community's Seventh Framework Programme [FP7/2007-2013] under grant agreement n° 258644,

<http://www.ict-chron.eu>. T. Jiménez would like to thank the Council of Education of the Regional Government of Castilla-León and the European Social Fund for their support.

Paper [I]: Experimental evaluation of prefiltering for 56 Gbaud DP-QPSK signal transmission in 75 GHz WDM grid

Robert Borkowski, Luis Carvalho, Edson Porto da Silva, Júlio César Diniz, Darko Zibar, Júlio Oliveira, and Idelfonso Tafur Monroy. Experimental evaluation of prefiltering for 56 Gbaud DP-QPSK signal transmission in 75 GHz WDM grid. *Optical Fiber Technology*, vol. 20, no. 1, pp. 39–43, January 2014.



Contents lists available at ScienceDirect

Optical Fiber Technology

www.elsevier.com/locate/yofte



Experimental evaluation of prefiltering for 56 Gbaud DP-QPSK signal transmission in 75 GHz WDM grid[☆]



Robert Borkowski^{a,*}, Luis Henrique H. de Carvalho^b, Edson Porto da Silva^b, Júlio César M. Diniz^b, Darko Zibar^a, Júlio César R.F. de Oliveira^b, Idelfonso Tafur Monroy^a

^a DTU Fotonik – Department of Photonics Engineering, Technical University of Denmark, 2800 Kgs. Lyngby, Denmark

^b CPqD – Centro de Pesquisa e Desenvolvimento em Telecomunicações, Campinas, SP, Brazil

ARTICLE INFO

Article history:

Received 30 August 2013

Revised 17 November 2013

Available online 18 December 2013

Keywords:

Optical prefiltering

Optical modulation

Quaternary phase shift keying

Coherent detection

Optical transmission

Wavelength division multiplexing

ABSTRACT

We investigate optical prefiltering for 56 Gbaud (224 Gbit/s) electrical time-division multiplexed (ETDM) dual polarization (DP) quaternary phase shift keying (QPSK) transmission. Different transmitter-side optical filter shapes are tested and their bandwidths are varied. Comparison of studied filter shapes shows an advantage of a pre-emphasis filter. Subsequently, we perform a fiber transmission of the 56 Gbaud DP QPSK signal filtered with the 65 GHz pre-emphasis filter to fit the 75 GHz transmission grid. Bit error rate (BER) of the signal remains below forward error correction (FEC) limit after 300 km of fiber propagation.

© 2013 The Authors. Published by Elsevier Inc. All rights reserved.

1. Introduction

One of the possible solutions to temporarily postpone fiber bandwidth exhaustion is to increase transmission symbol rates and spectral efficiency. Moving to dual polarization (DP) quaternary phase shift keyed (QPSK) transmissions at symbol rates of 56 Gbaud and beyond obtained by electrical time-division multiplexing (ETDM) is very demanding. This is due to a wideband nature of the transmitted signals, which set very high bandwidth (BW) requirements towards electrical components. Due to this, reported QPSK [1–3] or 16-QAM [4,5] transmission experiments at these high symbol rates are sparse. The wide optical spectrum of high symbol rate signals is also facing increased penalties due to cascaded filtering in fixed-grid reconfigurable optical add-drop multiplexers (ROADMs) [6].

With the advent of programmable optical filters, such as the WaveShaper (WS), controlled filtering at the transmitter (prefiltering) has recently been used to reduce bandwidth of signals with broad spectral support. While only a marginal performance penalty is introduced [7], it allows for transport in narrow grids resulting in increased spectral efficiency, as well as enhances signal tolerance

towards ROADMs filtering. Simultaneously, WS can be used to introduce pre-emphasis into the signal spectrum to combat BW limitation of electrical components as was recently reported for an 80 Gbaud system [3].

In this paper, we further investigate and compare different optical prefilters for 56 Gbaud DP-QPSK signal transmission. We analyze three different filter shapes (rectangular, Gaussian, pre-emphasis) and show that filtering can improve BER compared to unfiltered signal. We then analyze crosstalk from neighboring (interfering) channels and perform an experiment with five, 224 Gbit/s (DP QPSK and 16-QAM) 65 GHz-filtered channels aligned to 75 GHz grid, which leaves sufficient margin for propagation over at least 300 km of standard single-mode fiber (SSMF) with three ROADMs at 100 km spacing.

2. Experimental setup

Experimental setup is shown in Fig. 1. CW light at 1550.116 nm, being the channel under test (CUT), was originating from a 100 kHz-linewidth external cavity laser (ECL). The light source was followed by an optional pulse carver (PC). The PC was either clocked at 28 GHz which was resulting in a 67% duty cycle return-to-zero (67%RZ) pulse train or if no clock signal was present, the CW light was passing through without pulse carving, effectively removing PC from the setup. After the pulse carver, a 22 GHz BW in-phase/quadrature (I/Q) modulator was placed.

[☆] This is an open-access article distributed under the terms of the Creative Commons Attribution License, which permits unrestricted use, distribution, and reproduction in any medium, provided the original author and source are credited.

* Corresponding author. Fax: +45 4593 6581.

E-mail address: rbor@fotonik.dtu.dk (R. Borkowski).

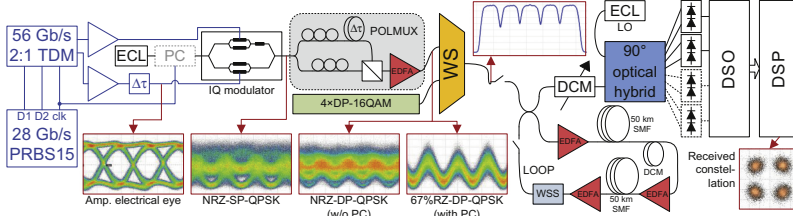


Fig. 1. Experimental setup. 56 Gbaud eye diagrams, optical spectrum (magnified in Fig. 3) and received constellation.

The electrical data signal, $2^{15} - 1$ pseudo-random binary sequence (PRBS-15), for the I/Q modulator originated from a 28 Gbit/s pattern generator with two outputs. Both electrical outputs produced sequences offset by a quarter of their length and were subsequently time-division multiplexed (TDM) to obtain 56 Gbit/s two-level electrical signal by interleaving both 28 Gbit/s input signals. Normal and inverted outputs of the TDM device were amplified, each to $4.4 V_{pp}$ (eye diagram shown in inset in Fig. 1), decorrelated by cables of different lengths and a delay line, and provided to I and Q inputs of the modulator to result in 112 Gbit/s (56 Gbaud) single polarization (SP) QPSK optical signal. This modulated signal was then polarization-division multiplexed by combining it with its delayed copy in the orthogonal polarization state. The obtained 224 Gbit/s (56 Gbaud) DP signal was subsequently amplified with erbium-doped fiber amplifier (EDFA) to account for components' losses and connected to one of the ports of the WS.

For experiments involving wavelength-division multiplexing (WDM), a subsystem generating four 28 Gbaud (224 Gbit/s) RZ-DP-16QAM interfering channels tightly surrounding the CUT was connected to another WS input. The WS was used to apply spectral shaping to connected input signals, separately to the CUT and the interfering channels, and combine them into one output signal.

For transmission experiments, signal was connected to a 2×50 km SSF loop with a dispersion compensating module (DCM) between both spans, a wavelength-selective switch (WSS) to emulate ROADM filtering and to equalize power, and EDFAs to compensate spans and WSSs losses. A variable DCM was connected at the loop output to fine-tune chromatic dispersion (CD) of the signal after propagation in the loop. The need for such accurate chromatic dispersion compensation was due to limited capabilities of the receiver, which are described further. For back-to-back experiments, the transmission loop was omitted and signal from the WS was directly connected to the receiver.

The receiver was built from discrete components as none of the available commercial 100G integrated coherent receivers exhibited sufficient performance with the CUT. The received signal was mixed with a local oscillator, CW signal from a 100 kHz-linewidth ECL spectrally separated from the CUT laser by a couple of hundreds of MHz, in a 90° optical hybrid. Four of the hybrid outputs, responsible for one of the polarizations, were supplied to two balanced photoreceivers (BPRXs) with 30 GHz BW. Since BPRXs were equipped with limiting transimpedance amplifiers (TIAs), their output amplitude was effectively limited to two levels. This, in turn, prevented digital signal processing-based (DSP-based) CD compensation and necessitated the use of DCM. One of the CUT polarizations was always aligned to the state of polarization received from the hybrid to assure minimum polarization mixing. Electrical signals from BPRXs were sampled at 80 GSa/s

(≈ 1.43 Sa/symbol) with 30 GHz-BW oscilloscope. Traces were captured and subsequently processed with offline DSP [7] algorithms to equalize received constellation.

2.1. Optical prefiltering

Unfiltered signal spectra are shown for reference in Fig. 2(a). Due to RZ shaping, the spectral support of RZ signal is approximately twice that of NRZ signal. Amplitude responses of filters applied to the WS are shown in Fig. 2(b–d). Designed and measured 3 dB and 10 dB responses are listed in Table 1.

The pre-emphasis filter (Fig. 2(d)) is an inverse of the transmitted signal spectrum in the interval equal to the filter BW and zero elsewhere. Effectively, it attenuates low- and mid-frequency components and results in approximately rectangular optical spectrum. The filter attenuation, α_{pre} , expressed in linear scale, where 1 corresponds to complete attenuation and 0 to no attenuation, is given by Eq. 1 as

$$\alpha_{pre}(f) = \begin{cases} 1 - \frac{\min(P(f))}{P(f)} & \text{for } -\frac{BW}{2} \leq f \leq \frac{BW}{2} \\ 1 & \text{otherwise} \end{cases} \quad (1)$$

where f is the optical frequency relative to the WDM channel center, $P(f)$ is the discrete optical power spectrum measured at the transmitter output, and BW is the filter 3 dB bandwidth. This filter is a zero-forcing equalizer applied at the transmitter that helps to mitigate intersymbol interference (ISI). The optical spectrum processed with a set of those filters is shown in Fig. 3(a).

We compare it with two, simpler to implement filters. Rectangular (Fig. 2(b)) filter, as defined by Eq. 2 has a flat amplitude response across its BW and a sharp cutoff outside of its BW. Its attenuation, α_{rect} , is specified as

$$\alpha_{rect}(f) = \begin{cases} 0 & \text{for } -\frac{BW}{2} \leq f \leq \frac{BW}{2} \\ 1 & \text{otherwise} \end{cases} \quad (2)$$

The specification of Gaussian filter is given by Eq. 3 (Fig. 2(c)). Its shape follows a Gaussian function with full width at half maximum equal to the filter BW. Spectral components outside of the WDM grid slot are cut off.

$$\alpha_{gauss}(f) = \begin{cases} 1 - \exp\left(-\frac{f^2}{2(BW/(2\sqrt{2\ln 2}))^2}\right) & \text{for } -37.5 \text{ GHz} \leq f \leq 37.5 \text{ GHz} \\ 1 & \text{otherwise} \end{cases} \quad (3)$$

As measured from the spectrum of the rectangular filter, the WS has a 0.85 dB/GHz roll-off in the transition band and bandwidth setting resolution of approximately 1 GHz.

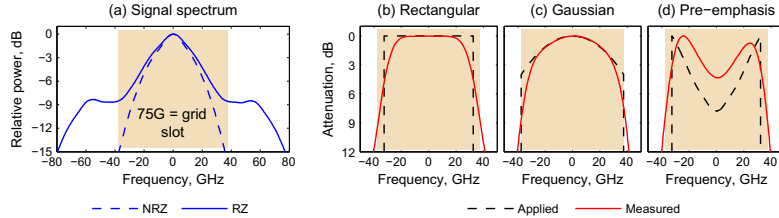


Fig. 2. (a) Comparison of 56 Gbaud DP-QPSK optical spectra for RZ and NRZ signals. (b–d) Applied and measured amplitude responses of implemented filters with 3 dB bandwidth of 65 GHz for transmission in 75 GHz grid (highlighted range).

Table 1

Designed (only filters) and measured 3 dB and 10 dB bandwidths for experimental signals and optical filters.

Signal/filter	Designed, GHz		Measured, GHz	
	3 dB	10 dB	3 dB	10 dB
RZ signal	–	–	32	128
NRZ signal	–	–	28	59
Rectangular	65	65	60	77
Gaussian	65	75	59	78
Pre-emphasis	65	65	64	77

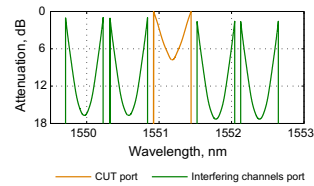


Fig. 4. Pre-emphasis filters applied to respective WS ports.

2.2. Optical prefiltering for WDM transmission

All channels in the WDM transmission experiment were equalized with a corresponding pre-emphasis filter. The back-to-back optical spectrum of the WDM system after filtering is shown in Fig. 3(a). The CUT was connected to one port of the WS, while interfering RZ-DP-16QAM channels were connected to another WS port. This was done to multiplex them together for transmission, and to prevent crosstalk to the CUT due to spectral overlap with interfering channels. Fig. 4 shows the filter applied to the interfering channels (green line), which is disjoint with the filter used for the CUT (yellow line). Possible strategies to introduce prefiltering into an actual system would be to use an optical equalizer as in [5] to either separately prefilter each channel at the output of each transmitter, or prefilter groups of odd and even channels, subsequently combining them for transmission in a narrow grid. Since both the CUT and interfering channels spectra were broader than 75 GHz slot of the transmission grid, the resulting spectral widths of signals after filtering with 65 GHz pre-emphasis filters were indistinguishable, as seen in Fig. 3(a).

3. Results

Back-to-back performance of the system as a function of optical signal-to-noise ratio (OSNR) is shown in Fig. 5(a). The system implementation penalty, as measured at BER of the forward error correction (FEC) limit of 3.8×10^{-3} , is 5 dB for both SP and DP signal. The horizontal separation between SP and DP curves is around 3 dB at FEC limit, indicating marginal penalty (theoretical minimum is 3 dB) due to polarization multiplexing. Only SP curve shows a small advantage of <1 dB for RZ shaping case. An error floor hits in around 1.5×10^{-4} and 3×10^{-4} for SP and DP cases respectively. Filter shapes under consideration are subsequently applied to the 67%RZ-shaped CUT while maintaining 23 dB OSNR. We start the investigation with a BW of 105 GHz for all filter shapes which is the minimum at which filter influence on the BER is negligible. As shown in Fig. 5(b), for rectangular and Gaussian filter shapes, the BER performance remains close to the reference for unfiltered RZ-DP signal, with the rectangular being slightly worse, until 65 GHz. For BWs lower than 65 GHz the BER starts to deteriorate, which for rectangular filter is very rapid due

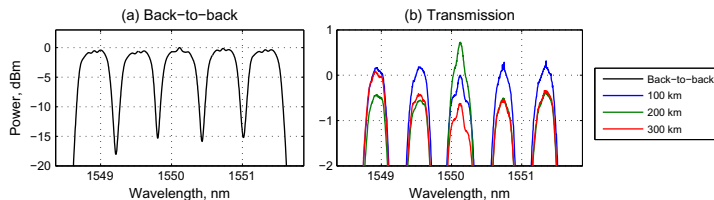


Fig. 3. (a) Back-to-back spectrum. (b) Evolution of transmission spectra after each loop circulation (power normalized w.r.t. the central QPSK channel at 100 km).

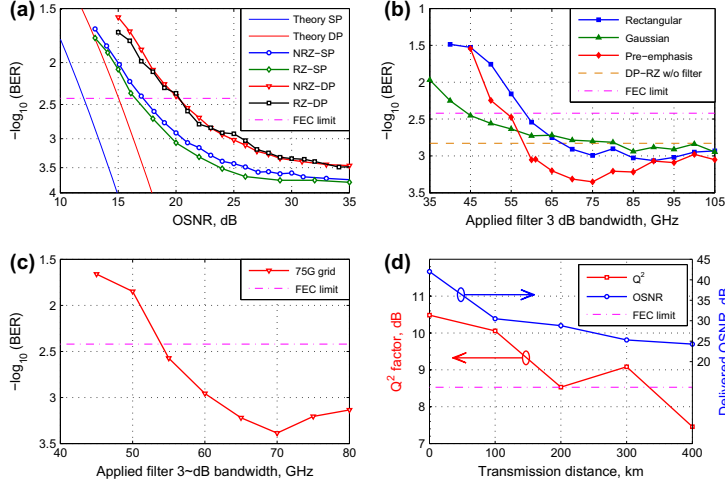


Fig. 5. (a) Back-to-back system performance. (b) Filtering performance of 56 Gbaud RZ-DP-QPSK signal at 23 dB OSNR. (c) Performance for varying bandwidth of pre-emphasis filter for transmission in 75 GHz grid at 23 dB OSNR. (d) BER performance and delivered OSNR of the CUT.

to strong ISI. For the pre-emphasis filter we can see an initial improvement in the BER from 3.0×10^{-3} at BW of 105 GHz down to a minimum of 4.4×10^{-4} at 75 GHz and again fast degradation below 60 GHz. This is explained by the fact that the pre-emphasis filter effectively works as amplification for high frequency components and counteracts the concatenated component frequency roll-off (which is steep as we are mostly using devices not designed to operate at 56 GHz). Thanks to transmitter-side pre-emphasis, noise amplification due to receiver-side equalization is less pronounced and in turn results in improved BER.

3.1. WDM transmission

We set up a WDM system with five channels in 75 GHz grid, as shown in Fig. 1, applied pre-emphasis filter to every channel, as described in Section 2.2, varied the filter BW and investigated crosstalk from interfering channels to the CUT. Results, shown in Fig. 5(c), indicate that the lowest crosstalk is obtained for a filter BW of 70 GHz. Considering cascaded ROADMs filtering, we decided to perform WDM transmission experiment with a filter BW of 65 GHz to increase margin for filter narrowing. The optical spectrum of the WDM signal, with each channel filtered with a corresponding pre-emphasis filter, is shown in Fig. 3(a). The evolution of this spectrum after each loop traversal, normalized to 0 dB for the CUT after 100 km, is presented in Fig. 3(b). The result of the WDM transmission experiment is shown in Fig. 5(d). We have managed to traverse 300 km (6×50 km) of SSMF with three WSSs in a compensated link while maintaining BER performance below the FEC limit.

4. Future work

Operating the system at high symbol rates is challenging and often requires a tradeoff between the bandwidth and linearity of

available electrical components. For instance, the coherent receiver used in the experimental setup was equipped with limiting TIAs. Because of this, accurate CD compensation was necessary at the end of the link to allow for successful signal digitization. We expect that a coherent receiver with linear TIAs, using adaptive CD compensation in DSP, will significantly improve the system performance. Moreover, even though both orthogonal polarization states were transmitted, only one of them could have been measured. For that reason an accurate polarization alignment of the signal entering the receiver was critical. Polarization state mismatch was negatively influencing BER, because crosstalk from non-received polarization could not have been mitigated in the follow-up DSP. We predict further BER improvement if data from both polarizations can be acquired and, subsequently, polarization demultiplexed with e.g. butterfly structure filter adapted by constant modulus algorithm (CMA) in digital domain. Despite those shortcomings, we still believe that our results are valid and provide an interesting input for further investigation of performance limits in optically-filtered 56 Gbaud systems. We also think that our work can provide guidelines when building or upgrading experimental setup to support high symbol rates.

5. Conclusions

We have compared different optical prefilters for 56 Gbaud DP-QPSK signal transmission. We found that for back-to-back case, an optical pre-emphasis filter (zero-forcing equalizer) with a bandwidth above 60 GHz resulted in BER improvement comparing to rectangular or Gaussian-shaped filters. We then demonstrated a 75 GHz-grid five-channel WDM transmission with channels shaped with 65 GHz 3 dB-bandwidth pre-emphasis filter, achieving 300 km transmission with BER performance below the FEC limit for the 56 Gbaud channel and passing through three WSSs.

Acknowledgment

We acknowledge Carolina Franciscangelis from CPqD for her help in performing experimental measurements.

References

- [1] P.J. Winzer, A.H. Gnauck, G. Raybon, M. Schnecker, P.J. Pupaiaikis, 56-Gbaud PDM-QPSK: coherent detection and 2500-km transmission, in: 35th European Conference and Exhibition on Optical Communication (ECOC), vol. 2009 – Suppl., Vienna, Austria, 2009, p. PD 2.7.
- [2] A.H. Gnauck, P.J. Winzer, G. Raybon, M. Schnecker, P.J. Pupaiaikis, 10×224 -Gb/s WDM transmission of 56-Gbaud PDM-QPSK signals over 1890 km of fiber, IEEE Photon. Technol. Lett. 22 (13) (2010) 954–956, <http://dx.doi.org/10.1109/LPT.2010.2048100>.
- [3] G. Raybon, P.J. Winzer, A.A. Adamiecki, A.H. Gnauck, A. Konczykowska, F. Jorge, J.-Y. Dupuy, L.L. Buhl, C.R. Doerr, R. Delbue, P.J. Pupaiaikis, All-ETDM 80-Gbaud (160-Gb/s) QPSK generation and coherent detection, IEEE Photon. Technol. Lett. 23 (22) (2011) 1667–1669, <http://dx.doi.org/10.1109/LPT.2011.2166111>.
- [4] P.J. Winzer, A.H. Gnauck, S. Chandrasekhar, S. Draving, J. Evangelista, B. Zhu, Generation and 1200-km transmission of 448-Gb/s ETDM 56-Gbaud PDM 16-QAM using a single I/Q modulator, in: 36th European Conference and Exhibition on Optical Communication (ECOC), No. 1, IEEE, Torino, Italy, 2010, p. PD2.2, doi:10.1109/ECOC.2010.5621371.
- [5] G. Raybon, A.L. Adamiecki, S. Randel, C. Schmidt, P.J. Winzer, A. Konczykowska, F. Jorge, J.-Y. Dupuy, L.L. Buhl, S. Chandrasekhar, X. Liu, A.H. Gnauck, C. Scholz, R. Delbue, All-ETDM 80-Gbaud (640-Gb/s) PDM 16-QAM generation and coherent detection, IEEE Photon. Technol. Lett. 24 (15) (2012) 1328–1330, <http://dx.doi.org/10.1109/LPT.2012.2203118>.
- [6] X. Zhou, L.E. Nelson, 400G WDM transmission on the 50 GHz grid for future optical networks, J. Lightw. Technol. 30 (24) (2012) 3779–3792, <http://dx.doi.org/10.1109/JLT.2012.2206013>.
- [7] E. Porto da Silva, L. Carvalho, C. Franciscangelis, J. Diniz, J. Oliveira, A. Bordonalli, Spectrally-efficient 448-Gb/s dual-carrier PDM-16QAM channel in a 75-GHz grid, in: Optical Fiber Communication Conference 2013, OSA, Anaheim, CA, 2013, p. JTh2A.39, doi:10.1364/NFOEC.2013.JTh2A.39.

Paper [J]: Reconfigurable digital coherent receiver for metro-access networks supporting mixed modulation formats and bit-rates

Antonio Caballero, Neil Guerrero Gonzalez, Valeria Arlunno, **Robert Borkowski**, Tien Thang Pham, Roberto Rodes, Xu Zhang, Maisara Binti Othman, Kamau Prince, Xianbin Yu, Jesper Bevensee Jensen, Darko Zibar, and Idelfonso Tafur Monroy. Reconfigurable digital coherent receiver for metro-access networks supporting mixed modulation formats and bit-rates. *Optical Fiber Technology*, vol. 19, no. 6, pp. 638–642, December 2013.



Contents lists available at ScienceDirect

Optical Fiber Technology

www.elsevier.com/locate/yofte



Reconfigurable digital coherent receiver for metro-access networks supporting mixed modulation formats and bit-rates



Antonio Caballero*, Neil Guerrero Gonzalez, Valeria Arlunno, Robert Borkowski, Tien Thang Pham, Roberto Rodes, Xu Zhang, Maisara Binti Othman, Kamau Prince, Xianbin Yu, Jesper Bevensee Jensen, Darko Zibar, Idelfonso Tafur Monroy

DTU Fotonik, Department of Photonics Engineering, Technical University of Denmark, Kgs. Lyngby, Denmark

ARTICLE INFO

Article history:

Received 6 June 2013
 Revised 26 August 2013
 Available online 28 October 2013

Keywords:

Coherent communications
 Phase modulation
 Radio-over-fiber systems
 Digital coherent receivers

ABSTRACT

A single, reconfigurable, digital coherent receiver is proposed and experimentally demonstrated for converged wireless and optical fiber transport. The capacity of reconstructing the full transmitted optical field allows for the demodulation of mixed modulation formats and bit-rates. We performed experimental validation of different modulation formats, including VCSEL based OOK, baseband QPSK, RoF OFDM and wireless IR-UWB over a 78 km deployed fiber link.

© 2013 Elsevier Inc. All rights reserved.

1. Introduction

Next generation metro-access networks will need to support diverse broadband services including converged wireless and wireline optical access over a unified fiber platform, satisfying bandwidth requirements [1] as well as fulfilling stringent power budget and chromatic dispersion constraints [2]. Future metro-access networks will also require agile re-configurability to seamlessly accommodate for emerging new services and increased bandwidth requirements [1]. The introduction of different modulation formats and bitrates into the metro-access networking scenario is creating a highly heterogeneous environment that represents a new challenge to tackle in the near future. Approaches looking for solutions to one or more of the above issues are radio-over-fiber systems for integrating baseband and wireless service delivery over optical fiber access networks [3]. The combination of high bitrate baseband has been proposed for the transport of wireless signal in the digital domain [4]. Most of these approaches focus on methods for generating the wireless signals carrying orthogonal frequency division multiplexing (OFDM) [5]; however, the detection is usually performed with independent receivers, increasing the complexity of these architectures.

A promising approach recently proposed to increase the capacity of passive optical networks (PON) is wavelength-division

multiplexing (WDM) combined with coherent detection. Compared to direct-detection (DD), coherent detection allows for closely spaced channels with increased receiver sensitivity to cope with the required large number of users and to extend the reach of metro-access networks [6,7]; also, coherent receivers does not require an arrayed waveguide grating (AWG) at the receiver to filter the undesired wavelengths [7], making this technology compatible with the passive optical splitting of legacy PONs. Digital coherent detection also allows for the detection of wireless signals [8] providing the required high linearity and high capacity of next generation wireless networks.

Although experimental demonstrations of converged service delivery have been reported in the literature [2,3] they use a dedicated receiver for each modulation or bit-rate. The approach of separate receivers is shown in Fig. 1, where different receivers are used to detect baseband signals, intensity-modulated (IM) or phase-modulated (PM), and analog signals, from a typical radio-over-fiber (RoF) such as WiFi or WiMAX to an ultra-wide band (UWB). The use of coherent detection allows reconfiguring the digital signal processing (DSP) software in the demodulator for each modulation format, thus there is only one receiver needed. Furthermore, it allows longer reach and avoids the use of an AWG to separate the different channels.

In this paper we present and experimentally demonstrate a single, reconfigurable, digital receiver supporting mixed modulation formats, baseband and wireless-over-fiber, with reconfiguration in the digital signal processing domain. We provide a detail description of the architecture and building blocks of the architecture.

* Corresponding author. Address: DTU Fotonik, B. 358 R. 105, 2800 Kgs. Lyngby, Denmark.

E-mail address: acaj@fotonik.dtu.dk (A. Caballero).

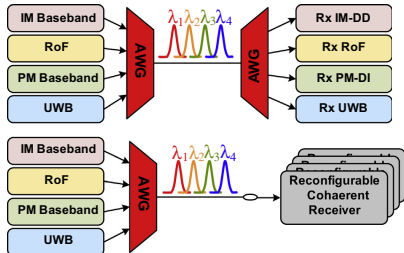


Fig. 1. Architecture of a WDM-PON with dedicated receivers (top) and with a single reconfigurable digital receiver (bottom).

Furthermore we detail the experimental demonstration first presented in [9] for 20 Gb/s non-return-to-zero quadrature phase-shift keying (NRZ-QPSK), optically phase-modulated 5 GHz OFDM RoF and 2 Gb/s impulse radio UWB (IR-UWB), and 5 Gb/s directly modulated vertical cavity surface emitting laser (VCSEL) after 78 km of deployed fiber link.

2. Single reconfigurable receiver

Recent advances in high-speed DSP and analog-to-digital (A/D) conversion (ADC) have enabled the integration of digital receiver into optical communication systems [8,10]. The main advantages digital receivers can offer over traditional signal demodulation schemes include the following:

- Cost effectiveness and compactness.
- Possibilities to adaptively compensate for channel impairments in the electronic domain (such as chromatic dispersion, polarization mode dispersion, etc.) using signal processing techniques.
- Design versatility and robust operation by enabling reception of different formats using the same receiver hardware based on the channel condition.
- Enhance performance, arising from the full recovery of the optical field information: digital coherent receivers enhanced OSNR tolerance, better compatibility with advanced modulation formats, and enhanced electronic equalization of linear and non-linear effects in the transmission link [11].

The first experimental demonstration of converge wired and wireless over deployed fiber [2] employed dedicated receivers for each signal. The baseband DQPSK signal was demodulated using a delay interferometer (DI); the RoF was detected using a photodiode (PD) and RF low-noise amplifier and for the UWB, also a PD was used. For the RoF using phase-modulation, a digital coherent receiver was used.

A single reconfigurable receiver in the uplink transmission, as proposed in this paper, has the benefit of demodulating different types of optical signals, with variable modulation formats and bit-rates. The use of coherent detection also benefits from improved sensitivity.

A schematic diagram of the employed single digital receiver is shown in Fig. 2. The single digital receiver first compensates for the chromatic dispersion of the link, which is a common impairment for all the modulation formats. For the analog detection (IR-UWB and PM-OFDM), the DSP first performs a recovery of the optical phase using a combination of optical carrier-recovery

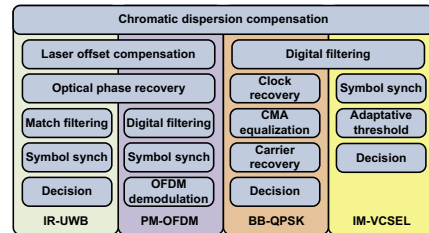


Fig. 2. Schematic diagram of the reconfigurable digital receiver.

digital phase-locked loop (PLL), to compensate for the lasers frequency offset, followed by linear signal demodulation [8], which extracts the phase of the optical field. Then, the IR-UWB is demodulated by match filter with the transmitted pulse-shape [11], whereas the PM-OFDM is demodulated using standard OFDM demodulation based on Schmidl training symbols [12]. For the baseband QPSK (BB-QPSK) a standard receiver is used, based on clock-recovery, constant-modulus algorithm (CMA) and carrier recovery [8,13]. The intensity modulated (IM) VCSEL is demodulated using match filter. An adaptive threshold is used afterwards to compensate for the absence of VCSEL temperature control and decision gating [14]. The reconfiguration for each modulation format was performed by digitally switching between the four signal demodulation DSP blocks. In our developed software, we first perform a switch from the 4 possible signals, loading their individual bitrates and modulation formats, the DSP modules needed for demodulation and their initialization parameters. As the possible modulation formats are finite, these initialization values can be stored in a modulation format database. In future, the identification of the modulation format could be automatized.

3. Experimental demonstration

Fig. 3 shows a block diagram of the heterogeneous optical network and setup used in the experiment. The field-deployed fiber connects the Kgs. Lyngby campus of the Technical University of Denmark (DTU) and the Taastrup suburb of Copenhagen. The fiber is a G.652 standard single-mode fiber (SMF) type (16.5 ps/nm/km chromatic dispersion, 0.20 dB/km attenuation). The total length of the fiber was 78 km, exceeding current standards but suitable for future longer reach PON. The total link loss was 27 dB. ITU standard operating wavelengths were used for all channels at 200 GHz separation due to equipment availability. The total launch power into the deployed fiber was kept to +4 dBm, with an equal launch power per carrier of -2 dBm. Due to the bitrates of this experiment and previous work in RoF [11] and baseband coherent [16], we would expect low penalty from closer WDM spacing, such as 50 GHz.

The optical spectrum each of the four different signals is shown in Fig. 4. At the receiver side, emulating the central office, an erbium doped fiber amplifier (EDFA) was used as preamplifier followed by an optical bandpass filter to reduced ASE noise. The optical power level to the coherent receiver was set to -11 dBm. A tunable external cavity laser (ECL), with a linewidth of 100 kHz, was used as local oscillator (LO) for all the received signal types. The in-phase and quadrature signals after the 90° optical hybrid were detected with two pairs of balanced photodiodes, having full-width at half-maximum bandwidth of 7.5 GHz. The detected photocurrents were digitized using a sampling oscilloscope at

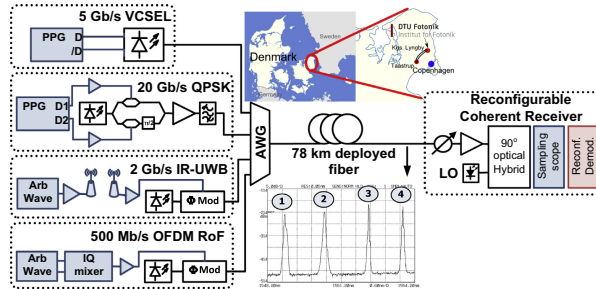


Fig. 3. Experiment layout of the heterogeneous optical network investigated in the experiment. Route of installed optical fiber is also shown. Reconfigurable receiver construction allows local oscillator (LO) tuning for channel selection. PPG: pulse pattern generator; Arb Wave: arbitrary waveform.

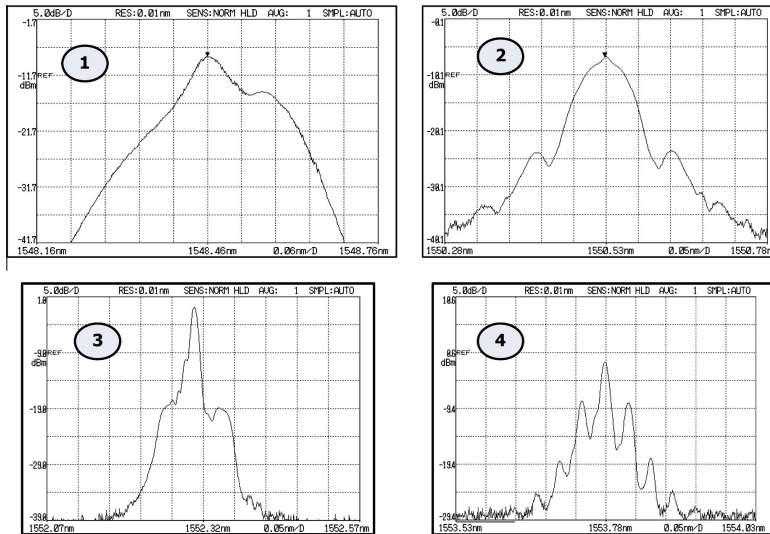


Fig. 4. Optical spectrums of the four different optical signals at the input of the fiber.

40 GSa/s for offline processing, with the receiver structure described in Fig. 2.

3.1. 5 Gb/s intensity-modulated and coherently detected VCSEL

A pulse pattern generator (PPG) at 5 Gb/s directly modulated a 1548.5 nm single-mode VCSEL. Single drive configuration was used for the VCSEL with a driving peak-peak voltage of 1 V. A pseudo random binary sequence (PRBS) with a length of $2^{15}-1$ was used for this experiment. The bias current of the VCSEL was used to tune the wavelength to the assigned AWG channel. Bias current was set to 14 mA. The output power of the VCSEL was measured to be 0.5 dBm.

3.2. 20 Gb/s NRZ-QPSK

The transmitter of the baseband QPSK subsystem consisted on a nested Mach-Zehnder modulator (MZM) driven by two independent electrical signals at 10 Gb/s with PRBS $2^{15}-1$. The laser source was a DFB centered at 1550.5 nm and with a value of the linewidth of 2 MHz.

3.3. 2 Gb/s phase-modulated IR-UWB

An Arbitrary Waveform Generator (AWG) with 24 GSa/s sampling rate was utilized to program a 5th order derivative Gaussian pulse, with good compliance with FCC mask [11]. A bipolar

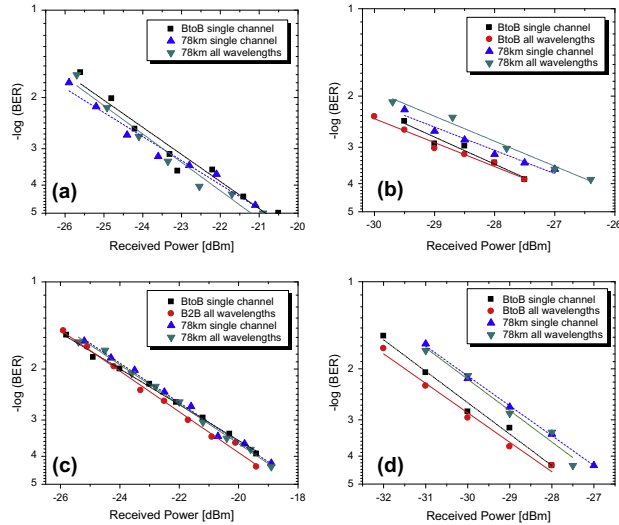


Fig. 5. Measured BER performances for (a) 5 Gb/s intensity-modulated VCSEL, (b) 20 Gb/s QPSK baseband, (c) 2 Gb/s phase-modulated IR-UWB, and (d) 5 GHz OFDM RoF.

modulation at a bit rate of 2 Gb/s was applied to the generated pulses with a PRBS $2^{11}-1$. The UWB signal was transmitted using an omni-directional antenna with 0 dBi gain and received after 1 m wireless transmission by a directive antenna with up to 12 dBi gain within the UWB frequency range. The received wireless signal was amplified by an electrical low noise amplifier, filtered and then amplified again to drive the optical phase modulator. The DFB laser source of this channel was set at 1552.3 nm.

3.4. 5 GHz OFDM RoF

The OFDM baseband signal was generated in software using a $2^{15}-1$ PRBS as input data stream. 256 4-QAM subcarriers were used with 26 samples cyclic prefix per OFDM symbol. The OFDM frame was composed of two Schmidl training symbols [13,15] followed by eight data symbols. The in-phase and quadrature signals were fed to an AWG with a 1.25 GSa/s rate, for a total bit rate of 500 Mb/s. The signal was then upconverted to a frequency of 5 GHz using a Vector Signal Generator (VSG), driving an optical phase modulator supplied with a DFB laser at 1553.78 nm.

4. Results

To demonstrate the performance of our reconfigurable digital coherent receiver, we measured bit error rate (BER) curves for back-to-back (B2B) and after 78 km of deployed fiber transmission (considering both single and all simultaneous channel performance) as a function of the received optical power. The results for each channel are shown in Fig. 5. For all four subsystems, a BER value below 10^{-3} (FEC threshold) is achieved for all considered scenarios. The worst receiver sensitivity achieved was -23 dBm, resulting in 21 dB link budget for +4 dBm total launch power.

4.1. 5 Gb/s coherently detected, intensity-modulated VCSEL

As we can see in Fig. 5a, the VCSEL coherently detected subsystem achieves a sensitivity of -24 dBm at 10^{-3} for both B2B and 78 km deployed fiber. As the chromatic dispersion and chirp were completely compensated by DSP no penalty was appreciated compared with the B2B case.

4.2. 20 Gb/s QPSK baseband

Fig. 5b shows that fiber transmission incurred in 1 dB power penalty difference at 10^{-3} BER. In the simultaneous presence of the other three channels, there was an observable *minor* 0.5 dB penalty both for back to back and after transmission. We attribute this penalty to the presence of the IM-VCSEL neighbour channel inducing cross-phase modulation. The receiver sensitivity was -28 dBm for the WDM transmission.

4.3. 2 Gb/s phase-modulated IR-UWB

As shown in Fig. 5c the measured BER performances of the UWB subsystem were consistent for all cases. The BER performance is below the FEC limit when the received optical power was higher than -23 dBm, including 1 m of wireless transmission.

4.4. 5 GHz OFDM RoF

Fig. 5d shows that for the case of four simultaneously integrated channels, OFDM suffered 0.5 dB of power penalty, for both B2B and 78 km fiber transmission compared to single OFDM channel transmission. This yielded receiver sensitivity at a BER of 10^{-3} of -29.5 dBm for the B2B system, and -28.5 dBm for the 78 km optical transmission link, respectively.

5. Conclusion

A single reconfigurable DSP enabled coherent receiver is proposed for long reach converged PON for uplink transmission. We experimentally demonstrated its performance for mixed modulation formats and bit rates over a deployed fiber link. In our reported experiment, four different types of wireline and wireless services including 20 Gb/s QPSK baseband, 5 Gb/s OOK, 5 GHz OFDM RoF and 2 Gb/s IR-UWB are successfully demodulated after transmission over 78 km deployed fiber link. The demonstrated links exceeds current access lengths and due to the low launch power and high sensitivity, we expect that minor penalty will be induced for closer WDM spacing. The receiver used the same optical front-end, is able to switch among baseband and wireless types of signals by DSP reconfiguring to baseband only. This demonstrated digital reconfigurable coherent receiver has potential to enable unified support for signal detection on highly heterogeneous next generation metro-access networks.

Acknowledgments

The authors thank Tektronix Denmark for the loan of the AWG7000 and Globalconnect Denmark for access to the deployed fiber. This work was partly supported by Danish Research Council under Grant OPSCODER and by the European Union FP7 Information Communication Technology (ICT)-ALPHA.

References

- [1] K. Sato, H. Hasegawa, Optical networking technologies that will create future bandwidth abundant networks, *J. Opt. Comm. Network*, 1 (2009) 81–83.
- [2] K. Prince, J.B. Jensen, A. Caballero, X. Yu, T.B. Gibbon, D. Zibar, N. Guerrero, A.V. Osadchii, I. Tafur Monroy, Converged wireline and wireless access over a 78-km deployed fiber long-reach WDM PON, *Photon. Technol. Lett.* 21 (2009) 1274–1276.
- [3] M. Popov, The convergence of wired and wireless services delivery in access and home networks, in: *Proc. of OFC*, 2010 (paper OWQ6).
- [4] A. Nirmalathas, P.A. Gamage, C. Lim, D. Novak, R. Waterhouse, Digitized Radio-Over-Fiber technologies for converged optical wireless access network, *J. Lightw. Technol.* 28 (2010) 2366–2375.
- [5] H. Yu-Ting, A novel lightwave centralized bidirectional hybrid access network: seamless integration of RoF with WDM-OFDM-PON, *Photon. Technol. Lett.* 23 (2011) 1085–1087.
- [6] H. Rohde, S. Smolorz, E. Gottwald, K. Kloppe, Next generation optical access: 1 Gbit/s for everyone, in: *ECOC* 2009, 10.5.5.
- [7] D. Lavery, M. Ionescu, S. Makovejs, E. Torrenço, S.J. Savory, A long-reach ultra-dense 10 Gbit/s WDM-PON using a digital coherent receiver, *Opt. Express* 18 (2010) 25855–25860.
- [8] A. Caballero, D. Zibar, I. Tafur Monroy, Performance evaluation of digital coherent receivers for phase-modulated Radio-Over-Fiber links, *J. Lightw. Technol.* 29 (2011) 3282–3292.
- [9] N.G. Gonzalez, A. Caballero, R. Borkowski, V. Arjunno, T.T. Pham, R. Rodes, X. Zhang, M.B. Öthman, K. Prince, X. Yu, J.B. Jensen, D. Zibar, I.T. Monroy, Reconfigurable digital coherent receiver for metro-access networks supporting mixed modulation formats and bit-rates, in: *OFC* 2011, OMW7.
- [10] L. Kazovsky, W.-T. Shaw, D. Gutierrez, N. Cheng, S.-W. Wong, Next-generation optical access networks, *J. Lightw. Technol.* 25 (2007) 3428–3442.
- [11] T.T. Pham, N. Guerrero Gonzalez, X. Yu, D. Zibar, L. Dittmann, I. Tafur Monroy, Robust BPSK impulse radio UWB-over-Fiber systems using optical phase modulation, in: *OFC* 2011, OTuF6.
- [12] V. Arjunno, R. Borkowski, N. Guerrero Gonzalez, A. Caballero, K. Prince, J.B. Jensen, D. Zibar, K.J. Larsen, I. Tafur Monroy, Radio over fiber link with adaptive order n-QAM optical phase modulated OFDM and digital coherent detection, *Microw. Opt. Technol. Lett.* 53 (2011) 2245–2247.
- [13] T. Pfau, S. Hoffmann, R. Noé, Hardware-efficient coherent digital receiver concept with feedforward carrier recovery for M-QAM constellations, *J. Lightw. Technol.* 27 (2009) 989–999.
- [14] J.B. Jensen, R. Rodes Lopez, D. Zibar, I. Tafur Monroy, Coherent detection for 1550 nm, 5 Gbit/s VCSEL based 40 km bidirectional PON transmission, in: *OFC* 2011, OTuB2.
- [15] T. Schmidt, D. Cox, Robust frequency and timing synchronization for OFDM, *Trans. Commun.* 45 (1997) 1613–1621.
- [16] M. Alfiad, M. Kuschnerov, T. Wuth, T.J. Xia, G. Wellbrock, E. Schmidt, D. van den Borne, B. Spinnler, C.J. Weiske, E. de Man, A. Napoli, M. Finkenzeller, S. Spaeller, M. Rehman, J. Behel, M. Chbat, J. Stachowiak, D. Peterson, W. Lee, M. Pollock, B. Basch, D. Chen, M. Freiberg, B. Lankl, H. de Waardt, 111-Gb/s transmission over 1040-km field-deployed fiber with 10G/40G neighbors, *Photon. Technol. Lett.* 21 (2010) 615–617.

Paper [K]: Experimental demonstration of adaptive digital monitoring and compensation of chromatic dispersion for coherent DP-QPSK receiver

Robert Borkowski, Xu Zhang, Darko Zibar, Richard Younce, and Idelfonso Tafur Monroy. Experimental demonstration of adaptive digital monitoring and compensation of chromatic dispersion for coherent DP-QPSK receiver. *Optics Express*, vol. 19, no. 26, pp. B728–B735, December 2011.

Experimental demonstration of adaptive digital monitoring and compensation of chromatic dispersion for coherent DP-QPSK receiver

Robert Borkowski,^{1,*} Xu Zhang,¹ Darko Zibar,¹ Richard Younce,²
and Idelfonso Tafur Monroy¹

¹ DTU Fotonik, Department of Photonics Engineering, Technical University of Denmark,
Ørstedes Plads, Building 343, DK-2800 Kgs. Lyngby, Denmark

² Tellabs, 1415 West Diehl Road, Naperville, IL 60563, USA

*rbor@fotonik.dtu.dk

Abstract: We experimentally demonstrate a digital signal processing (DSP)-based optical performance monitoring (OPM) algorithm for in-service monitoring of chromatic dispersion (CD) in coherent transport networks. Dispersion accumulated in 40 Gbit/s QPSK signal after 80 km of fiber transmission is successfully monitored and automatically compensated without prior knowledge of fiber dispersion coefficient. Four different metrics for assessing CD mitigation are implemented and simultaneously verified proving to have high estimation accuracy. No observable penalty is measured when the monitoring module drives an adaptive digital CD equalizer.

© 2011 Optical Society of America

OCIS codes: (060.1660) Coherent communications; (060.2330) Fiber optics communications.

References and links

1. S. J. Savory, "Digital filters for coherent optical receivers," *Opt. Express* **16**, 804–817 (2008).
2. F. Hauske, J. Geyer, M. Kuschnerov, K. Piyawanno, T. Duthel, C. Fludger, D. van den Borne, E. Schmidt, B. Spinnler, H. de Waardt, and B. Lankl, "Optical performance monitoring from FIR filter coefficients in coherent receivers," in *Optical Fiber Communication Conference, OSA Technical Digest (CD)* (Optical Society of America, 2008), paper OThW2.
3. M. Kuschnerov, F. N. Hauske, K. Piyawanno, B. Spinnler, A. Napoli, and B. Lankl, "Adaptive chromatic dispersion equalization for non-dispersion managed coherent systems," in *Optical Fiber Communication Conference, OSA Technical Digest (CD)* (Optical Society of America, 2009), paper OMT1.
4. F. N. Hauske, C. Xie, Z. P. Zhang, C. Li, L. Li, and Q. Xiong, "Frequency domain chromatic dispersion estimation," in *Optical Fiber Communication Conference, OSA Technical Digest (CD)* (Optical Society of America, 2010), paper JThA11.
5. D. Wang, C. Lu, A. P. T. Lau, and S. He, "Adaptive chromatic dispersion compensation for coherent communication systems using delay-tap sampling technique," *IEEE Photon. Technol. Lett.* **14**, 1016–1018 (2011).
6. B. Spinnler, "Equalizer design and complexity for digital coherent receivers," *IEEE J. Sel. Topics Quantum Electron.* **5**, 1180–1192 (2010).
7. M. Kuschnerov, F. N. Hauske, K. Piyawanno, B. Spinnler, M. S. Alfiad, A. Napoli, and B. Lankl, "DSP for coherent single-carrier receivers," *J. Lightwave Technol.* **27**, 3614–3622 (2009).
8. S. Haykin, *Adaptive filter theory* (Prentice-Hall, 2002).

1. Introduction

Coherent optical communication is already a commercially well established technology. One of the advantages of coherent receivers is that DSP algorithms, specifically impairment equalization schemes, can be implemented directly in the receivers' electronics. Chromatic dispersion, one of the most important factors contributing to signal degradation in long and ultra long haul optical communication systems, can be relatively easily canceled in the DSP circuit of a coherent receiver [1]. This enables operation of dispersion non-compensated links due to the fact that dispersion maps or CD compensation units are no longer necessary to ensure best reception quality and minimize number of received bit errors. Nonetheless, even for DSP-based dispersion filters it is usually assumed that CD value that accumulates in the signal is both known and constant enabling the use of a static CD filter at the receiver. Although this assumption is valid in submarine or terrestrial point-to-point links, it does not hold when mixed or coherent transport networks with routing capabilities are considered. In the general case, CD value of the incoming signal may change dynamically. This challenge is addressed by a DSP-based CD monitoring subsystem.

In literature different approaches to CD monitoring directly from the received data (blind monitoring) have been presented, such as: parameter extraction from FIR filter coefficients [2], time- [3] or frequency-domain [4] monitors placed before timing recovery stage and delay-tap sampling technique [5].

On the other hand, as to the authors' knowledge, no experimental trial of a monitoring module preceding timing recovery has been performed so far. In this paper we report on a successful experimental demonstration of CD estimation using the aforementioned method. We show that the receiver can adaptively adjust in order to mitigate signal degradation due to CD, even without prior knowledge of the fiber dispersion coefficient.

2. Blind chromatic dispersion monitoring for digital coherent receivers

We consider a polarization-division-multiplexing (PDM) quadrature phase-shift keying (QPSK) receiver consisting of the optical front-end and a DSP part, as shown in Fig. 1. The incoming optical signal is photodetected and sampled by analog-to-digital converters (ADCs) operating at twice the symbol rate. The CD monitor and equalizer block, which is of interest

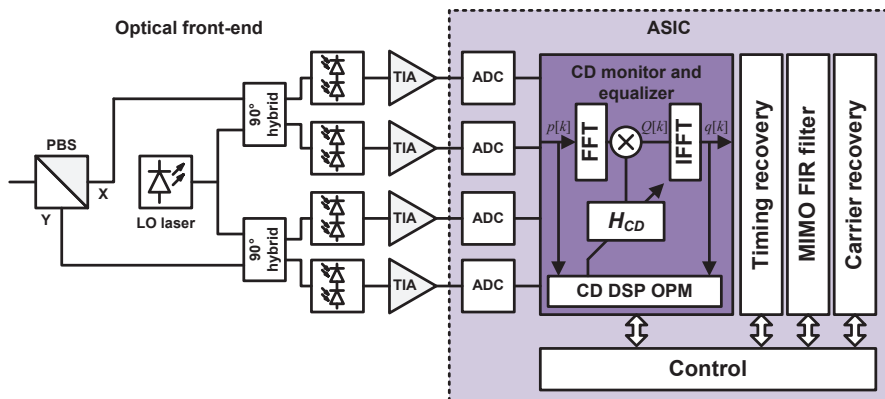


Fig. 1. Typical structure of a digital coherent receiver with CD monitoring and equalization block. The receiver in the figure monitors CD from time domain samples.

to this paper, is used for estimating and performing adaptive equalization of chromatic dispersion. Next, timing recovery takes place. A short, 7-tap finite impulse response (FIR) filter is then used for polarization demultiplexing and mitigation of residual impairments. Finally, carrier recovery is performed.

2.1. Generic scanning algorithm

The CD monitor and equalizer block in Fig. 1 uses a variable, transversal, frequency domain equalizer (FDE) for cancelation of inter-symbol interference (ISI) due to CD. The incoming signal $p[k]$ representing received complex optical field is first divided into blocks of length N , indexed consecutively with $k = 0 \dots N - 1$, and transformed to frequency domain. The resulting signal is then multiplied with the H_{CD} digital filter

$$H_{CD} = \exp \left(j f^2 \pi \frac{\lambda^2}{c} CD \right), \quad (1)$$

where f is the clock frequency, λ the signal wavelength, c the speed of light and CD the value of CD. The rationale behind using an FDE is the number of required complex multiplications as compared to time domain approach [6]. Next, the signal $Q[k]$ obtained after multiplication is transformed back to time domain as $q[k]$ and constitutes the output of the equalizer. Signals p and q (or Q , depending on particular method) are fed to a CD DSP OPM module which computes the metric J . Since the value of CD present in the channel is unknown, the transfer function H_{CD} may not be computed. However, due to the fact that H_{CD} has only one degree of freedom, adaptation can be performed by sweeping over a range of CD parameter, every time updating H_{CD} , until an optimal operating point is found. An interest range of CD values shall be specified, which in general will be different for each optical network and may depend on the topology and traffic characteristic. The CD parameter can be initialized as to coincide with the most probable CD value of the received signal in order to increase the convergence speed. The space of CD parameter is then gradually searched with a given resolution and the metric $J[CD]$ is computed for every value of CD under test.

As an engineering rule, CD scanning resolution for a simple maximum or minimum search-based metric shall not exceed 300 ps/nm with a recommended value of 200 ps/nm for a 28 Gbaud signal, which scales proportionally to the symbol rate squared. Once metric has been computed for all values lying within the range of interest, the metric is examined for a particular feature (e.g. minimum or maximum) which indicates the value of CD parameter that should be used to recalculate H_{CD} to mitigate the CD ISI.

The algorithm can be further extended to take average of the metric over multiple blocks or include multiple passes, each time narrowing the scanning range and increasing the scanning resolution. An example of a two-pass scan based on experimental data is shown in Fig. 2. Range between 0 ps/nm and 4000 ps/nm is swept with a step of 200 ps/nm (coarse scan). Once this initial estimate is obtained, a second pass with a resolution of only 20 ps/nm sets in and ranges 800 ps/nm centered around the previously found estimate (fine scan). This allows to increase the accuracy of the estimation. In theory, if no other impairment than CD is present in the signal, the maximum estimation error should be half of the scanning resolution. In practice, estimation error resulting from a single run is much greater because metrics are computed from blocks of finite length. Nonetheless, the accuracy of CD estimation at this stage is not strictly important because residual CD is compensated in the MIMO FIR filter that follows the CD equalizer in the receiver's DSP chain (comp. Fig. 1).

2.2. Dispersion metrics

This section provides a brief overview of algorithms for metrics computation. Four different metrics were implemented and experimentally verified in a transmission experiment. Figure 2 shows a comparison of those metrics generated from an experimental transmission of 20 Gbaud QPSK signal in a channel with 1280 ps/nm CD.

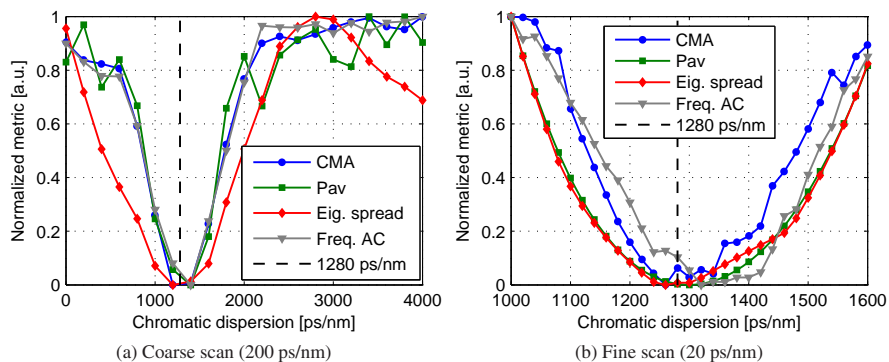


Fig. 2. Comparison of all metrics after normalization to $[0, 1]$ range. P_{av} metric was subtracted from 1 for clearness of comparison. Bold dashed vertical line shows the actual value of CD present in the channel (1280 ps/nm).

2.2.1. CMA metric

The first evaluated metric is described in [3, 7] and references provide its evaluation in computer simulations. The algorithm for this metric is based on a modified constant modulus algorithm (CMA) where a deviation from a constant power R_2 is the error function (metric). Since the received signal is sampled at twice the symbol rate, another normalization constant R_1 has to be used. Both R_1 and R_2 have to be constantly estimated from the power of odd and even samples of the received signal. The metric J is then computed

$$J[CD] = \frac{1}{N} \sum_{k=0}^{N-1} \left(\left| |q[2k+1]|^2 - R_1 \right| + \left| |q[2k]|^2 - R_2 \right| \right). \quad (2)$$

The required normalization constants R_1 and R_2 are determined for each block. First, the mean power of odd and even samples, \bar{q}_1 and \bar{q}_2 , is calculated

$$\bar{q}_1 = \frac{1}{N} \sum_{k=0}^{N-1} (q[2k+1])^2 \quad \bar{q}_2 = \frac{1}{N} \sum_{k=0}^{N-1} (q[2k])^2. \quad (3)$$

Based on the ratio of \bar{q}_2 to \bar{q}_1 , R_1 and R_2 normalization constants are determined as follows:

$$[R_1 \quad R_2] = \begin{cases} [R_a & R_c] & \text{if } \frac{\bar{q}_2}{\bar{q}_1} > \xi \\ [R_b & R_b] & \text{if } \xi^{-1} \leq \frac{\bar{q}_2}{\bar{q}_1} \leq \xi \\ [R_c & R_a] & \text{if } \frac{\bar{q}_2}{\bar{q}_1} < \xi^{-1} \end{cases} \quad (4)$$

with proposed empirically adjusted parameters $\xi = 1.25$, $R_a = 0.6$, $R_b = 1.5$ and $R_c = 2$ for the received complex signal power normalized to 1.

The curve of the metric presented in Fig. 2 was averaged over 8 different realizations, each having $N = 256$ samples.

2.2.2. Mean signal power

The second implemented metric is a simplified variant of the CMA-based metric. The mean power of samples at the input to the equalizer

$$P = \frac{1}{N} \sum_{k=0}^{N-1} |p[k]|^2 \quad (5)$$

is compared with the mean power of the signal after CD equalization and decimation to 1 sample/symbol stage. The post-decimation mean power, expressed in terms of signal q at the output of the CD equalizer is given by

$$\hat{P} = \frac{2}{N} \sum_{k=0}^{\frac{N}{2}-1} |q[2k]|^2. \quad (6)$$

Next, J metric is found according to

$$J[CD] = |P - \hat{P}|, \quad (7)$$

and the estimated value of CD parameter is indicated by the maximum of the metric.

In Fig. 2 the estimated CD value is found at a minimum as the metric was mirrored along the horizontal line at 0.5. Block size chosen for this metric was $N = 2048$.

2.2.3. Eigenvalue spread

An alternative metric, operating with time domain samples, relies on inspection of eigenvalue spread of the autocorrelation matrix. The concept, reviewed in [8], has not been used previously in relation to CD monitoring.

This metric uses samples from the CD equalizer after performing decimation to 1 sample/symbol.

The eigenvalue spread χ of the autocorrelation matrix \mathbf{R} is a quantitative measure of signal distortion. Specifically, \mathbf{R} is the following Toeplitz matrix of size $L \times L$

$$\mathbf{R} = \begin{bmatrix} r(0) & r^*(1) & \cdots & r^*(L-1) \\ r(1) & r(0) & \cdots & r^*(L-2) \\ \vdots & \vdots & \ddots & \vdots \\ r(L-1) & r(L-2) & \cdots & r(0) \end{bmatrix} \quad (8)$$

where r is the autocorrelation of the signal q calculated as

$$r(m) = \sum_{k=L}^{\frac{N}{2}-1} q[2k] q^*[2(k-m)] \quad (9)$$

and $*$ denotes complex conjugate. The eigenvalue spread of the autocorrelation matrix and the CD metric itself is then defined as

$$J[CD] = \chi(\mathbf{R}) = \frac{\lambda_{\max}}{\lambda_{\min}}, \quad (10)$$

where λ_{\max} and λ_{\min} are eigenvalues of \mathbf{R} with the largest and the smallest magnitudes respectively. If the dispersion was correctly compensated, the autocorrelation matrix is well-conditioned and the spread of eigenvalues approaches the theoretical minimum at 1. Otherwise, the matrix is ill-conditioned and the spread is significantly larger than that. This approach allows for construction of a minimum-search metric.

An engineering rule for the autocorrelation matrix size producing good results was found to be

$$L = \frac{CD_{\max} - CD_{\min}}{75}, \quad (11)$$

where in the numerator the maximum and minimum values of CD parameter (expressed in ps/nm) in the range of interest are used (units neglected). It should be noted that eigenvalues computation is an expensive task in terms of required processing power and, therefore, practical use of this metric might be limited.

In the curve shown in Fig. 2, block size was chosen to be $N = 16384$ and matrix size $L = 53$.

2.2.4. Frequency spectrum autocorrelation

The last metric, frequency spectrum autocorrelation, uses post-equalization samples before the inverse fast Fourier transform (IFFT) block. This method was studied in simulation in [4]. It uses signal Q , which is the frequency domain representation of the CD equalizer output after multiplication with the filtering function H_{CD} as presented in Fig. 1. First, a discrete circular autocorrelation is computed

$$U[m] = \frac{1}{N} \sum_{k=0}^{N-1} \text{csgn}(\bigcirc_m(Q[k])) \cdot Q^*[k], \quad (12)$$

where $\bigcirc_m(Q)$ is a circular shift operator that circularly shifts vector Q by m positions ($m \in N$) and csgn is a complex extension of the sign function sgn , defined as $\text{csgn}(x) = \text{sgn}[\Re(x)] + i \text{sgn}[\Im(x)]$, with \Re and \Im denoting, respectively, real and imaginary part of a complex number. It is not necessary for m to cover all possible shifts and thus m ranging from $-\lfloor 0.7 \frac{N}{2} \rfloor$ up to $\lfloor 0.7 \frac{N}{2} \rfloor$ has been used.

The metric function $J[CD]$ for a single CD value under test is then calculated as

$$J[CD] = \sum_m |U[m]|^2, \quad (13)$$

where summation over m covers all applied circular shifts.

The metric curve shown in Fig. 2 was obtained after averaging 20 realizations, each calculated from a block Q of size $N = 256$ samples as to smoothen the obtained curve.

3. Experimental setup

In order to experimentally prove that CD monitoring with the investigated approach is feasible, we use a single branch of a PDM-QPSK transmitter, as outlined in Fig. 3. A pattern generator provides the in-phase and quadrature inputs to the optical modulator at a bit rate of 20 Gbit/s resulting in a 40 Gbit/s QPSK optical signal. In order to test the monitoring algorithms for different magnitudes of CD affecting the signal, two cases are investigated: the back-to-back case (CD negligibly small) and transmission over 80 km of standard single-mode fiber (SSMF) with a dispersion coefficient of approximately 16 ps/nm/km, yielding 1280 ps/nm accumulated CD in total. Back-to-back trial was performed to test if the monitoring algorithm works correctly in a CD-free channel. As the next step, optical noise is added to the signal, varying the optical signal-to-noise ratio (OSNR) from 24 dB, down to 12 dB. An EDFA preamplifier and an attenuator just before the receiver is used to keep the power entering a 100G coherent receiver at a constant level equal to -10 dBm. The local oscillator (LO) is tuned to 1548.88 nm and the signal wavelength is less than 100 MHz apart. The signal and LO lasers are distributed feedback (DFB) narrow linewidth lasers (NLLs). Digital storage oscilloscope (DSO) is used to capture the voltage signal after conversion from optical to electrical domain. Traces are stored and processed offline.

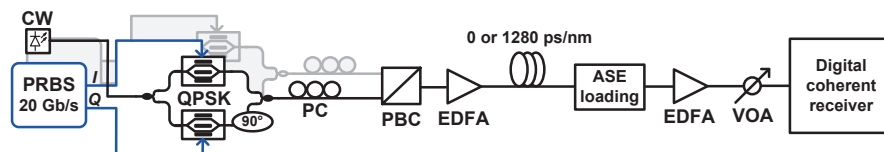


Fig. 3. Experimental setup of the transmission system. CW: continuous wave laser, PRBS: pseudorandom binary sequence generator, PC: polarization controller, PBC: polarization beam combiner, EDFA: erbium-doped fiber amplifier, ASE loading: amplified spontaneous emission noise loading, VOA: variable optical attenuator.

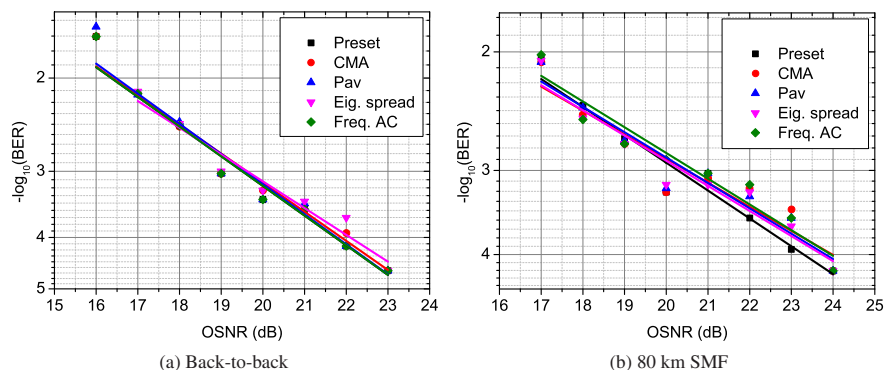


Fig. 4. BER vs. OSNR curves for each metric under investigation. *Preset*: reference line based on a priori known CD filter, *CMA*: constant modulus algorithm, *Pav*: mean signal power, *Eig. spread*: eigenvalue spread, *Freq. AC*: frequency spectrum autocorrelation.

4. Experimental results

Figure 4 shows bit error rate (BER) curves after demodulation of the traces using an equalizer driven by the monitoring module, where *Preset* is a reference line showing performance of the receiver when CD filter is manually set with an a priori known CD value of either 0 ps/nm (Fig. 4a) or 1280 ps/nm (Fig. 4b). Remaining lines show the performance of the receiver for different CD metrics as OSNR is varied for both transmission distances. It may be observed that regardless of the CD distortion present in the channel, lines depart only to a very small extent from the reference *Preset* line. This shows that both: each metric and the CD DSP monitor itself are reliable enough as not to introduce any penalty when compared to a CD filter with a fixed CD value. The FIR filter used for polarization demultiplexing is too short to compensate CD after 80 km of fiber transmission; effectively only residual CD is mitigated via the FIR filter, while bulk of the dispersion is removed by the FDE CD equalizer driven by the monitoring module. It is necessary to point out that this proof-of-concept works satisfactory with single polarization QPSK signal and it should be scalable to PDM-QPSK as CD affects both polarizations equally.

5. Conclusions

We experimentally demonstrated the use of DSP OPM algorithms for CD compensation and estimation module preceding timing recovery stage. This allows for an autonomous opera-

tion of a digital coherent receiver in a dispersion non-compensated coherent transport network. To the best of our knowledge this is the first demonstration showing feasibility of the presented receiver arrangement and algorithms in experimental setting. We found out that the four different metrics for assessing dispersion mitigation provide reliable estimations of CD so as no penalty is observed when compared to a CD filter whose value was fixed prior to the transmission.

Acknowledgments

We thank Teraxion for providing PureSpectrumTM-NLLs for this experiment. The research leading to these results is partially supported by the CHRON project (Cognitive Heterogeneous Reconfigurable Optical Network) with funding from the European Community's Seventh Framework Programme [FP7/2007-2013] under grant agreement no. 258644.

Paper [L]: Experimental demonstration of the maximum likelihood-based chromatic dispersion estimator for coherent receivers

Robert Borkowski, Pontus Johannisson, Henk Wymeersch, Valeria Arlunno, Antonio Caballero, Darko Zibar, and Idelfonso Tafur Monroy. Experimental demonstration of the maximum likelihood-based chromatic dispersion estimator for coherent receivers. *Optical Fiber Technology*, vol. 20, no. 2, pp. 158–162, February 2014.



Contents lists available at ScienceDirect

Optical Fiber Technology

www.elsevier.com/locate/yofte



Experimental demonstration of the maximum likelihood-based chromatic dispersion estimator for coherent receivers



Robert Borkowski^{a,*}, Pontus Johannisson^b, Henk Wymeersch^c, Valeria Arlunno^a, Antonio Caballero^a, Darko Zibar^a, Idelfonso Tafur Monroy^a

^aDTU Fotonik – Department of Photonics Engineering, Technical University of Denmark, DK-2800 Kgs. Lyngby, Denmark

^bPhotonics Laboratory, Chalmers University of Technology, SE-412 96 Gothenburg, Sweden

^cCommunication Systems Group, Chalmers University of Technology, SE-412 96 Gothenburg, Sweden

ARTICLE INFO

Article history:

Received 14 November 2013

Revised 16 January 2014

Available online 13 February 2014

Keywords:

Chromatic dispersion
Optical performance monitoring
Maximum likelihood
Digital signal processing
16 QAM
QPSK

ABSTRACT

We perform an experimental investigation of a maximum likelihood-based (ML-based) algorithm for bulk chromatic dispersion estimation for digital coherent receivers operating in uncompensated optical networks. We demonstrate the robustness of the method at low optical signal-to-noise ratio (OSNR) and against differential group delay (DGD) in an experiment involving 112 Gbit/s polarization-division multiplexed (PDM) 16-ary quadrature amplitude modulation (16 QAM) and quaternary phase-shift keying (QPSK).

© 2014 The Authors. Published by Elsevier Inc. This is an open access article under the CC BY license (<http://creativecommons.org/licenses/by/3.0/>).

1. Introduction

Linear impairments, in particular chromatic dispersion (CD) and polarization-mode dispersion (PMD) resulting from fiber transmission are now routinely mitigated by digital signal processing (DSP) in coherent receivers. This advancement allows for fiber-optic networks that no longer require dispersion compensating modules (DCMs) and two-stage amplification to perform reliable transmission. The major benefits of uncompensated links include: decrease in the noise figure (due to decrease in linear and nonlinear optical noise), reduction in link loss and latency, lower deployment capital expenditures.

As optical networks adopt flexibility and dynamic lightpath switching [1], the CD accumulated in the signal may change between two different connection requests, even if a source and destination are the same. Therefore a conventional approach, where a coherent receiver uses a static CD filter, does no longer apply. This makes an accurate adaptive CD estimation for dispersion unmanaged coherent photonic backbones indispensable.

Various approaches to non-data aided CD estimation in digital coherent receivers have been presented. One of the methods is based on parameter extraction from equalizer taps [2]. Due to a

limited number of filter taps in the receiver, this solution might only be used to monitor relatively small CD, roughly corresponding to a stretch of one fiber span in long haul network. To support longer links, other methods, based on CD scanning are used. In those techniques, the space of possible CD values is searched in small steps (20–200 ps/nm [3]) and a metric value is computed for each step. A characteristic feature of this metric, often global minimum or maximum, is used to indicate successful mitigation of CD. Diverse variants of this procedure, each using a different metric, have been shown so far. A method derived from constant modulus algorithm (CMA), where the metric is based on a departure from a fixed power threshold, is used in Refs. [3,4], delay-tap sampling estimator [5,6], autocorrelation of signal power waveform [7,8], clock tone search [9–11], Gardner time error detector variance [12]. Recently, another technique have been demonstrated, where the sweep over CD values is performed automatically when applying FFT on the autocorrelation of discrete spectrum [13].

In this paper we present an experimental investigation of a method for CD estimation based on the maximum likelihood (ML) criterion [14]. The approach is experimentally verified in a transmission experiment using 112 Gbit/s polarization division multiplexed (PDM) 16-ary quadrature amplitude modulation (16 QAM) and quaternary phase-shift keying (QPSK) optical signals and its performance is compared, and found better, to an alternative (reference) method derived from constant modulus algorithm

* Corresponding author. Fax: +45 4593 6581.

E-mail address: rbor@fotonik.dtu.dk (R. Borkowski).

criterion from [4]. (Please notice that this is not the CMA commonly used for polarization demultiplexing.)

2. CD estimator

In this section we shortly present the maximum likelihood CD estimator. The full derivation can be found in [14].

We consider a coherent optical communication system using polarization multiplexing. The data, phase, and polarization state of the received signal are unknown, as is the differential group delay (DGD) along an unknown axis. The received signal can be expressed in the frequency domain as

$$\mathbf{R}(f) = H(f)e^{j2\pi\eta f\tau}\mathbf{T}(f)\mathbf{S}(f) + \mathbf{N}(f) = \mathbf{X}(f) + \mathbf{N}(f),$$

where $H(f)$ is the transfer function of the CD, τ is an unknown propagation delay, the Jones matrix $\mathbf{T}(f)$ describes the polarization scrambling and DGD, $\mathbf{S}(f)$ is the Fourier transform of the transmitted signal, and $\mathbf{N}(f)$ is complex additive white Gaussian noise (AWGN) with power spectral density $N_0/2$ per each of the four real dimensions. The CD all-pass filter is described by

$$H(f) = \exp\left(-j\frac{\pi f^2 \lambda^2}{c} \int_0^L D(z) dz\right) = e^{j\pi\eta f^2},$$

where λ is the carrier wavelength, c is the speed of light, $D(z)$ is the dispersion parameter, L is the total system length, and η is the CD parameter to be estimated. The likelihood for the received signal is

$$p(\mathbf{r}|\eta, \tau, \mathbf{T}, \mathbf{a}) \propto \exp\left[-\frac{1}{N_0} \int \|\mathbf{R}(f) - \mathbf{X}(f)\|^2 df\right],$$

where we used Parseval's theorem to write the likelihood in the Fourier domain and denoted a vector representation of received signal in time domain, $\mathbf{r}(t)$, by \mathbf{r} . This expression depends on the data, represented by the sequence of transmitted symbols \mathbf{a} . To remove the dependency on \mathbf{a} , we use the second order Taylor expansion of $p(\mathbf{r}|\eta, \tau, \mathbf{T}, \mathbf{a})$ and take the expectation with respect to \mathbf{a} . We thus find an approximate expression for $p(\mathbf{r}|\eta, \tau, \mathbf{T})$. Further approximations allow us to remove the dependence on τ . However, the objective function still depends on \mathbf{T} . We solve this by optimizing over a small number of polarization states and DGD values. We formulate the final result in terms of the received signal after matched filtering. Thus, we introduce $\mathbf{Y}(f) = P^*(f)\mathbf{R}(f)$, where $P^*(f)$ is the transfer function of the filter matched to the transmitted pulse shape. For any M -ary quadrature amplitude modulation or M -ary phase-shift keying modulation format for $M > 2$, the final estimator turns out to be

$$\hat{\eta} = \arg \max_{\eta} \max_{\mathbf{M} \in \mathcal{S}} \left| \int_{-\infty}^{\infty} \mathbf{Y}^H(f) \mathbf{M} \mathbf{Y}(f + 1/T) e^{-j2\pi\eta f} df \right|, \quad (1)$$

where the set of matrices to test is

$$\mathcal{S} = \left\{ \begin{pmatrix} 1 & 0 \\ 0 & \pm 1 \end{pmatrix}, \begin{pmatrix} 0 & 1 \\ \pm 1 & 0 \end{pmatrix} \right\}.$$

3. Experimental setup

Fig. 1 shows the experimental setup, which can generate optical 16 QAM signal at 14 Gbaud or QPSK at 28 Gbaud. A pulse pattern generator (PPG) generates four copies of decorrelated electrical signals carrying binary pseudorandom bit sequences of length $2^{15} - 1$ (PRBS-15) which are then amplified. For 16 QAM, the PPG operates at 14 GHz and the resulting four signals are grouped in pairs, one signal from each pair is attenuated by 6 dB, and each

pairs is combined in a resistive combiner. This results in two four-level signals: in-phase (I) and quadrature (Q) components for the double-nested Mach-Zehnder modulator. In the optical domain, a 16 QAM signal at 56 Gbit/s is obtained. For QPSK, two amplified PPG outputs operate at 28 Gbit/s, generating two-level I and Q signals, which results in an optical QPSK signal at 56 Gbit/s. The light source used in the transmitter is an external cavity laser (ECL) with a linewidth of 100 kHz. Polarization division multiplexing is emulated by multiplexing the signal with its delayed copy in the orthogonal polarization, creating, respectively PDM-16 QAM and PDM-QPSK optical signals at 112 Gbit/s. An erbium-doped fiber amplifier is used at the transmitter to compensate for the insertion losses.

The signal is launched into a link without dispersion compensating fiber using a commercial wavelength division multiplexing (WDM) equipment with all other WDM channels turned off. An amplified spontaneous emission (ASE) noise loading stage is used only for back-to-back performance measurements. The transmission experiment is performed over links of 240, 400, 640, and 800 km lengths by using 3, 5, 8, and 10 spans, respectively of 80 km-long standard single-mode fiber, with nominal dispersion of 16.25 ps/(nm km) at the operating wavelength. Unless stated otherwise, the input power to the first span is 0 dBm and the optical signal-to-noise ratio (OSNR) is measured at the receiver in 0.1 nm bandwidth. A variable optical attenuator before the receiver is used to keep the power ratio between the signal and the local oscillator (LO) constant. For QPSK back-to-back measurements a DGD emulator is used to introduce delays of 20, 40, 60, and 80 ps.

3.1. Digital coherent receiver

The signal is received with a phase- and polarization-diversity digital coherent receiver whose structure is outlined in Fig. 2. The receiver consists of an opto-electronic front-end and a digital signal processing (DSP) stage.

3.1.1. Opto-electronic front-end

The front-end includes two polarization beam splitters (PBS) splitting the received signal and the local oscillator into two orthogonal polarizations (H – horizontal, V – vertical), two 90° hybrids for each polarization, a set of transimpedance amplifiers (TIAs) and analog-to-digital converters (ADCs). The ADCs are provided inside a real-time digital storage oscilloscope (DSO) with a 50 GS/s with 16 GHz bandwidth. The data is sampled by the DSO and the acquired traces are processed offline.

3.1.2. Digital signal processing

The offline processing stage begins with signal resampling to two samples per symbol by spline interpolation. The downsampled signal is then fed into the CD monitor and CD equalizer block, where the signal is first divided into blocks of fixed length and transformed to frequency domain. Dispersion mitigation is then performed blockwise by a transversal frequency domain equalizer due to low, logarithmically increasing, computational complexity for increasing dispersion magnitude, as compared to time domain equalization [4]. The variable transfer function generator, $H^{-1}(CD)$, is responsible for generating an inverse of the transfer function of fiber dispersion, according to the CD value supplied by the CD monitor. The CD value is swept with a resolution of 3 ps/nm until an optimum value indicated by the metric algorithm (estimator) is found. Depending on the specific test case, either an ML-based algorithm or the reference method is implemented inside CD monitor block in Fig. 2. To avoid aliasing when evaluating Eq. (1), ML CD estimator shall operate with four samples per symbol. Therefore the downsampled signal is again upsampled to four samples per symbol before entering ML CD monitor. Upsampling is necessary

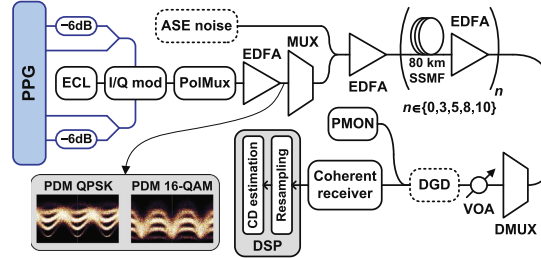


Fig. 1. The experimental setup. PPG: pulse pattern generator, ECL: external cavity laser, PolMux: polarization multiplexing stage, EDFA: erbium-doped fiber amplifier, (D) MUX: (de) multiplexer, SSMF: standard single-mode fiber, VOA: variable optical attenuator, DGD: differential group delay emulator, PMON: power monitor, DSP: digital signal processing stage.

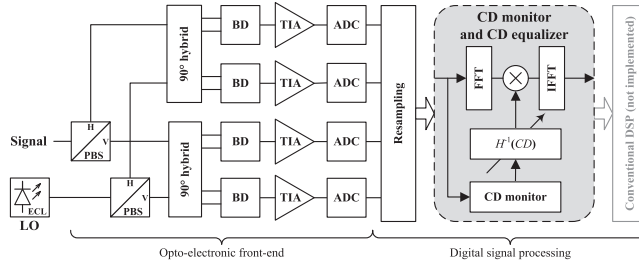


Fig. 2. Typical structure of a digital coherent receiver with CD monitoring and equalization block. The receiver in the figure monitors CD from time domain samples. LO: local oscillator, ECL: external cavity laser, PBS: polarization beam splitter, BD: balanced detector, TIA: transimpedance amplifier, ADC: analog-to-digital converter, (I) FFT: (inverse) fast Fourier transform.

to take into account the fact that the bandwidth of the transformed signal $\mathbf{Y}^H(f)\mathbf{Y}(f+1/T)$ increases and 2 samples/symbol is not sufficient to satisfy the sampling theorem.

After the frequency domain processing, the signal is subsequently transformed to time domain. In the next step, conventional DSP algorithms for a coherent receiver (*Conventional DSP* in Fig. 2) are used. Their structure typically follow the one presented in [15]. This includes a butterfly finite impulse response filter structure which combats the residual dispersion. It is important to emphasize that the CD monitoring algorithm considered in this work do not replace any of the conventional DSP blocks of a digital coherent receiver. This is a separate and complementary block used prior to the typical coherent receiver DSP, and is aimed at mitigation of the bulk dispersion. Without this block, the subsequent DSP algorithms will fail to operate correctly as a large CD values cannot be compensated for within the blind adaptive equalizer due to convergence issues. Since we only focus on the quality of CD estimates provided by the bulk CD monitors, there was no need to include any further DSP algorithms beyond the CD equalizer and CD monitor.

4. Results and discussion

The CD estimates provided by the ML-based estimator are compared against estimates obtained with the reference method

implemented with default parameters ($\xi = 1.25$, $R_a = 0.6$, $R_b = 1.5$, $R_c = 2$) [4]. The latter algorithm was chosen to provide a fair comparison base as: (i) the DSP structure in which the algorithm is implemented is very similar (the only difference is the algorithm inside *CD monitor* block in Fig. 2); (ii) previous results for that estimator report successful dispersion mitigation for both QPSK and 16 QAM modulation formats [10], which are also used in our experiment; (iii) it is well established, with an unambiguous description in the literature. The performance is measured using the standard deviation of the CD estimate, σ (in ps/nm), calculated from 1000 evaluations of sub-blocks of size N samples (Sa) within the same trace. The comparison was done with a CD scan resolution of 3 ps/nm.

Different plots of Fig. 3 show σ as a function of:

- Block size in Sa: (a) for back-to-back case (OSNR: 16 QAM 27.4 dB, QPSK 18.4 dB); (d) 240 km transmission (OSNR: 16 QAM 26.7 dB, QPSK 28.9 dB). In all presented cases, the standard deviation of the estimate decreases for increasing block lengths. This is explained by the fact that longer blocks allow to infer signal statistics with higher accuracy, consequently allowing for more precise dispersion estimation. The performance of ML for QPSK is shown to slightly outperform the reference. ML estimator is more accurate for 16 QAM than for QPSK, while the opposite is true for the reference method. This sets 16 QAM curves far apart, with

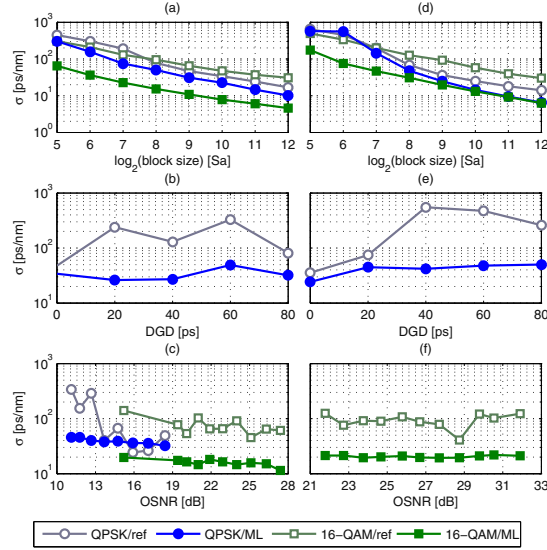


Fig. 3. Plots for back-to-back (a–c) and 240 km transmission (d–f). Plots show estimation standard deviation as a function of: (a,d) block size in samples; (b,e) DGD in ps; (c,f) OSNR in dB.

Table 1

Estimation results for all transmission distances. CD_0 – nominal CD value, m – estimated mean, Δ – mean estimation error (deviation of m from the nominal value), σ – standard deviation of the estimate.

L (km)	CD_0 (ps/nm)	OSNR (dB)	ML (ps/nm)			Reference (ps/nm)		
			m	Δ	σ	m	Δ	σ
QPSK								
0	0	18.4	−14	−14	33	−19	−19	46
240	3900	28.9	3886	−14	24	3879	−21	35
400	6500	27.0	6486	−14	36	6481	−19	287
640	10400	25.0	10397	−3	42	10396	−4	257
800	13000	22.3	13003	3	48	12994	−6	92
16 QAM								
0	0	27.4	−27	−27	11	−46	8	60
240	3900	26.7	3871	−29	20	3865	−35	90
400	6500	25.1	6471	−29	21	6470	−30	87
640	10400	23.0	10385	−15	24	10373	−27	65
800	13000	20.0	12987	−13	21	12989	−11	138

ML being significantly more accurate. The suboptimal performance of the reference estimator for 16 QAM may stem from the fact that this algorithm is derived from the constant modulus algorithm.

- DGD in ps for QPSK (constant block size of 512 Sa); (b) back-to-back (OSNR 18.4 dB); (e) 240 km transmission (OSNR 28.9 dB). Using ML estimation, standard deviation of the CD estimate is similar for all DGD values. This behaviour is expected and has been observed also in simulations [14]. The reference method, on the other hand, is sensitive to DGD and exhibits high σ for non-zero DGD.

- OSNR in dB (constant block size of 512 Sa); (c) back-to-back (by varying the amount of ASE noise); (f) 240 km transmission for 16 QAM only (the OSNR was adjusted by varying the input power to the first span from –5 dBm to 5 dBm in steps of 1 dBm).

The performance of the reference estimator deteriorates rapidly below 15 dB OSNR while ML remains almost unaffected. The improved performance of ML at low OSNR values agrees with simulation results [14]. The poor performance of the reference method in that regime is mainly caused by the outliers in CD estimates. The standard deviation of the CD estimates for

16 QAM using reference method is roughly one order of magnitude higher than for ML estimates and was also observed in subfigures (a,d). On the other hand, the ML estimator has virtually the same performance with low spread of estimates across wide range of OSNR values.

Table 1 shows CD estimation results for diverse transmission distances. It can be seen that for ML estimator the mean estimation error, Δ , which is the difference between the estimated mean and the nominal value, $\Delta = m - CD_0$, is lower in case of QPSK than for 16 QAM. On the other hand, the standard deviation of the estimate, σ is higher for QPSK. The estimates of the reference method are in general characterized by larger standard deviation than those provided by ML. In nearly all cases we notice a small underestimation, not exceeding 35 ps/nm, which might be due to the fact that the actual transmission link dispersion was lower than the assumed nominal value.

5. Conclusion

We have successfully experimentally verified the ML-based CD estimator for coherent transport networks by investigating 112 Gbit/s PDM-16 QAM and PDM-QPSK signals in the presence of variable amount of CD, ASE noise and DGD. The studied estimator was compared to an alternative method derived from the CMA criterion. The ML dispersion estimator was proven to correctly operate at OSNR below 15 dB and provided precise and repeatable CD estimates even with significant DGD. A substantial decrease of CD estimates' spread, especially for PDM-16 QAM, was observed with the ML dispersion estimator, as compared to the reference method.

Acknowledgments

We thank Neil Guerrero Gonzalez and Bangning Mao from European Research Center, Huawei Technologies Duesseldorf GmbH in Munich, Germany for their help in acquiring experimental data. We also thank Fabian Hauske for constructive comments. This work was partly supported by the EU FP7 project CHRON under Grant Agreement No. 258644.

References

- [1] I. Tafur Monroy, D. Zibar, N. Guerrero Gonzalez, R. Borkowski, Cognitive heterogeneous reconfigurable optical networks (CHRON): enabling technologies and techniques, in: 2011 13th International Conference on Transparent Optical Networks, IEEE, 2011, p. ThA1.2. doi:10.1109/ICTON.2011.5970833 <http://ieeexplore.ieee.org/lpdocs/epic03/wrapper.htm?arnumber=5970833>.
- [2] F.N. Hauske, J.C. Geyer, M. Kuschnerov, K. Piyawanno, T. Duthel, C.R. Fludger, D. van den Borne, E.-D. Schmidt, B. Spinnler, H. de Waardt, B. Lankl, Optical performance monitoring from FIR filter coefficients in coherent receivers – OSA technical digest (CD), in: Optical Fiber Communication Conference/National Fiber Optic Engineers Conference, Optical Society of America, 2008, p. OThW2. <http://www.opticsinfobase.org/abstract.cfm?URI=OFC-2008-OTHW2>.
- [3] R. Borkowski, X. Zhang, D. Zibar, R. Younce, I. Tafur Monroy, Experimental demonstration of adaptive digital monitoring and compensation of chromatic dispersion for coherent DP-QPSK receiver, Opt. Exp. 19 (26) (2011) B728–B735, <http://dx.doi.org/10.1364/OE.19.008728>. <http://www.opticsexpress.org/abstract.cfm?URI=oe-19-26-B728> and <http://www.ncbi.nlm.nih.gov/pubmed/22274093>.
- [4] M. Kuschnerov, F.N. Hauske, K. Piyawanno, B. Spinnler, M.S. Alfiad, A. Napoli, B. Lankl, DSP for coherent single-carrier receivers, J. Lightw. Technol. 27 (16) (2009) 3614–3622. <http://jlt.osa.org/abstract.cfm?URI=jlt-27-16-3614>.
- [5] D. Wang, C. Lu, A.P.T. Lau, S. He, Adaptive chromatic dispersion compensation for coherent communication systems using delay-tap sampling technique, IEEE Photon. Technol. Lett. 23 (14) (2011) 1016–1018, <http://dx.doi.org/10.1109/LPT.2011.2151280>. <http://ieeexplore.ieee.org/lpdocs/epic03/wrapper.htm?arnumber=5764498>.
- [6] V. Ribeiro, S. Ranzini, J. Oliveira, V. Nascimento, E. Magalhães, E. Rosa, Accurate blind chromatic dispersion estimation in long-haul 112 Gbit/s PM-QPSK WDM coherent systems, in: Advanced Photonics Congress, OSA, Washington, DC, 2012, p. SpTh2B.3. doi:10.1364/SPPCOM.2012.SpTh2B.3 <http://www.opticsinfobase.org/abstract.cfm?URI=SPPCOM-2012-SpTh2B.3>.
- [7] Q. Sui, A.P.T. Lau, C. Lu, Fast and robust blind chromatic dispersion estimation using auto-correlation of signal power waveform for digital coherent systems, J. Lightw. Technol. 31 (2) (2013) 306–312. <http://jlt.osa.org/abstract.cfm?URI=jlt-31-2-306>.
- [8] F.C. Pereira, V.N. Rozenal, M. Camera, G. Bruno, D.A.A. Mello, Experimental analysis of the power auto-correlation-based chromatic dispersion estimation method, IEEE Photon. J. 5 (4) (2013) 7901608, <http://dx.doi.org/10.1109/JPHOT.2013.2272782>. <http://ieeexplore.ieee.org/lpdocs/epic03/wrapper.htm?arnumber=6557429>.
- [9] F.N. Hauske, Z. Zhang, C. Li, C. Xie, Q. Xiong, Precise, Robust and least complexity CD estimation, in: Optical Fiber Communication Conference/National Fiber Optic Engineers Conference 2011, OSA, Washington, DC, 2011, p. JW4032. doi:10.1364/NFOEC.2011.JW4032 <http://www.opticsinfobase.org/abstract.cfm?URI=NFOEC-2011-JW4032>.
- [10] R.A. Soriano, F.N. Hauske, N. Guerrero Gonzalez, Z. Zhang, Y. Ye, I. Tafur Monroy, Chromatic dispersion estimation in digital coherent receivers, J. Lightw. Technol. 29 (11) (2011) 1627–1637. <http://jlt.osa.org/abstract.cfm?URI=jlt-29-11-1627>.
- [11] C. Malouin, P. Thomas, B. Zhang, J. O'Neil, T. Schmidt, Natural expression of the best-match search godard clock-tone algorithm for blind chromatic dispersion estimation in digital coherent receivers, in: Advanced Photonics Congress, OSA, Washington, DC, 2012, p. SpTh2B.4. doi:10.1364/SPPCOM.2012.SpTh2B.4. <http://www.opticsinfobase.org/abstract.cfm?URI=SPPCOM-2012-SpTh2B.4>.
- [12] J.C. Diniz, S. Ranzini, V. Ribeiro, E. Magalhães, E. Rosa, V. Parahyba, L.V. Franz, E.E. Ferreira, J. Oliveira, Hardware-efficient chromatic dispersion estimator based on parallel gardner timing error detector, in: Optical Fiber Communication Conference/National Fiber Optic Engineers Conference 2013, OSA, Washington, DC, 2013, p. OTh3C.6. doi:10.1364/OFC.2013.OTh3C.6. <http://www.opticsinfobase.org/abstract.cfm?URI=OFC-2013-OTh3C.6>.
- [13] C. Malouin, M. Arabaci, P. Thomas, B. Zhang, T. Schmidt, R. Marrocchia, Efficient, Non-data-aided chromatic dispersion estimation via generalized, FFT-based sweep, in: Optical Fiber Communication Conference/National Fiber Optic Engineers Conference 2013, OSA, Washington, DC, 2013, p. JW2A.45. doi:10.1364/NFOEC.2013.JW2A.45. <http://www.opticsinfobase.org/abstract.cfm?URI=OFC-2013-JW2A.45>.
- [14] H. Wymeersch, P. Johannisson, Maximum-likelihood-based blind dispersion estimation for coherent optical communication, J. Lightw. Technol. 30 (18) (2012) 2976–2982. <http://jlt.osa.org/abstract.cfm?URI=jlt-30-18-2976>.
- [15] S.J. Savory, Digital coherent optical receivers: algorithms and subsystems, IEEE J. Sel. Topics Quant. Electron. 16 (5) (2010) 1164–1179, <http://dx.doi.org/10.1109/JSTQE.2010.2044751>. <http://ieeexplore.ieee.org/lpdocs/epic03/wrapper.htm?arnumber=5464309>.

Paper [M]: Stokes space-based optical modulation format recognition for digital coherent receivers

Robert Borkowski, Darko Zibar, Antonio Caballero, Valeria Arlunno, and Idelfonso Tafur Monroy. Stokes space-based optical modulation format recognition for digital coherent receivers. *IEEE Photonics Technology Letters*, vol. 25, no. 21, pp. 2129–2132, November 2013.

Stokes Space-Based Optical Modulation Format Recognition for Digital Coherent Receivers

Robert Borkowski, Darko Zibar, Antonio Caballero, Valeria Arlunno, and Idelfonso Tafur Monroy

Abstract—We present a technique for modulation format recognition for heterogeneous reconfigurable optical networks. The method is based on Stokes space signal representation and uses a variational Bayesian expectation maximization machine learning algorithm. Differentiation between diverse common coherent modulation formats is successfully demonstrated numerically and experimentally. The proposed method does not require training or a constellation diagram to operate, is insensitive to polarization mixing or frequency offset and can be implemented in any receiver capable of measuring Stokes parameters.

Index Terms—Coherent detection, polarization multiplexing, modulation format recognition (MFR), modulation format detection (MFD), modulation format identification (MFI), Stokes space, Poincaré sphere, variational Bayesian expectation maximization (VBEM), Gaussian mixture models (GMM).

I. INTRODUCTION

WITH the advent of reconfigurable transmitters capable of signal generation using arbitrary coherent optical modulation format [1], it is no longer possible to ensure that the receiver unit will know the incoming modulation format in advance. This paradigm change calls for a new receiver functionality. Modulation format recognition (MFR) [2] is essential to guarantee that signals, which are using diverse complex modulation formats, are optimally acquired and demodulated. This can be realized with software-defined receiver (SDR) provided that the modulation format is recognized before the crucial steps of signal processing. Modulation format must be known in order to enable operation of receiver algorithms that are modulation format opaque. An example of such a subsystem is decision directed equalization, where the knowledge of modulation format allows for superior error performance compared to blind equalization algorithm [3].

Latest reports in the field of digital signal processing (DSP) for coherent optical communication indicate that the next generation of receivers will implement Stokes space-based algorithms due their lower complexity or faster convergence. An advantage of Stokes space is that polarization mixing, carrier frequency offset and phase offset do not affect the 3-dimensional (3D) representation of the signal in the Poincaré sphere. Recently conceived Stokes space-based DSP include:

Manuscript received July 22, 2013; revised August 26, 2013; accepted September 9, 2013. Date of publication September 17, 2013; date of current version October 9, 2013. This work was supported by the Cognitive Heterogeneous Reconfigurable Optical Network project with funding from the EU FP7 Programme (FP7/2007-2013) under Grant 258644.

The authors are with DTU Fotonik, Department of Photonics Engineering, Technical University of Denmark, Kgs. Lyngby 2800, Denmark (e-mail: rbor@fotonik.dtu.dk; dazi@fotonik.dtu.dk; acaj@fotonik.dtu.dk; vaar@fotonik.dtu.dk; idm@fotonik.dtu.dk).

Color versions of one or more of the figures in this letter are available online at <http://ieeexplore.ieee.org>.

Digital Object Identifier 10.1109/LPT.2013.2282303

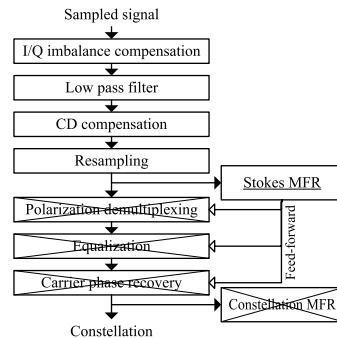


Fig. 1. DSP flow of a digital coherent receiver with the placement of Stokes MFR block. Crossed out blocks are not necessary to perform Stokes MFR. The location of constellation-based MFR [10] is shown for comparison.

polarization demultiplexing [4], [5], cross-polarization modulation compensation [6], PDL compensation [7] or OSNR monitoring [8].

Techniques for MFR have been well explored for wireless communications [9], and became widely used, e.g. in cognitive radio. In optical communication, this area has not been extensively investigated until very recently, mainly due to the static nature of fiber-optic networks. However, recently proposed cognitive optical networks architectures, such as CHRON [2], introduce reconfigurable and very dynamic networks where the receivers act autonomously and provide high degree of interoperability.

Literature lists four different methods that have been employed for optical MFR: i) monitoring from a constellation diagram with the use of k -means, which requires modulation transparent algorithms and entire receiver-side processing before MFR [10]; ii) artificial neural networks that need prior training [11]; iii) method based on signal cumulants [12]; iv) Stokes space and machine learning technique [13].

In this letter we expand upon our idea presented in [13]. By utilizing the DSP capabilities of a digital coherent receiver, we use Stokes space representation of the signal and employ a machine learning algorithm known as variational Bayesian expectation maximization (VBEM) [14] for Gaussian mixture models (GMM). The proposed method constitutes a major enhancement over the constellation analysis-based techniques, such as [10], as it allows for MFR at a considerably earlier stage in the receiver (cf. Fig. 1). The method does not require training, in contrast to neural network-based solution.

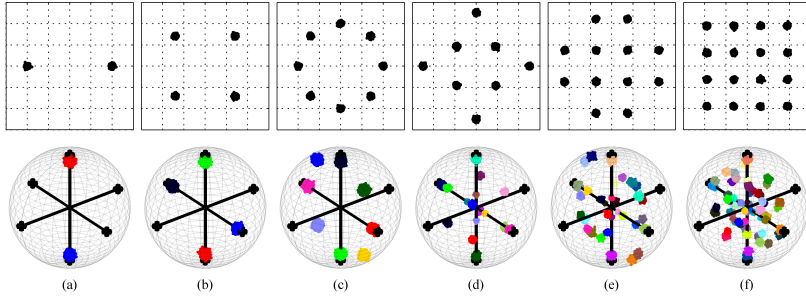


Fig. 2. Constellations (top row; only one polarization shown) and their corresponding Stokes space representation in the Poincaré (bottom row) for simulated data. (a) PDM BPSK, (b) PDM QPSK, (c) PDM 8-PSK, (d) PDM 8-QAM, (e) PDM 12-QAM, (f) PDM 16-QAM. Each color represents a separate cluster.

The information about recognized modulation format can be subsequently fed forward to the following DSP blocks to improve their performance. We report on successful optical modulation classification by discriminating from a possible set of BPSK, QPSK, 8-PSK, 8-QAM, 12-QAM and 16-QAM modulations.

II. PRINCIPLES

A. Stokes Space Transformation and Representation

Stokes parameters are calculated from samples of the received signal as $S_0 = |x|^2 + |y|^2$, $S_1 = |x|^2 - |y|^2$, $S_2 = 2\Re(xy)$, $S_3 = 2\Im(xy)$. Three-vector (S_1, S_2, S_3) after normalization by $\max(S_0)$ determines location of received data points inside a 3D lens [4] in the Poincaré sphere. The transformation equations essentially operate on relative interpolarization signal powers and phase differences. Due to this, the transformed signal becomes independent of the polarization mixing, carrier frequency offset and phase offset. After the transformation, each considered modulation format is characterized by a different signature – number of clusters (clouds of points). Signatures of polarization-division multiplexed (PDM) modulation formats under consideration – {BPSK, QPSK, 8-PSK, 8-QAM, 12-QAM, 16-QAM} – are shown in Fig. 2. Those modulation formats result in, respectively, $N = \{2, 4, 8, 16, 32, 60\}$ clusters. We apply VBEM-GMM [15] machine learning algorithm to the Stokes space-transformed samples to determine the number of separate clusters, and hence modulation format. The reason for choosing this algorithm instead of e.g. k -means as in [10] is twofold: it allows for convenient detection of number of mixture components and behaves well with mixtures where per-cluster variances and intercluster distances vary, which is the case for Stokes MFR.

B. Per-Cluster Noise in Stokes Space

Assuming a random received data, in-phase (I) and quadrature components (Q) of both polarizations for every cluster are independent and identically distributed (i.i.d.) normal random variables (RV). Since signal transformation to Stokes space

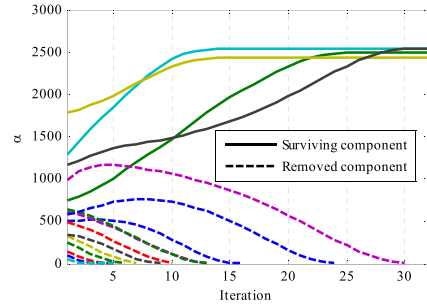


Fig. 3. Plot showing the value of α parameter for one VBEM-GMM run on simulated QPSK data. After the algorithm converges, only four components are left in the GMM, which is equivalent to four clusters in Stokes space, as shown in Fig. 2b.

cancels out phase information, the deterministic phase component (phase offset) can be disregarded.

The analytical evaluation of normally distributed variable after Stokes space transformation is very complex. However, by considering projections of per-cluster noise onto planes defined by normal unit vectors \hat{S}_1 , \hat{S}_2 and \hat{S}_3 we find that \hat{S}_1 projection has a noncentral chi-squared (χ^2) distribution with 4 degrees of freedom while projections onto \hat{S}_2 and \hat{S}_3 have product-normal distributions.

C. Variational Bayesian Technique for Gaussian Mixture Models

Due to analytically intractable noise probability distribution functions for Stokes-transformed samples, we simplify our considerations by assuming that after Stokes transformation, the per-cluster noise is normally (Gaussian) distributed. Following that, we can reuse the general result from VBEM for GMM which has been well studied in literature [14].

The algorithm provides an iterative framework to optimize a set of parameters in a maximum likelihood (ML) sense.

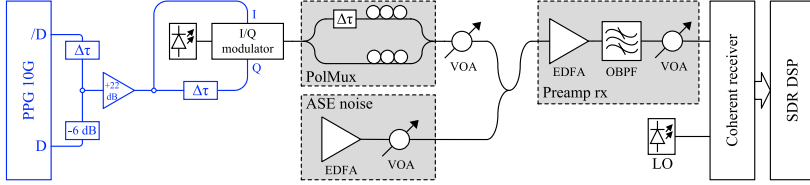


Fig. 4. Outline of the experimental setup. Blue - electrical subsystem, black - optical components. PPG - pulse pattern generator, Δt - delay line (electrical or optical), I - in-phase, Q - quadrature, PolMux - polarization multiplexing stage, ASE noise - amplified spontaneous emission noise loading stage, EDFA - erbium-doped fiber amplifier, VOA - variable optical attenuator, Preamp rx - preamplified receiver, OBPF - optical bandpass filter, LO - local oscillator, SDR DSP - software defined receiver digital signal processing.

Since the assumed underlying distribution is GMM, the set of variables to optimize are distribution parameters. The procedure iterates over two steps: expectation (E step) and maximization (M step), similar to the ones presented in [16]. In E step, the current model parameters are used to assign observed data to mixture components. In M step the model parameters are updated based on the data assignment from the previous step. Those two steps are iteratively applied until convergence is achieved. An example of one run of VBEM-GMM algorithm is shown in Fig. 3. The model is initialized with a large number of components that well exceeds the largest number of points in the Stokes space among detectable modulation formats (60 for 16-QAM). Each curve in Fig. 3 represents one component and the value α (concentration parameter) for every component is proportional to the number of points in the Stokes space that belong to particular mixture component. The initial means for the GMM are chosen randomly from among the set of all points in the Poincaré sphere, as in general case the actual position of the lens in 3D space may be arbitrary [4], [7]. In order to reduce the necessary computational effort and thus speed up the algorithm, we introduce a modification where components with low α values are removed from the mixture. The number of surviving components, \tilde{N} , roughly equivalent to the number of clusters formed in the Stokes space, is then used to compute a value of a simple cost function $j_N = |\tilde{N} - N|$. The cost function quantifies how close the detected number of clusters is to any of the considered modulation formats. The identification is done by finding $\min_N(j_N)$. It should be mentioned that \tilde{N} is just an approximation of the actual number of clusters because of an assumption by which non-normal noise distributions are approximated by a GMM.

III. SIMULATION AND EXPERIMENT SETUP

A. Numerical Simulation

The numerical simulation of the modulation format recognition was performed by transmitting $10^4 \times \log_2 M$ points, where M is the modulation order, of a 10 Gbaud PDM signal through an additive white Gaussian noise channel. Noise power was varied for every modulation format to keep electrical signal-to-noise ratio (SNR) at 30 dB. Next, a carrier frequency offset and phase offset were applied. The signal was then passed through a set of DSP algorithms as shown in Fig. 1 and modulation format was recognized. The maximum number of

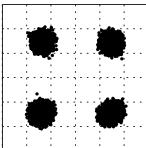
iterations for the algorithm was set to 100. The convergence was monitored by evaluating the variational lower bound and the number of iterations typically did not exceed 50. Fig. 3 shows an example in which the convergence was achieved after 32 iterations. The last redundant component was removed in iteration 30, after which the number of components stabilized at 4, which corresponds to QPSK modulation format (cf. Fig. 2b).

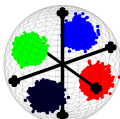
B. Experimental Validation

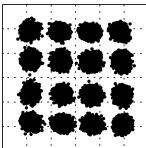
The experimental setup, with a reconfigurable transmitter and receiver, capable of generation and reception of PDM 16-QAM and PDM QPSK at 10 Gbaud, is shown in Fig. 4. An optical I/Q modulator was provided with a carrier signal originating from a 100 kHz-linewidth laser operating at 1550.116 nm. Electrical inputs to the modulator were generated by a 10 Gb/s pulse pattern generator (PPG) with two dependent outputs (one negated). One of the outputs was delayed to assure decorrelation, the other one was attenuated by 6 dB, and both were combined in a resistive combiner. By toggling the state of one of the PPG outputs, the electrical signal was either 4- or 2-level. Next, the signal was amplified, divided in a resistive splitter, one of the branches was decorrelated and both were supplied as in-phase (I) and quadrature (Q) signals to the I/Q modulator. This resulted in, respectively, 16-QAM at 40 Gb/s or QPSK at 20 Gb/s in optical domain. Optical output of the I/Q modulator was subsequently polarization multiplexed to create PDM 16-QAM at 80 Gb/s or PDM QPSK at 40 Gb/s. The output of the polarization multiplexing stage was connected to amplified spontaneous emission (ASE) loading stage. For 16-QAM, an optical SNR of 27 dB was set, while 19 dB was used for QPSK experiment. The noisy signal was then preamplified, filtered by a 0.33 nm-broad optical bandpass filter (OBPF) to remove out-of-band ASE noise and attenuated with a variable optical attenuator (VOA) to clamp the power at the front-end of a coherent receiver to an optimal level. Another 100 kHz-linewidth laser, offset by several hundred MHz from the carrier wavelength was used as a local oscillator signal (LO) and supplied to the integrated coherent receiver. A 40 GSa/s, 13 GHz bandwidth oscilloscope was used to digitize electrical data output by the coherent receiver. The acquired traces were subsequently processed offline by a set of DSP algorithms outlined in Fig. 1. 8×10^4 points were used for Stokes MFR.


TABLE I
COST FUNCTION VALUE FOR SIMULATION AND EXPERIMENTAL CASES.
RECOGNIZED MODULATION FORMATS WERE UNDERLINED

		Simulation						Exp.		
		PSK			QAM			QPSK	16QAM	
		2	4	8	8	12	16			
Cost function	PSK	2	<u>0</u>	2	6	14	30	58	2	48
	4	2	<u>0</u>	4	12	28	56	<u>0</u>	46	
	8	6	4	<u>0</u>	8	24	52	4	42	
	QAM	8	14	12	8	<u>0</u>	16	44	12	34
	12	30	28	24	16	<u>0</u>	28	28	18	
	16	58	56	52	44	28	<u>0</u>	56	<u>10</u>	









(a)

(b)

Fig. 5. Constellations (top row; only one polarization shown) and their corresponding Stokes space representation in the Poincaré (bottom row) for experimental data. (a) PDM QPSK, (b) PDM 16-QAM.

IV. RESULTS

Top rows of Figs. 2 and 5 show one of the received signal polarizations, respectively for simulation and experiment, while bottom rows show Poincaré spheres with Stokes space representation of received signal. Each color in the Poincaré spheres represent separate cluster obtained after transformation.

The VBEM-GMM algorithm was used to count the number of clusters in the Stokes space and the cost function was calculated for every tested case. Table I presents the summary of results for both numerical simulation and experimental data. Every column corresponds to one case and the row indicates value of the cost function. For numerical simulation, lowest values of the cost function are located on the diagonal, indicating that recognition was successful in all investigated cases. Recognition was also successful for experimental data, with lowest values of cost function being associated with actual experimentally transmitted modulation formats.

V. SUMMARY

In this letter we reported on an optical modulation format recognition method from Stokes space parameters using variational Bayesian expectation maximization for Gaussian mixture models algorithm. This machine learning algorithm is used to count the number of clusters in Stokes space and provides an input to a cost function used to identify the modulation format. By using the Stokes space representation of the received signal, the method is insensitive to polarization mixing, carrier frequency offset and phase offset. Unlike previously published methods, it does not require training nor full set of coherent DSP algorithms to work. The method successfully recognized PDM BPSK, QPSK, 8-PSK, 8-QAM, 12-QAM and 16-QAM in numerical simulation as well as 16-QAM and QPSK from experimental data. The technique can be used in any receiver capable of measuring Stokes parameters, in particular digital coherent receivers. The recognized modulation format can be used as an additional information improving performance of follow-up DSP blocks of the digital coherent receiver.

REFERENCES

- [1] K. Roberts and C. Laperle, "Flexible transceivers," in *Proc. ECOC*, 2012, pp. 1–3.
- [2] I. T. Monroy, D. Zibar, N. G. Gonzalez, and R. Borkowski, "Cognitive heterogeneous reconfigurable optical networks (CHRON): Enabling technologies and techniques," in *Proc. 13th ICTON*, Jun. 2011, pp. 1–4.
- [3] I. Fataadin, D. Ives, and S. J. Savory, "Blind equalization and carrier phase recovery in a 16-QAM optical coherent system," *J. Lightw. Technol.*, vol. 27, no. 15, pp. 3042–3049, Aug. 1, 2009.
- [4] B. Szafarek, B. Nebendahl, and T. Marshall, "Polarization demultiplexing in Stokes space," *Opt. Express*, vol. 18, no. 17, pp. 17928–17939, 2010.
- [5] Z. Yu, et al., "Polarization demultiplexing in Stokes space for coherent optical PDM-OFDM," *Opt. Express*, vol. 21, no. 2, pp. 3885–3890, 2013.
- [6] P. Serena, A. Ghazizadeh, and A. Bononi, "A new fast and blind cross-polarization modulation digital compensator," in *Proc. ECOC*, 2012, pp. 1–3, paper We.1.A.5.
- [7] N. J. Muga and A. N. Pinto, "Digital PDL compensation in 3D Stokes space," *J. Lightw. Technol.*, vol. 31, no. 13, pp. 2122–2130, Jul. 1, 2013.
- [8] T. Saida, et al., "In-band OSNR monitor for DP-QPSK signal with high-speed integrated Stokes polarimeter," in *Proc. ECOC*, 2012, pp. 1–3.
- [9] O. A. Dobre, A. Abdi, Y. Bar-Ness, and W. Su, "Survey of automatic modulation classification techniques: Classical approaches and new trends," *IEEE Commun. Surv. Tutorials*, vol. 1, no. 2, pp. 137–156, Apr. 2007.
- [10] N. G. Gonzalez, D. Zibar, and I. T. Monroy, "Cognitive digital receiver for burst mode phase modulated radio over fiber links," in *Proc. 36th ECOC*, Sep. 2010, pp. 1–3.
- [11] F. N. Khan, Y. Zhou, A. P. Lau, and C. Lu, "Modulation format identification in heterogeneous fiber-optic networks using artificial neural networks," *Opt. Express*, vol. 20, no. 11, pp. 12422–12431, 2012.
- [12] P. Isautier, A. Stark, K. Mehta, R. de Salvo, and S. E. Ralph, "Autonomous software-defined coherent optical receivers," in *Proc. OFC*, 2013, pp. 1–3, paper OTh3B.4.
- [13] R. Borkowski, D. Zibar, A. Caballero, V. Arlunno, and I. T. Monroy, "Optical modulation format recognition in Stokes space for digital coherent receivers," in *Proc. OFC*, 2013, pp. 1–3, paper OTh3B.3.
- [14] C. M. Bishop, "Approximate inference," in *Pattern Recognition and Machine Learning*, 3rd ed. New York, NY, USA: Springer-Verlag, 2006, ch. 10.
- [15] M. Chen, (2012). *Variational Bayesian Inference for Gaussian Mixture Model* [Online]. Available: <http://www.mathworks.com/matlabcentral/fileexchange/35362-variational-bayesian-inference-for-gaussian-mixture-model>
- [16] D. Zibar, et al., "Nonlinear impairment compensation using expectation maximization for dispersion managed and unmanaged PDM 16-QAM transmission," *Opt. Express*, vol. 20, no. 26, pp. B181–B196, 2012.

Paper [N]: Nonlinear impairment compensation using expectation maximization for dispersion managed and unmanaged PDM 16-QAM transmission

Darko Zibar, Ole Winther, Niccolo Franceschi, **Robert Borkowski**, Antonio Caballero, Valeria Arlunno, Mikkel Nørgaard Schmidt, Neil Guerrero Gonzalez, Bangning Mao, Yabin Ye, Knud J. Larsen, and Idelfonso Tafur Monroy. Nonlinear impairment compensation using expectation maximization for dispersion managed and unmanaged PDM 16-QAM transmission. *Optics Express*, vol. 20, no. 26, pp. B181–B196, November 2012.

Nonlinear impairment compensation using expectation maximization for dispersion managed and unmanaged PDM 16-QAM transmission

Darko Zibar,^{*1} Ole Winther,² Niccolo Franceschi,^{1,2} Robert Borkowski,¹ Antonio Caballero,¹ Valeria Arlunno,^{1,2} Mikkel N. Schmidt,² Neil Guerrero Gonzales,³ Bangning Mao,³ Yabin Ye,³ Knud J. Larsen,¹ and Idelfonso Tafur Monroy¹

¹ DTU Fotonik, Technical University of Denmark, Build. 343, DK-2800, Denmark

² DTU Informatics, Technical University of Denmark, Build. 305, DK-2800, Denmark

³ European Research Center, Huawei Technologies Duesseldorf GmbH, Riesstrasse 25, Munich, Germany

^{*} dazj@fotonik.dtu.dk

Abstract: In this paper, we show numerically and experimentally that expectation maximization (EM) algorithm is a powerful tool in combating system impairments such as fibre nonlinearities, inphase and quadrature (I/Q) modulator imperfections and laser linewidth. The EM algorithm is an iterative algorithm that can be used to compensate for the impairments which have an imprint on a signal constellation, i.e. rotation and distortion of the constellation points. The EM is especially effective for combating non-linear phase noise (NLPN). It is because NLPN severely distorts the signal constellation and this can be tracked by the EM. The gain in the nonlinear system tolerance for the system under consideration is shown to be dependent on the transmission scenario. We show experimentally that for a dispersion managed polarization multiplexed 16-QAM system at 14 Gbaud a gain in the nonlinear system tolerance of up to 3 dB can be obtained. For, a dispersion unmanaged system this gain reduces to 0.5 dB.

© 2012 Optical Society of America

OCIS codes: (060.0060) Fiber optics and optical communications; (060.1660) Coherent communications.

References and links

1. S. J. Savory, "Digital coherent optical receivers: Algorithms and subsystems," *IEEE J Sel. Top. Quantum Electron* **16**, 1164–1179 (2010).
2. R.-J. Essiambre, G. Kramer, P. Winzer, G. Foschini, and B. Goebel, "Capacity limits of optical fiber networks," *J. Lightwave Technol.* **28**, 662–701 (2010).
3. A. Lau and J. Kahn, "Signal design and detection in presence of nonlinear phase noise," *J. Lightwave Technol.* **25**, 3008–3016 (2007).
4. E. Ip and J. Kahn, "Compensation of dispersion and nonlinear impairments using digital backpropagation," *J. Lightwave Technol.* **26**, 3416–3425 (2008).
5. Z. Tao, L. Dou, W. Yan, L. Li, T. Hoshida, and J. C. Rasmussen, "Multiplier-free intrachannel nonlinearity compensating algorithm operating at symbol rate," *J. Lightwave Technol.* **29**, 2570–2576 (2011).
6. N. Stojanovic, Y. Huang, F. N. Hauske, Y. Fang, M. Chen, C. Xie, and Q. Xiong, "MLSE-based nonlinearity mitigation for wdm 112 gbit/s pdm-qpsk transmissions with digital coherent receiver," in *Proc. of OFC*, paper OTu3C.5, Los Angeles, California, USA, (2011).

7. D. Rafique, J. Zhao, and A. D. Ellis, "Compensation of nonlinear fibre impairments in coherent systems employing spectrally efficient modulation formats," *IEICE Trans. on Commun.* **E94-B**, 1815–1822 (2011).
8. D. Zibar, O. Winther, N. Franceschi, R. Borkowski, A. Caballero, A. Valeria, N. M. Schmidt, G. G. Neil, B. Mao, Y. Ye, J. K. Larsen, and T. I. Monroy, "Nonlinear impairment compensation using expectation maximization for pdm 16-qam systems," in *Proc. of ECOC*, paper Th1D2, Amsterdam, The Netherlands, (2012).
9. P. Winzer, A. Gnauck, C. Doerr, M. Magarini, and L. Buhl, "Spectrally efficient long-haul optical networking using 112-gb/s polarization-multiplexed 16-qam," *J. Lightwave Technol.* **28**, 547–556 (2010).
10. D. Zibar, J. C. R. F. de Olivera, V. B. Ribeiro, A. Paradisi, J. C. Diniz, K. J. Larsen, and I. T. Monroy, "Experimental investigation and digital compensation of dgd for 112 gb/s pdm-qpsk clock recovery," *Opt. Express* **19**, 429–437 (2011).
11. H. Meyr, M. Moeneclaey, and S. Fechtel, *Digital Communication Receivers / Synchronization, Channel Estimation, and Signal Processing* (Wiley, 1998).
12. J. Kurzweil, *An Introduction to Digital Communications* (John Wiley, 2000).
13. C. M. Bishop, *Pattern Recognition and Machine Learning* (Springer, 2006).
14. A. P. Dempster, N. M. Laird, and D. B. Rubin, "Maximum likelihood from incomplete data via the em algorithm," *J. Roy. Stat Soc. Series B*, **39**, 1–38 (1977).
15. N. G. Gonzalez, D. Zibar, A. Caballero, and I. T. Monroy, "Experimental 2.5-gb/s qpsk wdm phasemodulated radio-over-fiber link with digital demodulation by a k-means algorithm," *IEEE Photon. Technol. Lett.* **22**, 335–337 (2010).
16. A. Carena, V. Curri, G. Bosco, P. Poggiolini, and F. Forghieri, "Modeling of the impact of nonlinear propagation effects in uncompensated optical coherent transmission links," *J. Lightwave Technol.* **30**, 1524–1539 (2012).
17. F. Vacondio, O. Rival, C. Simonneau, E. Grellier, L. Lorcy, J.-C. Antona, S. Bigo, and A. Bononi, "On nonlinear distortions of highly dispersive optical coherent systems," *Opt. Express* **20**, 1022–1032 (2012).
18. A. Bononi, N. Rossi, and P. Serena, "Transmission limitations due to fiber nonlinearity," in *Proc. of OFC*, paper OW07, Los Angeles, California, USA, (2011).
19. E. Ip, N. Bai, and T. Wang, "Complexity versus performance tradeoff for fiber nonlinearity compensation using frequency-shaped, multi-subband backpropagation," in *Proc. of OFC*, paper OThF4, Los Angeles, California, USA, (2011).
20. S. Makovejs, D. S. Millar, D. Lavery, C. Behrens, R. I. Killey, S. J. Savory, and P. Bayvel, "Characterization of long-haul 112gb/s pdm-qam-16 transmission with and without digital nonlinearity compensation," *Opt. Express* **18**, 12939–12947 (2010).

1. Introduction

The application of digital signal processing (DSP) based coherent detection has allowed optical communication systems to operate closer to the nonlinear Shannon capacity limit by employing spectrally efficient modulation formats. Therefore, there is currently a lot of ongoing research on DSP based algorithms for signal detection and optical fibre channel impairment compensation. Linear signal processing algorithms can be effectively used to compensate for linear fibre channel impairments and have been demonstrated very successfully for higher order quadrature amplitude modulation (QAM) signaling [1]. However, for long-haul systems employing higher order QAM, nonlinear optical fibre impairments can severely limit the transmission distance as well as the achievable total capacity [2]. Mitigation of optical fibre nonlinearities is therefore very crucial as it will allow launching more power into the fibre and thereby enhancing the transmission distance. Additionally, mitigation of fibre nonlinearities will help us reduce the nonlinear crosstalk from the neighboring channel in a multi-channel transmission system.

It has been shown that nonlinear fibre impairments can be compensated by various techniques: digital backpropagation (DBP), maximum-likelihood sequence estimation, nonlinear polarization crosstalk cancelation, nonlinear pre- and post-compensation, RF-pilot, etc, [3–7] and references therein. Some of the mentioned methods suffer from complexity and, additionally, the achievable gain in the nonlinear tolerance is dependent on particular transmission scenarios. Therefore, efficient and widely applicable DSP algorithms for nonlinearity compensation are still open for research.

We have already demonstrated that for the dispersion managed links, the expectation maximization algorithm can be used to enhance system tolerance towards nonlinearities [8]. However, dispersion managed link will impact the signal propagation in a different way compared to

the dispersion unmanaged link, and it is therefore essential to investigate the benefits of EM for dispersion unmanaged link as well. In this paper, we consider both numerically and experimentally dispersion unmanaged link. Transmission distances of 240 km, 400 km and 800 km are investigated experimentally for the dispersion unmanaged link. For the consistency of the paper, results obtain for the dispersion managed link are included as well. We consider dispersion managed (link consisting of multiples stages of standard single mode fibre (SSMF) in combination with dispersion compensating fibre (DCF)) and dispersion unmanaged (link consisting of multiples stages of SSMF) polarization multiplexed 16-QAM single channel transmission. For the transmission link erbium doped fibre amplifier (EDFA) amplification is employed. First, it is investigated numerically, for the back-to-back case, if the expectation maximization (EM) algorithm can be effective in combating inphase and quadrature (I/Q) modulator nonlinearity, imbalance and laser linewidth. We investigate, also by numerical simulations, an improvement in nonlinear system tolerance that can be gained for PDM 16-QAM transmission. To begin with, we consider the case in which the chromatic dispersion is neglected and the system is impaired by self phase modulation induced nonlinear phase noise only. Finally, we move to a dispersion managed and unmanaged transmission system. As a proof of concept, an experimental set up employing dispersion managed and unmanaged PDM 16-QAM at 14 Gbaud is constructed and an improvement in the nonlinear system tolerance is investigated. The paper is ended with a conclusion and the future prospects of EM algorithm.

2. Numerical and experimental system set-up

In this section, a numerical and experimental set-up is presented. We first start by describing the numerical set-up used for simulations, and then we move to the experimental set-up. The section is concluded by a subsection describing the DSP algorithms used for signal equalization and demodulation.

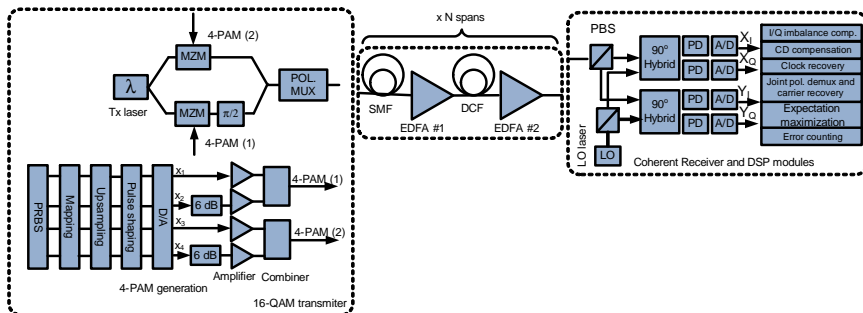


Fig. 1. Schematic diagram of the set-up used for simulations and experiment. PD: photodiode, PBS: polarization beam splitter, A/D: analog-to-digital converter, LO: local oscillator

2.1. Numerical set-up

The set-up used for the numerical investigations is shown in Fig. 1. All simulations are done using MATLAB (R2010a). For all numerical simulations, the baud rate is kept at 28 Gbaud resulting in the total bit rate of 224 Gb/s for the system under consideration. The transmitter and local oscillator (LO) laser phase noise is modeled as a random walk Wiener process. The output of the laser is then passed through an optical I/Q modulator. The I/Q modulator is driven by two four level pulse amplitude modulated (4-PAM) electrical signals, 4-PAM(1) and 4-PAM(2), in order to generate the optical 16-QAM signal. The module for generating 4-PAM

signals is shown in Fig. 1. It consists of pseudo-random binary sequence (PRBS) generator (generates four independent sequences of length $2^{15} - 1$), signal mapping, upsampling, pulse shaping filter (raised cosine), digital-to-analog converter (DAC), attenuators and electrical amplifiers. The actual impulse response of the driving amplifiers is not taken into consideration. It is assumed that the electrical amplifiers have sufficient bandwidth such that they don't induce any signal distortion. The method of 4-PAM signal generation is very similar to the one reported in [9]. The output of the I/Q modulator is then passed through a polarization multiplexing stage with a delay of 10 symbols, and the output is then amplified (EDFA). For the back-to-back numerical investigations, the generated PDM 16-QAM signal is coherently detected in a 90 degrees optical hybrid, photodetected and sampled at twice the baud rate by the analog-to-digital converter. We assume that the sampling frequency and the phase is not synchronized to the incoming signal and that the clock recovery is thereby performed by the DSP. The response of the analog-to-digital converter is modeled as a fourth-order Butterworth filter with a 3 dB bandwidth corresponding to 75% of the signal symbol rate. The sampled signal is then sent to the DSP modules which are described in subsection 2.3.

In this paper, we will also perform numerical investigations involving fibre transmission, and will therefore consider dispersion managed and unmanaged link. The dispersion managed link consists of a different number of stages where each stage consists of 80 km of SSMF and 17 km of a DCF. EDFA amplification is employed after the SSMF and the DCF spans, respectively, as shown in Fig. 1. For the SSMF we have the following fibre parameters: $\alpha_{smf}=0.2$ dB/km, $D_{smf}=17$ ps/nm/km and nonlinear coefficient is $\gamma_{smf}=1.3$ W⁻¹km⁻¹. For the DCF, we have the following parameters: $\alpha_{dcf}=0.5$ dB/km, $D_{dcf}=-80$ ps/nm/km and nonlinear coefficient is $\gamma_{dcf}=5.3$ W⁻¹km⁻¹.

2.2. Experimental set-up

The set-up used for the experimental investigations is very similar to the one shown in Fig. 1. For the experiment, the baud rate is kept at 14 Gbaud resulting in the total bit rate of 112 Gb/s. The transmitter and LO laser are both tunable external cavity lasers with a linewidth of ~ 100 kHz. The wavelength of the transmitter and LO laser is set to 1550 nm. Pulse-pattern generator outputs four copies, (x_1, x_2, x_3, x_4) , of a true PRBS of length $2^{15} - 1$. The PRBS sequences are first decorrelated by 270 bits, amplified and combined into a 4-PAM electrical signal. The two PRBS sequences x_1 and x_3 are independent, while x_2 and x_4 are inverted versions of x_1 and x_3 , respectively. The peak-to-peak amplitude of the 4-PAM signal used to drive an optical I/Q modulator is approximately 3 V. The delay in the polarization multiplexing stage is 10 symbols. Also, for the experiment we consider a dispersion managed and unmanaged link. For the experimental investigations we first consider dispersion managed link and then we move to dispersion unmanaged link. The dispersion managed link consists of 80 km of SSMF and 17 km of DCF with inline EDFA amplification. For the dispersion managed link, the DCF is just bypassed. The fibre parameters for SSMF and DCF used for the experiment are the similar to the one we have used in the numerical set-up. At the receiver, the 14 Gbaud PDM 16-QAM signal is then sampled at 50 Gs/s using a sampling scope with a nominal resolution of 8-bits and analog bandwidth of 17 GHz. The sampled signal is then send to DSP modules for the offline processing described in section 2.3.

2.3. Digital signal processing algorithms

The DSP modules consists of an I/Q imbalance compensation, interpolation (clock recovery) module, joint polarization demultiplexing and carrier recovery stage. We apply expectation maximization algorithm for nonlinearity compensation after joint polarization demultiplexing and carrier recovery. Within the expectation maximization algorithm, symbol demodulation is

embedded. The I/Q imbalance compensation algorithm employs Gram-Schmidt orthogonalization and is similar to the one reported in [1]. In order to make sure that we have a control signal for the clock recovery module, irrespective of the polarization mixing angle and the differential group delay, (DGD), a method reported in [10] is implemented. The implemented clock recovery module is a feedback structure similar to the one reported in [11]. It consists of an interpolator, timing error detector, loop filter and a number controlled oscillator (NCO). The timing error detector, which is the most crucial component, is a modified Gardner algorithm [10]. For the loop filter, an averaging filter is used. After, the clock recovery module a decimator is used in order to downsample the signal to one sample per symbol. The algorithm used for signal decimation is based on the maximum search method as proposed in [11]. The polarization demultiplexing stage is performed jointly with carrier frequency and phase estimation module. The polarization demultiplexing unit consists of a butterfly structure as the one reported in [1], and the carrier phase and frequency estimation unit is a decision-directed digital phase-locked loop [11]. The decisions from the digital phase-locked loop are then used as the error signal for the polarization demultiplexing. We found that the significant gain in the performance of the phase-locked loop can be obtained by properly designing the digital loop filter. We found that for the considered case proportional integrator filter was the best choice. We emphasize that the polarization demultiplexing and digital phase-locked loop are first trained in the blind mode using constant modulus algorithm and the switched to a decision directed mode as also reported in [1]. This type of joint equalization and phase/frequency estimation is described in more details in [12]. The EM algorithm is then applied after the polarization demultiplexing and carrier frequency/phase recovery stage. The task of the EM algorithm is then to learn the channel properties from the demodulated data without any prior knowledge. The information extracted from the channel is then used to compensate for the channel impairments and perform subsequent signal demodulation. After the EM stage, error counting is performed on ~ 100000 received symbols.

3. Theory

3.1. Statistical signal representation - mixture of Gaussians

In this section, we will first describe how a received signal can be modeled as a so called "Mixture of Gaussians, (MoG)" and then we will move into basic principles of the EM algorithm. For a more detailed treatment of MoG see [13], Chapter 9.2. Throughout, the entire section we will assume that the signal that is input to the EM algorithm contains one sample per symbol, and is obtained after polarization demultiplexing, frequency and phase recovery stage. We will refer to this signal as the demodulated signal.

The demodulated signal in x/y-polarization can be considered as a mixture of Gaussian densities (MoG) consisting of a number of components (clusters), where each of the components (clusters) can be described by a 2-D Gaussian distribution. For instance, in the case of 16-QAM, we have 16 clusters. For a 16-QAM signal constellation, in the absence of any impairment, we will have 16 distinct constellation points. However, in the presence of additive white Gaussian noise, around each of the 16 constellation points there will occur spread of symbols. The cluster is then defined as a grouping of the points/symbols around a mean value. Irrespective of the modulation format applied, (PSK or QAM), the demodulated signal can mathematically be expressed as a superposition of M Gaussian densities, where M is the number of clusters and corresponds to the number of constellation points. The probability density function of the demodulated signal is then expressed as:

$$p(\mathbf{x}) = \sum_{k=1}^M \pi_k N(\mathbf{x} | \mu_k, \Sigma_k) , \quad (1)$$

where k refers to each cluster in the constellation, π_k is a mixing coefficient (for the considered case of a signal where symbols have uniform distribution $\pi_k = 1/M$). $\mathbf{x} = [x_1, x_2]$ is a 2-D vector, corresponding to a detected symbol in the constellation (Inphase/Quadrature) plane and $N(\mathbf{x}|\mu_k, \Sigma_k)$ is a 2-D Gaussian density with mean μ_k and a 2×2 covariance matrix Σ_k [13]:

$$N(\mathbf{x}|\mu_k, \Sigma_k) = \frac{1}{2\pi|\Sigma_k|^{1/2}} e^{-\frac{1}{2}(\mathbf{x}-\mu_k)^T \Sigma_k^{-1}(\mathbf{x}-\mu_k)}, \quad (2)$$

where $|\Sigma_k|$ is the determinant of the covariance matrix and it expresses the area covered by the specific cluster k . The covariance matrix is defined as:

$$\Sigma_k = \begin{bmatrix} \text{var}(x_1) & \text{cov}(x_1, x_2) \\ \text{cov}(x_1, x_2) & \text{var}(x_2) \end{bmatrix} \equiv \begin{bmatrix} \sigma_{1,1}^2 & \sigma_{1,2}^2 \\ \sigma_{2,1}^2 & \sigma_{2,2}^2 \end{bmatrix}. \quad (3)$$

For the most general case, each cluster is described by its specific covariance matrix Σ_k . However, when the signal is mostly dominated by the additive Gaussian noise, the covariance matrices will be equal and diagonal, i.e. there is no correlation among symbols within the cluster. Additionally, the clusters will be circularly symmetric (equal variances) and the covariance matrix is then expressed as:

$$\Sigma_k = \Sigma = \begin{bmatrix} \sigma^2 & 0 \\ 0 & \sigma^2 \end{bmatrix}. \quad (4)$$

An example of the demodulated 16-QAM signal dominated by additive Gaussian noise is shown in Fig. 2(a). It is observed in Fig. 2(a) that all the clusters look similar. An example of the demodulated signal strongly impaired by laser phase noise is shown in Fig. 2(b). It is observed in Fig. 2(b) that the clusters are not similar. Indeed, the clusters belonging to the outer ring are elliptical. Here, we will distinguish between two cases: (1) the covariance matrix is still diagonal and $\sigma_{1,1}^2 \neq \sigma_{2,2}^2$; the clusters are stretched in either vertical or horizontal direction, (2) the covariance matrix is non-diagonal and in this case the shape and orientation of the cluster is arbitrary, all depending if there is positive or negative correlation. Finally, let's look at third case when the demodulated signal is severely impaired by non-linear phase noise, see Fig. 2(c). It is observed that in Fig. 2(c) not only outer cluster are affected but all the clusters experience distortion. It should also be noticed that the entire constellation is tilted (phase offset introduced), and the outer points have been compressed. This compression means that the mean values μ_k have been altered compared to the reference constellation. By reference constellation, it is meant the constellation which is free of any impairment.

In general, different optical channel impairments will have a different imprint on the received signal constellation. This information can then be used to determine the impairment and make optimal signal detection as explained next.

The optimal signal detection in maximum likelihood sense is obtained by maximizing a posteriori probability of the received symbol \mathbf{x} belonging to one of the clusters k , where $k = 1, \dots, M$:

$$\hat{k} = \underset{k}{\operatorname{argmax}} p(k|\mathbf{x}) \quad (5)$$

or in another words find a cluster k for which $p(k|\mathbf{x})$ is maximized. The a posteriori probability $p(k|\mathbf{x})$ is obtained from Bayes' theorem [13]:

$$p(k|\mathbf{x}) = \frac{\pi_k N(\mathbf{x}|\mu_k, \Sigma_k)}{\sum_{l=1}^M \pi_l N(\mathbf{x}|\mu_l, \Sigma_l)}. \quad (6)$$

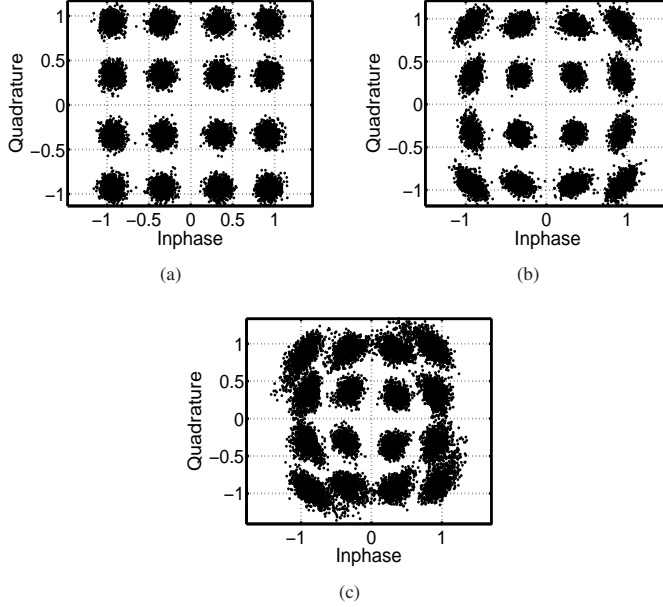


Fig. 2. Impact of different impairments on signal constellation for a 16-QAM signal. (a) Constellation of a signal dominated by additive noise. (b) Constellation of a signal dominated by phase noise. (c) Constellation of a signal dominated by non-linear phase noise.

Inserting the expression for the Gaussian distribution, the optimal decision, Eq. (5), reduces to a quadratic decision rule:

$$\hat{k} = \underset{k}{\operatorname{argmax}} \left\{ -\frac{1}{2} \mathbf{x}^T \Sigma_k^{-1} \mathbf{x} + \mathbf{w}_k^T \mathbf{x} + w_{k0} \right\} \quad (7)$$

with $\mathbf{w}_k = \Sigma_k^{-1} \mu_k$ and $w_{k0} = \log \pi_k - \log |\Sigma_k|/2 - \mu_k^T \Sigma_k^{-1} \mu_k/2$. In the case, when the covariance matrices are equal, the quadratic term in optimal decision rule in Eq. (7) are the same for all k and the decision rule becomes linear:

$$\hat{k} = \underset{k}{\operatorname{argmax}} \left\{ \mathbf{w}_k^T \mathbf{x} + w_{k0} \right\}. \quad (8)$$

However, in case when the signal constellation is distorted by nonlinear phase noise, laser phase noise, etc, Eq. (6) needs to be used in order to make optimum signal detection. In order to evaluate Eq. (6), M Gaussian densities, $N(\mathbf{x}|\mu_k, \Sigma_k)$ and thereby parameters $\pi \equiv \{\pi_1, \dots, \pi_k\}$, $\mu \equiv \{\mu_1, \dots, \mu_k\}$ and $\Sigma \equiv \{\Sigma_1, \dots, \Sigma_k\}$ describing Gaussian densities need to be determined. Next, we will show how to use a powerful method of EM in order to determine the parameters that generate the Gaussian mixture model. The EM will determine in a maximum likelihood sense the most likely parameters $\Xi = [\pi, \mu, \Sigma]$ that generated Gaussian densities.

3.2. Expectation maximization algorithm

In general, the EM is a numerical method of producing a solution to a maximum likelihood estimation for problems which can be simplified by introducing latent variables [13, 14]. In the

mixture model context the latent variables are the assignments. The set of parameters Ξ to be estimated, in the maximum likelihood sense, from the demodulated signal \mathbf{X} is governed by the following expression:

$$\hat{\Xi} = \underset{\Xi}{\operatorname{argmax}} p(\mathbf{X}|\Xi), \quad (9)$$

where $\mathbf{X} = [\mathbf{x}_1, \dots, \mathbf{x}_N]$, N is the length of the observation interval and the likelihood function of Ξ , $p(\mathbf{X}|\Xi)$, for independent identically distributed data is expressed as:

$$p(\mathbf{X}|\Xi) = \prod_{n=1}^N p(\mathbf{x}_n|\Xi) = \prod_{n=1}^N \sum_{k=1}^M \pi_k N(\mathbf{x}_n|\mu_k, \Sigma_k). \quad (10)$$

No closed-form analytical solution for Eq. (9) is available. Therefore, the iterative EM framework can be used to find a solution. The EM is a two step iterative procedure which is guaranteed to converge to the (local) maximum likelihood solution given in Eq. (9) [14]. The two step procedure, so called expectation (E) step and maximization (M) step for the particular case considered in this section is as follows [13]:

$$\textbf{E-step} : \gamma_{nk} \equiv p(k|\mathbf{x}_n) = \frac{\pi_k N(\mathbf{x}_n|\mu_k, \Sigma_k)}{\sum_{l=1}^M \pi_l N(\mathbf{x}_n|\mu_l, \Sigma_l)} \quad \text{for } n = 1, \dots, N \text{ and } k = 1, \dots, M \quad (11)$$

$$\textbf{M-step} : N_k = \sum_{n=1}^N \gamma_{nk} \quad (12)$$

$$\pi_k = \frac{N_k}{N} \quad (13)$$

$$\mu_k = \frac{1}{N_k} \sum_{n=1}^N \gamma_{nk} \mathbf{x}_n \quad (14)$$

$$\Sigma_k = \frac{1}{N_k} \sum_{n=1}^N \gamma_{nk} (\mathbf{x}_n - \mu_k)(\mathbf{x}_n - \mu_k)^T \quad \text{for } k = 1, \dots, M, \quad (15)$$

where γ_{nk} is called the responsibility and is nothing but a posteriori probability, Eq. (6), needed for optimal decisions.

The flow-chart describing the algorithm is shown in Fig. 3. To begin with, we initialize the EM with initial parameters for the means, covariance matrices and mixing coefficients and then the algorithms start to iterate in order to find most likely parameters. In the E-step, the current values of the parameters, Ξ^i at the iteration i , are used to evaluate the Eq. (11). The E-step expressed by Eq. (11) computes the probability of the received symbol belonging to one of the clusters, i.e. posterior probability. In the M-step we use those probabilities to re-estimate the parameters Ξ . In other words, in the M-step we are trying to find the parameters that maximize the probability that the data has been generated by a particular cluster. When making a parameter update resulting from the E step and followed by the M step, the likelihood function, $P(\mathbf{X}|\Xi^i)$, on the parameters will increase and will flatten out when the algorithm has converged. The convergence properties of the EM strongly dependent on the initialization. For the considered cases throughout the paper, we found that the EM algorithm will converge after 3 iterations. Once the EM algorithms has converged ($i > N_{iter}$), we use the results to perform the optimum signal detection governed by Eq. (5).

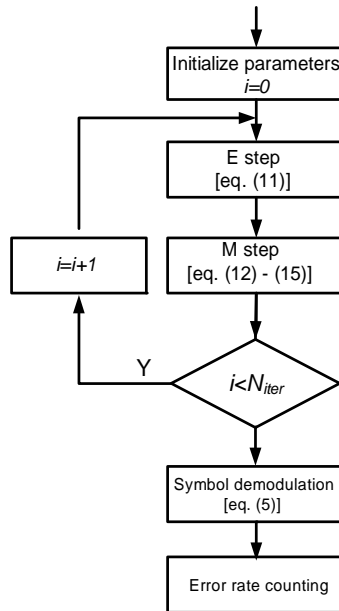


Fig. 3. Flow-chart illustrating the steps performed by the EM algorithm and subsequent signal demodulation. N_{iter} denotes the number of specified iteration.

4. Simulation results

4.1. Back-to-back investigation

First, we consider back-to-back case. It is investigated how the EM algorithm can be used to combat the combined effects of I/Q modulator nonlinearities and imperfection, and combined laser linewidth. We deliberately drive the I/Q modulator with large peak-to-peak amplitude, V_{pp} , of the electrical 4-PAM signal such that the constellation diagram of the 16-QAM signal is distorted. The resulting modulation depth of the modulator is then $m = V_{pp}/V_{\pi} = 2.12$. Furthermore, it is assumed that the phase shift between the inphase and quadrature branch of the I/Q modulator deviates from $\pi/2$ by 5%. In Fig. 4, $-\log[\text{BER}]$ is plotted as function of the combined laser linewidth for the optical signal to noise ratio (OSNR) of 25 dB. Figure 4 shows that compared to the case when no compensation is used (linear decision boundaries), the EM is very efficient in combating the combined impairments originating from I/Q modulator nonlinearities, non-ideal phase shift between the I and Q branches and combined laser linewidth.

4.2. Dispersion managed link

In order to investigate the effects of nonlinear phase noise only, the dispersion is numerically set to zero, i.e. transmission link consisting of 12 spans of SSMF with dispersion set to zero. The dominant nonlinear impairment is therefore the nonlinear phase noise originating from the EDFA amplification along the link. In order to determine the effectiveness of the EM algorithm, we also plot in the same figure $-\log(\text{BER})$ when k-means algorithm is used [13, 15]. The k-means algorithm, is another widely used clustering algorithm in nonlinear signal processing. It computes the means of the clusters and the information is used to perform minimum distance signal detection expressed by Eq. (8). In Fig. 5(a), $-\log(\text{BER})$ is plotted as a function of the

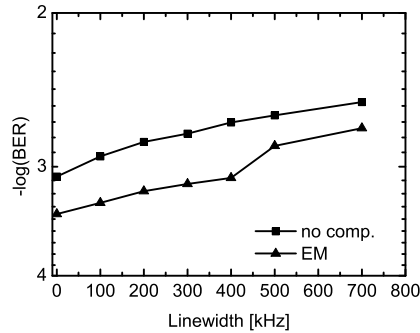


Fig. 4. BER as a function of combined laser linewidth for the back-to-back-case. The modulator modulation depth, $m = V_{pp}/V_{\pi} = 2.12$, I/Q imbalance: 5% and OSNR is 25 dB.

input signal power to the transmission span. In general, there is a relatively large improvement in the nonlinear system tolerance when using the EM algorithm. Figure 5(a) shows that by only using the k-means algorithm the system tolerance can be increased by approximately 1 dB for $-\log(\text{BER})$ of 3, while by using the EM, the system tolerance can be increased by 2.2 dB compared to the case when neither the EM nor k-means is used.

Next, we consider dispersion managed link consisting of SSMF and DCF as described in section 2.1. The total number of spans is 12. The results of $-\log(\text{BER})$ as a function of span input power are shown in Fig. 5(b). It is observed from Fig. 5(b) that by employing the EM system tolerance towards nonlinearities can be increased. The improvement in the nonlinear system tolerance is approximately 1.2 dB for the $-\log(\text{BER})$ of 3.

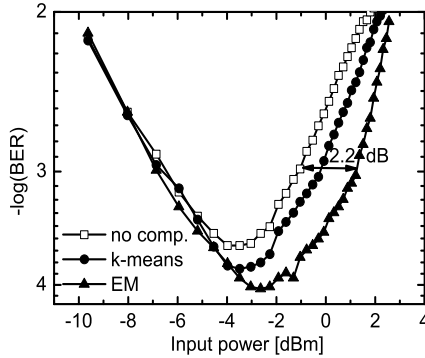
4.3. Dispersion unmanaged link

Next, we move to the case of dispersion unmanaged link. In Fig. 6(a), $-\log(\text{BER})$ is plotted as a function of the span input signal power. The total number of spans is 15. It is observed that there is no benefit of using the EM algorithm. This is because for the dispersion unmanaged links, the impact of the nonlinearity can be modeled as additive Gaussian white noise [16–18]. Therefore, all 16 covariance matrices are circularly symmetric and the optimum decision boundaries become linear as explained in Section 3. As the laser linewidth will also have an imprint on the signal constellation, next, we want to investigate if dispersion unmanaged links can benefit from the EM when impaired by laser linewidth and operate in the nonlinear regime. In Fig. 6(b), the $-\log(\text{BER})$ is plotted as a function of the combined laser linewidth. The number of spans for the unmanaged link is set 15 and the input signal power to the span is 1.4 dBm. It is observed in Fig. 6(b) that some improvement in the laser linewidth tolerance can be obtained when applying EM.

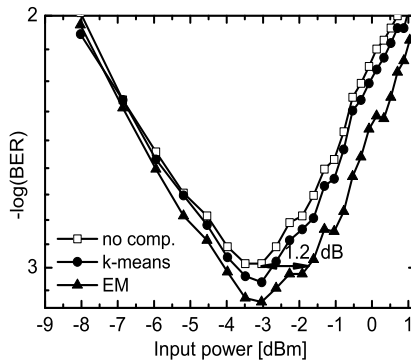
5. Experimental results

5.1. Dispersion managed link

First, we will demonstrate how EM can be effectively used to extract information from a severely distorted constellation and use this information to mitigate the impairments. Figure 7, shows a constellation diagram of a signal impaired by nonlinear phase noise after one span transmission through the dispersion managed link. We plot the recovered constellation diagram



(a)



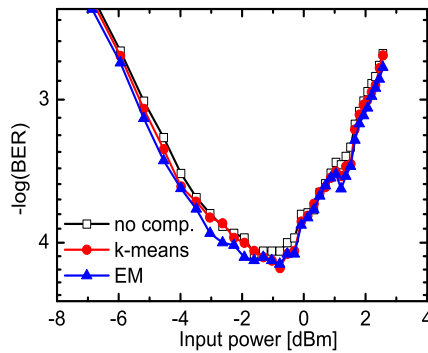
(b)

Fig. 5. The total number of spans is 12 and the combined laser linewidth is 200 kHz. (a) BER as a function of span input power for NLPN dominated transmission link, (dispersion numerically set to zero). (b) BER as a function of span input power for dispersion managed link. Transmission link consists of SSMF and DCF.

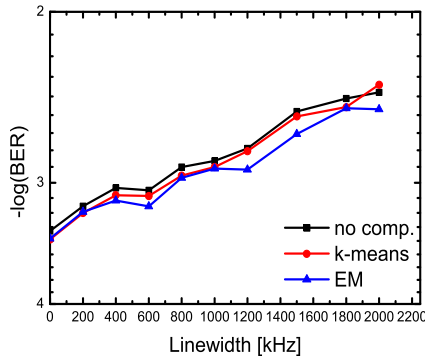
of the x polarization after the carrier recovery stage. Together with the constellation, we have also plotted optimal (nonlinear) decision boundaries obtained by applying Eq. (6) in conjunction with the EM algorithm.

It is observed from Fig. 7, that due to the nonlinear impairments, especially the outer constellation points are distorted. The inner constellation points are less affected due to lower power, however, all clusters experience a significant phase shift. In the case, no compensation is applied $-\log(\text{BER})$ is 1.30. For the case when the k-means is used the respective $-\log(\text{BER})$ is 2.04 while when the EM is applied $-\log(\text{BER})$ gets down to 3. This example demonstrates the capabilities of EM of compensating distorted and phase shifted constellations.

In Fig. 8(a), we plot the demodulated signal constellation for the input power of $P_{in} = 0$ dBm and the corresponding optimal decision boundaries after 800 km of transmission. It is observed that the demodulated signal constellation shown in Fig. 8(a) is distorted and therefore



(a)



(b)

Fig. 6. The total number of spans is 12. (a) BER as a function of span input power for dispersion unmanaged link. The combined laser linewidth is 200 kHz. (b) BER as a function of combined laser linewidth for dispersion unmanaged link.

the optimal decision boundaries are nonlinear. In Fig. 8(b), we plot $-\log(\text{BER})$ as a function of span input power after 800 km of transmission through dispersion managed link. It is observed that there is an improvement in the nonlinear system tolerance by employing the EM algorithm which is in accordance with simulation results. We observe up to 3 dB of improvement in nonlinear tolerance compared to the case when no compensation is used. The reason why we get more improvement for the experimental data may be attributed to the fact that the EM is also effective in compensating residual distortion induced on the signal. It is observed from the figure that only very little improvement can be obtained by using the k-means algorithm, and this is also in good agreement with the simulation results.

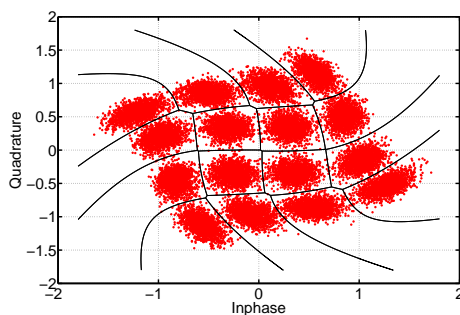
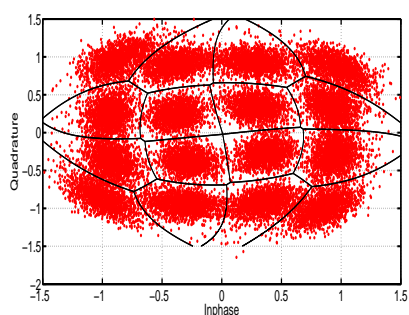
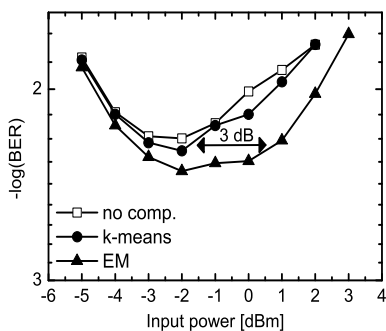


Fig. 7. Recovered constellation diagram impaired by nonlinear phase noise. Only a single transmission span is considered



(a)



(b)

Fig. 8. (a) Constellation diagram of the demodulated signal after 800 km of transmission through dispersion managed link. (b) BER as a function of span input power for dispersion managed link after 800 km of transmission.

5.2. Dispersion unmanaged link

For our next investigations, the DCF is removed and we consider 800 km of dispersion unmanaged signal transmission. In Fig. 9(a), the constellation diagram of the recovered signal is

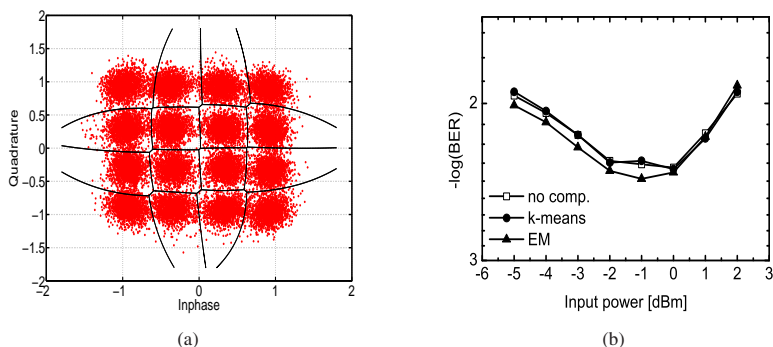


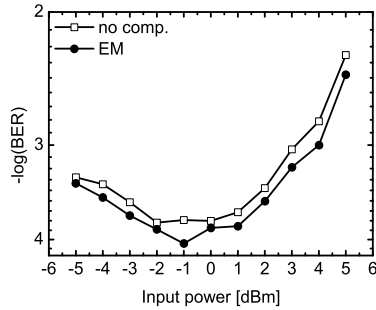
Fig. 9. (a) Constellation diagram of the demodulated signal after 800 km of transmission through dispersion unmanaged link. (b) BER as a function of span input power for dispersion unmanaged link after 800 km of transmission.

plotted together with the optimal decision boundaries for the input power of 0 dBm. It is observed in Fig. 9(a), that the clusters are not distorted in the same way as for the dispersion managed link. Indeed, the clusters seem to be more circularly symmetric and the optimal decision boundaries are very close to linear. This confirms the earlier observations reported in [16–18], that for the dispersion unmanaged links the effect of fibre nonlinearity corresponds to adding white Gaussian noise. There is however, some slight distortion in the shape of the clusters. In Fig. 9(b), $-\log(\text{BER})$ is plotted as a function of span input power. It is observed that for input power exceeding 0 dBm, there is no improvement in the nonlinear system tolerance when k-means or EM is used. However, for the input power less than 0 dBm shown in Fig. 9(b), there is an improvement of ~ 0.5 dB.

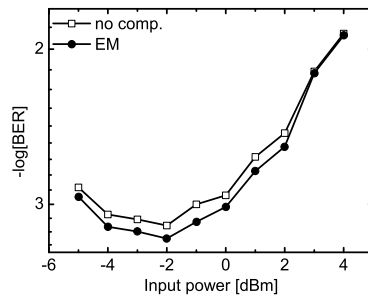
In order to investigate how nonlinearity compensation by the EM scales with transmission distance, $-\log(\text{BER})$ is plotted as a function of span input signal power for transmission distances of 240 km and 400 km, respectively, see Fig. 10. It is observed in Fig. 10(a) that an improvement in the nonlinear system tolerance of approximately 0.5 dB is observed for the entire range of the considered input optical power. For the transmission distance of 400 km, Fig. 10(b), a similar improvement of 0.5 is observed, however, the gain disappears for input power exceeding 2 dBm. One of the explanations could be that for input power exceeding 2 dBm the distortion is large and the EM cannot properly estimate the parameters.

6. Conclusion

We have shown that the expectation maximization algorithm is a powerful tool for combating system impairments, (fibre nonlinearities, I/Q imperfections and laser linewidth), which significantly distort the signal constellation. By the distortion, it is meant the deviation from circular symmetric shape. Additionally, we have demonstrated, experimentally that by using expectation maximization, up to 3 dB of improvement in nonlinear system tolerance can be obtained for 800 km long dispersion managed transmission link. For the considered dispersion unmanaged link of 240 km, 400 km and 800 km, an improvement of approximately 0.5 dB, is obtained. For a multi-channel WDM transmission system, the EM algorithm can potentially be beneficial as the inter-channel nonlinear effects will have an imprint on the constellation of the signal under constellation. The improvement in the nonlinear system tolerance offered by the EM, will depend on the modulation format of the neighboring channels, the spacing, as well as



(a)



(b)

Fig. 10. (a) BER as a function of span input power for dispersion unmanaged link after 240 km of transmission. (b) BER as a function of span input power for dispersion unmanaged link after 400 km of transmission.

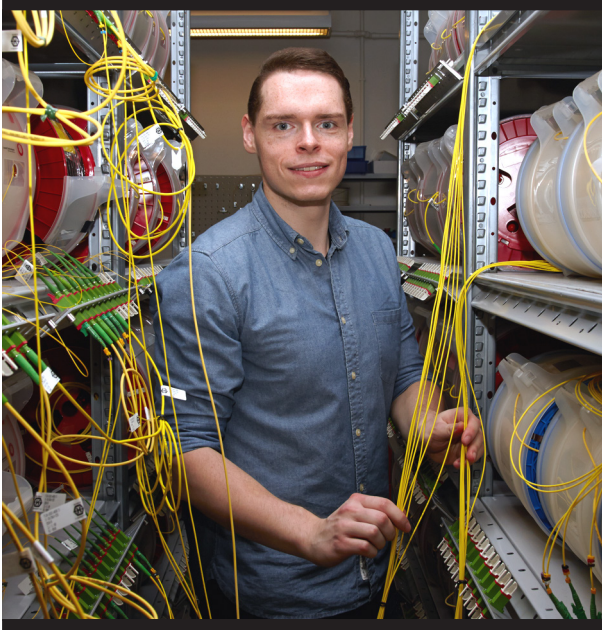
the number of neighboring channels. However, this is the topic that needs further investigations.

In order to see what benefits EM brings we need to relate the performance of the EM to a digital backpropagation, which has become a benchmark for nonlinearity compensation techniques. For the dispersion managed links, it has been numerically shown that up to 4 dB of improvement can be obtained [19]. The gain in the nonlinear system tolerance will though depend on the implementation of the digital backpropagation. For instance this gain reduces to 2 dB if 1 step/fiber digital backpropagation is used [19]. For the dispersion unmanaged links, an improvement of 3 dB for PDM 16-QAM signal has been shown experimentally [20]. As a rule of thumb, we may conclude that for dispersion unmanaged system digital backpropagation offers better performance, while for dispersion managed systems, depending on the implementation of digital backpropagation, the performance of the EM and digital backpropagation may be comparable. However, one technique does not have to exclude the other, as one may consider the combination of both techniques in combating optical fibre channel nonlinearities.

Acknowledgments

This work has been partly supported by the Danish Council for Independent Research, project CORESON and the CHRON (Cognitive Heterogeneous Reconfigurable Optical Net-

work) project, with funding from the European Community's Seventh Framework Programme [FP7/2007-2013] under grant agreement n° 258644, <http://www.ict-chron.eu>.



Copyright: Robert Borkowski
and DTU Fotonik
All rights reserved
ISBN: 978-87-93089-28-0

Published by:
DTU Fotonik
Department of Photonic Engineering
Technical University of Denmark
Ørstedss Plads, building 343
DK-2800 Kgs. Lyngby

Robert Borkowski was born in Lodz, Poland in 1987. He received M.Sc.Eng. and Ph.D. degrees from DTU Fotonik – Department of Photonics Engineering, Technical University of Denmark, respectively in 2011 and 2014.

During his Ph.D. he was working on various aspects of coherent communication systems, including digital signal processing algorithms for coherent receivers and optical performance monitoring routines, performing experimental trials as well as numerical simulations. He developed a novel modulation format recognition method for digital receivers based on Stokes space parameters and cluster analysis.

Dr. Borkowski was actively involved in the European FP7 project CHRON (Cognitive Heterogeneous Reconfigurable Optical Network). In 2012, he was a visiting researcher at CPqD in Campinas, Brazil. His research interests are in signal processing and machine learning applied to optical communications.